VOLUME 2

THE ASTROPHYSICAL JOURNAL

AN INTERNATIONAL REVIEW OF SPECTROSCOPY AND ASTRONOMICAL PHYSICS

SEPTEMBER 19

THE UNIVERSITY OF CHICAGO

CHICAGO, ILLINOIS

September 1951 Vol. 114, No. 1

THE ASTROPHYSICAL JOURNAL

AN INTERNATIONAL REVIEW OF SPECTROSCOPY AND ASTRONOMICAL PHYSICS

The Astrophysical Journal is published bimonthly by the University of Chicago at the University of Chicago Press, 5750 Ellis Avenue, Chicago 37, Illinois, during July, September, November, January, March, and May. ¶Two volumes are published per year, one beginning with the January issue and the other beginning with the July issue. The subscription price is $6.00 per volume or $12.00 per year; the price of single copies is $3.00. (Orders for service of less than a volume will be charged at the single copy rate.) ¶Postage is prepaid by the publishers on all orders from the United States and its possessions. No extra charge is made for postage to countries in the Pan American Postal Union. ¶Postage is charged extra as follows: for Canada, 20 cents per volume, 40 cents per year (total $6.20 per volume, $12.40 per year); on single copies 5 cents (total $3.05); for all other countries in the Postal Union, 40 cents per volume, $1.20 per year (total $6.40 per volume, $13.00 per year), on single copies 10 cents (total $3.10). Subscriptions are payable in advance. Please make all remittances payable to The University of Chicago Press, in United States currency or its equivalent by postal or express money orders or bank drafts.

The following is an authorized agent:

For the British Empire, except North America and Australasia: The Cambridge University Press, Bentley House, 200 Euston Road, London, N.W. 1, England. Prices of yearly subscriptions and of single copies may be had on application.

Claims for missing numbers should be made within the month following the regular month of publication. The publishers expect to supply missing numbers free only when losses have been sustained in transit, and when the reserve stock will permit.

Business correspondence should be addressed to The University of Chicago Press, Chicago 37, Illinois.

Communications for the editors and manuscripts should be addressed to: W. W. Morgan, Editor of The Astrophysical Journal, Yerkes Observatory, Williams Bay, Wisconsin.

Line drawings and photographs should be made by the author, and all marginal notes such as co-ordinates, wave lengths, etc., should be included in the cuts. It will not be possible to set up such material in type.

One copy of the corrected galley proof should be returned as soon as possible to the editor, Yerkes Observatory, Williams Bay, Wisconsin. Authors should take notice that the manuscript will not be sent to them with the proof.

The cable address is "Observatory, Williamsbay, Wisconsin."

The articles in this journal are indexed in the *International Index to Periodicals*, New York, N.Y.

Applications for permission to quote from this journal should be addressed to The University of Chicago Press, and will be freely granted.

Microfilms of complete journal volumes are available to regular subscribers only and may be obtained at the end of the year. Orders and inquiries should be addressed to University Microfilms, 313 North First Street, Ann Arbor, Michigan.

Notice to subscribers: If you change your address, please notify us and your local postmaster immediately.

Entered as second-class matter, July 12, 1949, at the Post-Office at Chicago, Ill., under the Act of March 3, 1879.
Acceptance for mailing at special rate of postage provided for in United States Postal Act of October 3, 1917, Section 1103, amended February 28, 1925.

[PRINTED IN U.S.A.]

THE ASTROPHYSICAL JOURNAL

AN INTERNATIONAL REVIEW OF SPECTROSCOPY AND ASTRONOMICAL PHYSICS

VOLUME 114 SEPTEMBER 1951 NUMBER 2

THE EVOLUTION OF GALAXIES AND STARS

C. F. VON WEIZSÄCKER
Max Planck Institut, Göttingen
Received May 17, 1951

ABSTRACT

I. Aims of the theory.—A hydrodynamical scheme of evolution is proposed, confined to events after the time when the average density in the universe was comparable to the density inside a galaxy at our time.

II. Hydrodynamical conditions.—Gas in cosmic space is moving according to hydrodynamics, mostly in a turbulent and compressible manner. Dust is carried with the gas, probably by magnetic coupling. Star systems cannot be described hydrodynamically and hence do not show turbulence and supersonic compressibility.

III. The spectral law of incompressible turbulence.—The relative velocity of two points at a distance l is proportional to $l^{1/3}$. This is deduced from the picture of a hierarchy of eddies.

IV. Compressibility and interstellar clouds.—A hierarchy of clouds is considered.

V. General evolutional scheme for a gaseous body.—A gravitationally stable, turbulent cloud is first flattened into a rotating disk, which then is dissolved into a uniformly rotating central body and a part returning into cosmic space. The time scale of these changes is somewhat larger than the diameter of the cloud divided by the turbulent velocity.

VI. The origin of galaxies.—They seem to have been formed by a competition between expansion and turbulence.

VII. The evolution of galaxies and spiral structure.—Irregular nebulae must be young, spirals intermediate, elliptical nebulae genetically old. Spiral structure is the distortion of turbulent clouds by nonuniform rotation. A bar is more stable than a disk. A two-armed spiral seems to be a distorted bar.

VIII. The origin of the stars.—Three groups of stars are considered instead of Baade's two populations: (*a*) stars belonging to the galactic center dynamically; (*b*) old stars belonging to the disk; (*c*) "young" stars. Stars could be formed as long as there were no stars present, because stellar radiation inhibits the contraction of clouds to form new stars.

IX. "Young stars."—They seem to be, more exactly, rejuvenated stars. The mechanism of the accretion of interstellar matter by a star is discussed hydrodynamically.

X. Rotation, planetary systems, and double stars.—Stars must be formed rotating because of the turbulence of the original clouds. They lose their rotation probably by a combined magnetic-hydrodynamic process. Both formation and loss of rotation provide gaseous disks in which planets and double stars can be formed. Modifications of the author's theory on the origin of planets are discussed.

XI. Giants and white dwarfs.—Giants seem to have highly condensed cores. Their model may be nonstationary, with a slowly expanding atmosphere. Planetary nebulae then would be special types of giants.

I. AIMS OF THE THEORY

The difficulty of cosmogonical theories lies in the interconnection of the facts. The evolution of a single object can be understood only if its temporal and spatial boundary conditions and the external forces acting on it are known. These are defined by the evolu-

tion of the larger system of which the object forms a part. So every single problem is likely to lead us back into the problem of the history of the universe. On the other hand, the evolution of large systems can be discussed only if we have some knowledge of the rules governing the evolutionary behavior of their parts. Hence cosmogony has, by necessity, developed as a sequence of general schemes, which, on the one hand, were needed to make the particular problems well defined, while, on the other hand, the very solutions of these particular problems usually disproved some of the fundamental assumptions of the scheme.

This paper again proposes such a general scheme with the purpose of giving a background for more specialized investigations which in the end should, if not supersede, at least correct the scheme. It follows the outline given by some older papers of the author.[1] Since these papers are partly inaccessible to American readers except in a few libraries, their main points are briefly restated and, if necessary, corrected. The results of new calculations, to be published elsewhere, are qualitatively described. The main new point of this paper is a more detailed theory of the origin of the stars.

There are parts of cosmic history for which we have every good reason to assume that they can be understood by applying no other fundamental laws of nature than those known today, while in other, more remote, parts of time and space modified laws may hold. This paper tries to confine the proposed theory strictly to the field of applicability of well-known laws. This excludes all discussions of models of the universe. The only element of general cosmological theories which is used is the assumption that the red shift of the spectral lines of extragalactic nebulae can be interpreted as a Doppler effect and that we must accordingly ascribe an age of not more than a few billion years to the systems which we observe today. The agreement in order of magnitude of this age with the intragalactic and radioactive age determinations seems to render this assumption fairly probable.

The largest system considered in the theory is a vicinity of galaxies. The motion in such a system is described by Newtonian mechanics in a Euclidean space. No cosmological constant and no permanent creation of matter are assumed, but most of the results would not be affected very much by such assumptions.

The earliest time considered is the moment when the average density of the matter from which the galaxies originated was comparable to the average density inside a galaxy today. The problem of the formation of chemical elements which probably belongs to an earlier time is therefore excluded from the theory, while the formation of separate galactic systems is included.

II. HYDRODYNAMICAL CONDITIONS

In cosmic space we know three different "states of aggregation" of matter: gas, dust, and stars. The first question of the theory is what form of mechanics is able to describe the average motions of matter in these states. We will find the following results: (1) The motion of the cosmic gas obeys the equations of hydrodynamics. In most cases it is turbulent and compressible. (2) The dust is built up from and is, in a first approximation, carried with the gas.

(3) The motion of the stars cannot be described by a hydrodynamical approximation. Hence the concepts of turbulence and of dynamical compressibility as used in hydrodynamics cannot be applied to a system of stars. More general methods of statistical mechanics must be used for them.

A system of separate bodies, moving freely in space under a common force (which in our case is gravity) can be statistically described to a first approximation by assigning a

[1] C. F. von Weizsäcker, *Zs. f. Ap.*, **22**, 319, 1943; **24**, 181, 1947; *Zs. f. Naturforschung*, **3a**, 524, 1948; *Fiat Review of German Science, Astronomy, Astrophysics and Cosmogony* ("Naturforschung und Medizin in Deutschland, 1939–1946," Vol. XX) (1948), p. 413; *Naturwiss.*, **35**, 188, 1948; W. Heisenberg and C. F. von Weizsäcker, *Zs. f. Phys.*, **125**, 290, 1948.

density of matter ρ and an average velocity v to every point in space in every moment of time. These quantities will obey the equations of hydrodynamics if the distances l, in which they change appreciably, are large compared with the mean free path λ of the single bodies:

$$\frac{l}{\lambda} \gg 1 . \tag{2.1}$$

The solutions of the hydrodynamical equations are turbulent if the Reynolds number,

$$R = \frac{\rho v l}{\mu} ,$$

is larger than a certain critical value. Here v and l are values of velocity and distance characteristic of the average flow of matter. The molecular viscosity μ is equal to $\rho v_{th} \lambda$, where v_{th} denotes the average thermal velocity of the molecules. The critical value of R at which an average laminar motion becomes unstable is of the order of magnitude 1000. The transition toward a turbulent motion, however, reduces the average velocity, and in a turbulent flow there are eddies whose proper motions and diameters define Reynolds numbers down to about 10.[2] So the condition for turbulence can be roughly written

$$\frac{v}{v_{th}} \frac{l}{\lambda} \gg 1 . \tag{2.2}$$

A gas is compressed by its internal hydrodynamical motion if the velocity of this motion is comparable to, or larger than, the velocity of sound, which is essentially equal to the thermal velocity of the molecules. So the condition for compressibility is

$$\frac{v}{v_{th}} \geqq 1 . \tag{2.3}$$

For *gas* atoms the effective cross-section for a collision, σ, will be the geometrical cross-section, 10^{-16} cm if the atoms are neutral, and considerably larger if they are ionized. The number n of gas particles per cubic centimeter is between 1 and 10 for ordinary interstellar space and higher in dense clouds. So the mean free path, according to the general formula

$$\lambda = \frac{1}{n\sigma} , \tag{2.4}$$

is

$$\lambda_{gas} < 10^{16} \text{ cm} , \tag{2.5}$$

in which λ_{gas} can be smaller by several orders of magnitude. But even 10^{16} cm is close to the lower limit of observable distances in cosmic space, and observable motions of interstellar gas will consequently be described fairly well by hydrodynamics.

Velocity differences inside a cosmic cloud of the order of magnitude 1 km/sec or more are observed, e.g., in the Orion nebula, and the sharpness of interstellar absorption lines gives an upper limit of only about 6 km/sec for the type of clouds observed by those lines.[3] The velocity differences between different clouds amount to 20 km/sec or in extreme cases to 70 km/sec. If we describe a whole galaxy as a hydrodynamical system, we have to use for v the differences between the rotational velocities of its different parts,

[2] W. Heisenberg, *Zs. f. Phys.*, **124**, 628, 1947.

[3] W. S. Adams, *Ap. J.*, **97**, 105, 1943; *Mt. W. Contr.*, No. 673; *Ap. J.*, **109**, 354, 1949; *Mt. W. Contr.*, No. 760.

which amount to several hundred km/sec. On the other hand, the temperature of interstellar gas is not higher than 100° K for the larger part of space, and about 10,000° K for *H* II regions.[4] The corresponding thermal velocities for hydrogen are roughly 1 km/sec and 10 km/sec. So, except for small structures, mostly inside *H* II regions, v/v_{th} will never be small compared to unity and in many cases will be much larger. It follows that the motion of the interstellar gas in general must show the characteristics both of turbulence and of compression. Turbulence means irregular fluctuations of velocity. Compression means that these fluctuations of velocity will produce fluctuations of density. Both effects are observed and will be discussed in the next section.

For *dust* we may assume an average particle size of 10^{-5} cm, giving $\sigma \approx 10^{-10}$ cm^2. Except for especially dense and small dust clouds (globules), one would assume an average space density of the dust not higher than 10^{-25} gm/cm^3. This figure follows from the assumption that the abundance ratio of heavy and light elements in stars should not deviate too much from the same ratio in the interstellar matter from which the stars were originally formed. This assumption, it is true, is open to doubt. But, since we know stars composed of heavy elements only (e.g., our earth) and since mechanisms have been proposed initiating the formation of a star by heavy elements only,[5] while, except for the radiation pressure of extremely luminous stars, no effects working in the opposite direction seem to exist, an estimate based on the ratio in our sun may seem conservative.

With these figures we would get roughly $n = 10^{-10}$ cm^{-3} and $\lambda = 10^{20}$ cm. This does not seem to fit well with the observational fact that there are structures of dust which certainly are not gravitationally stable and still show much finer details. The most conspicuous case is probably the thin filamentary structure in the Pleiades nebula, which is dust (since it is a reflection nebula) and whose smallest visible details are not larger than $2 \cdot 10^{15}$ cm. Such facts induce us to suspect that here the dust is carried with the gas. Its structure would then not be due to an interaction of dust particles with other dust particles but to their floating in the moving gas. We would have to assume that there is an uneven distribution of dust in the gas, perhaps due to the radiation pressure of the Pleiades B stars, and that this uneven distribution is then carried around with the eddies of the gas, thus making visible their kinematical pattern. The case would be similar to water clouds or tobacco smoke in our air. This idea seems to be supported by the fact that photographs of interstellar matter tend to show finer details in absorption or reflection than in emission.[6] Details in emission must be real density fluctuations of the gas, while details in absorption or reflection, according to the scheme here proposed, can render visible mere velocity fluctuations, even if they lie below the limit of compressibility.

As to the forces carrying the dust with the gas, only a tentative answer can be given here. The interaction may be caused by collisions of gas atoms with the dust particles or by a magnetic field. The latter coupling mechanism seems to be more efficient.

The coupling by collisions may be estimated as follows: A dust particle moving through the gas with a relative velocity v will change its momentum by its own order of magnitude in a time during which it is hit by a mass of gas comparable to its own mass. If v is small compared with the v_{th} of the gas molecules, this "frictional time scale" will be[7]

$$t_f = \frac{(4/3)\pi r^3 s}{4\pi r^2 \rho v_{th}} = \frac{r s}{3 \rho v_{th}}, \tag{2.6}$$

[4] L. Spitzer, Jr., *Ap. J.*, **93**, 369, 1941; **94**, 232, 1941; **95**, 329, 1942; **107**, 6, 1948; **108**, 276, 1948; **109**, 337, 548, 1949; **111**, 593, 1950; *Centennial Symposia* (Cambridge, Mass.: Harvard College Observatory, 1948), p. 87; *Science*, **109**, 461, 1949; B. Strömgren, *Ap. J.*, **89**, 526, 1939; **108**, 242, 1948.

[5] F. L. Whipple, *Centennial Symposia* (Cambridge, Mass.: Harvard College Observatory, 1948), p. 109; B. J. Bok, *Centennial Symposia*, p. 53.

[6] This was kindly pointed out to the author by Dr. Minkowski.

[7] L. Spitzer, Jr., cf. references n. 4.

where r and s are radius and density, respectively, of a dust particle. Table 1 gives values of t_f for different conditions. Now the gas changes its own velocity by its own order of magnitude during a "turbulent time scale," which, according to the spectral law (cf. next section), is

$$t_t = \frac{l}{v} = \frac{l_0^{1/3} l^{2/3}}{v_0}. \tag{2.7}$$

We may assume $v_0 = 10^5$ cm/sec and $l_0 = 10^{18}$ cm, thereby getting $t_t = 10^{12/3}$ sec or $t_t = 10^{13}$ sec for $l = 10^{18}$ cm, and $t_t = 10^{11}$ sec for $l = 10^{15}$ cm. The dust will take part in those motions of the gas for which $t_t > t_f$. This condition will scarcely be fulfilled for ordinary clouds if $l < 10^{18}$ cm. So, for a case like the Pleiades, recourse must probably be had to magnetic fields.

TABLE 1

FRICTIONAL TIME SCALE t_f IN SECONDS

v_m (CM/SEC)	ρ (GM/CM^3)		
	10^{-24}	10^{-22}	10^{-20}
10^5	10^{14} sec	10^{13} sec	10^{10} sec
10^6	10^{13} sec	10^{11} sec	10^{9} sec

It seems probable today that interstellar magnetic fields of about 10^{-6} gauss exist. For particles of mass m and charge Ze the Larmor period is

$$t_m = \frac{m c}{Z e H}, \tag{2.8}$$

which for $m = 3 \cdot 10^{-15}$ gm and $Z = 10$ would give $t_m \approx 2 \cdot 10^{10}$ sec. So $t_t > t_m$ would be fulfilled in general. This means a coupling of the dust particles to the lines of force, which, on the other hand, are coupled to the ionized part of the gas.

For a "gas" whose "molecules" are *stars*, even formula (2.1) is not fulfilled, as has been shown by Chandrasekhar.[8] Hence the hydrodynamical concepts cannot be applied to a system of stars. There will be fluctuations of both velocity and density in such a system, but they will correspond to the fluctuations in a gas produced by the random component of thermal motion rather than to turbulence or dynamical compressibility. In a gas, turbulence and dynamical compression (as shock waves and similar phenomena) are of a macroscopic, nonthermal origin. They correspond to solutions of the hydrodynamical equations which would not be substantially altered if, instead of the atomic theory, a continuum theory of matter were true. These fluctuations, if they occur at all, usually are much larger than the thermal fluctuations. But they can occur only if partial volumes of the gas can move as a bulk, transferring momentum only to immediately neighboring volumes. This condition breaks down for star systems. The mean free path of a star in a gravitationally stable star system is, except for extremely dense parts of the system, larger than the diameter of the whole system. So the local conditions in any partial volume of the system can interact directly with the local conditions in any other partial volume. But this "interaction" will seldom lead to a real exchange of momentum or other properties between individual stars. To a good approximation, the motion of a single star

[8] *Principles of Stellar Dynamics* (Chicago: University of Chicago Press, 1942), p. 74.

can be described as an unperturbed orbit in the common field of gravitation produced by the whole system.

A much discussed consequence of this fact is that in our galaxy (and similarly in clusters of galaxies, where the single galaxy plays the role of the single "star" in this analysis) an equipartition of the energies of the single stars cannot be reached within a few billion years. As far as this equipartition does not exist empirically, the theory seems satisfactory. But there are perhaps cases in which it would seem difficult to understand even the approximation toward equipartition which is actually displayed by some systems. Such cases have been considered arguments against the time scale which is now generally adopted.[9] It should, however, be remembered that equipartition is easily reached when the matter is not yet united in stars because then the high turbulent momentum transfer is available. Therefore, the sort or degree of equipartition in a system which is not dense enough to achieve it by stellar interactions may give a hint as to the stage of evolution of the system in which its gas was transformed into stars. We will use such indications in the later sections.

III. THE SPECTRAL LAW OF INCOMPRESSIBLE TURBULENCE

In this section the results of the modern statistical theory of turbulence are described as far as they are needed in this paper.[10] The main purpose is to introduce the concept of the hierarchy of eddies and to formulate Kolmogoroff's law in a way which seems most appropriate for astrophysical use.

We try to describe a turbulent flow. The fundamental concept of the theory is the "element of turbulence" or "eddy." This is a partial volume of the fluid having a rather common motion for an interval of time. This motion will, in general, contain a whirling component—hence the name "eddy." But the whirling is not the defining characteristic, and so the word "eddy" should not be understood as emphasizing the vorticity but rather as an abbreviation for "element of turbulence."

An eddy is characterized by its size, l. The eddy will be destroyed after having traveled a mean free path or "mixing length" which differs from l only by a numerical factor of the order of magnitude unity. Another characteristic of an eddy is its velocity v relative to neighboring eddies. According to a generally accepted similarity hypothesis, for eddies small compared with the largest eddies and large compared with the smallest eddies, all other statistical characteristics can be derived from l and the average value of v. If we want to give a mathematically precise meaning to these concepts, we had best use a Fourier analysis of the velocity field. Instead of the concept "eddy size," we then use the wave length of a Fourier component or its reciprocal value, the wave number k, and instead of v we use the Fourier amplitude corresponding to k.

There are eddies of all sizes from the spatial dimensions of the entire system down to a limit set by the molecular viscosity. The small eddies are inside the large ones. This is what we call the "hierarchy of eddies." It would not be meaningful to describe a particular turbulent flow by telling how many eddies of a given size exist there. The answer would be that they always touch each other, so that, for every eddy size, the number is just the total volume of the fluid divided by l^3. It is meaningful, however, to ask for the "strength" of the eddies of a given size l. This can be defined by the function $v(l)$ indicating the average velocity of an eddy of given size, or the average relative velocity of two points in the fluid at a distance l. The average kinetic-energy density of the eddies of

[9] J. Jeans, *Astronomy and Cosmogony* (Cambridge: At the University Press, 1928).

[10] G. J. Taylor, *Proc. R. Soc. London, A*, **151**, 421, 1935 ff.; T. von Kármán, *J. Aero. Sci.*, **4**, 131, 1937 ff.; A. V. Kolmogoroff, *C.R. Acad. Sci. U.S.S.R.*, **30**, 301, 1941; **32**, 16, 1941; L. Onsager, *Phys. Rev.*, **68**, 286, 1945; C. F. von Weizsäcker, *Zs. f. Phys.*, **124**, 614, 1947; W. Heisenberg, *Zs. f. Phys.*, **124**, 628, 1947; *Proc. R. Soc. London, A*, **195**, 402, 1949; S. Chandrasekhar, *Proc. R. Soc. London, A*, **200**, 20, 1949 ff.; G. K. Batchelor, *Proc. R. Soc. London, A*, **201**, 405, 1950, and previous publications.

size l is $\frac{1}{2}\rho v^2(l)$. In the language of Fourier analysis the same fact is usually represented by a function $F(k)$, defined by

$$\frac{1}{2}v^2 = \int^{\infty} F(k)\,dk\,, \tag{3.1}$$

where $\rho F(k)$ denotes the energy contained in the wave-number interval between k and $k + dk$, and the integral is the energy content of the eddies of the size $l = k^{-1}$. If the lower limit is put equal to zero, the integral is the total energy of the flow.

The spectral function $v(l)$ is determined by a consideration of the dissipation of energy. Under the influence of a viscosity η, the energy dissipated per unit time and volume is

$$S = \eta\,|\,\text{curl}\,\boldsymbol{v}\,|^2\,. \tag{3.2}$$

The energy of the larger eddies is not immediately transformed into heat, but it is first transferred to the eddies of somewhat smaller size. From these it flows to eddies of even smaller size and so on, until the smallest eddies transfer it to the thermal motion of molecules. The action of the eddies of a size l can be described phenomenologically by an "eddy viscosity,"

$$\eta_l = \rho l v\,. \tag{3.3}$$

This viscosity transfers the energy from the eddies somewhat larger than l to the eddies somewhat smaller than l. For dimensional reasons we must expect, in the average, for eddies of this size,

$$|\,\text{curl}\,\boldsymbol{v}\,|^2 = \text{Const.}\left(\frac{v}{l}\right)^2. \tag{3.4}$$

Hence the energy transferred through the eddies of size l is

$$S_l = \rho l v \left(\frac{v}{l}\right)^2 = \rho\,\frac{v^3}{l}\,. \tag{3.5}$$

If the situation is stationary, there must be a constant flow of energy through all eddy sizes, and therefore S_l must be independent of l. It follows that

$$v \propto l^{1/3}\,. \tag{3.6}$$

From equation (3.1) we see that then

$$F(k) \propto k^{-5/3}\,. \tag{3.7}$$

This law, which, in a different mathematical formulation, was first given by Kolmogoroff, can be used to estimate all other statistical properties of the eddies by purely dimensional arguments. The time scale of the dissolution of an eddy will be

$$t = \frac{l}{v} \propto l^{2/3}\,. \tag{3.8}$$

This means that small eddies dissolve (and form) more rapidly than large ones. Therefore, the assumption of a stationary state which was made in deducing formula (3.6) will hold for small eddies, even if the largest eddies are not stationary.

The eddy viscosity is proportional to $lv \propto l^{4/3}$. If we use η_l in the expression for the Reynolds number instead of μ, we find that this $R(\eta_l)$ is of the order of magnitude 1 for eddies somewhat larger than the ones characterized by l. Hence we can also interpret the spectral law by saying that the turbulence below the level l is kept just strong enough to

give to eddies above that level an "effective Reynolds number" not much larger than unity. If the turbulence below l were weaker than that, the motion above l would become more turbulent because of a lack of (eddy) viscosity; this increase of turbulence would show up just below l. If, on the other hand, the turbulence below l were stronger than indicated by the spectral law, its eddy viscosity would smooth out the motion above l, and thereby the turbulence below l would diminish.

When the energy flow reaches eddies for which the eddy viscosity is comparable to the molecular viscosity, it will be dissipated into heat; these are the "smallest eddies." According to Heisenberg, the limit is rather $\eta_l \approx 10\mu$; η_l/μ is the Reynolds number for l. This result was used in formula (2.2). Below the limit the spectral law takes the form

$$F(k) \sim k^{-7} . \tag{3.9}$$

Von Hoerner[11] has compared the spectral law with observations of radial velocities in the Orion nebula. Formula (3.6) can also be written

$$\frac{\partial \log v}{\partial \log l} = \frac{1}{3} . \tag{3.10}$$

In an empirical diagram showing $\log v$ as a function of $\log l$, the points can be represented by a straight line with the theoretical inclination 0.33 within the statistical error, while an inclination 0.40 might represent the observed points somewhat more closely. This slight deviation from the theory can perhaps be ascribed to compressibility.

These results will be modified by the consideration of magnetic fields. Turbulence tends to increase existing magnetic fields by lengthening the lines of force that are bound to follow the paths of the ionized particles. On the other hand, strong magnetic fields will prevent turbulent motions of ionized particles. These two effects will affect the spectrum by suppressing the turbulence, beginning from the lower end of the spectrum. The problem is very intricate. It has been treated by Biermann and Schlüter.[12]

IV. COMPRESSIBILITY AND INTERSTELLAR CLOUDS

This section describes the fundamental assumptions and results of a tentative theory of the interaction of turbulence and compressibility proposed by von Hoerner.[11] Supersonic velocities produce compression. In most terrestrial experiments we see single bodies moving with supersonic velocity through a fluid in which no other supersonic velocities are present. This leads to a single, fairly regular shock wave. In cosmic space similar phenomena may occur in the expanding shells of supernovae, as discussed by Oort and Burgers.[13] But this is probably not the average case of cosmic turbulence. In general, the energy source of cosmic turbulence will lie not in a single star but in the largest eddies, which probably should be identified with the rotational motion of the galaxy as a whole. Except for particular regions in their interior, galaxies are not rotating uniformly. The eddy viscosity produced by turbulence on a somewhat smaller scale tends to dissipate the kinetic energy of the relative motion of different parts of the galaxy caused by the non-uniform rotation, and this dissipated energy feeds the turbulence in the way described in the preceding section. The velocity differences involved in this process amount to 100 km/sec or a hundred times the average velocity of sound. Hence we would expect a very complicated statistical mixture of shock waves, if this concept can still be used at all.

Von Hoerner takes not shock waves but density fluctuations of the character of inter-

[11] To be published.

[12] *Zs. f. Naturforsch.*, **5a**, 237, 1950.

[13] J. M. Burgers, *Proc. Kon. Ned. Akad. Wet. Amsterdam*, **49**, 589, 1946; J. H. Oort, *M.N.*, **106**, 159, 1946.

stellar clouds as the fundamental concept of his theory. In analogy to the hierarchy of eddies in incompressible turbulence, he introduces a hierarchy of clouds. Every large cloud is assumed to consist of a certain number of smaller clouds. For the sake of simplicity, the space between the smaller clouds is treated as a vacuum. The smaller clouds, in their turn, consist of even smaller clouds, between which there is vacuum again. This hierarchical structure goes on until clouds are reached with an inner turbulent velocity small compared with the velocity of sound. Again, for simplicity, sharply distinct levels in this hierarchy are assumed and described by an index ν, which can have only integral values, larger ν designating larger clouds. A cloud at the level ν is called a C_ν. Instead of the single function $v(l)$ of the incompressible case, four functions of the index ν must be determined:

v_ν, the average velocity of the center of gravity of a cloud C_ν with respect to the center of gravity of the next larger cloud $C_{\nu+1}$ in which C_ν is contained;
ρ_ν, the average density of matter inside C_ν;
l_ν, the average diameter of a C_ν; and
N_ν, the average number of C_ν's contained in a $C_{\nu+1}$.

The functions ρ_ν and l_ν can be connected by the equation

$$\frac{\rho_\nu}{\rho_{\nu+1}} = \left(\frac{l_\nu}{l_{\nu+1}}\right)^{-3k_\nu}. \tag{4.1}$$

The exponent k_ν is called the degree of compression at the step ν. If $k_\nu = 0$, there is no compression at this step; k_ν must be smaller than unity.

It can be shown that k_ν also expresses the spectral law. Eliminating the index ν, we can write the law in analogy to formula (3.10)

$$\frac{\partial \log v}{\partial \log l} = \tfrac{1}{3} + k(l). \tag{4.2}$$

So the main task of the theory is the determination of the function k_ν or $k(l)$. This involves considerations of the mechanism of the formation and destruction of the density fluctuations here schematically described as separate clouds. We may consider two limiting cases. If we start from a uniform density throughout the whole volume, the supersonic velocities will soon produce strong density fluctuations by shock waves. If, on the other hand, we start from extreme density fluctuations, e.g., very small and dense clouds separated by distances large compared with their diameters, these clouds (unless gravitation were strong enough to keep them stable) would expand by the pressure of their internal temperature and turbulence; so a more uniform density distribution would be approached. Between the two limiting cases there must be an equilibrium between the compression produced by the collisions and the expansion during the time between the collisions. It is difficult to give an accurate model of these complicated processes, but von Hoerner could show that, with increasing ν and therefore increasing v_ν, the compression k_ν varies from 0 for $v_\nu \ll v_{th}$ to a limiting value k_∞ for $v_\nu \gg v_{th}$. For different assumptions about the mechanism of the collisions, k_∞ varies between 0.09 and 0.23, the value thought to be most probable lying at 0.12. The result about the spectral law of the Orion nebula seems to indicate that there $k_\nu \approx 0.07$, a reasonable value for the observed internal velocities of about 10 km/sec in the nebula.

The result can be expressed in still another way. We ask for the fraction f of the volume inside the largest clouds which is actually occupied by matter. This fraction will depend both on k_∞ and on the ratio between the sizes of the largest and the smallest clouds. If we

ascribe a diameter of 10^{22} cm (galaxy) to the largest clouds, and 10^{19} cm (3 parsecs) to the smallest clouds, we get the following values of f as a function of k:

$$k = 0.05\,, \quad 0.10\,, \quad 0.15\,;$$

$$f = 0.36\,, \quad 0.125\,, \quad 0.045\,.$$

The empirical value of f seems to lie somewhere between 0.05 and 0.15.

The analogy of this theory with the theory of the incompressible case is perhaps seen more clearly if we remark that, in addition to the eddy viscosity, we here get a "cloud pressure." Just as the kinetic energy density of molecules appears as gas pressure, the kinetic energy of the clouds below a given level acts as a pressure in the clouds of a higher level; and, since we have supersonic velocities, this cloud pressure is higher than the molecular pressure. And, just as the eddy viscosity serves to define an effective Reynolds number which, for successive levels of eddies in a stationary situation, can never exceed the order of magnitude 10, so we can define an "effective Mach number" for clouds above a level ν with respect to the "velocity of sound" defined by the velocities of clouds below this level. This effective Mach number again will stay small, and so the compression k in a single step can never become very high. This accounts for the existence of a limiting value k_∞. In a less abstract way we can say: Real shock waves in large dimensions cannot exist, since there are always density fluctuations in the next smaller level which immediately divert the wave fronts into statistically distributed directions. Here, again, the action of magnetic fields should be considered. The reader is referred to the paper by Biermann and Schlüter.[12]

V. GENERAL EVOLUTIONARY SCHEME FOR A GASEOUS BODY

In this section we try to describe the evolutionary trend as far as it does not depend on the special conditions by which galaxies, intragalactic clouds, stars, planets, etc., are distinguished.

We assume every gaseous body which we will consider to be formed as a part of a larger mass of gas that existed before the formation of the smaller body. The new body will be stable only if its gravitational energy is larger than its thermal energy:

$$\frac{GM^2}{R} > MkT\,. \tag{5.1}$$

This is Jeans's[14] condition. It is necessary, but not sufficient, for the actual formation of a separate stable body. If, like Jeans, we consider the original larger mass to have had uniform density and no inner motion, the gravitational instability of a slight density fluctuation might well lead to a first additional contraction. This contraction, however, will be stopped very soon by the conversion of the gravitational energy into heat, unless the heat can be at least partly removed, e.g., by radiation. Another insufficiency of the formula is that it gives only a lower limit to the mass of the body.

The picture becomes somewhat more definite if we assume that there is supersonic turbulent motion in the original mass. Then a hierarchy of clouds will be formed. Instead of Jeans's condition of stability, we will then get an equation in which the hydrodynamical velocity of the inner motion takes the role of the thermal energy:

$$\frac{GM^2}{R} \sim \frac{Mv^2}{2}\,. \tag{5.2}$$

Here we may write the sign of equality, since the mechanism of compressible turbulence

[14] Jeans, *op. cit.*, chap. xiii; G. Gamow and E. Teller, *Phys. Rev.*, **55**, 654, 1939; G. Gamow, *Phys. Rev.*, **74**, 505, 1948.

will provide for the formation of clouds not much larger than the lower limit. The further contraction of the clouds will again depend on the possibility of getting rid of part of the internal energy. Unlike the adiabatic compression of a quiet cloud, here the contraction is certainly accompanied by one irreversible process—the dissipation of turbulent energy.

If a turbulent cloud is stable and able to contract, the first step of the contraction will be a flattening. The contraction will first be caused by the decay of the inner turbulence and of the corresponding "cloud pressure." Now the part of the turbulent motion which is connected with a resulting angular momentum cannot easily vanish because of the conservation law. Thus a flat rotating disk will remain. Its largest diameter and rotational velocity will not be different by a large factor from the original diameter and turbulent velocity of the cloud. If these quantities are d and v, respectively, the time scale of the flattening will be

$$t = \alpha \frac{d}{v}, \tag{5.3}$$

where α may be put equal to 5, to give an estimate.

The disk will probably already have a central concentration of mass. Its rotation will not be uniform, and the differences in the rotational velocity will go on producing turbulence. The remaining extension of the disk in the direction perpendicular to its plane will be determined by this turbulence as long as its cloud pressure is higher than the molecular pressure.

The remaining turbulence exerts friction and thereby dissipates energy. Therefore, the rotation cannot be stable unless it becomes uniform. This will not be possible for a very extended mass of low density. On the other hand, the angular momentum prevents contraction of the body as a whole. The result will be the contraction of part of the body toward the center, while the gravitational energy set free by the contraction enables the rest of the mass to return to the surrounding cosmic space, carrying with it most of the angular momentum of the body. This evolution has been followed by analytical and numerical solutions of the hydrodynamical equations.[15]

For dimensional reasons the time scale of this loss of angular momentum will again be given by a formula like (5.3), where v can be taken to be the rotational velocity but with a much larger α, since now the turbulence is weaker than before and the process is more complicated. Perhaps we are not quite wrong in assuming an α of 100. But we should rather consider this process in more detail in the special cases.

VI. THE ORIGIN OF GALAXIES

Since the beginnings are the least-known part of history, we offer our hypothesis about the origin of galaxies with more hesitation than the theory about their further development. The actual motions of the galaxies are composed of two parts. One component is the systematic velocity of expansion as deduced from Hubble's law, which is predominant for galaxies far apart. The other component is an irregular proper motion of the single systems. For neighboring systems the relative velocity due to the second component is empirically of just the same order of magnitude as the relative velocity which would follow from Hubble's law alone.

According to the assumptions formulated in Section I, we may follow these motions back to the time t_0 when the galaxies just "touched each other." In the meantime, the velocities should have been essentially preserved by the law of inertia. At t_0 we would describe the first component as a systematic expansion of the part of the universe known to us and the second component as a turbulent motion superimposed on the expansion. It is encouraging for such a picture that the rotational velocities of the actual galaxies, too, are of the same order of magnitude as their irregular proper motions. We try to ex-

[15] R. Lüst and E. Trefftz, to be published (*Zs. f. Naturforsch.*).

plain the origin of the galaxies by the co-operation of these motions and of gravitation, while we do not try to deduce these motions from earlier states of the universe or from more fundamental principles.

The equality of the velocities of expansion and of turbulence for neighbors is just what we should expect if turbulent compression had determined the formation of the galaxies. In an expanding universe gravitational instability would not be sufficient to form subsystems, while turbulence could do it if its velocity v_t were large enough compared with the velocity of expansion v_{ex}. If r denotes the distance between two points in the universe at the time t_0, their relative velocity consists of the two components, one of which is given by Hubble's law:

$$v_{ex} = a\, r\,, \tag{6.1}$$

while the average value of the other follows from Kolmogoroff's law, which may be modified by considering compressibility and other deviations from stationary incompressible conditions:

$$v_t = b\, r^{1/3+k}\,. \tag{6.2}$$

In these equations a is Hubble's constant at the time t_0 (essentially $a = t_0^{-1}$), b is another constant which may be determined from the irregular motions as seen today, and k is perhaps a constant, perhaps a function of r, but in any case a number which will probably not exceed $\frac{1}{3}$. If $v_t > v_{ex}$, there is a chance that the two points approached each other at the moment t_0 and that they consequently became parts of the same galaxy. This condition defines a maximum value of r which we may identify with the size of the largest galaxy at the time of its formation. So the theory seems to explain that there is a maximum size of galaxies.

Yet the theory has several shortcomings which probably could be removed by closer consideration of the events at and before the time t_0. This transcends the restrictions we have imposed on ourselves in this paper, but we should at least mention the main problems.

First, the connection which probably exists between the two constants a and b is not understood. This may be the most fundamental problem of the theory because it involves the origin of cosmic turbulence, but probably it is the most difficult one, too.

Secondly, one might ask whether our considerations should not be applied to clusters of galaxies rather than to single galaxies. In a theory starting from the idea of a hierarchy of clouds we should probably not be surprised to find the aggregation of matter taking place in different levels at the same time. The competition between turbulence and expansion may lead to the looser aggregation in clusters for very large clouds and to the denser form which we call "galaxies" for somewhat smaller systems. The precise meanings of the quantities t_0, a, and b will not be clear without a more detailed theory of these distinctions.

Thirdly, the theory does not yet include another empirical fact concerning gravitation. Expressed in terms of an energy balance, the condition $v_{ex} = v_t$ means that for the actual galaxies the kinetic energies due to expansion and turbulence are equal. Now, empirically, the inner potential energy of gravitation of a large galaxy, being negative, has roughly the same absolute value as these two kinetic energies. This is seen most easily from the fact that the rotational velocities of galaxies are roughly as large as their "turbulent" translational velocities. The rotational energy of a flat galaxy is connected with its gravitational energy by the virial theorem. Therefore, even in assuming that the origin of the rotation is in the primary turbulence, we would not conclude a priori that the actual velocity of rotation must still be equal to the original velocity of turbulence; it would have had to adjust to the gravitational conditions by a shrinking or an expansion of the system. The empirical coincidence between the velocities of rotation and

translation therefore means that the systems did not need to readjust their densities very much after their separation. This may justify our choice of t_0 as the time when the average density of the known part of the universe was comparable to the density inside a galaxy today. But what does this coincidence mean cosmogonically?

At a given time, say, t_0, for every spherical part of the universe of average density, the inner gravitational energy and the kinetic energy of expansion are proportional to each other, no matter how large or how small the total mass of the sphere considered. Let r be the radius of the sphere and M its mass. Then M is proportional to r^3, and

$$E_{\text{grav}} = \text{Const.}\,\frac{M^2}{r} = \text{Const.}\;r^5\,, \tag{6.3}$$

$$E_{\text{exp}} = \text{Const.}\;M\,v^2 = \text{Const.}\,r^5\,. \tag{6.4}$$

Our coincidence now means that at t_0 they were not only proportional but roughly equal, while, later on, for a constant (though expanding) mass M, only E_{exp} remained constant, E_{grav} decreasing proportional to t^{-1}. Before t_0, if we may apply the simple picture of expansion to that time, both energies must have decreased with increasing time. So, from our observational indications, the first formation of galaxies seems to have taken place in the moment when the known part of the universe ceased to be "gravitationally coherent."

A fourth point which would need consideration is the mass distribution of galaxies, especially the fact that there seems to be a lower limit to the possible mass of a galaxy.[16] This is probably connected with the gravitational energy, too. Applying the spectral law (6.2), we find that the turbulent energy decreases more slowly for decreasing r than the potential energy of gravitation:

$$E_t = \text{Const.}\;M\,v_t^2 = \text{Const.}\,r^{11/3+2k}. \tag{6.5}$$

Hence, if condition (5.2) is approximately fulfilled for the largest systems, it cannot be fulfilled for systems much smaller than these. This, however, presupposes that all systems were formed at the same time. In the next section we shall find strong evidence for the assumption that some extragalactic nebulae, especially some of the smaller ones, were formed much later than t_0. So the mass distribution can be understood only in connection with the later evolution of the galaxies.

VII. THE EVOLUTION OF GALAXIES AND SPIRAL STRUCTURE

We assume galaxies to develop according to the scheme proposed in Section V. The time scale for the flattening of a galaxy connected with the decay of its original turbulence may be comparable to its actual period of rotation. The time scale for the loss of rotation can easily be ten or twenty times that period. Thus large galaxies like our own can be as old as the universe, without having yet reached their final stage. For small systems like the Magellanic Clouds or the companions of M 31, however, the time scale must be definitely smaller than the age of the universe. Consequently, they must be either still young in years or already old genetically. Probably systems of both types, including intermediate cases, occur in our neighborhood. Probably not all the original matter was exhausted in the formation of the oldest systems, and, moreover, the old systems must have lost matter in connection with the loss of angular momentum. So there may have been a chance for the formation of young systems from t_0 up to our time.

How to distinguish the stages of evolution? We will consider irregularity of shape and a high content of interstellar matter as indications of youth in a system. Irregularity indicates turbulence and must decay; even independently of our special model, we can conclude that an irregular shape cannot be a stable configuration in any system and there-

[16] Personal communication by Dr. Baade.

fore cannot be old in a time scale defined by the dimensions and inner velocities of the system.[17] Interstellar matter, on the other hand, can be converted into stars, while the opposite process will be rare; but here the time scale depends on details discussed in Section VIII. From these indications we conclude that irregular systems like the Magellanic Clouds are genetically the youngest systems, spirals are older (and probably the older, the "earlier" they are in Hubble's nomenclature), and elliptical nebulae are in a final stage which no longer shows the sort of evolution we consider here. We should keep in mind that the words "old" and "young" here always refer to the proper time scale of the system and that, of two systems of the same absolute age, the larger one will look "younger" today. So there is no objection to assuming that M 31 and its two companions are of the same absolute age, while the Magellanic Clouds must be definitely younger than our galaxy.

The most conspicuous semiregular pattern in galaxies to which we ascribe an intermediate stage in their evolution is spiral structure. We propose to explain it by the theory of Wilczynski and Brown,[18] adapted to the hydrodynamical model.

According to Baade,[19] spiral structure seems to be strictly connected with the appearance of dust. Even in the central part of M 31 some spiral structure is seen, not in the real distribution of the stars but as an absorbing cloud. It is improbable that large dust clouds should exist quite separately from gas (cf. Sec. II). So we take the presence of dust as an indication of the presence of gas. In fact, an increase in the density of dust by a factor of 10 would be much more conspicuous than a similar increase in the density of gas. So we conclude that spiral structure is produced by the interstellar gas. This view is strengthened by the fact that a spiral structure of the star distribution is conspicuous only in "young" stars.

We try to understand spiral structure as a hydrodynamical effect. Spirals are rotating and turbulent. Since they are flat, their turbulence is no longer the original one; it must be produced by nonuniform rotation. Every system, however, which is at the same time turbulent and nonuniformly rotating must, of necessity, show a spiral pattern. Every cloud formed by the turbulence will be distorted by the rotation into a segment of a spiral. This phenomenon is shown by milk put into a cup of coffee after stirring.

The main objection against the older versions of this theory probably was that the spiral arms should be wound many times around the nucleus, while actual spirals never wind more than two or three times. This difficulty no longer exists in the hydrodynamical theory, since turbulence dissolves the clouds as well as creates them, and the time scale for their dissolution is comparable to the period of rotation.

If the theory is correct, the arms should trail behind (move in the direction of their convex side), except if there are regions where the angular velocity increases with increasing distance from the center. Babcock's[20] measurements seem to indicate that such a region exists in M 31, while the spiral structure certainly does not change the direction of winding in that region. But Babcock's measurements certainly do not refer to the interstellar matter in that region, and additional observations may be needed.[21]

The abundance of systems with just two spiral arms is probably caused not by turbulence but by gravitation. In fact, for "late" spirals, which contain most interstellar matter and look most turbulent, the spiral structure, though conspicuous in all large clouds, cannot, in general, be described by the concept of two long, coherent arms. The number 2 is most evident in the least turbulent-looking systems like barred spirals. We may understand the bars as elongated equilibrium figures of rotation similar to Jacobi's

[17] H. Shapley, *Galaxies* (Philadelphia: Blakiston Co., 1943), pp. 216 ff.

[18] E. Z. Wilczynski, *Ap. J.*, **4**, 97, 1896; *A.J.*, **20**, 67, 1899; E. W. Brown, *Observatory*, **51**, 277, 1928.

[19] Private communication.

[20] *Lick Obs. Bull.*, **19**, 41, 1939.

[21] I am grateful to Dr. N. U. Mayall for an interesting discussion on this point.

liquid ellipsoids. In a rotating disk of circular symmetry, no gravitational energy can be gained by concentrating the mass toward the center, since the conservation of angular momentum prevents such a dislocation; but all the matter moving on the same circular orbit around the center can be moved toward two opposing single points on the circle without changing the angular momentum, but with a gain of gravitational energy. Hence a bar is a more stable structure than a disk. But the bar can be kinematically stable only if the system rotates uniformly. Uniform rotation presupposes a gravitational potential quadratic in the distance from the center. Hence it will be possible in the neighborhood of a potential minimum. This may explain the fact that barred spirals have bars near the center and spiral structure in the outer parts.

Regular spirals with two arms, according to this explanation, would be close enough to uniform rotation not to destroy the "bar" entirely but to distort it strongly.[22] Both in M 31 and in M 33 the easily visible spiral arms lie in regions where the rotation does not deviate strongly from uniformity. It is remarkable in M 31 that outside the nucleus (which has its own, higher angular velocity) there is another region of nearly uniform rotation. The fact that some barred spirals show a small spiral inside the nucleus (a "wheel inside the bar") raises the same problem even more clearly. A very special law of mass distribution is needed to achieve this effect, and it is not to be expected a priori that the system during its formation should assume this special mass distribution. The only explanation I can offer is that turbulent friction tends to establish a uniform rotation and that it may set up hydrodynamical currents achieving the necessary rearrangement of the masses.

Spiral structure as a turbulent pattern cannot last forever. Two final developments can be imagined. The interstellar matter can either be absorbed by the stars or be lost, together with an amount of angular momentum. According to the following sections, both events will happen, but probably with a preference for the loss into cosmic space. In any case a system consisting of stars alone will be the final stage. Such a system can preserve its internal motion for a time long compared with the age of the universe.

VIII. THE ORIGIN OF THE STARS

The distribution of stars and of interstellar matter gives us some indications about the possible processes of formation of the stars. We may use Baade's[23] two populations as a starting point of an empirical discussion. These populations were first distinguished by three criteria:

Physical parameters of the stars: Their H-R diagrams are different.

Spatial distribution: Population I is found in the disk of spirals, especially in the arms; population II in the nuclei of spirals, in elliptical nebulae, and in globular clusters.

Kinematical properties: In the neighborhood of our sun, population I prefers circular orbits, population II elliptical orbits.

There has been some discussion whether the two populations are sharply distinguished or whether they indicate extreme points of a continuous range of types. Baade maintains that they are sharply distinguished, but he partly separates the criteria, e.g., by saying that a large percentage of the stars in spiral disks belong to population II.[24] We cannot try to discuss these difficult observational questions here. To have a nomenclature that would not involve too many special assumptions, we propose to characterize every type of star by three numbers, x, y, and z. The first number should classify it according to its physical parameters, the second one according to its spatial position, and the third number should describe its kinematical properties. In this paper we shall only use integers for

[22] Dr. A. Schlüter is considering the possibility that spiral arms are stabilized by magnetic fields (private communication).

[23] *Ap. J.*, **100**, 137, 1944; *Mt. W. Contr.*, No. 696.

[24] Private communication.

x, y, z, leaving it to further discussion if some of them should rather be considered to vary within a continuous range of values.

With respect to physical parameters, we accept the distinction of two groups as defined by their color-luminosity diagrams. We write $1yz$ for Baade's population I, and $2yz$ for Baade's population II, as far as populations I and II are defined by the H-R diagram. But we want to give some emphasis to a subgroup of I by calling it $0yz$. These are the stars that can be seen by merely physical arguments to be young (or "rejuvenated"; cf. next section). For most of them several independent criteria of youth apply. The early types of the main sequence must be young because they exhaust their hydrogen rapidly. This criterion may even include the A stars in group $0yz$, if there is no mixing process of matter inside the stars.[25] The O and B stars of the main sequence and the supergiants are mostly connected with dust.[26] Just as in the preceding chapter, we shall assume the dust to be the tracer for the presence of gas. Then we may conclude that these stars, if any, have a chance of still acquiring large amounts of interstellar matter. Finally (cf. Sec. X), rotation seems to be a sign of youth in a star, and this property is confined to early main-sequence stars down to the early F stars.

We might ask if all $1yz$ stars are young, so that we might identify $0yz$ and $1yz$. But if the sun is a typical population I star, as Baade maintains, this population also contains old stars, since the sun cannot plausibly be assumed to be younger than the earth. So, if the sun is to be retained in group $1yz$, this group must be defined by other parameters than age, and $0yz$ is only a subgroup of population I. We do not try to solve this problem in this paper.

With respect to spatial distribution, the three areas of which Baade's group II is the only population seem to have something in common. According to our picture, elliptical nebulae are old spirals that have lost their spiral arms; so, in general, we will expect them to behave similarly to the nuclei. Globular clusters (and the few stars in the space between them) may be considered to form an extended "atmosphere" of the galactic center. Such an atmosphere may be a remnant of an original cloud, but, even if the original cloud had completely disappeared, a new atmosphere would probably have been formed. For the virial theorem postulates a high average velocity for the stars in the center, and in every reasonable statistical distribution this means that there must be some stars present which have enough energy to move very far away from the center.

We shall call all stars belonging to the "center plus atmosphere" or to an elliptical system, group $x2z$. Baade's empirical result is expressed by saying that for them always $x = z$. As long as we do not know exactly what the distinction between $1yz$ and $2yz$ means, we cannot deduce this result theoretically. But it seems understandable that no young stars of this type, i.e., no $02z$ stars, exist, since interstellar matter is very scarce in those regions of space today.

Besides the center plus atmosphere, spirals possess a flat disk of stars. We call the stars contained in this disk group $x1z$. According to Baade, there exist stars both of type $11z$ (e.g., the sun) and $21z$.

Inside the disk we can again distinguish as a subgroup the stars contained only in spiral arms; we shall call them group $x0z$. Empirically,[27] arms seem to be whiter than the rest of the disk. It seems possible that in this group always $x = 0$. That means that only young stars are confined to arms, as we should suppose if the arms are the concentrations of interstellar gas. Stars that accidentally occur within an arm but belong to a type which is also present in the rest of the disk should not be included in group $x0z$.

Kinematically, we may distinguish stars in circular orbits and stars in eccentric orbits: $xy1$ and $xy2$. It is probable that circular orbits are typical of disk stars, so in $xy1$

[25] This possibility was pointed out to the author by Dr. Chandrasekhar.

[26] Both Drs. Baade and Nassau kindly discussed the evidence with the author.

[27] C. K. Seyfert and J. J. Nassau, *Ap. J.*, **101**, 179, 1945.

we expect $y = 1$ or 0, while x may be 0, 1, or 2. For $xy2$ stars, $x = 0$, and probably even $x = 1$, seem to be excluded.

The concentration of disk stars toward the galactic plane is a criterion that is in some way coupled with kinematical properties. The more strictly circular the orbit is, the more concentrated toward the plane the stars seem to be. $00z$ stars are certainly the most concentrated ones, as O and B stars. These kinematical criteria are the ones which show the most continuous variation of the parameters.

We may summarize this analysis by mentioning the groups of stars we have found:

000: Young stars, moving in spiral arms and in circular orbits.
111: Population I, including old stars like our sun.
212: Population II in the disk. It is doubtful if also 211 stars exist.
222: Population II in the center plus atmosphere.

If we now try to apply the ideas of Section V to the formation of stars, we seem to encounter a paradox. The time scale for the formation of a cloud of stellar mass as defined by formula (5.3) is much shorter than the age of the galaxy. Choosing $l = 3 \cdot 10^{18}$ cm and $v = 10^5$ cm/sec, we get about $t = 5 \cdot 10^8$ years. If the formation of stars is possible at all today, it is not to be understood why there still should be as much interstellar matter present as we find in the surroundings of our sun. We are led to the suspicion that no formation of stars is possible today, except perhaps under conditions which generally are not fulfilled. This view is strengthened by the analysis of Section IX, which seems to show that the stars of group 000 are not, in general, newly formed but rather rejuvenated and that even this process of rejuvenation needs peculiar external conditions.

On the other hand, the stars are there, so the conditions for their formation must once have been better. What was the difference between then and now? We propose that it consisted in the fact that when the stars were formed there were no stars present. In other words, the presence of stars inhibits the formation of new stars. Consider a cloud of stellar mass before it has started to contract appreciably. It must be an equilibrium between gravitation and gas pressure if it is stable at all. It can contract further only if it can radiate away part of its thermal energy. This is probably possible if no stars are in the neighborhood. If stars are present, however, they will maintain the temperature of the cloud by their radiation as long as it is still transparent to their light, and so the contraction cannot start. In fact, we know that the interstellar matter in our surroundings is kept at a temperature of at least 50° K by the stars,[4] and at these temperatures clouds of stellar mass and a density smaller than about 10^{-18} gm/cm^3 are not dynamically stable at all but will expand.

What, then, do we know about the conditions under which the formation of stars began? We have empirical indications that at least the stars of group $x1z$ (stars in the disk) were formed after the decay of the initial turbulence or in its last phase. Else they would not now be concentrated in the galactic plane. For stars, once formed, no longer suffer turbulent friction, and therefore a system of stars should approximately retain its kinematic structure and hence the general characteristics of its shape as they were at the time of the formation of the stars. Thus globular clusters seem to have formed their stars before much of their turbulence decayed, while the opposite conclusion applies to the galaxy.

If clouds are formed inside a galaxy by a compressible turbulence caused by rotation, they cannot be expected to be gravitationally stable from the outset. The galaxy as a whole is just in such an equilibrium between gravitational and centrifugal forces. For smaller clouds the gravitational energy decreases more rapidly with decreasing size than the kinetic energy of their internal turbulence (cf. Sec. VI). But the smallest clouds can dissipate energy by their internal incompressible turbulence. The time scales of this dissipation and of the expansion of the cloud caused by the same internal turbulence and by temperature are of the same order of magnitude, both being determined by the same val-

ues of v and l. The dissipation will be especially high in the moment of the collision of two such clouds under a still supersonic relative velocity. Therefore, the smallest clouds have a good chance of becoming gravitationally stable if they are able to radiate away the heat produced. If they can cool down to the temperature T, we would expect their total mass to be given by Jeans's condition, which can be written:

$$M = \left(\frac{KT}{G}\right)^{3/2} \rho^{-1/2}. \tag{8.1}$$

As a function of ρ and T, Table 2 gives M, roughly estimated. The real star masses lie in the region between 0°.2 and 5° for $\rho = 10^{-23}$ and between 1° and 10° for $\rho = 10^{-21}$.

We do not attempt to estimate the temperature to which the clouds really can be cooled down. Hence two possibilities must be considered: either the clouds will reach temperatures as required—say, a few degrees—or they stay at a higher temperature.

TABLE 2

MASS OF SMALLEST CLOUDS

ρ (Gm/Cm³)	T			
	100° K	10° K	1° K	0°.1 K
10^{-23}	10^{37} gm	$10^{35.5}$ gm	10^{34} gm	$10^{32.5}$ gm
10^{-21}	10^{36} gm	$10^{34.5}$ gm	10^{33} gm	$10^{31.5}$ gm

In the first case the temperature reached seems to determine the average mass of the stars. In the second case a secondary effect must have been active, reducing the masses of the stars to the values observed today. Radiation pressure may have been such an effect, since we know that for the highest known star masses the radiation pressure at the surface is strong enough to blow away the upper layers of the atmosphere. This, however, would lead to the unpleasant result that the larger part of the cloud's mass would not be kept in the star but would become interstellar matter again. Since we assume that existing stars prohibit the formation of new stars, we would be left with more interstellar matter than is actually observed.

Observational facts seem to indicate a compromise. Empirically, we do not find appreciable amounts of interstellar matter in the regions of pure group 222, which always are regions of high density. If we assume that in regions both of high and of low density the same temperature of a few degrees was reached, this would lead to the formation of stars of about solar mass in the regions of high density but to stars of about ten times that mass in the regions of low density. Therefore, only in the regions of low density did radiation pressure have a good chance to return a part of the mass into interstellar space.

It should not be forgotten, however, that the hydrodynamical process connected with the loss of angular momentum also carries matter back into cosmic space. A more detailed theory will be needed to describe these processes.

IX. "YOUNG" STARS

The stars of group 000 either can have been formed as entirely new individuals or can be older stars which were rejuvenated by the accretion of interstellar matter.

The only possible mechanism which could lead to the recent formation of new stars seems to be the one proposed by Spitzer and Whipple.[4, 5] They assume the formation of clouds consisting mainly of dust which is brought together by a "quasi-gravitational" action of radiation pressure. We shall not try here to find out whether such conditions

can exist. Every star, be it formed recently or at an earlier time, may have a chance of growing by the accretion process. We shall discuss this problem without deciding how the original star was formed.

Hoyle and Lyttleton[28] have proposed a mechanism for the accretion of interstellar matter by stars. We shall rediscuss the question under hydrodynamical aspects. Consider a star of mass M and a small volume of interstellar matter of density ρ, which, if following a straight path of inertial motion, would pass the star at a smallest distance r with the velocity v. The total duration of the encounter is roughly

$$\tau = \frac{r}{v}. \tag{9.1}$$

The force exerted on the gas by the star is

$$f = \frac{GM\rho}{r^2}. \tag{9.2}$$

The total momentum transferred by this force is approximately

$$p = f\tau = \frac{GM\rho}{rv}. \tag{9.3}$$

This momentum is equal to the original momentum ρv at a distance

$$r_0 = \frac{GM}{v^2}. \tag{9.4}$$

Particles hitting an area of the order of magnitude r_0^2 are therefore deflected by a large angle.

Now we introduce the ideas of hydrodynamics. In general, r_0 is larger than the mean free path of gas particles. Accordingly, we assume that all matter entering a sphere of radius r_0 will be maintained as a turbulent cloud surrounding the star. The turbulent friction causes a loss of kinetic energy, by which at least a part of the matter in this sphere is forced to stay in the gravitational field of the star, and so in the end to be united with the star. The total mass inside the sphere is roughly $r_0^3\rho$, and it is replenished in the time $\tau(r_0)$. Thus the increase of the star's mass per unit time is

$$\frac{\partial M}{\partial t} = \gamma r_0^3 \rho \frac{v}{r_0} = \gamma \rho r_0^2 v = \gamma \frac{G^2M^2\rho}{v^3}, \tag{9.5}$$

where γ is a numerical constant probably not much smaller than unity. This is the formula of Hoyle and Lyttleton. A high initial mass of the star and a small relative velocity between the star and the cloud favor a rapid increase of the mass. But both quantities must be close to the acceptable limits, in order to give an appreciable effect in "historic" times. The solution of equation (9.4) is

$$M = \frac{v^3}{\gamma G^2 \rho (t_1 - t)}. \tag{9.6}$$

Thus, for the finite time $t = t_1$, M would diverge. Before that moment several of our approximations (e.g., ρ = Const., v = Const.) would break down, but t_1 may be used to measure the time scale of the increase of the star's mass. If M_0 is the initial mass,

$$t_1 = \frac{v^3}{\gamma G^2 \rho M_0}. \tag{9.7}$$

[28] *Proc. Cambridge Phil. Soc.*, **35**, 405, 592, 1939.

The value of t_1 is given in Table 3 for $\rho = 10^{-23}$ and different M_0 and v. We see that only very small velocities, together with a mass about ten times that of the sun, give reasonably short time scales. In very dense clouds the times are somewhat shorter. But, in general, we would conclude that only a star which starts with a mass larger than that of the sun and which stays inside a very quiet cloud for more than 10^7 years has a chance of increasing its mass considerably. For $M = 2 \cdot 10^{34}$ gm, $\rho = 10^{-23}$ gm/cm^3, and $v = 10^4$ cm/sec, we get roughly $r_0 = 10^{19}$ cm = 3psc, a rather large feeding volume.

TABLE 3

TIME SCALE t_1 FOR THE INCREASE OF A STAR MASS FROM THE INITIAL VALUE M_0, ASSUMING $\rho = 10^{-23}$ GM/CM^3 AND DIFFERENT VALUES FOR v

v (CM/SEC)	M_0 (GM)		
	$2 \cdot 10^{32}$	$2 \cdot 10^{33}$	$2 \cdot 10^{34}$
10^4	$3 \cdot 10^9$ years	$3 \cdot 10^8$ years	$3 \cdot 10^7$ years
$3 \cdot 10^4$	10^{11} years	10^{10} years	10^9 years

X. ROTATION, PLANETARY SYSTEMS, AND DOUBLE STARS

If a star originates or is rejuvenated in one of the ways described above, it must rotate. If we assume $r_0 = 10^{18}$ cm and $v = 10^4$ cm/sec, a resultant average rotational velocity of the original cloud of 10^3 cm/sec may be a conservative estimate. By contraction to a final radius of 10^{11} cm, the conservation of angular momentum would lead to a rotational velocity of the star of 10^{10} cm/sec = 10^5 km/sec, while $5 \cdot 10^2$ km/sec is the limit of stability. Even if most of the angular momentum is carried away, the stars must originate rotating.

This mechanism provides a rotating disk of gas around an originating star as was supposed in the author's work on the origin of planets.[29] Yet still another mechanism for the formation of such a gaseous disk can have existed, connected with the loss of rotation by the stars. We shall try to describe this second mechanism without deciding in which phase of the evolution of the sun our solar system was built.

In discussing the rotation, we will consider only main-sequence stars. Giants, except for very early supergiants,[30] do not show any rotation. This is not very surprising. Their radii are so large that any large rotational velocity would destroy the star by its centrifugal force. White dwarfs, on the other hand, can uphold a high rotational velocity with a small angular momentum, comparable to that of our sun, and so we should not be surprised if we should, as a rule, find them rotating. For main-sequence stars, however, the distinction between rotating and nonrotating stars must be genetically significant. Visible rotation for them is empirically limited to the types which also for other reasons must be considered to be "young" stars. Not all stars of those types rotate, it is true. On the other hand, no stars of other types (except binaries) rotate with a measurable velocity.

We conclude that there must be a mechanism by which stars can lose their angular momentum. Ter Haar[31] has pointed out that the mechanism connected with the dissolu-

[29] *Zs. f. Ap.*, 22, 319, 1943.

[30] This exception was mentioned to the author by Dr. Nassau.

[31] *Ap. J.*, 110, 321, 1949.

tion of an original gas cloud around the sun will not suffice. Probably the magnetic coupling first considered by Alfvén[32] will be a working mechanism. Such a coupling would carry an ionized cloud around the sun like a rigid body. This can be true only up to a distance from the sun at which the period of a planetary orbit around the sun is equal to the sun's rotational period. Probably beyond that distance hydrodynamical transport mechanism must take its place. Calculations about this problem are now being carried out at the Max Planck Institut für Physik.

Lüst[15] has shown that there exist solutions of the hydrodynamical equations with turbulent friction in which a rotating disk of finite mass carries an infinite angular momentum from the center toward infinity. These solutions presuppose a boundary condition expressing a stationary transfer of angular momentum from the central body to the innermost part of the disk. This boundary condition may schematically describe the effect of Alfvén's mechanism. If the total angular momentum transferred is finite, the disk will not directly disappear into infinity but will be extended into a distance from the central body corresponding to the angular momentum transferred. From there on, the disk will develop and in the end dissolve, according to solutions without a momentum transfer at the center. The distance to which a disk is carried can be estimated as follows: The angular momentum of a body revolving around the sun at a distance r, according to Kepler's third law, is proportional to $r^{1/2}$. If the sun originally rotated with a velocity close to the stability limit and if the fraction f of the sun's mass had to carry this angular momentum from the sun's surface to a distance r, then r will be f^{-2} times the sun's radius. For $f = \frac{1}{10}$, this would be approximately the radius of the orbit of the earth. So the disk required by the theory of the origin of the planets can be formed in this way too.

Here I want to point out what other parts of my paper on the origin of the planets ought to be changed or modified in the light of new information. The regular system of vortices drawn there now seems to me to be too particular a description of a more general consequence of the theory of turbulence. Tuominen[33] has pointed out that Bode's law can formally be derived from Prandtl's rule that the average eddy size is proportional to the distance from the wall, the sun in this case being the wall. This, however, would in itself give only an average rule for the location of eddies and not a well-defined sequence of distances at which planets must originate. Such a sequence is given by Kuiper's new theory.[34] In this theory the gravitational action of the disk on itself is considered, and it is assumed that it forms "protoplanets," within which the later planet is built up while the protoplanet in the end is dissolved again.

The growth of planets out of small bodies which are themselves formed by chemical forces must take place inside the protoplanets as well, as was considered in the original picture. The absence of the rare gases on the earth is a clear indication of this "cold" formation of the earth. This fact and the later heating-up of the earth have been considered in detail by Urey and H. Brown.[35]

For the formation of double stars, two ways seem still to be open, and perhaps both of them are used: the immediate formation of two centers in an original rotating cloud or the growth of a planet or a protoplanet to the size of a full, stable companion. Whether double stars could ever be formed by the breakup of a single star seems very doubtful now, and I want explicitly to revoke my tentative hypothesis connecting supernovae with such an event.

[32] *Ark. f. mat., astr. och fysik*, Vol. **28A**, No. 6, 1942.

[33] *Ann. d'ap.*, **10**, 179, 1947.

[34] I am extremely grateful to Dr. Kuiper for the opportunity to see his paper before publication and for many discussions.

[35] H. Urey, to be published; H. Brown, *Ap. J.*, 111, 641, 1950. I am very grateful to Drs. Urey and Brown for many interesting discussions.

XI. GIANTS AND WHITE DWARFS

That white dwarfs are stars which have exhausted their hydrogen now seems generally accepted. No satisfactory model, however, seems yet to have been given for giants in general. We shall use the name "giants" here for all stars right on and above the main sequence. There are giants in group 222. Hence giants can be old stars. It is therefore necessary to find a model for at least some giants that will provide an energy source which will outlast nuclear energy sources. The only sufficient source known in the physics of today is gravitation. Enough gravitational energy can be available only if the giant contains a highly condensed core.[36]

This idea puts the giants in one family with the white dwarfs. It would not exclude the possibility that some giants (especially subgiants) still produce energy by nuclear reactions outside an isothermal core.[37] But this certainly cannot be the theory of highly luminous old giants, because the nuclear energy would not suffice for them. The difference between giants and white dwarfs must then be that giants are above Chandrasekhar's[38] limiting mass and therefore have ample energy resources in their contraction toward a density comparable to the density in the atomic nucleus. The theory proposed here would assume that luminous giants are not in a final state but that their core is still contracting and thus liberating energy.

The main objection to this picture is that stationary models of such stars are always very small and dense, lacking the large atmosphere which would be seen as a giant star from outside. Yet such small stars cannot be stable at their surface if they are highly luminous. The radiation pressure must drive the atmosphere outward. If there are no stationary solutions for stars with such extended atmospheres, the real solutions must be nonstationary, with an atmosphere moving slowly but steadily outward (or containing other systematic motions). A planetary nebula would then be a special type of giant in which the atmosphere happens to be transparent to visible light. As far as I know, no calculations for such models have as yet been made.

It can be asked what determines the rate of release of gravitational energy from the contracting core. Perhaps it is given by the rate of loss of the angular momentum remaining in the core. It is not sure a priori how far a mass-luminosity relation can be expected for such models.

For the stars of group 111 this would lead to the conclusion that the B-type supergiants are a later stage of evolution than the B-type main-sequence stars. But, since evolution at such luminosities is rapid, they can still be young stars on an absolute-time scale.

[36] P. Jordan, *Die Herkunft der Sterne* (1947), pp. 38 ff.

[37] R. S. Richardson and M. Schwarzschild, *Ap. J.*, **108**, 373, 1948; G. Gamow and E. Teller, *Phys. Rev.*, **55**, 791, 1939; G. Gamow and G. Keller, *Rev. Mod. Phys.*, **17**, 125, 1945; G. Gamow, *Phys. Rev.*, **67**, 120, 1945; A. Reiz, *Ann d'ap.*, **10**, 301, 1947.

[38] *M.N.*, **95**, 207, 226, 676, 1935; *An Introduction to the Study of Stellar Structure* (Chicago: University of Chicago Press, 1939).

A THEORY OF INTERSTELLAR POLARIZATION*

LYMAN SPITZER, JR., AND JOHN W. TUKEY
Princeton University
Received November 20, 1950

ABSTRACT

A detailed analysis is given of the polarization of starlight produced by ferromagnetic grains, oriented by an interstellar magnetic field. Lack of information on the optical properties of large elongated grains with a high refractive index prevents a consideration of grains with a circumference very much bigger than 8000 A, the longest wave length at which polarization measures have been made. Grains of about this size, with a mean radius of 1.3×10^{-5} cm and composed primarily of *Fe*, *Mg*, and their compounds, are shown to arise from collisions between ordinary grains, containing predominantly H_2O, NH_3, and CH_4. It is estimated that one out of every four grains is compound, with a shell of ices surrounding a dense nucleus of this sort. It is quite possible that such nuclei will be ferromagnetic; if so, they will all be highly magnetized single domains. However, a magnetic field of about 2×10^{-3} gauss is apparently required to orient these grains sufficiently to explain the observed polarization.

Larger grains, which could be oriented by weaker fields, might form in two ways. First, the individual nuclei might stick together, forming long rods; this process will take place at an appreciable rate only if most of the grains occur in concentrations in which the density is one or two orders of magnitude greater than the assumed average cloud density. Second, successive collisions between compound nuclei and other grains would be expected to produce some ferromagnetic grains with relatively large radii. Since the optical properties of such large grains are unknown, whether or not they could explain the observed polarization is uncertain.

The polarization of light from distant stars, found by Hiltner[1] and Hall,[2] is perhaps one of the most unexpected discoveries of modern astrophysics. The observations indicate that light from distant stars is polarized only if the stars are reddened and that the effect is independent of the physical properties of the stars. More recent evidence[3, 4] supports these indications. It seems reasonable to infer that the solid particles or grains producing the interstellar extinction are somehow responsible for the polarization. If the grains were elongated and also oriented by some force, the observational results could be explained.

A magnetic field provides an evident force which might orient grains. In view of the very long relaxation time for galactic magnetic fields, any field present in the galaxy during its formation would presumably still be present. Moreover, magnetic fields can be produced by turbulence of the interstellar gas, as suggested by Fermi.[5] According to this mechanism, turbulence in an extended, electrically conducting medium will increase the magnetic induction B until equipartition of energy is established between the magnetic energy density, $B^2/8\pi$, and the density of kinetic energy, $\frac{1}{2}\rho v^2$. An average interstellar density of one H atom per cubic centimeter, and a root-mean-square cloud velocity of 22.5 km/sec, the value adopted by Oort and van de Hulst,[6] yield a value of 1.0×10^{-5} gauss for B. A more detailed hydrodynamic theory by Batchelor[7] shows that isotropic

* This work was supported in part by a contract with the Office of Naval Research.

[1] *Science*, **109**, 165, 1949; *Nature*, **163**, 283, 1949.

[2] *Science*, **109**, 166, 1949.

[3] W. A. Hiltner, *Ap. J.*, **109**, 471, 1949.

[4] J. S. Hall and A. H. Mikesell, *A.J.*, **54**, 187, 1949.

[5] *Phys. Rev.*, **75**, 1169, 1949. The relevance of these fields to the polarization problem was first pointed out by Hiltner (*Ap. J.*, **109**, 471, 1949).

[6] *B.A.N.*, **10**, No. 376, 187, 1946.

[7] Paper presented at the Paris conference on "Problems of Motions of Gaseous Masses of Cosmical Dimensions," August, 1949 (*Proc. R. Soc. London, A*, **201**, 405, 1949).

turbulence in a highly conducting and homogeneous medium will, in fact, lead to rapid equipartition between kinetic and magnetic energy densities, although the magnetic fields deduced are somewhat less than 10^{-5} gauss. Similar conclusions have been reached by Schlüter and Biermann.[8] Hence a magnetic field of 10^{-5} gauss in interstellar space is at least a very plausible assumption. On this basis the attempt to interpret the polarization observations reduces to the explanation of why the grains are elongated and how they are oriented by this magnetic force.

At the present time, at least two theories for the orientation of the grains have been advanced. One, by the present authors,[9] assumes that at least a small percentage of the grains are ferromagnetic; the high permanent magnetization of small ferromagnetic particles would then account for their orientation. Another theory, by Davis and Greenstein,[10] relies on paramagnetic relaxation to orient rapidly rotating grains. This theory represents a substantially modified version of one published earlier by these same authors.[11] The present paper is devoted to a detailed exposition of the theory based on ferromagnetic grains. No detailed attempt is made to compare the predictions of these two theories, and it is possible that no final decision can be made between them at the present time.

The first section below summarizes the observational data on interstellar polarization. Section II discusses the theory of extinction by a small elongated particle, while Section III analyzes the polarization produced by many grains, partially oriented by a magnetic field. Section IV discusses collisions between grains and the nature and density of the ferromagnetic grains which may be formed by these collisions. Comparison between theory and observation is presented in Section V.

I. OBSERVATIONAL DATA

a) CORRELATION BETWEEN p AND E_1

A plot of observed values of the polarization against the values of the color excess E_1 measured by Stebbins, Huffer, and Whitford[12] is given by Hall.[2] Table 1 shows a summary of more extensive observations obtained more recently by Hall and Mikesell.[13]

TABLE 1

OBSERVED AVERAGE PERCENTAGE POLARIZATION

Galactic Longitudes	Color Excess E_1					
	0.00	0.10	0.20	0.30	0.40	0.50
10°–59°	0.23	0.98	1.15	1.31	.....	2.58
60–79	0.18	1.54	1.21	2.54	2.66	.....
80–120	0.46	2.32	2.83	3.45	3.53	.....
130–170	0.08	.....	1.98	1.94	.....	.....
320–360	0.23	1.01	1.23	1.14	1.93	2.25
Averages for all stars:						
Polarization	0.28	1.43	1.75	2.44	2.58	2.71
Color excess	−0.01	+0.11	+0.19	+0.29	+0.38	+0.50
No. of stars	39	55	164	73	26	12

[8] *Zs. f. Naturforsch.*, **5a**, 237, 1950.

[9] L. Spitzer, Jr., and J. W. Tukey, *Science*, **109**, 461, 1949.

[10] *Ap. J.*, **114**, 206, 1951.

[11] *Phys. Rev.*, **75**, 1065, 1949.

[12] *Ap. J.*, **91**, 20, 1940.

[13] *Pub. U.S. Naval Obs.*, Vol. **17**, Part I, 1950. We are much indebted to Dr. Hall for communicating these results to us in advance of publication.

The stars are arranged by galactic longitudes and by intervals of 0.10 (centered at 0.00, 0.10, etc.) in E_1; mean values of the polarization, p, are given for all the stars in each group. No values are given for groups containing less than four stars.

Two conclusions are apparent from these data. In the first place, the polarization is very small when E_1 is less than 0.05. Oort[14] has shown that the zero point of the photoelectric color excesses for early B stars requires a correction of at least -0.02 and possibly as great as -0.05. The observations are certainly consistent with the belief that p vanishes when there is no selective extinction. In the second place, in each region the polarization tends to increase with E_1. The ratio of p to E_1 varies on the average, however, from 0.095 for low E_1 to 0.050 for high E_1, provided that a zero-point correction of -0.04 is adopted for the color excesses. Some tendency for the ratio p/E_1 to decrease with increasing E_1 may be expected theoretically. However, some of this observed trend may result from the combined effect of observational selection and variations in the properties of clouds. We therefore represent the observational data by the approximate mean relation,

$$p = 0.08E_1 . \tag{1}$$

b) ORIENTATION OF PLANE OF POLARIZATION

The distance over which the plane of polarization is unchanged in direction should give an indication of the scale of the magnetic fields which are presumably orienting the interstellar grains. A plot showing the direction of the plane of polarization (plane containing the magnetic vector) for all stars measured has been given by Hall and Mikesell.[4] It is evident from this diagram that these directions mostly lie within 45° of the normal to the galactic plane. Moreover, deviations from the normal seem highly correlated with one another over separations of about 30°. Apparently, the orienting force may be analyzed into components which include a uniform component and a varying component with a normal scale of some 100 or 200 parsecs, the distance subtended by 30° at the probable distance of 200–400 parsecs for most of the clouds measured.

c) VARIATION OF p WITH WAVE LENGTH

Measures of polarization at different wave lengths are not, as yet, very extensive. Hall[2] reports no significant change in percentage polarization between 3700 and 6200 A; a change as great as 25 per cent of p would not be excluded by these observations, however. Observations at λλ 4200, 5500, and 8000 have been obtained for two stars by Hiltner.[15] For one star these observations seem to exclude a change as great as 10 per cent of p as the wave length varies from 4200 to 8000 A. For the other star, the polarization at λ 8000 is about 80 per cent of its values at λ 4200 and λ 5500. Apparently, the relative change of p with wave length is different for different stars, with changes ranging from less than 0.1 to about 0.3 times the change to be expected if p were proportional to the extinction. Additional observations along this line are very desirable and may be expected to throw much light on the whole problem.

II. EXTINCTION CROSS-SECTION OF A SINGLE GRAIN

a) SMALL PROLATE SPHEROIDS

The absorption and scattering of light by spheroids, small compared to the wave length, have been analyzed by Gans.[16] We shall let σ_T be the extinction cross-section for radiation whose electric vector is perpendicular (or transverse) to the spheroid's axis,

[14] *B.A.N.*, **8**, No. 308, 233, 1938.

[15] W. A. Hiltner, *Phys. Rev.*, **78**, 170, 1950. We are much indebted to Dr. Hiltner for communicating these results to us in advance of publication.

[16] *Ann. d. Phys.*, **37**, 881, 1912.

and σ_A or $\sigma_T(1+R)$ the extinction cross-section for radiation whose electric vector is parallel to this axis. Then Gans's results indicate that

$$1+R=\frac{|1+(m^2-1)P'/4\pi|^2}{|1+(m^2-1)P/4\pi|^2}, \tag{2}$$

where m is the index of refraction of the spheroid (here assumed in a vacuum) and where, for a prolate spheroid, the depolarization factors P and P' are given by the equations

$$\frac{P}{4\pi}=\frac{1-e^2}{e^2}\left\{\frac{1}{2e}\log\frac{1+e}{1-e}-1\right\}, \tag{3}$$

$$\frac{P}{4\pi}+2\,\frac{P'}{4\pi}=1, \tag{4}$$

where the quantity e is the eccentricity of the ellipse generating the spheroid. Evidently, if x is the ratio of the major to the minor axis of the ellipsoid, then

$$e^2=1-\frac{1}{x^2}. \tag{5}$$

Values of R for different values of m and x are given in Table 2; only real indices of

TABLE 2

RATIO $1+R$ OF EXTINCTIONS FOR TWO STATES OF POLARIZATION

RATIO OF AXES x	INDEX OF REFRACTION						
	1.1	1.2	1.4	1.7	2.0	2.5	3.0
1.1	1.015	1.029	1.057	1.092	1.121	1.158	1.182
1.2	1.025	1.050	1.097	1.159	1.200	1.278	1.325
1.5	1.065	1.132	1.268	1.466	1.647	1.902	2.098
2.0	1.100	1.205	1.433	1.799	2.141	2.751	3.250
3.0	1.143	1.303	1.671	2.336	3.106	4.521	5.962
5.0	1.180	1.389	1.902	2.930	4.283	7.238	10.90
10.0	1.206	1.452	2.080	3.440	5.419	10.42	17.91
∞	1.221	1.488	2.190	3.783	6.250	13.14	25.00

refraction are considered. Evidently, for spheroids of low eccentricity and with an index of refraction near unity, R does not differ much from unity. In this region we have the simple approximation

$$R=\tfrac{8}{5}(x-1)\,|\,m-1\,|, \qquad \begin{matrix}\text{for } |\,m-1\,| \ll 1\,,\\ \text{and } (x-1)\ll 1\,.\end{matrix} \tag{6}$$

As x approaches infinity, with m finite, the denominator of equation (2) approaches 1, while $P'/4\pi$ becomes equal to $\frac{1}{2}$; hence we have

$$R=\tfrac{1}{4}\,|\,m^2+1\,|^2-1\,, \qquad \text{for } x\gg 1\,. \tag{7}$$

Values from equation (7) are given in the bottom line of Table 2.

b) GRAINS OF ARBITRARY SIZE AND SHAPE

For small grains of arbitrary shape certain general results can be given. As long as all dimensions are small compared with the wave length, the extinction will depend only on the orientation of the grain with respect to the electric vector and not on the orientation with respect to the direction of propagation. If the incident electrical field is a vector $\boldsymbol{E}$, then at great distance r the electrical vector in the scattered wave will be a vector $f(r)\Psi \cdot \boldsymbol{E}$, where $f(r)$ is a function of position and Ψ is a dyadic. This dyadic can be diagonalized, and the extinction cross-sections for radiation polarized along the three principal axes set equal to σ_1, σ_2, and σ_3. If the electric vector of the radiation has direction cosines l, m, and n along the three principal axes, then clearly the extinction coefficient $\sigma(l, m, n)$ is given by

$$\sigma(l, m, n) = \sigma_1 l^2 + \sigma_2 m^2 + \sigma_3 n^2 . \tag{8}$$

If two of the cross-sections—say, σ_2 and σ_3—are equal, the grain is uniaxial (at this frequency) and is optically indistinguishable from a spheroid. In the present theory, only uniaxial grains need be considered, since, when any grain is rotated about its magnetic axis, the resultant average cross-sections are those of a uniaxial grain; as will be shown below, it is only these average cross-sections that are needed.

When a grain has dimensions comparable to or greater than a wave length, these results may require modification. In particular, the extinction cross-section will then depend on the orientation of the grain with respect to the wave front, as well as with respect to the electric vector. For a fixed orientation with respect to the wave front, two principal axes, A and B, both in the plane of the wave front, can be defined as before, and we have

$$\sigma(l, m) = \sigma_A l^2 + \sigma_B m^2 , \tag{9}$$

where l and m are now the direction cosines of the electric vector with respect to the axes A and B. For a small uniaxial grain, one of these axes—say, the A-axis—will be the projection of the grain axis on the plane of the wave front, and we may write

$$\sigma_A = \sigma_T (1 + R \sin^2 \gamma) , \tag{10}$$

$$\sigma_B = \sigma_T , \tag{11}$$

where γ is the angle between the grain axis and the direction of propagation. For a grain of arbitrary size, equations (10) and (11) are still applicable, provided that the grain is uniaxial, but the quantities R and σ_T may depend on γ.

Unfortunately, precise values of R and σ_T for large, elongated particles are not available. It is evident physically that, when the dimensions of a grain approach $\lambda/2\pi$, the value of σ_T will approach roughly the geometrical cross-section. The value of R is more difficult to estimate, and the Gans theory can presumably not be applied when $R\sigma_T$ much exceeds the geometrical cross-section. Computations for infinite cylinders with refractive indices of 1.50 and 1.25 have been carried out by van de Hulst;[17] but no computations are presently available for the larger refractive indices of interest in the present paper. In subsequent numerical work we shall set R equal to unity for particles whose axial ratio is about 2 and whose minor axes are about equal to $\lambda/2\pi$. This value, about half the predictions obtained from the Gans theory, for an index of refraction between 2.5 and 3, seems relatively conservative.

[17] *Ap. J.*, 112, 1, 1950.

III. POLARIZATION BY MANY GRAINS

We consider an assembly of grains in kinetic equilibrium at some temperature T and subject to an external magnetic field $\boldsymbol{B}$. The extinction produced by this assembly for light polarized in a particular plane may be computed if the properties of the individual grains and of the magnetic field $\boldsymbol{B}$ are known. We first treat a set of small, identical, uniaxial grains in a uniform magnetic field, discussing later the more general cases.

a) IDENTICAL UNIAXIAL GRAINS IN A UNIFORM FIELD

Each grain is assumed to have uniform permanent magnetization I parallel to the principal axis. Since the grains are considered uniaxial, σ_2 will equal σ_3, and we may use the notation developed for a prolate spheroid, with $(1 + R)\sigma_T$ and σ_T representing σ_1 and σ_2, respectively.

The orientation of the grains in a magnetic field $\boldsymbol{B}$ may be found from the usual Langevin formula. It is evident, from the assumption of kinetic equilibrium, that $F(\theta)d\theta$, the fraction of grains with their major axes inclined at an angle between θ and $\theta + d\theta$ to the magnetic field, will be given by the expression

$$F(\theta) = K \sin \theta e^{-U(\theta)/kT}, \tag{12}$$

where K is a normalization factor chosen so that the integral of $F(\theta)d\theta$ from 0 to π is unity. The factor $\sin \theta d\theta$ is proportional to $d\omega$, the element of solid angle. The potential energy $U(\theta)$ of a body with volume V and uniform magnetization I, when placed in a uniform magnetic field, is given by

$$U(\theta) = -IBV \cos \theta, \tag{13}$$

independent of the body's shape. With this substitution, equation (12) becomes

$$F(\theta) = \frac{g \sin \theta e^{-g \cos \theta}}{2 \sinh g}, \tag{14}$$

where

$$g = \frac{IBV}{kT}. \tag{15}$$

The computation of the extinction produced by grains oriented according to equation (14) is straightforward. Figure 1 shows the geometry of the situation. The z-axis is chosen along the direction of propagation. The magnetic field $\boldsymbol{B}$ is inclined at an angle ϕ to the z-axis, and the x-axis is chosen to lie in the plane defined by $\boldsymbol{B}$ and the z-axis. The plane containing the electric vector and the direction of propagation will here be called the "plane of vibration." The orientation of this plane differs by 90° from the orientation of the plane of polarization used by Hall. We let σ_x designate the extinction cross-section of a grain for radiation with the plane of vibration parallel to the xz-plane (electric vector parallel to the x-axis), and σ_y the corresponding cross-section for radiation with the plane of vibration parallel to the yz-plane (electric vector parallel to the y-axis). We compute the mean values of σ_x and σ_y for a single grain, averaged over all orientations.

Let the vector q denote the direction of the major axis of the grain. Also, let α and β be the angles made by q with the x- and y-axis, respectively; then the direction cosines l_x and l_y for the two electric vectors relative to the major axis of the grain are $\cos \alpha$ and $\cos \beta$, respectively. Under these conditions, equations (9), (10), and (11) give, after some reduction,

$$\sigma_x = \sigma_T + \sigma_T R \cos^2 \alpha, \tag{16}$$

$$\sigma_y = \sigma_T + \sigma_T R \cos^2 \beta . \tag{17}$$

The form of these equations also follows immediately from equation (8). From spherical trigonometry, cos α and cos β may be expressed as functions of θ, ϕ, ϵ_1, and ϵ_2, where ϵ_1 is the angle between the qB-plane and the xBz-plane, while ϵ_2 is the corresponding angle between the qB- and the By-plane. The appropriate relations are

$$\cos \alpha = \cos\theta \sin \phi + \sin\theta \cos \phi \cos \epsilon_1 , \tag{18}$$

$$\cos \beta = \sin\theta \cos \epsilon_2 . \tag{19}$$

To determine mean values of σ_x and σ_y, denoted by S_x and S_y, we must average equations (16) and (17) over all θ, with $F(\theta)$ in equation (14) as a weighting factor. If equations (18) and (19) are inserted into equations (16) and (17), the cross-product term averages to zero, the integrations can be carried out directly, and we have

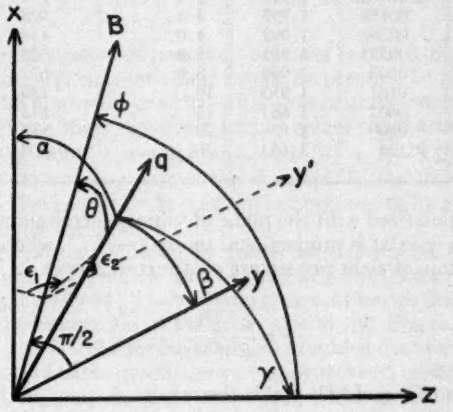

FIG. 1.—Orientation of grain axis q and magnetic field B

$$S_x = \sigma_T + R\sigma_T \left\{ \sin^2 \phi \left(1 + \frac{2}{g^2} - \frac{2}{g} \coth g \right) + \cos^2 \phi \left(\frac{\coth g}{g} - \frac{1}{g^2} \right) \right\}, \tag{20}$$

$$S_y = \sigma_T + R\sigma_T \left(\frac{\coth g}{g} - \frac{1}{g^2} \right). \tag{21}$$

Thus for the difference of the two extinctions we may write

$$S_x - S_y = R\sigma_T M(g) \sin^2 \phi , \tag{22}$$

where we define

$$M(g) = 1 + \frac{3}{g^2} - \frac{3 \coth g}{g} . \tag{23}$$

The function $M(g)$ has the following developments:

$$M(g) = \begin{cases} 1 - \dfrac{3}{g} + \dfrac{3}{g^2} & g > 3 , \\ \frac{1}{15} g^2 - \frac{2}{315} g^4 & g < 1 , \end{cases} \tag{24}$$

accurate to better than 1 per cent within the ranges indicated. Values of $M(g)$ are listed in Table 3. The values of $d \log M/d \log g$, which are also given, will indicate the extent to which $M(g)$ varies as g^2.

The resultant polarization follows at once from these results. The transmitted in-

TABLE 3

VALUES OF $M(g)$

$g=IBV/kT$	$M(g)$	$(dM/dg)\times g/M$	$g=IBV/kT$	$M(g)$	$(dM/dg)\times g/M$
0.10	0.000666	1.998	2.0	0.194	1.464
0.15	.00150	1.995	3.0	.328	1.121
0.20	.00266	1.992	4.0	.437	0.868
0.30	.00595	1.984	5.0	.520	0.694
0.40	.0105	1.970	8.0	.672	0.419
0.50	.0163	1.953	10	.730	0.329
0.80	.0402	1.861	15	.813	0.213
1.0	.0609	1.828	20	.858	0.157
1.5	0.124	1.653	30	0.903	0.103

tensity of radiation polarized with the plane of vibration containing the x-axis (electric vector parallel to the x-axis) is proportional to $\exp(-NS_x)$, where N is the total number of grains in the line of sight per square centimeter. Hence

$$p = \frac{e^{-NS_y} - e^{-NS_x}}{e^{-NS_y} + e^{-NS_x}}. \tag{25}$$

The use of equations (22) and (23) yields the result

$$p = \tanh\left\{\tfrac{1}{2} N \sigma_T \, RM(g) \sin^2\phi\right\}. \tag{26}$$

b) GRAINS OF ARBITRARY SHAPE IN A NONUNIFORM MAGNETIC FIELD

First we consider small triaxial grains, uniformly magnetized in some direction not necessarily along the principal axis. This situation may be simplified by the consideration that the grain may be rotated to any position about the magnetic axis without change of potential energy, and it is only the direction of the magnetic axis that affects U. Hence, in computing the extinction coefficients, we may first take an average value for a fixed orientation of the magnetic axis. It is clear that, when this average is taken, the resultant extinction coefficient will be that of a uniaxial grain with its axis parallel to the direction of magnetization. It is these average values of σ_T and $\sigma_T(1+R)$ that must be used in equation (26).

When grains of different sorts are present, it is readily shown that $\sigma_T RM(g)$ must be integrated over all particle sizes. In addition, if $\boldsymbol{B}$ varies with position, an average value of $M(g)$ must be taken. This average becomes relatively simple if g is sufficiently small that $M(g)$ may be replaced by $g^2/15$, the leading term in equation (24) for small g. In this case it is readily shown from equations (9), (20), and (21) that, for light polarized in any particular direction $\boldsymbol{j}$, the average extinction cross-section, σ_j, is given by

$$\begin{aligned}\sigma_j &= \sigma_T + \frac{R\sigma_T}{3} + \frac{R\sigma_T I^2 V^2}{15 k^2 T^2}\left(-\tfrac{1}{3}B^2 + B_j^2\right) \\ &= \sigma_T\left[1 + \frac{R}{3}\left(1 - \frac{B^2 I^2 V^2}{15 k^2 T^2}\right)\right] + \frac{R\sigma_T I^2 V^2 B_j^2}{15 k^2 T^2},\end{aligned} \tag{27}$$

where B_j is the component of $\boldsymbol{B}$ in the direction of the vector j. Evidently if B_j varies with position, the mean extinction cross-section, S_j, will contain a term proportional to $\overline{B_j^2}$, where the bar denotes a space average, taken along the line of sight. If we define the x-axis to lie in the direction of maximum $\overline{B_j^2}$, subject, of course, to the condition that this axis is perpendicular to the line of sight, then equation (26) becomes, for weak orientation and small polarization,

$$p = \frac{N\sigma_T R I^2 V^2}{30k^2T^2} B_{\text{eff}}^2, \tag{28}$$

where

$$B_{\text{eff}}^2 = \overline{B_x^2} - \overline{B_y^2}. \tag{29}$$

Evidently, there are a number of possible situations in which $\overline{B_y^2}$ may differ from $\overline{B_x^2}$. In the first place, a uniform magnetic field might be present. In the second place, the magnetic field could be randomly oriented with a magnitude independent of direction, and the difference between these two mean-square values could arise solely from spatial fluctuations of the field; would be small compared to $\overline{B_x^2} + \overline{B_y^2} + \overline{B_z^2}$; and would, on the average, increase with the square root of the distance. In the third place, all components of the magnetic field could be fluctuating but preferentially greater in magnitude along one axis than along the other.

Lastly, we consider effects produced by grains large compared to the wave length. Equations (9), (10), and (11), which lead to the basic equations (16) and (17) in the present analysis, are generally valid for uniaxial grains, although, for large grains, σ_T and R will vary with γ, the inclination of the grain axis to the direction of wave propagation. Hence equation (26) is valid for large grains, provided that we take average values of σ_T and R. The values of these quantities as γ approaches 0 (grain axis parallel to the direction of propagation) may have an important effect on the term in brackets in equation (27) but should have considerably less effect on the last term, which determines the polarization. It is physically evident that the polarization must be caused by grains whose axes are inclined to the direction of propagation. For large grains we shall therefore use equations (26) and (28) with σ_T and R evaluated at γ equal to $\pi/2$.

IV. FORMATION OF FERROMAGNETIC GRAINS

The familiar Lindblad[18] theory of the growth of interstellar grains assumes that virtually all atoms which strike the grain surface will stick. As pointed out by van de Hulst,[19, 20] this theory requires modification in the case of *H*, *He*, and *Ne*, which will evaporate rapidly at grain temperatures exceeding some 5° K. Of the remaining elements, *C*, *N*, and *O* are the most abundant, and Oort and van de Hulst[6] have stressed that a typical grain will be composed of the hydrogen compounds of these three elements, with other substances less abundant. This conclusion may require modification if sometime during its life a grain is heated up, the more volatile constituents tending to evaporate, leaving behind the more refractory elements and compounds. An evident mechanism which may heat up an appreciable fraction of the grains is a direct collision between two grains. The possibility that such collisions might lead to fusion of the two grains and formation of a new "secondary" grain has been analyzed by Oort and van de Hulst[6] and in more detail by van de Hulst,[20] who suggests that selective evaporation might

[18] *Nature*, **135**, 133, 1935.

[19] *Centennial Symposia* (Cambridge, Mass.: Harvard College Observatory, 1948).

[20] *Rech. Astr. Obs. Utrecht*, Vol. 11 Part 2, 1949.

modify the chemical composition of the secondary particles. The present section attempts a quantitative discussion of the effect which collisions may be expected to have on the equilibrium composition of the interstellar grains. First, the evaporation occurring when two grains collide is considered, and, second, some of the chemical reactions that might occur on collision are discussed. Finally, the particle density of ferromagnetic grains in interstellar space and the size and shape of such grains are treated briefly.

a) EVAPORATION OF ATOMS FROM A GRAIN

Collisions between high-speed interstellar grains are exceedingly complicated to analyze in detail, and the present discussion is tentative and exploratory. We shall simplify the problem by assuming that a collision produces a grain at a high internal temperature. Thus the shock waves produced by the impact—which might conceivably break a grain into a number of separate pieces—are neglected, and only the heat generated is considered. Also, we shall discuss here only the evaporation of chemically inert compounds, postponing until later a consideration of the chemical reactions which may occur.

The composition of a typical grain may be determined from the relative abundance of elements given by Kuiper, based on work by Unsöld, Greenstein, and others. We assume that He, Ne, and solid H do not stick to the grain but that all other elements are present in about the same abundance as in the stars and nebulae, mostly as compounds with H. The resulting composition is given in Table 4.

TABLE 4

COMPOSITION OF INTERSTELLAR GRAINS

Compound	Per Cent by Weight	Compound	Per Cent by Weight	Compound	Per Cent by Weight	Compound	Per Cent by Weight
H_2O	42	CH_4	15	SiH_4	6	Mg	3
NH_3	16	Fe	13	H_2S	5	Others	<1

We shall consider, first, the following very idealized problem: A grain of chemically inert molecules of different types is suddenly given a large amount of internal energy; we wish to find its final state. We shall consider, first, that the only molecules present are H_2O and Fe_2O_3; if the abundance of the latter is increased somewhat to represent the Mg atoms also, the relative abundance of H_2O and Fe_2O_3 molecules by number is about 20 to 1. The resultant density of matter in the grain is 1.2 gm/cm^3. The presence of CH_4 and NH_3 molecules will be considered subsequently.

The internal energy, u, in calories per gram, produced by a collision is simply computed. For direct, central collision between two grains of equal mass, moving at a relative velocity V cm/sec, we have

$$u = 3.0 \times 10^{-9} V^2 \text{ cal/gm} . \tag{30}$$

Next we consider the range of values for u within which selective evaporation of the H_2O occurs. At the lower limit we have the value of u which will just heat the grain up to 0° C without melting it. In computing this value of u, which we denote by u_0, the presence of Fe_2O_3 molecules is neglected; the specific heat of H_2O decreases with decreasing temperature, but a rough integration yields a value of about 70 cal/gm for u_0. A grain heated to 0° C will cool rapidly by sublimation. Loss of energy by radiation may be neglected here; even if the absorption coefficient of the grain in the infrared were equal to its geometrical cross-section—an assumption which grossly overestimates the rate of radiation—radiation losses of energy would be less than evaporation and sublimation

losses, even at 1000° K. If all the internal energy is assumed to go into sublimation, about 9 per cent of the ice will sublime.

When u exceeds u_0, the additional energy will go at first into selective evaporation of the H_2O molecules. If u is 150 cal/gm, for example, the ice will just melt, and the evaporation of about 11 per cent of the H_2O molecules will just freeze the remainder. We denote this value of u by u_1. If u is 250 cal/gm, the grain will be heated to 100° C, and about a third of the H_2O molecules will evaporate. With increasing u, the grain will form initially a superheated droplet, which will evaporate rapidly. A limiting upper value, u_2, is reached when the internal temperature of this droplet is so great that the molecules literally fly apart. When this occurs, the Fe_2O_3 molecules will be pushed outward by the H_2O molecules, and there will probably be no grain left, even though the temperature may be insufficient to evaporate the Fe_2O_3 molecules, had they been sticking together initially. The value of u_2 is very uncertain. We shall here set u_2 equal to 1000 cal/gm, which is sufficient to evaporate all the H_2O at a temperature of about 700° C.

This value may be compared with the value obtained by the methods of Oort and van de Hulst.[6] They compute the energy needed to evaporate a grain at 100° C, which, for a grain of H_2O initially near 10° K, amounts to 790 cal/gm. However, a grain with this much energy would have an initial temperature of about 600° C (provided that we take a specific heat of about 1.1 for superheated water), and the molecules evaporating at the surface would have a kinetic temperature of this amount. The remaining molecules would then have insufficient energy for all to evaporate. Thus the heat required to evaporate a grain completely is apparently somewhat greater than the value considered by Oort and van de Hulst. (The specific value of 250 cal/gm which they use is based on a different composition from that considered here.)

The final state of the Fe_2O_3 molecules must also be considered. If most of the H_2O evaporates, the residue will evidently be solid Fe_2O_3. If only a small fraction of the H_2O evaporates, the Fe_2O_3 may still solidify to form a separate mass of ferric oxide inside the grain, provided that the grain is liquid for a sufficiently long time. The time of solidification of a small water droplet at 0° C may be computed from the rate of evaporation at this temperature, which may be found from the known vapor pressure. If the radius of the drop is 10^{-5} cm, the solidification time[21] is about 10^{-5} sec. If some nucleus is present to which every colliding Fe_2O_3 molecule sticks, the radius of this nucleus will increase initially at some 10^3 cm/sec, according to the familiar Lindblad formula,[18] and will grow to include all Fe_2O_3 molecules in less than 10^{-5} sec. The latent heats of vaporization and fusion liberated in this solidification will evaporate a large part of the remaining H_2O. We conclude that, for any value of u between u_1 and u_2, all the Fe_2O_3 will condense into solid form, the amount of H_2O remaining decreasing as u increases from u_1 to u_2.

Equation (30) may be used to give the values of V corresponding to this range for u. A solid core of Fe_2O_3 will form if two ice grains collide with a relative velocity of between 2.2 and 5.8 km/sec. To relate this conclusion to actual grains, we must take the other elements into account. The CH_4 and NH_3 will boil off on collision. The latent heats of vaporization of these substances are much less than that of water, and hence, after the grain has cooled appreciably, these substances will carry away only a fraction of the energy per unit mass which they have contributed. Whether SiH_4 and H_2S boil away is less certain, but we shall assume that 30 per cent of the mass of the grain goes off, carrying only half its original energy as computed from equation (30). The range of relative velocities within which a solid core of Fe (and Mg) compounds will form is then reduced to between 2.0 and 5.2 km/sec.

Another very similar case is that in which unattached Fe atoms are distributed throughout an H_2O grain and, upon collision and heating, combine with one another to form metallic Fe. The latent heat of vaporization of metallic Fe is very large, amounting

[21] This analysis was first carried out by E. Schatzman (cf. L. Spitzer, Jr., and E. Schatzman, *A.J.*, **54**, 195, 1949).

to 90 kcal per gram atom at 3000°,[22] or 1600 cal/gm; at lower temperatures this latent heat will be somewhat greater. Thus the solidification of all the *Fe* in a grain, about 30 per cent as abundant by mass as H_2O, would provide enough energy to evaporate most of the ice. Thus, for any value of u between u_1 and u_2, a core of metallic *Fe* would form, with relatively little H_2O remaining.

Alternatively, the heating required to melt a grain could be provided by the heavy nuclei in cosmic radiation, as suggested by Spitzer and Schatzman.[21] However, the absence of *Li* and *Be* nuclei in the cosmic radiation, as observed by Bradt and Peters,[23] shows that the particles in cosmic radiation have not been traveling through interstellar space for more than a fraction of the some ten million years required for an equilibrium distribution of nuclear charges to be set up. This result casts grave doubt on whether the heavy nuclei observed in the cosmic radiation are actually present in interstellar space; and the effect of such particles on the grains will not be considered further.

b) CHEMICAL REACTIONS WITHIN A GRAIN

There are many possible chemical transformations which might occur when two grains collide. Since exact thermodynamic equilibrium cannot be assumed, a very detailed analysis of the many complicated physical and chemical processes occurring might be required to yield reliable results. The present discussion is very tentative and simply explores some of the most evident possibilities.

One possibility that should at least be mentioned is that most of the atoms in the grain are originally bound only by physical forces of van der Waals type, since, as a grain grows in a low-temperature H I region, the atoms strike the grain surface at such a low velocity that they may lack the activation energy necessary for chemical binding. In such a case the heating produced by a collision would provide sufficient energy to allow chemical binding. Much additional heat would be generated by such chemical processes. In this situation the heat available for evaporation might considerably exceed the values found above. Since this situation is not only very complicated but also somewhat unlikely, we shall not consider it further. A somewhat more likely possibility is that individual *H* atoms will become chemically bound to *C*, *N*, *O*, *Si*, *S*, and similar atoms on impact but that reactions between these hydrogen compounds occur only when the grain is heated. Uncertainties in the rate of chemical reactions make a quantitative discussion of these processes very difficult. However, certain reactions can be shown to be strongly exothermic and may be expected to occur. A number of major reactions are discussed below from this viewpoint.

Let us first consider the reactions which may be expected between an *Fe* core, if one forms, and the surrounding material. Such a core is not likely to be oxidized. Most oxygen atoms are likely to be held in water molecules, and *Fe* cannot displace *H* from liquid H_2O or from NH_3 or CH_4. Among other reactions with the more abundant elements is

$$Fe + H_2S = FeS + H_2 + 18 \text{ kcal} . \tag{31}$$

The heat of reaction indicated is simply the difference between the heats of formation[24] of the compounds involved and indicates the energy that could be liberated. A reaction between H_2S and *Mg*, similar to that between H_2S and *Fe*, is also energetically possible, while H_2S has no natural reactions with CH_4, NH_3, H_2O, or SiH_4. Since the abundance of *S* is apparently less than that of *Fe*, it seems unlikely that all the *Fe* might be converted to *FeS*, especially since much H_2S may be expected to escape.

[22] *International Critical Tables* (Washington: National Research Council, 1926), 1, 102.

[23] *Phys. Rev.*, 80, 943, 1950. We are much indebted to Dr. Bradt and Dr. Peters for communicating their results to us in advance of publication.

[24] *Handbook of Chemistry and Physics* (Cleveland: Chemical Rubber Publishing Co., 1947).

If the *Fe* atoms can react with other elements before sticking together to form liquid or solid *Fe*, a number of reactions become possible. In particular, atomic iron may perhaps be expected to displace *H* from liquid water, forming ferrous and ferric oxides. Such oxides might be reduced to metallic *Fe* by the following reactions:

$$2FeO + SiH_4 = 2Fe + SiO_2 + 2H_2 + 61 \text{ kcal}, \tag{32}$$

$$2Fe_2O_3 + 3SiH_4 = 4Fe + 3SiO_2 + 3H_2 + 187 \text{ kcal}, \tag{33}$$

provided that the gaseous SiH_4 does not escape or react first with H_2O, according to the equation

$$SiH_4 + 2H_2O = SiO_2 + 4H_2 + 53 \text{ kcal}. \tag{34}$$

The H_2 released in this reaction or present within the grain as absorbed gas might conceivably reduce *Fe*, according to the reaction

$$FeO + H_2 = Fe + H_2O + 4 \text{ kcal}. \tag{35}$$

According to Latimer,[25] reaction (35) may produce metallic *Fe* in the somewhat similar case of planet formation

Reactions involving other atoms are also of interest. Between the abundant compounds CH_4, NH_3, and H_2O, the only reaction which seems energetically possible is

$$NH_3 + H_2O\,(\text{liquid}) = NH_4OH + 8 \text{ kcal}. \tag{36}$$

While some ammonium hydroxide may be expected to form, the reaction is reversible, and the NH_4OH, unless it reacts first with other compounds, may be expected to be converted back into NH_3 as the latter evaporates. Hence one may expect that most of the NH_3, like the CH_4, will evaporate from the grain at a temperature of 273° K or above. On the other hand, we have seen that an appreciable fraction of *Si* and perhaps also of *S* may fail to evaporate. There seems no way for *Mg* to evaporate at the temperatures under consideration. This element is most likely to remain as *MgO*, since metallic *Mg* can readily displace hydrogen from H_2O, *FeO*, or SiO_2.

Evidently, the final state of the grain is uncertain. A ferromagnetic particle seems a good possibility, however, since metallic iron and the oxide Fe_3O_4 are definitely ferromagnetic, and Fe_2O_3 is also ferromagnetic when precipitated from a water solution The magnesium iron spinel, $MgFe_2O_4$, is also ferromagnetic.[26] Thus, unless *FeO*, *FeS*, $FeSiO_3$, or related compounds are the end-products, a collision between two grains of the sort considered is very likely to produce a ferromagnetic grain. We shall assume here that all dense grains formed in this way are, in fact, ferromagnetic.

c) DENSITY AND SIZE OF FERROMAGNETIC GRAINS

We shall assume here, following the theory of Oort and van de Hulst,[6] that grains are destroyed when two clouds collide or when grains between the clouds collide with a cloud. Such encounters lead to high-speed collisions between individual grains, which then evaporate, at least partially. In accordance with this theory, we assume that, in equilibrium, ferromagnetic grains will be produced at the same rate as that at which they are destroyed. The formation will take place when ordinary ice grains collide, are fused, and the more volatile constituents evaporate. For simplicity we assume here that the destruction probability is the same as that of primary ice grains, postponing until later a more detailed discussion of this process. We determine, below, the ratio *q* between the number of collisions which form ferromagnetic grains and the number of collisions which evaporate the ordinary grains entirely.

[25] *Science*, 112, 101, 1950.

[26] J. L. Snoek, *Physica*, 3, 463, 1936.

According to Oort and van de Hulst,[6] any collision between two grains with a relative velocity exceeding 2.9 km/sec will destroy the grains. Here we shall take 2.0 km/sec as the critical velocity for the destruction of two ordinary ice grains, since the fusion taking place at this velocity results in the evaporation of an appreciable fraction of the lighter constituents of the grain. We have already seen that collisions at velocities between 2.0 and 5.2 km/sec will probably lead to a ferromagnetic particle. Since the velocity of the grain penetrating a cloud varies inversely as the first power of the time, the distance traveled varies logarithmically with the velocity (eq. [7] of note 6), and we find

$$q = \frac{\log 5.2/2.0}{\log v_0/2.0} = 0.40\,, \tag{37}$$

where v_0 is the initial velocity of the grain relative to the cloud, here set equal to 22.5 km/sec. Evidently a considerable fraction of the interstellar grains should be at least partially ferromagnetic.

The previous discussion has tacitly assumed that the dense grain resulting from a collision will contain all the heavy atoms in each of the two colliding grains. Such an outcome is not probable. When two grains collide at several kilometers per second, the resultant angular momentum is generally great enough to disrupt a liquid grain almost immediately against the strong cohesive force of surface tension. It seems improbable that all the angular momentum will be concentrated in a single grain, even momentarily. If the collision is sufficiently fast, the strength of the solid grains may be ignored, and only those parts of each grain which collide physically with each other will be stopped, the ends flying on unobstructed and carrying away most of the angular momentum. A detailed analysis of these processes would be very difficult, and we shall assume here that half the mass of the two colliding grains is available for the formation of a dense ferromagnetic grain.

Each dense grain formed in this way will serve as a nucleus for the condensation of interstellar atoms, and a shell of ices will grow, surrounding the ferromagnetic core. Since the nuclei already have appreciable radii, the resultant compound grains will be somewhat larger than the ordinary ice grains.

We now compute the relative number of compound grains per cubic centimeter in equilibrium. Let y be the ratio of the particle densities of compound grains and ordinary grains. Since we have assumed equal mean lives for these two types of grains, the ratio of the number of compound grains destroyed by collisions per second per unit volume to the corresponding number of ordinary grains destroyed is also equal to y. The ratio of the number of ferromagnetic nuclei formed per second per unit volume to the corresponding number of ordinary grains destroyed is $q(1 + y)/2$, the factor $1 + y$ arising from the fact that fusion of a compound grain can also produce a new ferromagnetic nucleus. It is clear that collisions involving compound grains will have a different value of q and will produce ferromagnetic nuclei of different sizes than will collisions between two ice grains; such differences, which may be responsible for the large ferromagnetic grains suggested in the last section, are ignored here.

Evidently, in equilibrium, the number of ferromagnetic nuclei formed per unit volume per second must equal the corresponding number of compound grains destroyed. Hence the two ratios discussed in the preceding paragraph must be equal, and we have

$$y = \tfrac{1}{2} q\,(1 + y)\,, \tag{38}$$

which yields

$$y = \frac{q}{2 - q} = 0.25\,, \tag{39}$$

if the numerical value for q is taken from equation (37). This value is considerably greater

than the value 0.06 found by van de Hulst[20] for the ratio of particle densities of secondary and primary grains. This difference results from the larger radius taken for a secondary grain by van de Hulst, who assumed that the mass of a secondary grain equaled the sum of the masses of the two primary grains; evidently, the larger the grains when they start out, the sooner they will be destroyed by collisions, and the fewer of them there will be.

The particle density n_{gF} of ferromagnetic particles and the sizes of these grains depend on the properties of the ordinary interstellar grains. We shall here adopt the distribution obtained by van de Hulst,[20] who fitted the theoretical distribution obtained by Oort and van de Hulst[6] to the observations of selective extinction. In this distribution the total number of grains per cubic centimeter is 1.52×10^{-13}, the root-mean-square radius is 2.4×10^{-5} cm, and the average mass per particle is 9.1×10^{-14} gm. The average mass of a particle on evaporation (the mass averaged over the derivative of the distribution function of the radii) has the value 2.6×10^{-13} gm, the difference resulting from the lower destruction rate of the smaller grains. If, in a typical collision, CH_4, NH_3, and H_2O evaporate, leaving behind a residue of Fe and Mg oxides containing 19 per cent of the mass of one of the grains, the mass of the resultant grain will then average 5.0×10^{-14} gm, about half the average mass of an ordinary grain. If a density of about 5 gm/cm^3 is assumed for the new grain produced in a collision, the corresponding volume is 10^{-14} cm^3, and the radius is 1.3×10^{-5} cm. From equation (39) and the number of ordinary grains per cubic centimeter obtained by van de Hulst, we see that the total number of ferromagnetic grains is 3.8×10^{-14} cm^{-3}, corresponding to a space density of 1.9×10^{-27} gm/cm^3—about an eighth of the space density 1.38×10^{-26} gm/cm^3 found for the ordinary grains by van de Hulst. If, in accordance with Strömgren's results,[27] we assume that the density within a cloud is some twenty times the average, we find

$$n_{gF} = 7.6 \times 10^{-13} \text{ cm}^{-3} . \tag{40}$$

It should be emphasized that this relatively high abundance of compound grains is quite independent of the argument concerning the presence of ferromagnetism within the relatively dense nuclei. Even if no ferromagnetism were present, the presence of these compound grains, each with a dense nucleus of high refractive index, would in any case require serious modifications in the theory of interstellar extinction. Evidently, the distribution adopted for the ordinary ice grains may require some modification, thus requiring changes in the number and properties of compound grains found above.

Finally, we must consider the elongation of the ferromagnetic grains. The particles formed by fusion are likely to be elongated, if solidification of a crystal from a liquid is assumed. Ferromagnetic grains with a length about twice their mean thickness will be considered here.

In addition, we must consider the sticking-together of these grains to form elongated needles. The grains are moving very slowly in kinetic equilibrium, and their strong mutual magnetic attraction will produce collisions between them. Two grains which collide will stick together, with opposite poles of the two nuclei as close together as possible. The tendency of tiny Fe particles to stick together in chains is well illustrated by laboratory experiment.[28] In computing the number of grains which collide and stick, we shall neglect the presence of the outer shell of ices, considering only the ferromagnetic nucleus. We shall assume that all ferromagnetic grains have the same radius.

Two grains, each of volume V and with a uniform magnetization I, separated by a distance r, will have a mutual potential energy $-2I^2V^2/r^3$, multiplied by a function of the orientation of the two grains; this function equals unity when the grains have the

[27] *Ap. J.*, **108**, 242, 1948.

[28] D. Beischer and A. Winkel, *Naturwiss.*, **25**, 420, 1937.

orientation of minimum potential energy, with magnetic axes collinear and opposite poles facing each other. When $2I^2V^2/r^3$ is about equal to $3kT/2$, the mean kinetic energy of rotation at the kinetic temperature T, the alignment of the grains will, on the average, begin to approach that of minimum potential energy.

An exact discussion of the paths followed by the two grains would be rather complicated. If the force is assumed to vary exactly as $6I^2V^2/r^4$, however, the analysis becomes simple. We shall let p be the usual impact parameter (distance of closest approach if no interaction were present). Then it may be shown that a direct collision will occur if $2I^2V^2/p^3$ is equal to or greater than $2/3^{3/2}$ times the mean translational kinetic energy $3kT/2$.

The collisional cross-section σ_c is then given by

$$\sigma_c = 3^{1/3}\pi\left(\frac{2I^2V^2}{kT}\right)^{2/3}. \tag{41}$$

For a single grain, the mean time t_c between such collisions is given by

$$t_c = \frac{1}{n_{gF}\sigma_c v_g} = \frac{(kT)^{1/6}\rho_g^{1/2}}{3^{5/6}2^{2/3}\pi n_{gF} V^{5/6} I^{4/3}}. \tag{42}$$

The numerical values to be substituted in equations (41) and (42) may be found partly in the preceding paragraphs of this section, partly in the next section. If we set T equal to 60° K, ρ_g to 5 gm/cm^3, I to 400, V to 10^{-14} cm^3, and n_{gF} to 7.6×10^{-13} cm^{-3} (from eq. [40]), we find that σ_c equals 1.1×10^{-5} cm^2 and t_c is 5.3×10^9 years. If all the *Fe* is assumed in metallic form, the magnetic moment IV of each grain is increased by a factor 1.8, and this computed time becomes less by a factor of 0.45.

These computed values of the time required for grains to stick together, comparable to the short-time scale of 3×10^9 years, imply that this particular mechanism is not important, especially since Oort and van de Hulst give 5×10^7 years for the mean life of an interstellar grain before evaporation. However, the value of n_g in equation (38) is somewhat uncertain. It is not impossible that density fluctuations, filaments, etc., are found inside clouds and that the mean value of n_g is some five times as great as the assumed value, corresponding to a total grain density of about 10^{-24} gm/cm^3. If, at the same time, the mean life of an interstellar grain before evaporation were increased by a factor of about 20, possibly by the influence of electromagnetic fields in hindering collisions, chains of ferromagnetic particles might be expected to form in appreciable amounts. We shall therefore keep this possibility in mind in the following section.

V. COMPARISON WITH OBSERVATION

The theoretical results may now be compared with the observational data summarized in Section I. One important conclusion may be drawn at once from the relative constancy of p with wave length. According to the theory of extinction by small particles, R is independent of the wave length, while the extinction cross-section increases rapidly with decreasing wave length. These two variations combine to give a polarization which increases with decreasing wave length, in conflict with observation. Hence the thickness of a typical grain cannot be small compared to the wave length of visible light, and the values of R given in Section II are not applicable. Until some theory for the optical properties of large elongated grains is available, no precise quantitative theory of interstellar polarization by grains is possible.

If a value is estimated for R, equation (28) is still valid for small polarization produced by partial orientation of large grains. The present theory may therefore be used at least to estimate the order of magnitude of the magnetic field needed to explain the observations. First we discuss below the values which may be assumed for the various

physical parameters which describe the grains and which enter into equation (28). An evaluation of B_{eff} is then obtained from the observed values of p. Finally, the fluctuations in B_{eff} are considered.

a) ASSUMED PROPERTIES OF THE GRAINS

The quantities N and σ_T in equation (28) refer to ferromagnetic grains, and in this section we shall denote these quantities by N_{gF} and σ_{TF}. From the preceding section we see that σ_{TF} is 6.0×10^{-10} cm^2, and over a path length of 1000 parsecs the average value of N_{gF} is 1.2×10^{8} cm^{-2}. Hence $N_{gF}\sigma_{TF}$ averages 0.072 per kiloparsec. The photoelectric color excess E_1, on the other hand, averages[29] about 0.17 mag/kpc. Thus we rewrite equation (1) in the form

$$p = 0.19 N_{gF}\sigma_{TF} . \tag{43}$$

If this equation is combined with equation (28), we have

$$B_{\text{eff}} = \frac{2.4kT}{R^{1/2} I V} . \tag{44}$$

This equation may be used to determine B_{eff}.

Next we consider the value of R that may be assumed. The indices of refraction for *Fe*, Fe_2O_3, and $MgFe_2O_4$ are[30] about $2.5 - 3.5i$, 3, and 2.3, respectively. While these values refer to about 6000 A, the corresponding values at 8000 A are not likely to be very different. From Table 2 we see that, for a prolate spheroid with x equal to 2, the value of $1 + R$ is about 3 for these indices of refraction. For particles of the size considered here, the Gans theory is not applicable, and R is presumably less than 2. We shall here set R equal to 1, at 8000 A; this value seems not unreasonable in view of the likelihood that the grains responsible for the polarization begin to be small for infrared radiation.

The magnetization I may be taken equal to the saturation magnetization produced in a ferromagnetic substance by very strong external fields. It is well known that an ordinary ferromagnetic solid is divided into small regions, called "domains," in each of which the magnetization I has always its saturation value, denoted by I_∞. When an external field is applied to a large ferromagnetic body, these individual domains are progressively aligned with the field, producing the observed dependence of magnetization on B for a large sample. Both theory[31] and observation[32] indicate that sufficiently small ferromagnetic particles will be single domains and will thus be permanently magnetized, with I equal to I_∞. The exact radius up to which a particle will remain a single domain is not entirely certain but is apparently[33] greater than 2×10^{-5} cm, especially if the particle's length much exceeds its radius.

Values of the saturation intensity I_∞ for ferromagnetic substances include[34] 2000 gauss for Fe_2Co and 470 for Fe_3O_4 (magnetite). These values refer to room temperature, and at low absolute temperatures slightly higher values of I will be found. Since the most likely ferromagnetic grain in interstellar space is probably a compound of *Fe*, *O*,

[29] J. Stebbins, C. H. Huffer, and A. Whitford, *Ap. J.*, **92**, 193, 1940.

[30] Landholt and Börnstein, *Physikalisch-chemische Tabellen* (Berlin: J. Springer, 1923), **2**, 907; 3. Ergänzungsband, **2**, 1485, 1936. The values for *Fe* depend on the presence of impurities; the value adopted here is that found for electrolytic *Fe* and for most steels.

[31] C. Kittel, *Phys. Rev.*, **70**, 965, 1946.

[32] W. C. Elmore, *Phys. Rev.*, **54**, 1092, 1938.

[33] We are indebted to Dr. C. Kittel for this information.

[34] National Research Council, *International Critical Tables* (New York: McGraw-Hill Book Co., 1929), **6**, 376.

and *Mg*, we shall set I equal to 400. We shall also consider grains containing metallic *Fe*, with I equal to 1600.

The volume V of a ferromagnetic grain we have already found to be 10^{-14} cm^3. The shell of ices surrounding the nucleus is unimportant in this connection, since only the volume of ferromagnetic material must be used in equation (28). If all the *Fe* is in metallic form, the value of V for the *Fe* in the grain becomes 4.5×10^{-15} cm^3. If f grains are stuck together in a chain, these values must be increased by a factor f.

Lastly, we must evaluate the kinetic temperature T. It is evident from equation (28) that the mean value of B_{eff}^2/T^2 is required. Hence regions of low T will have the predominant effect. According to a recent analysis[35] of interstellar temperatures, the most probable value of T in *H* I regions, where most of the obscuration presumably occurs, is about 60°. Large fluctuations about this value seem very likely, and the value of T to be used in equation (28) should be less than 60°. We shall accordingly set T equal to 30°.

b) REQUIRED VALUE OF *B*

If we insert into equation (42) the numerical values found above, we obtain

$$B_{\text{eff}} = \frac{2.5 \times 10^{-3}}{f} \text{ gauss}, \tag{45}$$

for a grain composed of *Fe*, *O*, and *Mg*. If the *Fe* within the grain is in metallic form, however, we find

$$B_{\text{eff}} = \frac{1.4 \times 10^{-3}}{f} \text{ gauss}. \tag{46}$$

We see from equation (44) that the value of g for these two types of grains is about 2, provided that B does not much exceed B_{eff}. According to Table 3, $d(\log M)/d(\log g)$ is about 1.5 for this value of g, and equation (28), which is based on the assumption that this derivative is exactly 2, is somewhat approximate, although the error should not be very large.

Evidently, if f is unity, the value of B_{eff} must be about 2×10^{-3} gauss for ferromagnetic grains of the size considered here. This field is about 10^2 times as great as the values obtained from simple equipartition arguments, although our present knowledge of interstellar magnetic fields is so fragmentary that a field of this order cannot be excluded.

On the basis of the present theory, there are at least two possible ways in which the polarization observations might be explained with weaker fields. First, we have seen in the previous section that an appreciable number of ferromagnetic grains would be expected to stick together if the density times the lifetime of grains were two orders of magnitude greater than has previously been assumed. If f were to be as great as 10, for example, B_{eff} could be reduced to 10^{-4} gauss. While large values of f do not seem at all likely, they cannot be excluded at the present time.

Second, grains of larger volume could be oriented by weaker fields. If there are present in interstellar space ferromagnetic grains with mean radii of some 5×10^{-5}cm, these could be oriented appreciably by fields only about 2 per cent as great as those found above, or about 3×10^{-5} gauss for grains containing metallic *Fe*. If the value of $N_g r \sigma_{Tr}$ for such grains were about equal to that assumed for the smaller grains, they would produce a gray extinction of about 0.1 mag/kpc, which would be difficult to detect from ordinary extinction measures. The total space density of matter in such large grains would be about 10^{-26} gm/cm^3, about the same as that of the ordinary ice grains. If the value of R for such large grains were as great as unity, such grains could explain the observed polarization with fields of the order of 10^{-5} gauss.

[35] L. Spitzer, Jr., and M. P. Savedoff, *Ap. J.*, 111, 593, 1950.

It is possible that such large ferromagnetic grains might grow from successive collisions of compound nuclei. For example, when two compound grains of the sort considered in the previous section collide at moderate velocities, with the more volatile substances evaporating, the mass available for a dense grain would be six times that of either nucleus, and the resultant grain might well have a mass some three times as great. While such grains would not be formed very rapidly, they would not be destroyed so rapidly as would the ice grains. When a compound grain collides with an ice grain at high speed, most of the energy may be expected to go into heating up the ices to a very high temperature, possibly even into dissociating some of the hydride molecules. The nucleus itself has such a low specific heat that, after the lighter materials of high specific heat have evaporated, the nucleus, even at a temperature of 5000° K, will not have enough thermal energy to provide the latent heat of evaporation for more than a fraction of its mass. Moreover, at such a high temperature, radiative losses of energy would be relatively rapid. Thus we see that, while a compound grain is readily destroyed in a collision, in the sense that the shell melts or evaporates, the refractory nucleus is relatively difficult to destroy, especially if its mass is large compared to the mass of the average ice grain with which it collides. It follows that the average size and mass of the dense nuclei are probably greater than computed in the previous section. More computations would be needed to determine the detailed distribution of grain sizes. Until more information on the optical properties of large particles is available, such further computations do not seem warranted.

c) FLUCTUATIONS OF B

It is evident from Section I that p fluctuates in amount for stars of the same color excess and also shows some fluctuation in direction. The fluctuation in amount might result from changes in the relative number and size of ferromagnetic grains—in y, R, or σ_{TF}—as well as in B or T, and is therefore difficult to interpret unambiguously at the present time. The fluctuations of the plane of vibration, however, can apparently be explained only by variations in the direction of the effective magnetic field.

We have already seen that the observations indicate that the orienting force can be analyzed into two components—a uniform field which orients the major axes of the grains perpendicular to the galactic plane and a fluctuating component. If we consider that the magnitude of the fluctuating field is independent of direction and that this field is randomly oriented, then this field will cancel out, on the average, leaving only the effects cause by statistical fluctuations. This picture would suggest that fluctuations in the direction of polarization should become smaller, on the average, for stars at increasing distances. It may be noted that the observed decrease of the ratio p/E_1 as E_1 increases is consistent with this picture.

Another interpretation is also possible. From equation (29) we note that $B_{\perp}^2$ is simply $\overline{B_x^2} - \overline{B_y^2}$. If the random magnetic fields are not isotropic, with fields in the x-direction systematically greater than in the y-direction, polarization will result even if the scale of the field is very small. Thus, even if the average magnetic field in a particular direction is small, the average root-mean-square field in the x-direction may considerably exceed that in the y-direction. Fluctuations in the plane of polarization might then be due to changes in the preferential axis for the small-scale magnetic fields. If one accepts the assumptions of Oort and van de Hulst,[6] the cloud velocities are greater parallel to the galactic plane than they are perpendicular to it, and the greatest magnetic fields should perhaps be parallel to the galactic plane. Since these arguments are quite uncertain, no definite conclusions can be drawn along this line at the present time, except for the general inference that the observed fluctuations in polarization do not appear to be inconsistent with the present theory.

We are indebted to Drs. Leverett Davis and Jesse Greenstein for several discussions and helpful suggestions.

THE POLARIZATION OF STARLIGHT BY ALIGNED DUST GRAINS

LEVERETT DAVIS, JR.
PHYSICS DEPARTMENT, CALIFORNIA INSTITUTE OF TECHNOLOGY
and
JESSE L. GREENSTEIN
MOUNT WILSON AND PALOMAR OBSERVATORIES
CARNEGIE INSTITUTION OF WASHINGTON
CALIFORNIA INSTITUTE OF TECHNOLOGY
Received January 4, 1951

ABSTRACT

Polarization of starlight may arise from absorption and scattering by elongated dust grains that are at least partially aligned by a magnetic field. We assume that the grains contain mostly compounds of hydrogen with about 12 per cent iron by weight, presumably also in compounds. The theory of Gans is used to compute the scattering and absorption by a spheroidal grain small compared to the wave length, the component of the light with its electric vector parallel to the grain's long axis being preferentially weakened. The polarization and extinction of light are then computed for a cloud of small particles (mean radius 10^{-6}–3×10^{-5} cm) having any specified distribution of orientations.

Our mechanism for orienting the rapidly spinning grains (angular velocities of the order of 10^5–10^6 rad/sec) is the small nonconservative torque due to paramagnetic relaxation in material containing a few per cent of iron. The magnitude of the paramagnetic absorption is estimated from theory and experiment. This torque tends to make the short axis of the grain the axis of rotation, which is still very rapid, and to set this short axis along the magnetic field (orientation rate of the order of 10^{-12}–10^{-13} rad/sec). Thus the maximum extinction coefficient is for light with its electric vector perpendicular to the field. An approximate statistical theory based on a relaxation time (of the order of 10^{12} sec) for the orientation of the grains gives the distribution of orientations to be expected when this tendency toward orientation is balanced by the tendency toward random alignment caused by the bombardment of the grains by the interstellar gas. Small prolate grains of eccentricity such that the ratio of diameters lies in the range 1.2–1.7 will be sufficiently aligned to produce the observed ratio of polarization to color excess, $p/E_1 \leqslant 0.18$, in a magnetic field of 10^{-4}–10^{-5} gauss.

The theory predicts that for uniform magnetic fields and interstellar matter of constant temperature and composition the polarization should be proportional to the color excess. The direction of the observed polarization vectors indicates that over regions of several hundred parsecs in the Milky Way the magnetic field is mainly parallel to the plane of the galaxy, perhaps nearly uniform along a spiral arm or perhaps making random whirls mainly in the plane of the galaxy. Since the interstellar grains are larger than those to which the Gans theory applies and since the predicted wave-length dependence of the extinction is incorrect, it is not surprising that the theory gives an incorrect wave-length dependence of the polarization. Qualitative considerations indicate that the predicted ratio p/E_1 is not too far from the correct order of magnitude and that present observations of the wave-length dependence do not necessarily contradict the rest of our theory, which can be extended when extinction coefficients are known for large grains.

Observational data are summarized in § 1, and the nature of the grains is treated in § 4; our theory is given in outline in § 3, and the mathematical details are worked out in §§ 5–7. In § 8 we show that torques due to eddy currents or to static charges on the grain are unimportant.

1. SUMMARY OF OBSERVATIONAL INFORMATION

The polarization of starlight transmitted through interstellar dust and gas was recently discovered by W. A. Hiltner[1, 2, 3] and John S. Hall.[4, 5, 6] Their data yield three striking characteristics of the polarization.[7]

[1] *Science*, **109**, 165, 1949.

[2] *Ap. J.*, **109**, 471, 1949.

[3] *Phys. Rev.*, **78**, 170, 1950.

[4] *Science*, **109**, 166, 1949.

[5] Hall and Mikesell, *A.J.*, **54**, 187, 1949.

[6] Hall and Mikesell, *Pub. U.S. Naval Obs.*, Vol. **17**, Part I, 1950.

[7] We are greatly indebted to both Hall and Hiltner for permission to use their results before publication.

(i) They have shown that a correlation exists between the available measurements of the polarization p and the photoelectric measurements by Stebbins, Huffer, and Whitford[5] of the interstellar reddening E_1. Large polarization is very rare among stars of small reddening, and a rough upper limit seems to exist for the polarization associated with a given reddening. Stars of large reddening show a range of polarization from nearly zero to this limit. Thus it seems probable that interstellar absorption is a necessary, but not a sufficient, condition for the appearance of polarization. This conclusion is well documented by Hall and Mikesell's detailed review[6] of the correlations of the polarization with other quantities. We shall express this in numerical form, following Hall in using the conventional definition of the polarization, p. As discussed in § 5.3 below, p is 0.46 times the perhaps more convenient definition used by Hiltner. In a plot of p as a function of E_1, the correlation diagram can be bounded by a straight line that gives the normal maximum value of p for a given E_1. This shows that, approximately,

$$p \leqslant 0.18 E_1 , \tag{1}$$

where the natural uncertainties at low values are augmented by the uncertain location of the zero point of the E_1 scale. The mean value of p/E_1 is considerably lower, near 0.09. We do not consider in these estimates the apparently nearly unreddened stars listed by Hall and Mikesell[6] in their Table IV. Since E_1 and the interstellar absorption are very highly correlated, we can introduce the known ratio of the color excess to the absorption at the photographic effective wave length and obtain

$$p \leqslant 0.020 A_{pg} . \tag{2}$$

Under the most favorable conditions, which occur in the galactic plane, this is equivalent to a statement that the extinction coefficient of the dust varies over a range of about 5 per cent with the plane of vibration.

(ii) In general, the vectors representing the polarization of different stars show approximate parallelism for small galactic latitude over a considerable range of galactic longitude. There is, however, only a correlation of directions, not completely uniform alignment. In our discussion we shall describe the polarization in terms of the plane of vibration, the plane in which the electric vector of the radiation has its maximum; we do not use the older "plane of polarization," which lies at right angles to this and which is used by Hall and Mikesell. In the region of the galactic center and in Cygnus there is considerable disorder, but in the Perseus region the planes lie within $\pm 6°$ of parallelism over an area 8° square. According to Hall and Mikesell, the plane of vibration lies approximately in the galactic plane from galactic longitude 80° to 120° and perhaps up to 170°.

(iii) Hiltner[3] has shown that the polarization varies more slowly with wave length than does the interstellar absorption.

We may now briefly discuss the implications of these observations.

(i) The correlation of polarization and color excess indicates that a cloud of interstellar particles can produce a polarization which, under favorable conditions, reaches the upper limit given by equation (2). The fact that the polarization is often less than the maximum can be explained if the mechanism producing the polarization either (1) varies from region to region in strength or effectiveness in producing observable results or (2) has a random orientation from one complex of dust to another, so that the observed net polarization arises from random composition of the polarization vectors. The first possibility is exemplified if the polarization is due to the alignment of dust grains, and the aligning mechanism is more effective in certain regions than in others. As an example of the second possibility, note that, if there are n regions, the average polarization will be $n^{1/2}$ times

[5] *Mt. W. Contr.*, No. 621; *Ap. J.*, 91, 20, 1940.

that produced by one region, while the reddening is n times. Then p/E_1 will be $n^{-1/2}$ times the ratio in a single cloud.

(ii) The rough parallelism of the planes of vibration suggests that the polarization does not arise in individual stars, circumstellar clouds, or any other small regions of space, since there seems to be no reason why such objects should have parallel axes. In fact, since strong interstellar absorption over the region of approximate parallelism sets in at a distance of 300–500 psc, we conclude that a region with an extension of at least 200 psc across the line of sight produces an essentially constant direction of polarization. In the direction of Sagittarius and Cygnus, where the direction of polarization is more erratic and the ratio p/E_1 somewhat smaller, one might accept the random composition of the effects of small clouds discussed above.

(iii) The color-dependence data imply either that the constituent of interstellar space responsible for polarization is not the one responsible for the main absorption or that, although one constituent does both, the difference in the extinction coefficients of beams of light having different planes of polarization shows less dependence on the wave length than does the sum of the extinction coefficients. Even the former alternative does not imply that dust could not be responsible for the polarization; it could imply that the dust has a wide range of sizes, with different size ranges being dominant in each of the two phenomena.

2. POSSIBLE SOURCES OF POLARIZATION

The polarization must be due to some anisotropy in space. No obvious mechanisms exist that would polarize light by direct interaction with anisotropic gravitational or electromagnetic fields or with matter moving anisotropically. The simplest mechanism is an absorption that depends on the plane of vibration of the light, thus implying some type of alignment in the absorbers. Certain fields with which the absorbers might be aligned cannot be essentially uniform over large enough regions, as in the case of electric fields which are suppressed by the high conductivity of interstellar space. Most other fields produce no alignment of any kind, as in the case of gravitational fields or fields of light-flux. The one exception is a magnetic field, since it is made essentially permanent by the high conductivity and since it exerts an aligning torque on any body with a magnetic moment.

Let us consider sources of absorption which under special conditions might produce polarization. The Thomson scattering by electrons cannot be a source of polarization because of the large mass of ionized material required to produce appreciable absorption. It also does not seem probable that electron spins can be aligned in a magnetic field B unless $B\mu \approx kT$, where $\mu = 9 \times 10^{-21}$ erg/gauss is the magnetic moment of an electron. Fields of $B \approx 10^4 T$ gauss would be required. Also there seems to be no way for aligned electrons to produce polarization by Thomson scattering.

Atomic continua are negligible except shortward of the Lyman limit. The absorption by H^- from its ground state has not as yet been considered in interstellar space. We may estimate the number of H^- ions per cubic centimeter from

$$\frac{n_{H^-}}{n_H n_e} = 4.16 \times 10^{-10}\, \theta_c^{3/2}\, \theta_e 10^{0.75\theta_c} \left(\frac{T_c}{T_e}\right)^{1/2} \frac{kT_e}{W}, \tag{3}$$

where T_c and T_e are the color and electron temperatures and W is the dilution. In a cool H I region $n_e = 10^{-3}\, n_H$, and then $n_{H^-} = 1.6 \times 10^{-10}\, n_H^2$; the absorption is $1.5 \times 10^{-5}\, n_H^2$ per kiloparsec. This is negligible unless $n_H > 10^2$, i.e., unless the average space density along the line of sight is about one hundred times the Oort limit. In a dense dark nebula of large extent, H^- may have to be considered as a source of absorption; unlike dust, its absorption decreases shortward. However, we cannot suggest any mechanism by which H^- can produce differential extinction in a magnetic field.

Dust is believed to be the most important absorbing constituent in space. Polarization

is observed to be partially correlated with color excess, which is almost surely due to absorption by dust. Contrary to the cases mentioned above, there exists an obvious mechanism that could produce a polarization of light by aligned dust grains and several mechanisms that might align the grains.

3. THE BASIS OF POLARIZATION BY PARAMAGNETIC RELAXATION: SUMMARY OF RESULTS

In this section we treat the physical basis for the alignment of dust grains by a magnetic field and the resulting polarization of starlight, emphasizing the assumptions and approximations made and summarizing the conclusions that can be drawn. The extensive mathematical derivations are postponed until later sections.

3.1. *The equipartition of angular velocity.*—The essential problem that any theory must meet is the necessity of aligning elongated dust grains in spite of the tendency toward rapid spin caused by collisions with the hydrogen atoms or ions in space. In the absence of any aligning torque, the orientation of the grains would be completely random, and, by the equipartition theorem, their mean kinetic energy of rotation, R_e, would be equal to the mean kinetic energy of the atoms of the interstellar gas. Thus, if T denotes the kinetic temperature of the gas and a the average radius of a grain whose internal density is ρ_g, the mean rotational energy is

$$R_e = \tfrac{3}{2} kT = 2.07 \times 10^{-16} T \text{ ergs}. \tag{4}$$

Since its average moment of inertia is $\bar{I} \approx (\frac{8}{3})\, a^5 \rho_g$, the grain would have a root-mean-square angular velocity, the equipartition angular velocity, of

$$\omega_e = \left(\frac{2R_e}{\bar{I}}\right)^{1/2} = 1.57 \times 10^{-8} \left(\frac{T}{a^5 \rho_g}\right)^{1/2} \text{ rad/sec}$$

$$= 5.0 \times 10^5 \text{ rad/sec in } H\,\text{I} \text{ regions} \tag{5}$$

$$= 6.0 \times 10^6 \text{ rad/sec in } H\,\text{II} \text{ regions}.$$

The numerical values are for illustration only. For this purpose we shall use the values $a = 10^{-5}$ cm, $T = 10^2$ in H I regions and 10^4 in H II regions. We shall take n_H, the number of atoms per cubic centimeter, as 10 in H I regions and 1 in H II regions. The internal temperature of the grains will be taken to be $T_g = 10°$ K.

Briefly, these figures were selected for the following reasons. The grain is heated by stellar radiation of energy density sufficient to maintain a black body at about 3° K. The low infrared emissivity of most substances results in the particle's heating until it can radiate as much as a black body at 3° K; an estimate of 10°–25° K seems reasonable. The kinetic temperature of the gas, T, will lie in the range 5,000°–10,000° in regions where hydrogen is ionized (H II regions), as it does in emission nebulae. In neutral hydrogen regions (H I) the temperature can be much lower; Spitzer and Savedoff[9] have computed the energy balance in these regions. It seems probable that $T < 200°$ K; $T \approx 100°$ K seems to be a reasonable value to adopt at present. The density in H I regions may be taken as $n_H = 10$ from studies of interstellar lines.[10] The grain size is discussed in § 4.

3.2. *The alignment of spinning bodies.*—It is possible to align a spinning body by applied torques in several distinct ways. First, one can apply a torque that tends to produce

[9] *Ap. J.*, 111, 593, 1950.

[10] B. Strömgren, *Ap. J.*, 108, 242, 1948.

the desired alignment directly, as in a compass needle; this is the mechanism of Spitzer and Tukey[11, 12] and of Spitzer and Schatzman.[13] However, unless the torque is relatively large, it will be almost completely counterbalanced by the gyroscopic torque, leaving a precession as the only appreciable effect. More precisely, the work done by the applied torque when the body is rotated through a radian in the most favorable direction must be of the order of magnitude of the mean kinetic energy of rotation if alignment is to be produced in this way. When the applied torque is derivable from a potential, it follows that this potential energy must be of the order of kT. Thus, in order to get large enough torques, Spitzer and Tukey suppose the grains to be ferromagnetic and at fairly low kinetic temperatures; if the particles have a radius of 3×10^{-5} cm and if the kinetic temperature of the gas is 10° K, a field of at least 10^{-4} gauss is necessary. Evaporation of the volatile constituents of some grains is suggested as the source of pure ferromagnetic particles, and the very low kinetic temperature required may be attained in favorable regions of dense H I clouds. This hypothesis would naturally receive strong support if the observations should establish that polarization occurs only in neutral hydrogen regions of very low temperature. We adopt the hypothesis that, in general, the grains exist and polarization occurs in both H I and H II regions and that, even in H I regions, the grains are somewhat dielectric rather than pure metallic in character, having high albedo. Absorption of light in H II regions, providing color excess without polarization, would dilute the polarization greatly on the Spitzer and Tukey theory.

In an attempt to work with the small aligning torques characteristic of less specialized paramagnetic and diamagnetic substances and to deal with temperatures that might run as high as 10,000° K—a value appropriate for diffuse emission nebulae or H II regions—Davis and Greenstein[14] originally proposed that the kinetic energy of rotation could be very much less than the mean energy of the hydrogen atoms if, during the long intervals between collisions, the grains were braked almost to zero angular velocity by small torques produced by hysteresis or similar effects. It can be objected, however, that no magnetic hysteresis, in the strict meaning of the term, can occur, since either the ferromagnetic domains will be too small and isolated or the iron atoms will be so diluted by other atoms that there will be no ferromagnetism present. Although there might well be some braking action due to the magnetic analogue of dielectric loss, it would not leave the particles motionless but, rather, spinning rapidly about the magnetic lines of force. Such considerations lead to a second basic method[14] of aligning rigid bodies, a method in which small nonconservative torques are used to damp out nutations and to cause a noncircular precession that will carry the dynamic axis to the desired position. A familiar example is provided by a rapidly spinning top. By far the largest torque is produced by gravity, but this produces only a circular precession, not an alignment in which the top hangs down vertically from its pivot. The very small frictional torques at the pivot damp out the wobbles or nutations and then cause the axis to rise slowly against gravity until the axis is vertical and the top "sleeps." We shall find that, if there is a galactic magnetic field, very small torques should act on the dust grains in such a way that a significant, or indeed an almost complete, alignment might be expected, even though the kinetic energy of rotation is but little affected.

3.3. *The torque due to paramagnetic absorption.*—A consideration of the various torques that might act on a grain of dust rotating in a magnetic field whose strength is of the order of 10^{-5} gauss leads one to conclude (cf. § 8) that the torques due to eddy currents and the Rowland effect are probably completely negligible, the important torque being due to paramagnetic absorption. Paramagnetic absorption is the magnetic analogue of dielectric loss and may be thought of as due to internal friction that hinders the alignment of the atomic dipoles by an applied field. Thus, when a grain rotates with the vector

[11] *Science*, **109**, 461, 1949.

[12] *Ap. J.*, **114**, 187, 1951.

[13] *A.J.*, **54**, 195, 1949.

[14] *Phys. Rev.*, **75**, 1605, 1949; **78**, 84, 1950; *A.J.*, **55**, 71, 1950.

angular velocity ω, the magnetization, M, is dragged along with the material and, as shown in Figure 1, *a*, is not parallel to the field,[15] B.

The analysis of § 6.1 shows that the magnetization is, except for a term that can be ignored,

$$M = \chi'' \omega^{-1} (\omega \times B), \tag{6}$$

where χ'' is the imaginary part of the complex susceptibility and measures the angle through which M is dragged away from B. If V is the volume of the grain, its magnetic moment is VM, and the torque on this dipole in a magnetic field is

$$L = VM \times B = V\chi'' \omega^{-1} (\omega \times B) \times B \tag{7}$$

in Gaussian units. Although these expressions are derived only for grains that rotate about an axis fixed in the grain, we assume that they hold approximately in the actual

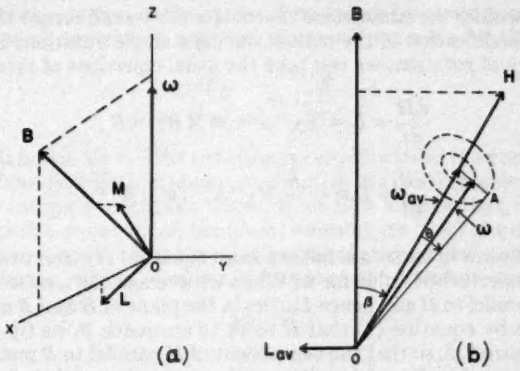

FIG. 1.—*a*, schematic representation of the magnetization, M, and torque, L, produced by rotation with angular velocity ω in a magnetic field, B. (Note that each dotted line locating a vector is parallel to one of the co-ordinates axes.) *b*, the nutational motion of the grain and the average torque.

nutational motion. We suppose (cf. § 4) that the dust grains consist mainly of crystals of such substances as ice, methane, and ammonia with various heavier atoms present as diffuse impurities. In particular, about one atom in one hundred should be iron or a similar atom having a large magnetic moment. Hence the grain will be paramagnetic. Both theory and experiment indicate tentatively (cf. § 6.2) that χ'' should be of the order of

$$\chi'' = 2.5 \times 10^{-12} \frac{\omega}{T_g}, \tag{8}$$

where T_g, the internal temperature of the grain, may be expected to be about 10° K.

3.4. *The motion produced by paramagnetic absorption.*—As a preliminary to determining the effect of this torque on the general nutational motion of the grain, we must first describe the motion of an axially symmetric grain[16] when no torque acts. We shall treat

[15] We describe the magnetic field in terms of B, the magnetic flux density, measured in gauss rather than in terms of H, the magnetic field intensity, measured in oersteds. This follows the current strong trend in physics and is based on the undesirability of taking as primary a quantity defined in terms of nonexistent magnetic poles. In this connection it should be noted (*Nature*, 135, 419, 1935) that at London in 1934 the International Union of Pure and Applied Physics adopted the oersted as the unit of H. Since we do not use H for the magnetic field, we are free to use it for the angular momentum in accordance with a fairly prevalent custom in classical mechanics.

[16] L. Page, *Introduction to Theoretical Physics* (2d ed.; New York: D. Van Nostrand Co., 1933), pp. 133–137.

the grains of dust as spheroids, in order to simplify the mathematical complexities of working with grains of arbitrary shapes. This should not affect our understanding of the phenomena or the order of magnitude of our numerical estimates. Here $\boldsymbol{H}$, the angular momentum vector, is constant, remaining fixed in space, and, as indicated in Figure 1, *b*, the axis of symmetry OA moves on a circular axis about $\boldsymbol{H}$, the grain spinning about OA. The angular velocity vector, $\boldsymbol{\omega}$, is obtained as the sum of the rotations about $\boldsymbol{H}$ and OA. Therefore, $\boldsymbol{\omega}$ moves both in space and through the grain, always lying in the plane of $\boldsymbol{H}$ and OA. We denote this type of motion as "nutational motion," and by "one nutation" we mean one rotation of OA about $\boldsymbol{H}$ as determined by a nonrotating observer. We use the term "precession" to denote a very slow motion of $\boldsymbol{H}$ due to small external torques. The orientation is given by the angles β and θ, where β is the angle between $\boldsymbol{B}$ and $\boldsymbol{H}$ and θ is the angle between $\boldsymbol{H}$ and the axis of symmetry. When there is no torque, these angles remain constant.

We can now consider the cumulative effects of a very small torque that produces only an infinitesimal modification of the motion during a single nutation. Thus, letting R be the kinetic energy of rotation, we can take the usual equations of motion,

$$\frac{d\boldsymbol{H}}{dt} = \boldsymbol{L} = V\chi''\omega^{-1}(\boldsymbol{\omega}\times\boldsymbol{B})\times\boldsymbol{B}, \tag{9}$$

$$\frac{dR}{dt} = \boldsymbol{L}.\boldsymbol{\omega} = -V\chi''\omega^{-1}(\boldsymbol{\omega}\times\boldsymbol{B})^2, \tag{10}$$

where the second form in each case follows from equation (7), and average over a nutation, using the unperturbed value for $\boldsymbol{\omega}$. When we average the torque as given by equation (7), $\boldsymbol{\omega}_{av}$ is parallel to $\boldsymbol{H}$ and hence $\boldsymbol{L}_{av}$ lies in the plane of $\boldsymbol{H}$ and $\boldsymbol{B}$ and is normal to $\boldsymbol{B}$. Therefore, we see by equation (9) that $\boldsymbol{H}$ tends to approach $\boldsymbol{B}$, its tip moving along the dotted line of Figure 1, *b*, so that the component of $\boldsymbol{H}$ parallel to $\boldsymbol{B}$ remains constant and the component normal to $\boldsymbol{B}$ vanishes. Thus β decreases. To see that, for prolate spheroidal grains, θ increases, we note that the right-hand side of equation (10) is negative; hence R decreases, except when $\boldsymbol{\omega}$ is parallel to $\boldsymbol{B}$. Therefore, if such a torque acted long enough, it would make $\boldsymbol{H}$ parallel to $\boldsymbol{B}$ and would make R as small as possible, subject to the condition that the component of $\boldsymbol{H}$ along $\boldsymbol{B}$ remain fixed. To achieve this requires that the grain rotate about its shortest axis or, more precisely, the shortest principal axis of the ellipsoid of inertia. (This may be seen from the Poinsot construction, since there $[2R]^{1/2}/H$ is the distance from the center of the inertia ellipsoid to the invariable plane. See also § 7.1.) Thus the state toward which the torque urges the grains is one in which they spin about $\boldsymbol{B}$ with their long axes normal to $\boldsymbol{B}$, with $\boldsymbol{\omega}$ parallel to $\boldsymbol{H}$ and $\boldsymbol{B}$ so that there is no further decrease in R. The angle β would be zero and θ would be $\pi/2$ for prolate grains. If we start with the randomly oriented equipartition distribution, then the exact calculations of §§ 6 and 7 show that for reasonably eccentric grains the average rate at which the angles approach these end values is of the order of $0.1\chi''B^2/\omega_c a^2$, which is about 10^{-18} rad/sec if $B = 10^{-5}$ gauss and $a = 10^{-5}$ cm.

3.5. *The distribution parameter* F.—This tendency toward orientation due to paramagnetic relaxation is countered by the tendency toward the randomly oriented equipartition distribution due to the collisions of the atoms with the dust grains. The amount by which any particular distribution varies from the equipartition distribution can be measured by a quantity F whose proper definition is given in § 5.2 but which here we visualize in simplified terms. We picture the randomly oriented equipartition distribution as one in which one-third of the grains have their axes of symmetry in each of three mutually perpendicular directions, the directions chosen being the direction OZ of the magnetic field $\boldsymbol{B}$, a line OY normal to $\boldsymbol{B}$ in the plane containing $\boldsymbol{B}$ and the light-beam, and a line OX normal to this plane (cf. Fig. 4). In a nonisotropic distribution we picture

the fraction F of the grains as having been rotated from OZ to OX and OY; thus $\frac{1}{3} - F$ of the grains have their axes of symmetry parallel to $\boldsymbol{B}$ and $\frac{1}{3} + \frac{1}{2}F$ have theirs in each of the perpendicular directions. For example, if the torque due to paramagnetic relaxation has oriented all grains with their axis of symmetry normal to $\boldsymbol{B}$, then F is $\frac{1}{3}$. Both the true definition of F and the simple picture lead to the same expression for the polarization in the case of grains that are small compared to the wave length; hence in this case no error is introduced by the use of the simple description.

3.6. *The kinetic theory of the grains.*—An adequate treatment of the statistical mechanics of a spheroidal dust grain bombarded by atoms and acted upon by a weak torque of a very general character, one not derivable from a potential, will not be attempted here. Instead, we shall give an elementary, inexact treatment from which only estimates of order of magnitude can be hoped for. We start by considering the rate at which an arbitrary distribution would tend toward the equipartition distribution if nothing but collisions affected the motion of the grains. Proceeding by analogy with the equations governing other more completely analyzed systems,[17] we write for the rate at which F is changed

$$\left.\frac{dF}{d\tau}\right|_{\text{coll}} = -\frac{F}{\tau}, \tag{11}$$

where τ is the relaxation time. This equation is certainly valid if we regard it as defining τ as a function of the distribution; our approximation lies in using under all circumstances that same crude estimate of τ given below. If we now assume that, in addition to collisions, certain weak torques act on the grain, we compute in § 7 the rate at which these torques, acting alone, would affect the distribution of orientations and hence the value of F. This rate of change, which, of course, depends on the distribution considered, can be denoted by

$$\left.\frac{dF}{dt}\right|_{\text{torque}}$$

and can be calculated exactly for any specified distribution from the expressions for the average rates of change of θ and β given in § 7.1. If both the torques and the collisions act, the system will approach a steady state, in which the sum of the two rates of change of F must be zero. Hence

$$F = \tau \left.\frac{dF}{dt}\right|_{\text{torque}}. \tag{12}$$

In § 7.2 we calculate F approximately from this equation by using on the right-hand side the equipartition distribution, which is known, rather than the correct, but unknown, steady-state distribution. This approximation should be satisfactory when the torques are so small that the two distributions do not differ greatly; it becomes completely invalid as F approaches $\frac{1}{3}$ or $-\frac{2}{3}$, since then the right-hand side is zero. Equation (12) shows that τ can be pictured as the time available for the applied torques to alter the distribution before collisions stop further drift away from the equipartition distribution.

We must now estimate τ. Because our simple approach could be in error by one or two powers of 10, we shall ignore some numerical factors of the order of unity. Letting m_d denote the mass of a dust grain, its average moment of inertia is $\bar{I} = 0.4a^2m_d$, and its equipartition angular momentum is, by equation (5),

$$H = \bar{I}\omega_e = (0.8\, R_e a^2 m_d)^{1/2}. \tag{13}$$

Since $2a/3$ is the average radius of a collision and $v_H = (2R_e/m_H)^{1/2}$ is the root-mean-

[17] Cf. J. H. Jeans, *The Dynamical Theory of Gases* (1st ed.; Cambridge: At the University Press, 1904), p. 294.

square velocity of the hydrogen atoms (m_H is their mass), the average angular momentum imparted to a grain by a hydrogen atom that sticks to the grain is

$$\Delta H = \tfrac{2}{3} a m_H v_H = \left(\frac{m_H}{m_d}\right)^{1/2} (2R_c^{\frac{4}{3}} a^2 m_d)^{1/2} \approx \left(\frac{m_H}{m_d}\right)^{1/2} H . \tag{14}$$

During the collision, which initially changes the angular velocity but not the orientation of the grain, the vector $\boldsymbol{H}$, shown in Figure 1, *b*, swings through an angle of the order of $(m_H/m_d)^{1/2}$ radians while $\boldsymbol{B}$ and OA remain fixed. Thus the average change of β and θ in a collision is of that order. Since the collisions are random, the root-mean-square change in angle produced by n collisions is $(nm_H/m_d)^{1/2}$, and the number of collisions required to produce a change of one radian is $n = m_d/m_H$. We shall take τ to be the average time required for this number of collisions. Now, for grains containing many molecules, the average time between the impacts of the hydrogen on a particular grain is

$$t_{H,d} = \frac{1}{\pi a^2 v_H n_H} = \frac{2.02 \times 10^{-5}}{a^2 n_H T^{1/2}} \text{ sec} , \tag{15}$$

$$= 2.02 \times 10^3 \text{ sec in both } H\text{ I and } H\text{ II} .$$

Thus we shall use, as the best available estimate of the relaxation time,

$$\tau = \frac{t_{H,d}\, m_d}{m_H} = \frac{5.05 \times 10^{19} \rho_g a}{n_H T^{1/2}} , \tag{16}$$

$$= 5.05 \times 10^{12} \text{ sec in both } H\text{ I and } H\text{ II} .$$

Next consider a criterion that will indicate whether a suggested source of torque is large enough to be worth considering in detail. If a torque is to change the orientation significantly in the time τ, it must change the angular momentum by an amount that is not very small compared to the total angular momentum and hence must not be small compared to

$$L_R = \frac{H}{\tau} = \frac{5.19 \times 10^{-28} a^{5/2} n_H T}{\rho_g^{1/2}} . \tag{17}$$

Another possibility is that the retarding torque could be great enough to reduce the angular velocity imparted to a nonrotating grain in a single collision to zero in the time $t_{H,d}$ between collisions. Then any directional effect whatever would align the grains. But this torque is greater than L_R by a factor of about $(m_d/m_H)^{1/2}$; hence we do not consider it further.[18]

3.7. *The approximate value of* F.—On the basis of this argument we conclude (cf. §§ 7.2 and 7.3) that for prolate spheroidal grains of reasonable eccentricity and for small deviations from the equipartition distribution

$$F \doteq F_l \quad \text{if} \quad |F_l| \ll \tfrac{1}{3} , \tag{18}$$

[18] We are indebted to Dr. Spitzer for pointing out a correction to τ. He has shown (*Ap. J.*, **93**, 369, 1941) that in an H II region more electrons than protons strike an uncharged grain because of the higher velocity of the former. Thus an electrostatic potential is built up that attracts protons and makes the collision probabilities equal. The effective cross-section of the grain for protons and the average angular momentum imparted per collision are increased by a factor of about 3.5. Therefore, we should decrease $t_{H,d}$ and τ and increase L_R in H II regions, with a consequent increase by a factor of $(3.5)^{3/4} = 2.6$ in the magnetic fields required by our mechanism.

where we have introduced, as a parameter measuring the relative importance of collisions and paramagnetic relaxation,

$$F_l = \tau \left.\frac{dF}{dt}\right|_{\text{torque}}^{\text{equipartition}} = \frac{1.6 \times 10^{10} \chi'' a^{3/2} \rho_g^{1/2} B^2}{T n_H} = \frac{6.3 \times 10^6 B^2}{a T^{1/2} n_H T_g} . \tag{19}$$

$$F_l = 6.3 \times 10^6 B^2 \text{ in both } H\text{ I} \text{ and } H\text{ II} \text{ regions} .$$

When F_l is large, the deviation from the equipartition distribution is large and F approaches $\frac{1}{3}$, as discussed above; thus

$$F = \tfrac{1}{3} \quad \text{if} \quad |F_l| \gg \tfrac{1}{3} . \tag{20}$$

For intermediate values of F_l we should get a satisfactory rough approximation by using equation (18) when $F_l < \frac{1}{3}$ and equation (20) when $F_l > \frac{1}{3}$, although any reasonable interpolation formula should be an improvement.

3.8. *The approximate polarization expected.*—We now turn to a consideration of the effect on a beam of light of dust grains oriented in this way. We wish to compare the weakening due to absorption and scattering of a beam whose plane of vibration contains B with that of a beam whose plane of vibration is turned through 90° and with that of unpolarized light; we are not interested in making absolute calculations of any of these quantities. It has been established that nearly spherical dust grains, mainly dielectric in composition, can produce the observed interstellar reddening and absorption with very moderate space density. It is generally assumed that a wide range of grain sizes exists, with the maximum contribution to the extinction produced by sizes slightly less than a wave length. Exact theoretical results and extensive computations exist for dielectric and metallic spherical grains. At present, exact computations for spheroidal grains much smaller than the wave length can be based on the work of R. Gans;[19] the theory of infinite cylinders of any size has been developed by P. Wellman[20] and H. C. van de Hulst.[21] We know of no usable theoretical or experimental data on the effects of spheroidal grains whose diameter is comparable to the wave length. Accordingly, we shall, of necessity, use the expressions for very small grains in the hope that this will give us the order of magnitude of the expected effect. We obviously cannot hope thus to predict the correct wavelength dependence of the polarization; a consideration either of the results of Wellman and of van de Hulst for large cylinders or of the fact that very large grains will produce only shadows with no polarization indicates that the ratio of polarization to total absorption deduced from small grains is likely to be too large.

In § 5.1 detailed calculations for a small prolate spheroidal grain show that it weakens a beam of light so polarized that its electric vector is parallel to the long axis of the grain more than light polarized at right angles, in the ratio σ_A/σ_T. The values obtained for this ratio are given in Table 2; they range from 1.33 for dielectric grains having a ratio of axes $x = \frac{5}{3}$, to 1.95 for dielectric grains having $x = 5.02$, and to 4.08 for metallic grains having $x = 5.02$. The effect of a small grain inclined at any specified angle to the light is easily expressed in terms of σ_A/σ_T, a simplification of the theory that does not hold for the larger grains. Hence we can compute (cf. § 5.3) the effect of a distribution of small grains whose orientation is specified by F. The most interesting result is that, if the grains are all of the same size, the ratio of the polarization to the total absorption is

$$\frac{p}{A_{pg}} = 2.07 F \cos^2 \nu \, \frac{(\sigma_A/\sigma_T) - 1}{(\sigma_A/\sigma_T) + 2} , \tag{21}$$

[19] *Ann. d. Phys.*, **37**, 881, 1912.

[20] *Zs. f. Ap.*, **14**, 195, 1937.

[21] *Ap. J.*, **112**, 1, 1950.

where $(\pi/2) - \nu$ is the angle between the magnetic field and the beam of light.

3.9. *Interpretation of results.*—According to equation (2), the left side of equation (21) must be at least 0.02 in some regions. Suppose that the grains are completely aligned, with their long axes normal to $\boldsymbol{B}$ so that $F = \frac{1}{3}$ and take $\nu = 0$, then $\sigma_A/\sigma_T = 1.09$. The values of the ratio quoted above and in Table 2 show that this condition is easily met by grains of quite moderate eccentricity. If the grains have considerable eccentricity, there is a fairly large factor of safety that could be used to allow for the fact that σ_A/σ_T is considerably less for large grains than for small. Alternatively, many of the grains might be spherical or of a size that was not easily aligned. It follows from equations (19) and (20) that F will be of the order of $\frac{1}{3}$, provided that $B \geqslant 2.3 \times 10^{-6}$ gauss for our standard illustrative conditions or $B \geqslant 4.0 \times 10^{-5}$ gauss for $a = 3 \times 10^{-5}$ cm, other conditions being unchanged. If the effect of charge in *H* II regions is considered,[18] this becomes $B \geqslant 10^{-4}$ gauss. With lower temperatures or lower hydrogen density or smaller particles, smaller fields or a smaller value of χ'' would suffice. On the other hand, if we wish to assume that the mean σ_A/σ_T of all grains is, say, 1.33, then $F = \frac{1}{5}$ and B would be 2.3×10^{-5} gauss if $a = 3 \times 10^{-5}$ cm. Thus the proposed mechanism seems adequate to explain quantitatively the observed polarization with fields somewhere in the range from 10^{-4} to 10^{-5} gauss.

Throughout the above discussion we have, for simplicity, assumed that the ellipsoids are prolate. If they are oblate, neither the plane of polarization nor the order of magnitude of the effect is changed. Equation (21) holds, but both $(\sigma_A/\sigma_T) - 1$ and F are negative, the sign of equation (19) being changed. The limiting value for complete alignment is $F = -\frac{2}{3}$, so that the limits in equations (18) and (20) require a corresponding change.

Without undertaking an extensive interpretation of the observations in terms of this theory, we may draw a few quite speculative inferences as to the probable nature of the magnetic field. The first is that the observed uniformity in the planes of vibration mentioned in § 1 (ii) implies a corresponding uniformity, on the basis of this theory, in the direction of the magnetic field averaged in space and time. The average is to be taken over a time of the order of τ, which is about 1.7×10^5 years, since the orientation of the grains will not follow shorter-period fluctuations in the field. The light observed often travels 1000 psc and must traverse several independent complexes of dust and gas. The detailed structure of the field cannot deviate from point to point too wildly from the average, or the ratio of polarization to reddening would be smaller than that observed. Thus the very irregular magnetic field proposed by E. Fermi[22] in his theory of the origin of cosmic rays seems less plausible than a nearly uniform field. Perhaps the observed motion of gas clouds is to be accounted for by magneto-hydrodynamic waves,[23] in which the lines of force do not deviate far from their original direction, the gas moving with the lines of force like beads on a taut vibrating string rather than at random.

The second point is that, in our theory, $\boldsymbol{B}$ is normal to the long axis of the grains and to the conventional plane of polarization (not the plane of vibration) of the light and cannot lie too close to the line of sight. Thus one can get a suggestion of the path of the lines of force from Hall and Mikesell's[6] Figures 4–7, showing the planes of polarization, and from the fact that the lines must be continuous. The suggestion seems to be that for galactic longitudes 80°–120° or perhaps even to 170° the lines of force lie in the plane of the galaxy, possibly along a spiral arm of dust and gas. This inference is consistent with the remark of Hall and Mikesell[6] that in Cygnus, where they observe a relatively small and randomly oriented polarization, one may be looking along a spiral arm. For in this case the component of $\boldsymbol{B}$ normal to the line of sight would be small and randomly oriented. A theory of the nature of the interstellar magnetic field proposed by Schlüter

[22] *Phys. Rev.*, **75**, 1169, 1949.

[23] H. Alfvén, *Cosmical Electrodynamics* (Oxford: Clarendon Press, 1950), pp. 76–88.

and Biermann[24] indicates that the magnetic field will affect the nature of turbulent motions. The smaller eddies will be rapidly damped out. The larger eddies will presumably still show the effect of the anisotropic driving force, i.e., galactic rotation; hence the lines of force would be in the galactic plane. A field in which the lines of $\boldsymbol{B}$ make random small-scale whirls in the galactic plane would produce a polarization of the type observed if our theory is correct. The magnitude of the polarization for a given average field strength would be half that produced by a uniform field normal to the line of sight.

The tentative value of 10^{-4} to 10^{-5} gauss for B in regions of maximum polarization suggested by our theory does not seem unreasonable if we consider the energies available. The corresponding energy densities are $E_B = B^2/8\pi \approx 4 \times 10^{-10}$ to 4×10^{-12} erg/cm^3 or 4×10^{-31} to 4×10^{-33} gm/cm^3. This is so much less than the mass density of interstellar matter, $\rho \approx 10^{-24}$ gm/cm^3, that it produces no gravitational effects. The larger value of E_B is of the order of the density of kinetic energy due to galactic rotation, $E_R = \frac{1}{2}\rho v_{\text{rot}}^2 \approx 8 \times 10^{-10}$ erg/cm^3 if $v_{\text{rot}} \approx 3 \times 10^7$ cm/sec; thus the mechanism that set the galaxy rotating would have enough energy to produce the magnetic field. If there is any galactic magnetic field at all, it follows from the arguments of Alfvén, as discussed by Fermi,[22] that it will be increased by the peculiar motion of the interstellar gas clouds until $E_B \approx E_p = \frac{1}{2}\rho \bar{v}_p^2 \approx 3 \times 10^{-12}$ erg/cm^3 if $\bar{v}_p \approx 2 \times 10^6$ cm/sec. The scale of irregularity in $\boldsymbol{B}$ will be that of the peculiar motions of the gas clouds. If the magnetic field is to have the uniformity we ascribe to it on the basis of the observations described in § 1 (ii), then it must dominate the peculiar motions, requiring that $E_B \gg E_p$. This supports a value of B of the order of 10^{-4} gauss for the regions where polarization is observed.

4. COMPOSITION, SIZE, AND PHYSICAL PROPERTIES OF THE DUST GRAINS

Special theories exist for the growth of interstellar grains out of the interstellar gas. It is generally assumed that the abundance of the elements in space is the same as on the surface of the stars and that the particles grow by successive random captures of the interstellar atoms on a small nucleus. Hydrogen and helium are overwhelmingly abundant, but, even at the low temperatures of the solid grains, they would evaporate rather than remain in the solid, unless chemically bound. From Harrison Brown's compilation of astrophysical and terrestrial abundance data[25] we adopt in Table 1 the abundances of

TABLE 1

ADOPTED ABUNDANCES OF THE ELEMENTS IN SOLID GRAINS

Element	Atomic Weight	Stellar Abundance by Number	Weight Bound in Grain	Percentage by Weight	Percentage by Number of Atoms
H	1	1600	6.0	14	72
C	12	0.36	4.3	10	4
N	14	0.73	10.3	23	9
O	16	1.00	16.0	36	12
Mg	24	0.040	0.96	2	0.5
Al	27	0.004	0.11	0.3	0.05
Si	28	0.046	1.27	3	0.6
S	32	0.016	0.51	1	0.2
Fe	56	0.083	4.7	11	1.0
Ni	58	0.006	0.34	0.8	0.07

[24] *Zs. f. Naturforsch.*, **5a**, 237, 1950.

[25] *Rev. Mod. Phys.*, **21**, 625, 1949.

interest here. In the fourth column we estimate the contribution to the weight of the grain of elements bound chemically. Except for hydrogen, this is obtained from the abundance times the weight; for hydrogen it is given by the number that could be chemically bound, mainly as H_2O, NH_3, and CH_4, etc. Only 0.4 per cent of the original hydrogen is thus permanently bound. If H_2 is formed catalytically in the particle, a small part may be absorbed and retained in the solid lattice and on the surface. This amount, however, would be less than the number of other molecules in the solid, since H, H_2, and He tend to evaporate. In the next to the last column is given the final abundance by weight. We find that most of the mass is in the form of compounds based on C, N, O, and H (H_2O, NH_3, CH_4) and that a wide variety of compounds of lower abundance could be formed involving Fe, Mg, Al, Si, and S. We shall not consider grains in which the Fe is so concentrated that the grains are ferromagnetic, a case considered by Spitzer and Tukey.[12] Whether more complex compounds will, in fact, occur depends on the evolution of the particle. If the solid is bombarded with heavy elements at thermal energies in an H II region, collisions involving several electron-volts occur. Such heavy atoms entering the solid may have sufficient energy of activation to produce chemical combinations. Further, the continuous local heating by proton and perhaps by cosmic-ray bombardment favors chemical combination and migration of ions to begin the process of crystal formation. It is quite possible that moderately complex molecules are formed and that the grains show the irregular, but generally nonspherical, character of terrestrial solids. The major difference from rocks, of course, is the preponderance of the frozen solid state of ordinarily gaseous compounds of hydrogen. If only simple compounds are formed, approximately 4 per cent would contain Fe. Whether or not the shape of grains formed by random collision would be spherical cannot be stated in the presence of these complex mixtures. In the growth of pure substances—say, solidified gases—it is very likely that semicrystalline structures would occur and that the final grains would be appreciably elongated. Another serious question would be whether the grains are compact solids of moderate density and normal indices of refraction or whether they would grow as open, spongelike flakes (similar to snow or some industrial metallic smoke or dust) which would have very low density and low index of refraction. Assuming the grain to be compact in order to provide sufficient mechanical strength to withstand the rapid rotation, we find from Table 1 that it is a dielectric of low index of refraction—say, 1.2 to 1.4—of low density, ρ_v, which we take as unity, and with a small imaginary component in the index of refraction, perhaps of the order of 0.05, due to iron and its compounds.

Spherical dust grains of radius less than 10^{-2} cm have sufficiently large mass-absorption coefficients to account for the interstellar absorption; a size somewhat less than a wave length of light will also produce the correct space reddening. The more recent theoretical work[26, 27, 28] has emphasized the importance of a wide frequency distribution of sizes, with numbers increasing rapidly as the size decreases. The proper choice of the typical grain size depends on the nature of the frequency distribution and may differ in the theory of interstellar polarization from the choice in the theory of reddening. H. C. van de Hulst[28] has developed a theory of the frequency distribution and applied it to the observed interstellar reddening. The number of dielectric grains ($m = \frac{4}{3}$) varies as $f(a/a_1)da/a_1$; his Table 10 and solution 15 of his Table 14 contain the details. The value of $f(a/a_1) = 0.064$ with $a = a_1 = 4 \times 10^{-5}$ cm, the value of $f(a/a_1) \approx 1$ for $a < 2 \times 10^{-5}$ cm. The mean radius would be very small, but the size most effective in producing interstellar extinction is near 4×10^{-5} cm. The small spheroid theory of Gans does not hold if $\alpha = 2\pi a/\lambda > 1$. We show below that the extinction by the grains may be metallic in character if $\alpha < 1$. If this is confirmed, the required modification of the frequency distribution will probably give a most effective size different from a_1 and between 10^{-5} and

[26] J. L. Greenstein, *Harvard Circ.*, No. 422, 1938.

[27] J. L. Greenstein, *Ap. J.*, **104**, 403, 1946.

[28] H. C. van de Hulst, *Rech. Astr. Obs. Utrecht*, Vol. 11, Part II, 1949.

3×10^{-5} cm. However, we shall see that there are many serious problems in the transmission coefficient of partially oriented spheroids if $a > 1$; since we shall not now try to explain the wave-length dependence of the polarization, it will be simplest if we limit ourselves to the orientation problem for typical particles with $a = 10^{-5}$ cm, and use the order-of-magnitude polarization predicted by the electric-dipole scattering of pure dielectric spheroids. Van de Hulst[21] has found a possible fit to both the wave-length dependence of polarization and the absorption for infinite cylinders of radius 4×10^{-5} cm.

One comment may be made on the basis of Table 1, which predicts a small but finite complex index of refraction, due to the 4 per cent abundance of iron by number of molecules. The complex index of refraction can then be roughly estimated as

$$m = n - ik = 1.4 - 0.05i\,. \tag{22}$$

Van de Hulst[28] has shown that the phase shift of a ray through the center of a sphere is

$$\rho^* = 2a\,(n-1) - 2a\,(n-1)\,i \tan\beta\,, \tag{23}$$

$$\tan\beta = \frac{k}{n-1}\,. \tag{24}$$

The complex part of ρ^* represents a decay of the wave and permits an evaluation of the true absorption within the particle. For our case β is 7°; if one examines his Figure 5, it is clear that the grain has a small but finite absorption, as well as scattering; more importantly, the high maximum found in the extinction coefficient near $2a(m-1) = 4$ and the minimum near $2a(m-1) = 8$ both nearly disappear because of the disappearance of resonance effects. Furthermore, if $a < 1$, it is possible that the metallic absorption by the particle will be important. Greenstein[26] showed that the ratio of the absorption K to the scattering S by a grain, if $k < n$ and $a < 1$, is

$$\frac{K}{S} = \frac{9}{a^3}\frac{nk}{(n^2-1)^2}\,. \tag{25}$$

If we adopt the 4 per cent iron abundance, with the refractive index $m = 1.4 - 0.05i$, we find that K is of the order of, or larger than, S when a is less than 0.88. Our approximation in equation (25) is not valid for so large an a, but it is clear that metallic absorption becomes important near this point; for visible radiation, this size corresponds to 8×10^{-6} cm. We must then expect particles at the maximum of the frequency function to be effectively metallic absorbers, with an extinction coefficient nearly proportional to $1/\lambda$, while those of larger size act as dielectric scattering agents; since the latter have $a > 1$, we expect a wave-length dependence also near $1/\lambda$ or slower. Thus, rather than the $1/\lambda^4$ dielectric scattering of very small dielectric spheres, the present theory essentially predicts the $1/\lambda$ law over a wide range of wave length. These complexities will have to be taken into account when an attempt is made to explain the small wave-length dependence of the polarization.

5. THE POLARIZATION PRODUCED BY ORIENTED DUST GRAINS

The discussion of the previous sections indicates that we should consider in detail the polarization that would be produced by nonspherical, partially oriented grains of dust. Rather than consider mixtures of grains of arbitrary and varying shapes and chemical composition, we shall consider a model in which all grains are spheroids of the same eccentricity and composition. The resulting expressions for the polarization would be needed in almost any theory in which the polarization is produced by oriented dust grains.

5.1. *The scattering and absorption of a single spheroidal particle.*—R. Gans[19] has treated the absorption and scattering of light by small dielectric spheroids. His procedure is to

compute the induced dipole moment on the assumption that the electric field is uniform over the particle and then to compute the absorption and scattering from this. Thus it is essential that the method be applied only to particles small compared to the wave length and of a composition such that the magnetic component of the electromagnetic wave is unimportant. Define σ_A to be the extinction cross-section in square centimeters of a single spheroid whose axis of symmetry is parallel to the electric vector in the light; similarly, define σ_T to be the extinction cross-section for a spheroid whose transverse axis is parallel to the electric vector, i.e., whose axis of symmetry is normal to the electric vector. The procedure used to compute σ_A and σ_T may be outlined as follows: Let $2a_A$ be the length of the axis of symmetry, $2a_T$ that of the transverse axis, and $x = a_A/a_T$ the ratio of the axes. Then the so-called "depolarization factors" are, in terms of x rather than the more conventional eccentricity e, used by Gans:

$$P = \frac{4\pi}{x^2-1}\left[\frac{x}{(x^2-1)^{1/2}}\cosh^{-1}x - 1\right] \text{for prolate spheroids}, \tag{26}$$

$$P = \frac{4\pi}{1-x^2}\left[1 - \frac{x}{(1-x^2)^{1/2}}\cos^{-1}x\right] \text{for oblate spheroids}, \tag{27}$$

$$P' = 2\pi - \tfrac{1}{2}P. \tag{28}$$

Let m be the complex index of refraction and V the volume of the particle. Two cases are to be considered. In the first, the dielectric case, $m = n$ is real, and the process is one of pure scattering. Here

$$\sigma_A = \frac{128\pi^5 a^6}{3\lambda^4}\left[\frac{m^2-1}{3+(m^2-1)(3P/4\pi)}\right]^2 = \frac{128\pi^5 a^6}{3\lambda^4}G_A, \tag{29}$$

where G_A has been introduced as a convenient abbreviation defined by equation (29). In the second, the metallic case, m is complex. If its imaginary part is large, the process is one of pure absorption with negligible scattering, and

$$\sigma_A = \frac{8\pi^2 a^3}{\lambda} Im\left[\frac{1-m^2}{3+(m^2-1)(3P/4\pi)}\right] = \frac{8\pi^2 a^3}{\lambda}H_A. \tag{30}$$

The quantities σ_T, G_T, and H_T are obtained by replacing P by P'. Equation (29) shows an essential similarity to Rayleigh scattering with the cross-section proportional to a^6/λ^4; equation (30) shows metallic absorption with a cross-section proportional to a^3/λ, if we neglect the variation of n with λ. In either case polarization exists if $P \neq P'$. Table 2 contains the detailed results of some computations, with final results for oblate spheroids. The ratio σ_A/σ_T is given, together with γ the ratio of the moments of inertia, Γ, and $100\Gamma\rho_g Va^2/I$, quantities required below in the theory of the orientation of the spheroids. These dynamic parameters are computed by means of equations (91)–(94). Note that the index of refraction adopted for the metallic case involves a large value of the absorptivity, k. A trial computation for $m = 2^{1/2}(1 - 0.5i)$ gave about half the polarization. Table 2 shows that completely aligned small particles give appreciably different extinction coefficients in two planes of polarization when the deviation from a sphere is quite small. A ratio of axes of 1.091 gives about 2.7 per cent polarization, p, for the dielectric and 7.2 per cent polarization for the metallic particle if the absorption is 1 mag. This is further discussed in § 3.9.

The variation of σ_A and σ_T with wave length should properly include the variation of the index of refraction with wave length. A trial computation made with $x = 1.25$ showed that a large change of refractive index, $\delta n = 0.01$, changed $(\sigma_A/\sigma_T) - 1$ by 3 per cent. This is small compared to the corresponding change in the $1/\lambda^4$ or $1/\lambda$ factor in

each σ. Since, in the dipole approximation for small grains, $(\sigma_A/\sigma_T) - 1$ measures p/A and p/E_1, where p is the polarization, A the absorption, and E_1 the color excess, this might lead one to expect that these ratios would be essentially independent of the wave length for any reasonable variation in the index of refraction. Since we know that A varies roughly as $1/\lambda$, an observable change in p could be expected from blue to infrared. This is not in agreement with Hiltner's observations,[3] thus proving that the dipole-scattering approximation is insufficient. Spheroids with $2\pi a/\lambda$ near unity would have a smaller

TABLE 2

EXTINCTION CROSS-SECTIONS AND INERTIAL PROPERTIES OF SMALL GRAINS

	Prolate Spheroids					
e	0	0.4	0.8	0.9	0.95	0.98
$a_A/a_T=x$	1	1.091	1.667	2.294	3.203	5.025
G_A for $n=2^{1/2}$	0.06250	0.06487	0.07590	0.08416	0.09175	0.09973
G_T for $n=2^{1/2}$	0.06250	0.06140	0.05707	0.05471	0.05285	0.05126
σ_A/σ_T for $n=2^{1/2}$	1.000	1.058	1.328	1.538	1.738	1.945
H_A for $m=2^{1/2}(1-i)$	0.6000	0.6612	1.0105	1.2352	1.3739	1.4163
H_T for $m=2^{1/2}(1-i)$	0.6000	0.5714	0.4640	0.4135	0.3764	0.3465
σ_A/σ_T for $m=2^{1/2}(1-i)$	1.000	1.158	2.18	2.99	3.65	4.08
γ	1	1.095	1.889	3.132	5.628	13.126
$100\,\Gamma$	0	0.303	1.816	1.888	1.800	1.358
$100\,\Gamma\rho_s\,Va^2/I$	0	0.804	6.38	8.16	9.76	9.97
	Oblate Spheroids					
e	0	0.4	0.8	0.9	0.95	0.98
x	1	0.916	0.600	0.436	0.312	0.199
σ_A/σ_T for $n=2^{1/2}$	1	0.952	0.732	0.605	0.505	0.398
σ_A/σ_T for $m=2^{1/2}(1-i)$	1	0.870	0.422	0.258	0.169	0.105
γ	1	0.920	0.680	0.595	0.549	0.520
$-100\,\Gamma$	0	0.311	1.71	2.55	3.09	3.48
$-100\,\Gamma\rho_s\,Va^2/I$	0	0.732	3.02	3.66	3.56	2.96

polarization but would also have a smaller change of polarization with wave length, as van de Hulst has shown for semi-infinite cylinders.[21] It is difficult to put these arguments on a quantitative basis at present, both because of the lack of theoretical computations for spheroids near a wave length in size and because then it is much more difficult to treat obliquely inclined grains.

Consider, now, a spheroid whose axis of symmetry makes the angle α (not to be confused with $2\pi a/\lambda$) with the electric vector of the radiation; let $\sigma(\alpha)$ be its extinction coefficient. In the approximation in which $\sigma(\alpha)$ is computed from the dipole moment induced by a quasi-static field that is uniform over the grain, one can resolve the electric field into components along and normal to the axis of symmetry and easily find that

$$\sigma(\alpha) = \sigma_A \cos^2\alpha + \sigma_T \sin^2\alpha = \sigma_T + (\sigma_A - \sigma_T)\cos^2\alpha\,. \tag{31}$$

If $a \gtrsim \lambda$, this derivation breaks down; indeed, even the definition of $\sigma(\alpha)$ breaks down, since the angle between the direction of propagation and the axis of symmetry must be

considered. In this case a qualitative understanding of the situation can be obtained from a consideration of the three extinction coefficients, σ_E, σ_B, and σ_S, where the subscript indicates that the axis of symmetry is parallel, respectively, to $\boldsymbol{E}$, the electric vector of the wave; to $\boldsymbol{B}$, the magnetic vector; and to $\boldsymbol{S}$, the propagation vector. The complexity of the situation is apparent when one realizes that, if $a \ll \lambda$, $\sigma_E = \sigma_A$, $\sigma_B = \sigma_S = \sigma_T$, while, if $a \gg \lambda$, σ is measured by the area of the shadow and diffraction pattern, and $\sigma_E = \sigma_B \neq \sigma_S$. A schematic representation of the situation for prolate spheroids is shown in Figure 2, with the assumption that the index of refraction has a small complex part. We shall see below that, if all the grains are aligned in one of the three directions, the total absorption is proportional to $\frac{1}{3}(\sigma_E + \sigma_B + \sigma_S)$ but that the polarization is proportional to $\sigma_E - \sigma_B$. Thus we see from the figure that A and p have the same dependence on λ for $a \ll \lambda$, that p is zero and A is independent of λ for $a \gg \lambda$, and that there is a range near $\lambda = 2\pi a$ in which p is independent of λ because the σ_E and σ_B curves are parallel, while A varies with λ because all three curves are rising.

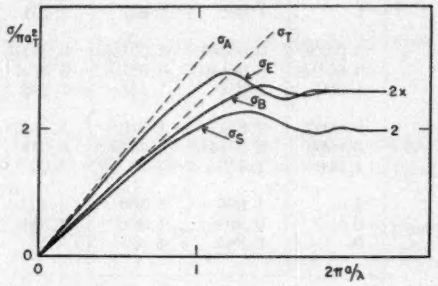

FIG. 2.—A schematic representation of the extinction cross-sections of a prolate spheroid; each cross-section, σ, is expressed in units of πa_1^2; $x = a_A/a_T$.

Returning to the case in which $\lambda \gg a$, we next ask: What is the average effect of a spinning grain upon which no torques act? Then $\boldsymbol{H}$, the angular momentum of the grain, will remain fixed in space and the axis of symmetry, OA, will nutate around it, making the constant angle θ with $\boldsymbol{H}$ and moving at a constant rate around $\boldsymbol{H}$ in the circular cone indicated by the dotted circle in Figure 3. We wish to average over all positions of OA on this cone. Before we can do this, we must make more definite the situation contemplated. We suppose that $\boldsymbol{B}$ is a uniform field that lays down a unique direction in space and that exerts small torques on the grains. We shall later take it to be a magnetic field, but for the present its only purpose is to specify a unique direction. We consider a beam of light for which $\boldsymbol{S}$, the direction of propagation, makes the angle $(\pi/2) + \nu$ with $\boldsymbol{B}$. To locate $\boldsymbol{H}$, the angular momentum, we give β, its polar angle, and ϕ, its azimuthal angle measured from the plane of $\boldsymbol{B}$ and $\boldsymbol{S}$. To locate OA, the axis of symmetry, we use the polar and azimuthal angles θ and ψ, respectively, with respect to $\boldsymbol{H}$ as pole. Then, if no torques act on an axially symmetric grain, ϕ, β, and θ remain constant while ψ increases at a uniform rate. By "one nutation" we shall mean one revolution of A about $\boldsymbol{H}$, i.e., a motion in which ψ increases by 2π. In order to get the average effect of a grain, we average over a nutation. Also, by the symmetry of the situation, even if the presence of $\boldsymbol{B}$ alters the distribution of orientations of OA over β and θ and produces a precession in which ϕ varies slowly, all values of ϕ are equally likely. Hence we shall average over ϕ and ψ.

We see from equation (31) that the quantity to be averaged is the square of the cosine of the angle between the axis of symmetry and $\boldsymbol{E}$, the electric vector in the plane-polarized light. Hence we must resolve the light into two plane-polarized components, one of

intensity I_π, with its $E = E_\pi$ parallel to the plane of B and S; the other of intensity I_σ, with its $E = E_\sigma$ perpendicular to B, as shown in Figure 4. Let α_π denote the angle between E_π and OA, α_σ the angle between E_σ and OA. Hence, by equation (31), the average energy removed from I_π by the grain is

$$I_\pi[\sigma_T + (\sigma_A - \sigma_T)\overline{\cos^2 \alpha_\pi}] = I_\pi \sigma_\pi(\beta, \theta, \nu, a), \tag{32}$$

where the bar indicates the average over ϕ and ψ and the equation defines σ_π. Likewise the average energy removed from I_σ is

$$I_\sigma[\sigma_T + (\sigma_A - \sigma_T)\overline{\cos^2 \alpha_\sigma}] = I_\sigma \sigma_\sigma(\beta, \theta, \nu, a), \tag{33}$$

where σ_σ is a coefficient giving the mean effect of a single grain on a light-wave whose plane of vibration is normal to B.

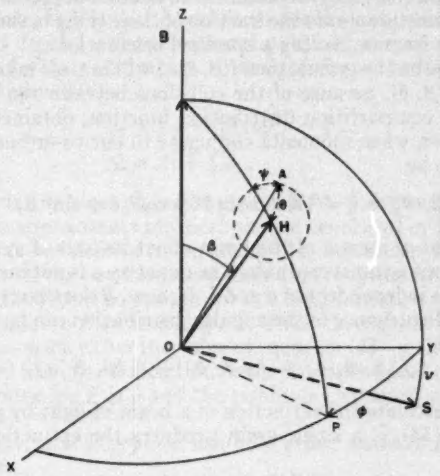

FIG. 3.—The angles defining the orientation

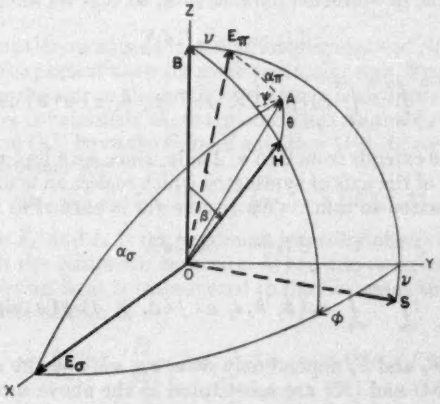

FIG. 4.—The orientation of the electric vector of the radiation for the two planes of polarization

By a straightforward application of analytic geometry and spherical trigonometry, the averages in equations (32) and (33) can be evaluated, giving (cf. Appendix 1)

$$\sigma_\sigma = \sigma_T + (\sigma_A - \sigma_T)\,\tfrac{1}{2}\,(1 - \cos^2\beta\,\cos^2\theta - \tfrac{1}{2}\sin^2\beta\,\sin^2\theta)\,, \tag{34}$$

$$\sigma_\pi = [\sigma_T + (\sigma_A - \sigma_T)\,(\cos^2\beta\,\cos^2\theta + \tfrac{1}{2}\sin^2\beta\,\sin^2\theta)]\cos^2\nu + \sigma_\sigma \sin^2\nu\,. \tag{35}$$

5.2. *The effect of many grains.*—Let y be the distance measured along the light-ray in centimeters. Let

$$f(\beta,\ \theta,\ a)\ \rho(a)\ n_d(y)\ d\beta\ d\theta\ da \tag{36}$$

be the number of grains of dust per cubic centimeter with mean radius a in the range from a to $a + da$, and so oriented that β lies between β and $\beta + d\beta$ and θ lies in the range from θ to $\theta + d\theta$. In equation (36), $n_d(y)$ represents the number of grains of all sizes and orientations per cubic centimeter; $\rho(a)da$ the fraction of these lying in the indicated size range; and $f(\beta, \theta, a)d\beta d\theta$ the fraction having a specified orientation.

If β exerts no torque on the grains, then $f(\beta, \theta, a)$ will in time take on the equipartition value, denoted by $f_e(\beta, \theta)$, because of the collisions between the grains and hydrogen atoms and ions. The equipartition distribution function, obtained from the Maxwell-Boltzmann distribution when momenta conjugate to our co-ordinates are used (cf. Appendix 2), is found to be

$$f_e(\beta,\ \theta) = \tfrac{1}{2}\gamma^{1/2}\sin\beta\,\sin\theta\,(\gamma\cos^2\theta + \sin^2\theta)^{-3/2}\,, \tag{37}$$

where I is the moment of inertia of the grain about its axis of symmetry and γI is its moment of inertia about a transverse axis. The quantity a is not included as an argument of f_e, since the latter is independent of a and I. If, now, $\boldsymbol{B}$ does exert a small torque on the grains, the resulting disturbance in the angular distribution can be specified by the function $f_1(\beta, \theta, a)$, where

$$f(\beta,\ \theta,\ a) = f_e(\beta,\ \theta) + f_1(\beta,\ \theta,\ a)\,. \tag{38}$$

Next we wish to calculate the extinction of a beam of light by grains distributed according to equation (38), if a single grain produces the extinction described in § 5.1. Define N by

$$dN = n_d(y)\,dy\,, \tag{39}$$

and measure distance along the beam by N rather than by y. The light-loss of a beam polarized with its plane of vibration parallel to $\boldsymbol{B}$, so that its intensity is I_π, is

$$dI_\pi = -S_\pi I_\pi dN\,, \tag{40}$$

where

$$S_\pi = \int_0^\infty \int_0^{\pi/2} \int_0^\pi \sigma_\pi(\beta,\ \theta, \nu,\ a)\, f(\beta,\ \theta,\ a)\, \rho(a)\, d\beta d\theta d\theta da\,. \tag{41}$$

The integration over θ extends from 0 to $\pi/2$ only, since we adopt the convention that A is always on that end of the axis of symmetry which makes an acute angle with $\boldsymbol{H}$. Likewise, for a beam polarized so that its electric vector is normal to $\boldsymbol{B}$,

$$dI_\sigma = -S_\sigma I_\sigma dN\,, \tag{42}$$

with

$$S_\sigma = \int_0^\infty \int_0^{\pi/2} \int_0^\pi \sigma_\sigma(\beta,\ \theta, \nu,\ a)\, f(\beta,\ \theta,\ a)\, \rho(a)\, d\beta d\theta d\theta da\,. \tag{43}$$

It may be seen that S_π and S_σ depend only on ν, σ_A, σ_T, and the distribution function.

When equations (34) and (35) are substituted in the above integrals, rather formidable-appearing expressions are obtained. However, the integrals over the angles can be

separated from the integrations over a and the results expressed in terms of three functions, defined as follows:

$$F(a) = -\int_0^{\pi/2}\int_0^{\pi} (\cos^2\beta\cos^2\theta + \tfrac{1}{2}\sin^2\beta\sin^2\theta)\, f_1(\beta, \theta, a)\, d\beta d\theta\,, \tag{44}$$

$$S_t = \frac{1}{3}\int_0^{\infty} (2\sigma_T + \sigma_A)\,\rho(a)\,da\,, \tag{45}$$

$$S_p = \frac{3}{2}\int_0^{\infty} (\sigma_A - \sigma_T) F(a)\,\rho(a)\,da\,. \tag{46}$$

The physical meaning of these functions will be developed below, where it will be found that F provides a simple description of the distribution, while S_tN is the optical depth for the beam as a whole, $S_\pi N$ is the optical depth for the component polarized parallel to $\boldsymbol{B}$, $S_\sigma N$ is the optical depth for the component polarized normal to $\boldsymbol{B}$, and $S_pN\cos^2\nu$ is the "optical depth" for the polarization. A straightforward reduction of equations (41) and (43) gives (cf. Appendix 3):

$$S_\pi = S_t - S_p(\cos^2\nu - \tfrac{1}{3})\,, \tag{47}$$

$$S_\sigma = S_t + \tfrac{1}{3}S_p\,. \tag{48}$$

We shall show that, in the most plausible model, $S_p > 0$; hence $S_\pi < S_\sigma$.

Consider, first, the approximate physical picture developed in § 3.5, where F, the distribution integral, was not defined by equation (44) but rather as a characteristic of a distribution in which all the particles have their axes of symmetry parallel either to the X, the Y, or the Z axis. If f_1 is computed for this distribution, we find that F as defined by equation (44) is equal to F as used in § 3.5. Thus, throughout our discussion the distribution integral represents either the value of equation (44) or the fraction of the grains that have been turned from the $\boldsymbol{B}$ direction to the two orthogonal directions. Clearly, the maximum possible value for F is $\frac{1}{3}$ and the minimum, attained when all the grains are parallel to $\boldsymbol{B}$, is $-\frac{2}{3}$.

5.3. *The polarization, total absorption, and color excess produced by dust.*—If S is a constant, the solution of

$$dI = -SI\,dN \tag{49}$$

is

$$\Delta m = -(\tfrac{5}{2})\log_{10}\frac{I}{I_0} = 1.086SN\,, \tag{50}$$

where Δm is the absorption measured in stellar magnitudes and SN is the optical depth.

Let us assume for the present that, for some particular star, $\boldsymbol{B}$ is uniform over all parts of the light-path from the star to the earth where there is an appreciable density of dust, and that $\rho(a)$ and f are constants in these regions. Thus S_π and S_σ are independent of N, and equations (40) and (42) have the form of equation (49). In each of the two planes of polarization the absorptions are

$$\Delta m_\pi = 1.086S_\pi N\,, \qquad \Delta m_\sigma = 1.086S_\sigma N\,. \tag{51}$$

If $S_\pi < S_\sigma$, then $I_\pi > I_\sigma$, and I_π is the maximum intensity observed as a plane polarizer is rotated, while I_σ is the minimum intensity. When the polarizer is rotated from the position in which the most light is transmitted to that in which the least is transmitted, the observed magnitude change is

$$\Delta m_p = -(\tfrac{5}{2})\log_{10}\frac{I_\sigma}{I_\pi} = \Delta m_\sigma - \Delta m_\pi = 1.086N(S_\sigma - S_\pi)\,, \tag{52}$$

$$\Delta m_p = 1.086NS_p\cos^2\nu$$

where we have used equations (47) and (48). The quantity Δm_p is that used by Hiltner. On the other hand, the degree of polarization is obtained from the classical definition

$$p = \frac{I_\pi - I_\sigma}{I_\pi + I_\sigma} = \frac{1 - \exp(-S_p N \cos^2 \nu)}{1 + \exp(-S_p N \cos^2 \nu)} \doteq \tfrac{1}{2} S_p N \cos^2 \nu = 0.4605 \Delta m_p , \tag{53}$$

provided that $S_p N \ll 1$. We shall use p, defined by equation (53) exclusively, in order to follow the notation in Hall and Mikesell's catalog,[6] although from a theoretical and observational point of view the quantity Δm_p is more satisfactory.

The total intensity of light as observed when there are no polarizers in the photometer is $I = I_\pi + I_\sigma$, while if there were no dust it would be $2I_0$. Hence the absorption due to dust is

$$\begin{aligned} \Delta m_T &= -\left(\tfrac{5}{2}\right) \log_{10} \left[\frac{I_\pi + I_\sigma}{2 I_0}\right], \\ &= -1.086 \ln \\ &\quad \left\{\exp\left[-\tfrac{1}{2}(S_\pi + S_\sigma) N\right] \frac{\exp\left[\tfrac{1}{2}(S_\sigma - S_\pi) N\right] + \exp\left[-\tfrac{1}{2}(S_\sigma - S_\pi) N\right]}{2}\right\} \\ &\doteq 1.086 \left[S_t - S_p\left(\tfrac{1}{2}\cos^2 \nu - \tfrac{1}{3}\right)\right] N \doteq 1.086 S_t N = A_{pg} , \end{aligned} \tag{54}$$

since $S_p N \ll 1$, $S_p \ll S_t$. The color excess E_1 is about $\Delta m_T / 9$, hence

$$E_1 = 0.121 N S_t \tag{55}$$

and

$$\frac{p}{E_1} = 4.14 \frac{S_p}{S_t} \cos^2 \nu , \tag{56}$$

a result showing that, on the basis of the assumed homogeneity of $\boldsymbol{B}$ and $\rho(a)$, p/E_1 is independent of N and hence of E_1.

It is easy to obtain a rough evaluation of the right-hand side of equation (56) by assuming in equations (45) and (46) that all the grains are of the same size. Hence,

$$\frac{p}{E_1} = 18.6 F \cos^2 \nu \, \frac{(\sigma_A / \sigma_T) - 1}{(\sigma_A / \sigma_T) + 2} . \tag{57}$$

Equation (21) for p/A_{pg} is obtained on the same assumptions. From this we see that the experimental value of 0.18 for the maximum observed value of p/E_1 could be explained by taking $\nu = 0$, $F = \frac{1}{3}$ (i.e., all grains lined up normal to $\boldsymbol{B}$), and $\sigma_A/\sigma_T = 1.086$, or by taking $\nu = 0$, $F = \frac{1}{15}$ (i.e., one-fifth of the grains lined up) and $\sigma_A/\sigma_T = 1.52$. Reference to Table 2 shows that the first value of σ_A/σ_T corresponds to very moderate eccentricities. The second is such that we would not expect much smaller values of F to lead to an attractive theory unless the dust grains are assumed to have relatively large elongations (axes in ratio 2:1 or more). It must be emphasized that this treatment is useful in dealing with rough orders of magnitude. Since it assumes that particles of only one size are present and that this size is small compared to the wave length, it will give an incorrect dependence of the interstellar absorption on wave length; thus little weight is to be attached to the fact that it also gives an incorrect dependence on wave length of p and of p/E_1.

6. THE TORQUE DUE TO PARAMAGNETIC ABSORPTION

We now turn to a consideration of the processes which might lead to a partial orientation of the grains of dust, starting with what appears to us to be the most likely mechanism, paramagnetic absorption. We develop an expression for the torque to be expected

and, in the next section, for the effect of this torque on the distribution function. Later we consider briefly other mechanisms which might be suspected of producing orientation.

6.1. *The nature of the phenomena.*—The magnetic properties of many substances are such that if the substance is put in a magnetic field $\boldsymbol{B}$, whose magnitude varies sinusoidally, so that

$$\boldsymbol{B} = \boldsymbol{e}B_0 \cos(\omega t + \delta), \tag{58}$$

where $\boldsymbol{e}$ is a fixed unit vector, then the magnetization is [29]

$$\boldsymbol{M} = \boldsymbol{e}B_0 [\chi' \cos(\omega t + \delta) + \chi'' \sin(\omega t + \delta)]. \tag{59}$$

Here χ' and χ'' are the real and imaginary parts of the complex susceptibility; their numerical values as functions of ω will be considered below. When $\omega = 0$, then $\chi'' = 0$ and $\chi' = \chi_0$, the ordinary static susceptibility. The amount of heat generated by the alternating magnetic field is determined by the value of χ''. This absorption of energy from a changing magnetic field is called "paramagnetic absorption."

Next suppose the magnetic field, $\boldsymbol{B}$, to be constant and the grain to rotate with the constant angular velocity ω about an axis fixed in the grain and in space. Let $OXYZ$ be axes fixed in space and $Oxyz$ be rotating axes fixed in the grain, taking both OZ and Oz along ω. Let $\boldsymbol{e}_X$, $\boldsymbol{e}_Y$, and $\boldsymbol{e}_Z$ be the unit vectors in the stationary system and $\boldsymbol{i}$, $\boldsymbol{j}$, and $\boldsymbol{k}$ be those in the rotating system. Choose the origin of time so that

$$\boldsymbol{e}_X = \boldsymbol{i}\cos\omega t - \boldsymbol{j}\sin\omega t, \qquad \boldsymbol{e}_Y = \boldsymbol{i}\sin\omega t + \boldsymbol{j}\cos\omega t, \qquad \boldsymbol{e}_Z = \boldsymbol{k} = \frac{\boldsymbol{\omega}}{\omega}. \tag{60}$$

No generality is lost if OX is oriented as shown in Figure 1, *a* and

$$\boldsymbol{B} = B_X \boldsymbol{e}_X + B_Z \boldsymbol{e}_Z. \tag{61}$$

Then equations (60) show that, from the point of view of an observer rotating with the particle,

$$\boldsymbol{B} = B_Z \boldsymbol{k} + B_X \left[\boldsymbol{i}\cos\omega t + \boldsymbol{j}\cos\left(\omega t + \frac{\pi}{2}\right)\right]. \tag{62}$$

Hence he sees three fields, each described by equation (58), superposed, and, if the magnetization can be obtained by superposition, it is given by equation (59) as

$$\begin{aligned}\boldsymbol{M} &= \chi_0 B_Z \boldsymbol{k} + B_X [\boldsymbol{i}(\chi' \cos\omega t + \chi'' \sin\omega t) + \boldsymbol{j}(-\chi' \sin\omega t + \chi'' \cos\omega t)] \\ &= \chi_0 B_Z \boldsymbol{e}_Z + \chi' B_X \boldsymbol{e}_X + \chi'' B_X \boldsymbol{e}_Y.\end{aligned} \tag{63}$$

The physical interpretation of this is that the component of $\boldsymbol{M}$ along $\boldsymbol{\omega}$ is the same as though there were no rotation, the component at right angles to $\boldsymbol{\omega}$ is reduced in the ratio χ'/χ_0 and is dragged along by the rotation through the relatively small angle $\tan^{-1}(\chi''/\chi')$.

Since $V\boldsymbol{M}$ is the magnetic moment of a grain of volume V, the torque due to magnetization is given by equations (63) and (61) as

$$\boldsymbol{L} = V\boldsymbol{M} \times \boldsymbol{B} = V(\chi_0 - \chi')\omega^{-2}(\boldsymbol{B}\cdot\boldsymbol{\omega})(\boldsymbol{\omega}\times\boldsymbol{B}) + V\chi''\omega^{-1}(\boldsymbol{\omega}\times\boldsymbol{B})\times\boldsymbol{B}, \tag{64}$$

where the last expression is arranged to formulate the result in a way independent of the co-ordinate axes. We shall see in later sections that, since the first term is perpendicular to $\boldsymbol{\omega}$, it does not affect the rotational energy; although it produces a precession (i.e., changes ϕ in the notation of Fig. 3), it has no significant effect on the distribution of orientations, because $VB^2(\chi_0 - \chi') \ll kT$. For similar reasons we neglect an additional

[29] C. J. Gorter, *Paramagnetic Relaxation* (New York: Elsevier Pub. Co., 1947), p. 20.

very small torque, of the order of $\chi_0^2 B^2 V$, which tends to rotate the long axis of the grain into parallelism with $\boldsymbol{B}$.[30] Hence the term in χ'' produces the entire effect by its cumulative action. These points are touched on again in § 8.1.

We shall use equation (64) for $\boldsymbol{L}$ not only when $\boldsymbol{\omega}$ is fixed in the body but also when the body is nutating. This seems a reasonable assumption which greatly simplifies the subsequent analysis as compared to that necessary with slightly more accurate assumptions; but it must be remembered that, actually, $\boldsymbol{\omega}$ moves through the body relatively rapidly, unless the body is greatly elongated. We shall assume that the magnitude of $\boldsymbol{\omega}$ is given by ω_e from equation (5).

6.2. *The magnitude of* χ''.—The magnitude of the effect produced by paramagnetic absorption depends on the magnitude of χ''. We now estimate theoretically the value of χ'' for a material of the type discussed in § 4, that is, one in which each atom of a strongly magnetic element such as *Fe, Ni, Cr, Gd*, etc., is diluted by about 100 diamagnetic atoms. No significant error should be introduced if all the magnetic atoms are considered to be *Fe;* on the basis of Table 1 we shall regard *Fe* as comprising 12 per cent of the mass of the grain. We also show that experiment tends to confirm the theoretical estimate of χ''. Our treatment has been guided by suggestions from Gorter and Van Vleck and depends upon results given in Gorter's *Paramagnetic Relaxation*.[29] Unfortunately, it seems to be neither possible to find the required result in a directly quotable form nor desirable to give here a treatment sufficiently extensive to stand independently. Hence we shall combine a number of Gorter's formulas, leaving to him the discussion of their significance and the definition of some of the quantities that do not occur in our final result.

The case of interest to us seems to be governed by Gorter's equation (82) (p. 97), which should hold for frequencies of the order of ω_e,

$$\chi'' = \frac{\chi_0 \omega}{\omega_0} \left(\frac{\pi}{2}\right)^{1/2} \exp\left(-\frac{\omega^2}{2\omega_0^2}\right), \tag{65a}$$

where, with $2\pi\nu = \omega$, from his equation (80) and the related definitions we get

$$h\frac{\omega_0}{2\pi} = 2\beta^2 \left[8S(S+1)\sum_{p \neq q} r_{pq}^{-6}\right]^{1/2}. \tag{65b}$$

Here $\beta = eh/4\pi mc = 0.927 \times 10^{-20}$ erg/gauss is the Bohr magneton, S is the spin quantum number of the magnetic ions, and for Σr_{pq}^{-6} we may take $7.2n_e^2$, where n_e = number of *Fe* ions per cc. This value is the one given by Gorter on page 13 for a face-centered cubic lattice; the small difference in the coefficient of n_e for other arrangements is not significant for our purposes. In Table III (p. 15) Gorter gives 5.92 as the value of $2[S(S+1)]^{1/2}$ for Fe^{+++}; other magnetic ions have comparable, although usually somewhat smaller, values. Hence, if $n = 10^{-24} n_e$ = number of *Fe* ions per cubic angstrom, we have

$$\omega_0 = 3.66 \times 10^{12} n\,. \tag{66}$$

If Curie's law holds, we can use the expressions on page 6 of Gorter to evaluate χ_0. If T_g is the internal temperature of the grain, then we have

$$\chi_0 = \frac{n_e g^2 J(J+1)\beta^2}{3kT_g} = \frac{7.28n}{T_g}, \tag{67}$$

where in obtaining the second form we used data given above and the value $g[J(J+1)]^{1/2} = 2[S(S+1)]^{1/2} = 5.92$ taken from Gorter (p. 15, Table III) and from the discussion on page 18.

[30] W. R. Smythe, *Static and Dynamic Electricity* (2d ed.; New York: McGraw-Hill Book Co., Inc., 1950), p. 421.

Before substituting equations (66) and (67) in equation (65a), we can reduce the latter to an even more convenient form for estimating the order of magnitude of χ'' by noting that, if $\omega/\omega_0 < 0.7$, the exponential may be taken to be unity. Thus we have

$$\chi'' = 2.5 \times 10^{-12} \frac{\omega}{T_g}, \tag{68}$$

provided that

$$10^{-2} > n > 6 \times 10^{-21} \left(\frac{T}{a^5 \rho_g}\right)^{1/2} = 1.9 \times 10^{-7} \text{ in } H\,\text{I} \\ = 1.9 \times 10^{-6} \text{ in } H\,\text{II}. \tag{69}$$

These limitations on the validity of equation (68) arise as follows. The lower limit on n arises from the condition that $\omega/\omega_0 < 0.7$ and follows from equations (5) and (66). The upper limit is required, according to Gorter (private communication), in order not to enter the range where Curie's law breaks down because the iron atoms get so close together that the interactions are strong. Material whose density is ρ_g and which contains 12 per cent *Fe* by weight must have $0.12 \times 10^{-24}\ \rho_g$ gm of *Fe* atoms, each weighing 9.37×10^{-23} gm in each cubic angstrom. Hence $n = 1.3 \times 10^{-3}\ \rho_g$, and we see that the composition adopted in Table 1 easily satisfies condition (69) for all except very small grains ($a \ll 10^{-6}$).

It will be noted that χ'' as given by equation (68) is independent of the number of *Fe* ions per cubic angstrom as long as condition (69) is satisfied, that is, over a wide range of concentrations. This surprising and fortunate result means that our conclusions do not depend in a sensitive way on the amount of magnetic material in the grains. Let us consider the origin of this result. In χ_0 we find a term proportional to n giving the expected proportionality of the effect to the amount of *Fe*. But in equation (65) we note that the farther the resonance at ω_0 is from the frequency of interest, $\omega = \omega_e$, the smaller is the effect of each ion. Also we would expect the resonance frequency to be higher when the "coupling" is stronger, that is, when the density of interacting ions is greater, a result in agreement with equation (66). Combining the two tendencies, the result appears plausible.

Since the theoretical derivation of equation (68) is based on many assumptions and simplifications, it is most desirable that its predictions be compared with experiment. Gorter's discussion on pages 67–68 shows that the general dependence of χ''/χ_0 on T and ω is correctly given by equation (68) for frequencies up to 10^6 sec^{-1} and temperatures of the order of 70° K and that the dependence on n is roughly correct. The numerical value of this ratio for $FeNH_4(SO_4)_2 \cdot 12H_2O$ deduced from his Table XV, which is based on experiment, is 65 per cent of the value deduced from our equations (66) and (68); values for a number of other substances show that our result is a quite reasonable estimate of the order of magnitude of χ''.

7. THE EFFECT OF A TORQUE ON THE DISTRIBUTION INTEGRAL

We now wish to consider the effect of a torque so small that the change in angular momentum during a single nutation is negligible and only cumulative effects are significant. Thus we can describe the motion as in § 5.1, using Figure 3, with the modification that the angles β and θ are regarded as changing very slowly rather than being constant. To simplify our notation, we shall work out their rates of change for the torque considered in the previous section, although the modification for any other small torque is straightforward. In the latter parts of this section we consider the effect of these changes on the distribution integral.

7.1. *The mean rates of change of β and θ.*—We must first develop a somewhat more extensive description of the motion when there is no torque. Consider the plane through the angular momentum, $\boldsymbol{H}$, and the axis of symmetry, $\boldsymbol{e}_A$, shown in Figure 5, *a*. Because

of the symmetry, the angular velocity ω must lie in this plane. Let θ, θ_H, and θ_ω be the angles indicated where θ is as defined above, and let e_A and e_T be the unit vectors in this plane along and normal to the axis of symmetry, respectively. Since we have defined I to be the moment of inertia about e_A and γI to be that about e_T and since these are principal axes of inertia, we can write the angular velocity and angular momentum as

$$\omega = e_A \omega \cos\theta_\omega + e_T \omega \sin\theta_\omega , \tag{70}$$

$$H = e_A H \cos\theta + e_T H \sin\theta \tag{71}$$

$$= e_A I\omega \cos\theta_\omega + e_T I\gamma\omega \sin\theta_\omega . \tag{72}$$

From equations (71) and (72) it follows that

$$\cos\theta_\omega = \frac{H}{I\omega}\cos\theta, \quad \sin\theta_\omega = \frac{H}{I\gamma\omega}\sin\theta . \tag{73}$$

Since $\theta_H = \theta - \theta_\omega$, it then follows that

$$\cos\theta_H = \frac{H}{I\gamma\omega}(\gamma\cos^2\theta + \sin^2\theta),$$

$$\sin\theta_H = \frac{H}{I\gamma\omega}(\gamma - 1)\sin\theta\cos\theta . \tag{74}$$

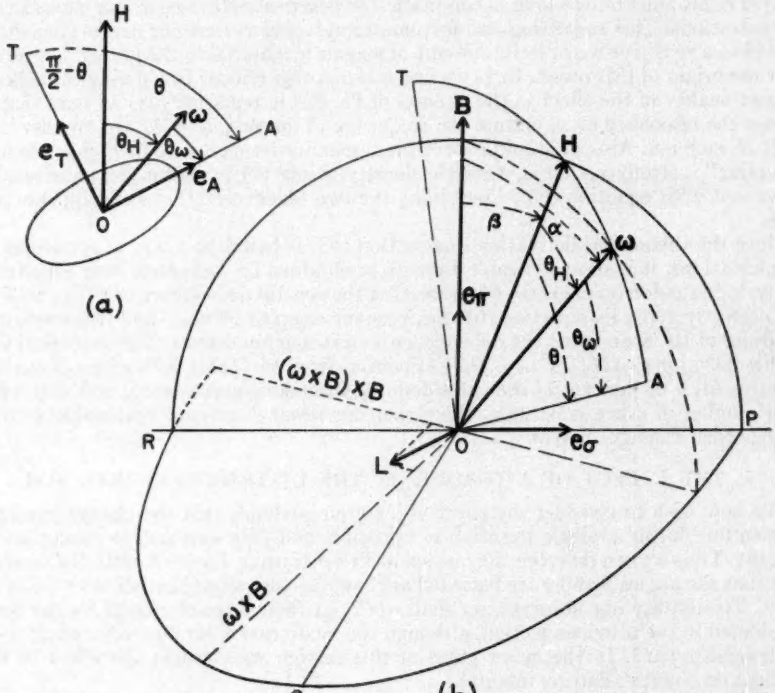

FIG. 5.—*a*, the angles between H, ω, and the axis of symmetry, A. *b*, the relations between ω, H, B, and L. The angles are $\angle HOA = \theta$; $\angle BOH = \beta$; $\angle BO\omega = \alpha$; $\angle BHA = \psi$; $\angle HO\omega = \theta_H$; $\angle \omega OA = \theta_\omega$.

The kinetic energy of rotation is

$$R = \tfrac{1}{2}\left[I(\omega\cos\theta_\omega)^2 + I\gamma(\omega\sin\theta_\omega)^2\right], \tag{75}$$

so that, by equations (75) and (73),

$$\frac{2I\gamma R}{H^2} = \gamma\cos^2\theta + \sin^2\theta\,. \tag{76}$$

Further, by equations (74) and (76)

$$\frac{2R}{H\omega} = \cos\theta_H\,. \tag{77}$$

As our basic equations of motion we take

$$\dot{\boldsymbol{H}} = \boldsymbol{L} = V(\chi_0 - \chi')\omega^{-2}(\boldsymbol{B}\cdot\boldsymbol{\omega})(\boldsymbol{\omega}\times\boldsymbol{B}) + V\frac{\chi''}{\omega}(\boldsymbol{\omega}\times\boldsymbol{B})\times\boldsymbol{B}, \tag{78}$$

$$\dot{R} = \boldsymbol{\omega}\cdot\boldsymbol{L} = -V\frac{\chi''}{\omega}\left[\omega^2B^2 - (\boldsymbol{\omega}\cdot\boldsymbol{B})^2\right], \tag{79}$$

where the dot indicates differentiation with respect to time and where we have used equation (64). Next we average these over one nutation to get $[\dot{H}]_{av}$ and $[\dot{R}]_{av}$. We see from Figure 3 that a knowledge of the former of these gives the average rate at which β is changing. Equation (76) allows us to obtain the average rate at which θ changes from $[\dot{H}]_{av}$ and $[\dot{R}]_{av}$.

In order to carry out the averaging, consider Figure 5, *b*, which is the same as Figure 3 except that $\boldsymbol{\omega}$ and the various vectors needed to determine $\boldsymbol{L}$ have been added and the system has been rotated about $\boldsymbol{B}$. In the nutational motion, the plane containing O, T, $\boldsymbol{H}$, $\boldsymbol{\omega}$, and OA, i.e., the plane of Figure 5, *a*, rotates with constant angular velocity $\dot{\psi}$ about $\boldsymbol{H}$, the angles θ, θ_ω, and θ_H remaining constant. If, as $\boldsymbol{\omega}$ moves in a circle about $\boldsymbol{H}$, we first average over positions that are mirror images in the plane BOH, so that the values of α are the same, we see that the average over a nutation of $\boldsymbol{\omega}\times\boldsymbol{B}$ lies along OQ, i.e., along the vector $\boldsymbol{H}\times\boldsymbol{B}$, and that the average of $(\boldsymbol{\omega}\times\boldsymbol{B})\times\boldsymbol{B}$ lies along OR, i.e., along the vector $-\boldsymbol{e}_\sigma$ which lies in the plane of $\boldsymbol{B}$ and $\boldsymbol{H}$. Hence the first term on the right-hand side of equation (78) causes $\boldsymbol{H}$ to precess around $\boldsymbol{B}$ but produces no change in β or in H, the magnitude of $\boldsymbol{H}$. Thus, although $(\chi_0 - \chi')$ contributes to the torque, it does not affect the distribution of orientations, and we shall drop it from our treatment. The average of the last term of equation (78) is

$$\begin{aligned} V\frac{\chi''}{\omega}\left[(\boldsymbol{\omega}\times\boldsymbol{B})\times\boldsymbol{B}\right]_{av} &= V\frac{\chi''}{\omega}\left([\boldsymbol{\omega}]_{av}\times\boldsymbol{B}\right)\times\boldsymbol{B} \\ &= -V\frac{\chi''}{\omega}\omega B^2\sin\beta\cos\theta_H\boldsymbol{e}_\sigma \end{aligned} \tag{80}$$

because $[\boldsymbol{\omega}]_{av}$ is directed along $\boldsymbol{H}$ and has the magnitude $\omega\cos\theta_H$. Hence $\boldsymbol{H}$ tends to spiral toward $\boldsymbol{B}$, its projection on $\boldsymbol{B}$ remaining constant.

If $\boldsymbol{H}$ is resolved into components $\boldsymbol{H}_\tau$ and $\boldsymbol{H}_\sigma$ along $\boldsymbol{B}$ and OP, respectively, we see from equations (79) and (80) that

$$\begin{gathered} [\dot{H}_\tau]_{av} = 0\,, \\ \left[\frac{dH_\sigma}{dt}\right]_{av} = \left[\frac{d(H_\tau\tan\beta)}{dt}\right]_{av} = -V\frac{\chi''}{\omega}\omega B^2\sin\beta\cos\theta_H\,. \end{gathered} \tag{81}$$

It follows from this and equation (74) that the average rate of change of β is

$$[\dot{\beta}]_{av} = -\frac{\chi''}{\omega}\frac{VB^2}{I\gamma}\sin\beta\cos\beta(\gamma\cos^2\theta+\sin^2\theta). \tag{82}$$

Next turn to the calculation of the average rate of change of θ. We shall need the expression

$$\left[\frac{dH^2}{dt}\right]_{av} = \left[\frac{d}{dt}(H_\pi^2+H_\sigma^2)\right]_{av} = -2V\frac{\chi''}{\omega}\omega B^2 H\sin^2\beta\cos\theta_H. \tag{83}$$

Also average equation (79):

$$\begin{aligned}[\dot{R}]_{av} &= -V\frac{\chi''}{\omega}\omega^2B^2(1-[\cos^2\alpha]_{av}) \\ &= -V\frac{\chi''}{\omega}\omega^2B^2(1-\cos^2\theta_H\cos^2\beta-\tfrac{1}{2}\sin^2\theta_H\sin^2\beta),\end{aligned} \tag{84}$$

with $[\cos^2\alpha]_{av}$ from equation (109) suitably modified. Now differentiate equation (76), solve for $\dot{\theta}$, and average. Reduce the resulting expression with the aid of equations (77) and (74):

$$\begin{aligned}[\dot{\theta}]_{av} &= -\frac{I\gamma R}{H^2(\gamma-1)\sin\theta\cos\theta}\left\{\frac{[\dot{R}]_{av}}{R}-\frac{1}{H^2}\left[\frac{dH^2}{dt}\right]_{av}\right\} \\ &= \frac{I\gamma V\chi''B^2\omega}{H^2(\gamma-1)\sin\theta\cos\theta}\sin^2\theta_H(1-\tfrac{1}{2}\sin^2\beta) \\ &= \frac{\chi''}{\omega}\frac{VB^2}{I\gamma}(\gamma-1)\sin\theta\cos\theta(1-\tfrac{1}{2}\sin^2\beta).\end{aligned} \tag{85}$$

It might appear that the above treatment somewhere omits an important consideration, since it seems to imply that a torque due to the first term on the right-hand side of equation (78) or due to a permanent magnetization of the grain along its axis of symmetry produces only a precession and does not affect the distribution of orientations. It is indeed true that such torques affect the distribution, the effect being easily computed from the Maxwell-Boltzmann distribution when, as is usual, the torque is derivable from a potential energy. But the effect on the distribution is insignificant unless this potential energy is of the same order as R, since the cumulative effect is null.

7.2. *The distribution integral when the relaxation time is short.*—Consider the case in which the collisions of atoms and ions with the dust grains are so frequent that the distribution remains relatively near the equipartition value, the effect of the torques being to produce a small perturbation. Evaluate the distribution integral with equation (12). The problem then is to calculate the rate at which F changes when β and θ for each grain are changing as given by equations (82) and (85). Regard each grain as characterized by a representative point in β-θ space, the density of the representative points being just $f(\beta, \theta, a)$ as defined in § 5.2. These points move with the velocity

$$v = [\dot{\beta}]_{av}e_\beta + [\dot{\theta}]_{av}e_\theta, \tag{86}$$

where e_β and e_θ are unit vectors along the co-ordinate axes. Since the representative points never vanish, the usual equation of continuity gives

$$\frac{\partial f}{\partial t} = -\operatorname{div}(vf). \tag{87}$$

It follows that if we evaluate the derivative as the system is passing through the equipartition distribution,

$$\frac{\partial f_1}{\partial t} = -\frac{\partial}{\partial \beta}\{[\dot{\beta}]_{av} f_e\} - \frac{\partial}{\partial \theta}\{[\dot{\theta}]_{av} f_e\}. \tag{88}$$

To form the derivative with respect to t of F, as defined by equation (44), we need only differentiate f_1 under the integral sign, using equation (88). Hence, from equation (12),

$$F(a) \doteq F_l(a) \equiv \tau \int_0^{\pi/2}\int_0^{\pi} (\cos^2\beta\cos^2\theta + \tfrac{1}{2}\sin^2\beta\sin^2\theta) \left(\frac{\partial}{\partial\beta}\{[\dot{\beta}]_{av} f_e\} + \frac{\partial}{\partial\theta}\{[\dot{\theta}]_{av} f_e\}\right) d\beta d\theta, \tag{89}$$

where we introduce F_l for the value of the integral in any case. $F = F_l$ only for the linear range where the perturbation from the equipartition distribution is small, i.e., when $|F_l| \ll \frac{1}{3}$. We can now substitute from equations (37), (82), and (85), reducing equation (89) by an integration of elementary functions (cf. Appendix 4) to

$$F \doteq F_l = \frac{\Gamma(\gamma)\, V\chi'' B^2 \tau}{I\omega_e}, \tag{90}$$

where $\Gamma(\gamma)$ is an abbreviation for a constant that depends only on the eccentricity of the spheroid, being

$$\begin{aligned}
\Gamma(\gamma) &= \frac{2}{15\gamma^{1/2}(\gamma-1)^{1/2}}\left[\frac{2\gamma+1}{\gamma-1}\sinh^{-1}(\gamma-1)^{1/2} - 3\left(\frac{\gamma}{\gamma-1}\right)^{1/2}\right] \text{ if } \gamma > 1 \\
&= \frac{-2}{15\gamma^{1/2}(1-\gamma)^{1/2}}\left[\frac{2\gamma+1}{1-\gamma}\sin^{-1}(1-\gamma)^{1/2} - 3\left(\frac{\gamma}{1-\gamma}\right)^{1/2}\right] \text{ if } 0 < \gamma < 1 \\
&= \frac{8(\gamma-1)}{225\gamma}[1 - \tfrac{1}{7}(\gamma-1) + \ldots] \quad \text{if} \quad |\gamma-1| \ll 1,
\end{aligned} \tag{91}$$

where in the last form the term neglected is of order $(\gamma-1)^2$.

In Table 2 we have tabulated for a variety of grain shapes the values of various quantities of interest. If a_A is the radius of the grain along the axis of symmetry, a_T is the radius in the transverse direction, and a is the mean radius, used throughout our paper, the quantities tabulated are obtained from equation (91) and

$$V = \tfrac{4}{3}\pi a_A a_T^2 = \tfrac{4}{3}\pi a^3, \tag{92}$$

$$\gamma = \frac{I\gamma}{I} = \frac{\rho_g V(a_A^2 + a_T^2)/5}{\rho_g V(a_T^2 + a_T^2)/5} = \frac{1}{2}\left(\frac{a_A^2}{a_T^2} + 1\right), \tag{93}$$

$$\frac{100\Gamma\rho_g V a^2}{I} = 250\left(\frac{a_A}{a_T}\right)^{2/3}\Gamma. \tag{94}$$

Consulting Table 2, we see that over the plausible range of (a_A/a_T) we can take

$$100\Gamma\frac{V}{I} = \pm\frac{5}{a^2\rho_g} \tag{95}$$

without introducing errors as great as those due to our lack of knowledge of τ.

By substitution of equations (95), (68), and (16) we can now reduce equation (90) to

$$F_l = \pm \frac{6.31 \times 10^6 B^2}{aT^{1/2} n_H T_g} \tag{96}$$

$$= \pm\ 6.31 \times 10^8 B^2 \text{ in both } H\text{ I} \text{ and } H\text{ II},$$

the sign being + for prolate and − for oblate spheroids.

7.3. *The distribution integral when the relaxation time is very long.*—If we compare equation (90) with equations (82) and (85), we see that, to within a factor of the order of unity, F_l is just τ times the average rate of change of the orientation angles, provided that Γ is introduced to allow for averaging over all orientations. Thus, when $|F_l| \ll \frac{1}{3}$, the angles change but little during the relaxation time, which is to be regarded as the time available for the applied torque to alter the orientation before the collisions stop further drift away from equipartition. On the other hand, when $|F_l| \gg \frac{1}{3}$, the relaxation time is so long that the collisions do not affect the distribution significantly and the torque orients the grains to the maximum degree possible. It then follows from equation (82) that β approaches 0 if $\beta < \pi/2$ initially and β approaches π if $\beta > \pi/2$. That is, the angular momenta all line up either parallel or antiparallel with the magnetic field. Recalling that $0 \leqslant \theta \leqslant \pi/2$, we see from equation (85) that for prolate spheroids, where $\gamma > 1$, θ approaches $\pi/2$, while for oblate spheroids, where $\gamma < 1$, θ approaches 0. In either case the long dimension of the spheroid becomes normal to $\boldsymbol{H}$ and $\boldsymbol{B}$. Thus, by the discussion at the end of § 5.2, $F = \frac{1}{3}$ for prolate spheroids and $F = -\frac{2}{3}$ for oblate spheroids when $|F_l| \gg \frac{1}{3}$.

8. OTHER METHODS OF PRODUCING POLARIZATION

8.1. *Torques due to permanent magnetization.*—When the orientation of the grains can be specified directly without investigating $\boldsymbol{H}$, the angular momentum, it is convenient to set $\beta = 0$ in all our formulae and to regard θ as being the angle between $\boldsymbol{B}$ and the axis of symmetry. The resulting expressions enable one to treat situations, such as that considered by Spitzer and Tukey,[12] where the grains are assumed to have a permanent magnetization $\boldsymbol{M}$ along the axis of symmetry. Then the angular distribution function, f, defined by the expression (36) with β and $d\beta$ omitted, is easily found from the Maxwell-Boltzmann distribution law, and evaluation of equation (44) then gives

$$F(a) = -\left\{\tfrac{2}{3} + 2g^2 - \frac{2}{g}\coth g\right\}, \tag{97}$$

where $g = VMB/kT$. Our $F(a)$ is $-\frac{2}{3}M(g)$ in the notation of Spitzer and Tukey. Substitution in the equations of § 5.3 then gives an expression for p that is in agreement with their equation (26). The fact that F is less than zero means that the magnetic field required to produce a given orientation of the grains by this mechanism is at right angles to that required when paramagnetic relaxation, or any dissipative mechanism, produces the orientation. The fact that the limiting value here is $-\frac{2}{3}$, while for the case of § 3 it is $\frac{1}{3}$, means that a field strong enough to give complete alignment requires here a smaller value of σ_A/σ_T.

If $VMB/kT \ll 1$, the distribution is not much affected, and the polarization is very small. Similarly one can show that the torque described by the first term of equation (64) produces no significant effect. In a mixture of such a torque and a nonconservative torque of the type treated in § 7, one can treat the case in which the latter torque produces only a small perturbation merely by replacing the f_e of § 7 by the Maxwell-Boltzmann equipartition distribution for the conservative torque.

8.2. *Eddy currents.*—Among the possible torques that might act on a body rotating in a magnetic field is that due to eddy currents in a conductor. We may estimate the order

of magnitude of this torque by assuming the grain of dust to be a sphere of conductivity σ e.m.u. and permeability κ. We find that u, the ratio of the diameter of the grain to the skin depth of the eddy currents, is

$$u = 2a(2\pi\omega\kappa\sigma)^{1/2} = 6.3\times10^{-4}(\kappa\sigma)^{1/2}\left(\frac{T}{a\rho_g}\right)^{1/4}, \tag{98}$$

where we have used equation (5) for ω, the angular velocity of the grain. Thus u is small compared to unity for all plausible values of the parameters. Rotation in a uniform field is equivalent to the action on a stationary sphere of two alternating fields at right angles and 90° out of phase. Hence the torque is twice the power absorbed in an alternating field divided by the angular velocity. We use the expression for the power given by W. R. Smythe,[31] converting it to e.m.u. and keeping only the lowest-order terms in u. The result is

$$L_E = \frac{6\pi a^5\omega\kappa^2\sigma B^2}{45+30(\kappa-1)+5(\kappa-1)^2}. \tag{99}$$

Such a torque will not affect the motion significantly if $L_E/L_R \ll 1$. If we substitute from equation (17) for L_R, and from equation (5) for ω, and take $\kappa = 1$, we get

$$\frac{L_E}{L_R} = 1.3\times10^{19}\frac{aB^2\sigma}{n_H T^{1/2}} = 1.3\times10^{12}\sigma B^2, \text{ in } H\text{ I and } H\text{ II regions}. \tag{100}$$

As κ approaches infinity, the ratio approaches a value nine times as great. Now for pure iron at a temperature of 5° K, σ is of the order of 0.02 e.m.u. Impurities would diminish the conductivity very greatly, and, if the grains have the composition assumed in § 4, σ will be smaller by at least 10^7. Thus, if B is of the order of 10^{-4} gauss, eddy currents produce negligible effects unless the grains are assumed to be very good metallic conductors. If the grains were pure iron, eddy-current effects would probably significantly modify the type of behavior discussed by Spitzer and Tukey.

8.3. *The Rowland Effect.*—If the dust grains bear electrostatic charges, then, as follows from Rowland's famous experiment, torques will act on them as they rotate in a magnetic field.[32] If the potential of the grain is of the order of a few volts, then it is easy to show that for this reason the grains have a magnetic moment per unit volume of the order of 10^{-4} e.m.u. For magnetic fields of the order of 10^{-5} gauss, the resulting torque on the grains is much larger than L_R as given by equation (17) and hence is a torque whose effects should be examined with some care. On the other hand, its direction is such that it might be expected to produce mainly precession without appreciable alteration of the distribution of orientations. Indeed, we shall now show that the distribution of orientations is completely unchanged by the Rowland effect.

Our procedure is to obtain a Hamiltonian for the system; then the distribution of orientations in the steady state is obtained from the basic theorems of statistical mechanics. We shall consider only the rotational motion of the grain, since the inclusion of translatory degrees of freedom, as is apparently suggested by Hiltner,[2] should not affect the orientation. Assume that all effects due to motion of the charge relative to the grain have been accounted for in the treatment of eddy currents and hence assume that the charges are fixed with respect to the grain.

The Lagrangian for a rigid body is obtained by adding together the well-known

[31] *Static and Dynamic Electricity* (2d ed.; New York: McGraw-Hill Book Co., Inc., 1950), p. 400.

[32] The authors are indebted to Dr. Olin C. Wilson for the suggestion that this torque should be investigated. Some such torque was also suggested by Hiltner (*Ap. J.*, 109, 471, 1949).

Lagrangians of the charged particles into which the body can be divided. Thus we get, for the rigid grain of dust,

$$\mathfrak{L} = \tfrac{1}{2}\boldsymbol{\omega}\cdot\boldsymbol{I}\cdot\boldsymbol{\omega} + \tfrac{1}{2}\boldsymbol{B}\cdot\boldsymbol{J}\cdot\boldsymbol{\omega}\,, \tag{101}$$

where $\boldsymbol{\omega}$ is regarded as expressed in terms of Eulerian angles and their derivatives; $\boldsymbol{I}$ is the familiar tensor of inertia defined in terms of integrals over the volume of certain functions of position multiplied by the mass density; and $\boldsymbol{J}$ is a tensor defined in exactly the same way except that the charge density replaces the mass density.

Let us denote the Eulerian angles used to specify the orientation of the grain by q_i, $i = 1, 2, 3$. Then $\boldsymbol{\omega}$ is linear in $\dot{q}_i$, although a somewhat complicated function of q_i. Thus equation (101) may be written as

$$\mathfrak{L} = \tfrac{1}{2}A_{ij}\dot{q}_i\dot{q}_j + C_i\dot{q}_i\,, \qquad A_{ij} = A_{ji}\,, \tag{102}$$

where a single index can have any of the values 1, 2, 3 while we sum over any index that occurs twice in a single term—i.e., the usual summation convention. The quantity A_{ij} comes from the first term of equation (101) and does not involve B, the magnetic field, while C_i comes from the second term and is zero when $B = 0$. From equation (102) we obtain the generalized momenta,

$$p_i = \frac{\partial\mathfrak{L}}{\partial\dot{q}_i} = A_{ij}\dot{q}_j + C_i\,, \tag{103}$$

and the Hamiltonian

$$\mathfrak{H} = p_k\dot{q}_k - \mathfrak{L} = \tfrac{1}{2}A_{ij}\dot{q}_i\dot{q}_j\,, \tag{104}$$

where $\mathfrak{H}$ is to be expressed in terms of q_i and p_i by means of equation (103).

The usual statistical mechanical procedures now give (cf. Appendix 2), as the number of grains whose representative points lie in a region $\delta\tau$ of phase space,

$$\delta N = c_1\int\!\!\int\!\!\int_{\delta\tau}\!\!\int\!\!\int\!\!\int\exp\left\{\frac{-\mathfrak{H}}{kT}\right\}dq_1dq_2dq_3dp_1dp_2dp_3\,, \tag{105}$$

where c_1 is a normalization constant. The regions $\delta\tau$ that interest us are those in which the q_i, i.e., the orientation, are confined to a narrow range while the p_i range over all possible values. We now change variables in equation (105) from p_i to $v_i = \dot{q}_i$. The appropriate expression for $\mathfrak{H}$ is already available in equation (104); we note that it is independent of B. The change of variables does not affect our description of $\delta\tau$. The Jacobian of the transformation is found from equation (103) to be the determinant of the matrix A_{ij}, and this is independent of B. Thus the expression for the angular distribution has been formulated in such a way that nowhere does the magnetic field enter; hence the distribution must be completely independent of the field.

We are deeply indebted to both Dr. W. A. Hiltner and Dr. John S. Hall for the observational material made available to us before publication. Dr. J. H. Van Vleck and Dr. C. J. Gorter have been most helpful in the discussion of paramagnetic relaxation. We are particularly grateful to Dr. Lyman Spitzer for discussions of all phases of the problem and for his many helpful suggestions on reading our manuscript.

APPENDIXES

Appendix 1. *Derivation of equations (34) and (35).*—We wish to compute $\overline{\cos^2 a_\sigma}$ and $\overline{\cos^2 a_\pi}$, where the angles are shown in Figure 4 and the average is over ϕ and ψ. Denote the direction cosines of OA by $\cos a_X$, $\cos a_Y$, and $\cos a_Z$. Then, since the direction cosines of E_π are 0: $\sin\nu$: $\cos\nu$,

$$\cos a_\pi = \sin\nu\cos a_Y + \cos\nu\cos a_Z\,, \tag{106}$$

$$\cos a_\sigma = \cos a_X . \tag{107}$$

By spherical trigonometry

$$\cos a_Z = \cos\beta\cos\theta + \sin\beta\sin\theta\cos\psi . \tag{108}$$

Now, when we average over ψ, we readily obtain

$$\overline{\cos^2 a_Z} = \cos^2\beta\cos^2\theta + \tfrac{1}{2}\sin^2\beta\sin^2\theta ; \tag{109}$$

and this result is unchanged if we next average over ϕ. When we average first over ϕ and then over ψ, we see by symmetry that

$$\overline{\cos^2 a_X} = \overline{\cos^2 a_Y} = \tfrac{1}{2}(1 - \overline{\cos^2 a_Z}) . \tag{110}$$

Therefore,

$$\overline{\cos^2 a_\sigma} = \tfrac{1}{2}(1 - \cos^2\beta\cos^2\theta - \tfrac{1}{2}\sin^2\beta\sin^2\theta) , \tag{111}$$

which gives equation (34) on substitution in equation (33).

When we square equation (106) and average over ϕ, we note that $\cos a_Y \cos a_Z$ averages to zero. Then, substituting from equations (109) and (110), we get

$$\overline{\cos^2 a_\tau} = \tfrac{1}{2}\sin^2\nu(1 - \cos^2\beta\cos^2\theta - \tfrac{1}{2}\sin^2\beta\sin^2\theta) + \cos^2\nu(\cos^2\beta\cos^2\theta + \tfrac{1}{2}\sin^2\beta\sin^2\theta) , \tag{112}$$

which gives equation (35) on substitution in equation (32).

Appendix 2. *The equipartition distribution.*—We wish to derive equation (37), the expression for the equipartition distribution, which is the distribution when no torques act on the grain except during collisions with atoms. In this case we have a Maxwell-Boltzmann distribution, and the usual statistical mechanical procedures give

$$\delta N = c_1 \int\int\int\int_{\delta\tau}\int\int\int \exp\frac{-R}{kT}\, d\lambda d\psi d\phi dp_\lambda dp_\psi dp_\phi \tag{113}$$

as the number of particles whose representative points lie in a region $\delta\tau$ of phase space, where c_1 is a normalization constant; R is the kinetic energy of rotation of a grain; T is the temperature of the gas molecules whose collisions produce the equipartition distribution; λ, ψ, and ϕ are angles defined below that specify the orientation of the grain; and p_λ, p_ψ, and p_ϕ are the conjugate momenta needed to complete the phase space. Hence our problem is to define suitable co-ordinates and then select a region $\delta\tau$ in phase space such that δN gives us $f_\sigma(\beta, \theta)$.

As shown in Figure 6, let $OXYZ$ be a system of nonrotating co-ordinates with O at the center of mass and OZ directed along $\boldsymbol{B}$. Let $Oxyz$ be a system of axes fixed in the particle with Oz along the axis of symmetry, and let λ, ϕ, and ψ be the usual Eulerian angles, λ replacing θ, which is used for the angle between $\boldsymbol{H}$ and the axis of symmetry. Note that temporarily we shall not use ψ with the same meaning as in § 5. The moments of inertia of the spheroid are $I_{zz} = I_{yy} = \gamma I$, $I_{xx} = I$. The kinetic energy of rotation is

$$R = \tfrac{1}{2} I[\gamma(\dot\lambda^2 + \dot\psi^2\sin^2\lambda) + (\dot\phi + \dot\psi\cos\lambda)^2] . \tag{114}$$

The conjugate momenta, p_λ, p_ψ, and p_ϕ, are defined in the usual way by $p_\lambda = \partial R/\partial\dot\lambda$, etc. Any standard treatment of the dynamics of rigid bodies gives the expression for the angular momentum, $\boldsymbol{H}$, referred to axes fixed in the spheroid in terms of the Eulerian

angles and their rates of change. The expressions for the momenta and the abbreviation

$$\pi_\psi = \frac{p_\psi - p_\phi \cos\lambda}{\sin\lambda} \tag{115}$$

then enable us to write

$$R = \tfrac{1}{2}(I\gamma)^{-1}(p_\lambda^2 + \pi_\psi^2 + \gamma p_\phi^2), \tag{116}$$

$$H^2 = p_\lambda^2 + \pi_\psi^2 + p_\phi^2, \tag{117}$$

$$\cos\theta = \frac{\boldsymbol{H}\cdot\boldsymbol{e}_z}{H} = \frac{p_\phi}{H}, \tag{118}$$

where $\boldsymbol{e}_z$ is a unit vector along OA.

The dependence of f_e on β is easily found. In our present discussion, $\boldsymbol{B}$ is regarded as a

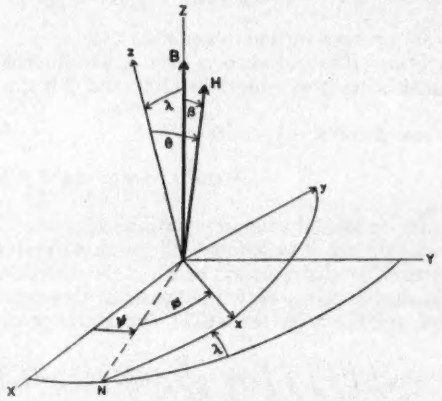

FIG. 6.—The Eulerian angles

vector that specifies a unique direction in space but that does not affect the orientation of the grain. Hence $\boldsymbol{H}$ is oriented at random over a sphere and f_e must be proportional to $\frac{1}{2}\sin\beta d\beta$. Thus we need only select $\delta\tau$ so as to give the dependence on θ; that is, to include those values of the canonical co-ordinates and momenta for which θ lies in the range $d\theta$. Now that we have equation (113), we no longer need to use canonical variables but can change to the set λ, ψ, ϕ, p_λ, π_ψ, p_ϕ. The Jacobian of the transformation is $\sin\lambda$. We note that R and θ do not depend on λ, ψ, and ϕ; hence we can carry out the integration over these variables and write equation (113) in the form

$$\delta N = c_2 \int\int_{\delta\tau}\int \exp\frac{-R}{kT}\, dp_\lambda d\pi_\psi dp_\phi, \tag{119}$$

where c_2 is one of a series of normalization coefficients, c_n, whose evaluation we shall postpone. Equations (117) and (118) show that we can regard

$$p_\lambda = H\sin\theta\cos\alpha, \qquad \pi_\psi = H\sin\theta\sin\alpha, \qquad p_\phi = H\cos\theta \tag{120}$$

as being Cartesian co-ordinates in a space whose spherical polar co-ordinates are H, θ, and α. In our complete phase space we see that p_λ, p_ψ, and p_ϕ, and hence π_ψ, run from

$-\infty$ to $+\infty$. Thus H runs from 0 to ∞, θ from 0 to π, and a from 0 to 2π. In the region $\delta\tau$ of interest, the only change to be made is that θ is restricted to the range $d\theta$. If we express R and $dp_\lambda\, d\pi_\psi\, dp_\phi = H^2 \sin\theta\, dH\, d\theta\, da$ in terms of the new variables, equation (119) becomes

$$\delta N = c_2 \int_0^\infty \int_\theta^{\theta+d\theta} \int_0^{2\pi} \exp\left[-\frac{H^2(\sin^2\theta + \gamma\cos^2\theta)}{2I\gamma kT}\right] H \sin\theta\, dH\, d\theta\, da\,, \tag{121}$$

$$= c_3 \sin\theta\,(\gamma\cos^2\theta + \sin^2\theta)^{-3/2} d\theta\,.$$

If we now multiply the left side of equation (121) by $\frac{1}{2}\sin\beta d\beta$, to give the dependence on β found above, and evaluate c_3 by integration over all θ and β, we get equation (37). In this normalization we return to the convention, used everywhere except in the present section, that θ lies between 0 and $\pi/2$.

Appendix 3. *The derivation of equations (44)–(48).*—For purposes of derivation it is convenient to regard S_l and S_p as being defined by equations (47) and (48) rather than by equations (45) and (46).

Using equations (41), (43), (34), and (35), one finds that

$$S_l = \frac{S_\pi + (2\cos^2\nu - \sin^2\nu) S_\sigma}{3\cos^2\nu} = \int_0^\infty \int_0^{\pi/2} \int_0^\pi \frac{\sigma_A + 2\sigma_T}{3} f(\beta,\theta,a)\, \rho(a)\, d\beta\, d\theta\, da\,, \tag{122}$$

$$S_p = \frac{S_\sigma - S_\pi}{\cos^2\nu} = \int_0^\infty \int_0^{\pi/2} \int_0^\pi (\sigma_A - \sigma_T)(\tfrac{1}{2} - \tfrac{3}{2}\cos^2\beta\cos^2\theta - \tfrac{3}{4}\sin^2\beta\sin^2\theta) \tag{123}$$

$$\times [f_e(\beta,\theta) + f_1(\beta,\theta,a)]\, \rho(a)\, d\beta\, d\theta\, da\,.$$

If we next consider the definitions of f, f_e, and f_1 in § 5.2, it is evident that

$$\int_0^{\pi/2} \int_0^\pi f(\beta,\theta,a)\, d\beta\, d\theta = \int_0^{\pi/2} \int_0^\pi f_e(\beta,\theta)\, d\beta\, d\theta = 1\,, \tag{124}$$

$$\int_0^{\pi/2} \int_0^\pi f_1(\beta,\theta)\, d\beta\, d\theta = 0\,. \tag{125}$$

Now $f_e = \sin\beta[f_e/\sin\beta]$, where from equation (37) $f_e/\sin\beta$ is independent of β. Hence, by equation (124),

$$\frac{1}{2}\int_0^{\pi/2} \int_0^\pi \left[\frac{f_e(\beta,\theta)}{\sin\beta}\right] \sin\beta\, d\beta\, d\theta = \int_0^{\pi/2} \left[\frac{f_e(\beta,\theta)}{\sin\beta}\right] d\theta = \tfrac{1}{2}\,. \tag{126}$$

Therefore,

$$\int_0^{\pi/2} \int_0^\pi (\tfrac{3}{2}\cos^2\beta\cos^2\theta + \tfrac{3}{4}\sin^2\beta\sin^2\theta) \left[\frac{f_e(\beta,\theta)}{\sin\beta}\right] \sin\beta\, d\beta\, d\theta \tag{127}$$

$$= \int_0^{\pi/2} (\cos^2\theta + \sin^2\theta) \left[\frac{f_e(\beta,\theta)}{\sin\beta}\right] d\theta = \tfrac{1}{2}\,.$$

It follows from equation (124) and the fact that σ_A and σ_T are independent of β and θ that equation (122) is equivalent to equation (45). It follows from equations (124), (125), and (127) that equation (123) is equivalent to equations (46) and (44).

Appendix 4. *The evaluation of the parameter F.*—Substitution in equation (89) shows

that equation (90) holds, provided that

$$\Gamma(\gamma) = \frac{1}{2\gamma^{1/2}} \int_0^{\pi/2} \int_0^{\pi} (\cos^2\beta \cos^2\theta + \tfrac{1}{2}\sin^2\beta \sin^2\theta) \times \left[\frac{\partial(-\sin^2\beta\cos\beta)}{\partial\beta} \times \frac{\sin\theta}{(\gamma\cos^2\theta + \sin^2\theta)^{1/2}} + \frac{\partial}{\partial\theta}\left\{ \frac{\sin^2\theta\cos\theta}{(\gamma\cos^2\theta+\sin^2\theta)^{3/2}} \right\} (\gamma-1)\sin\beta(1-\tfrac{1}{2}\sin^2\beta) \right] d\beta d\theta . \quad (128)$$

The differentiations and integrations over β are easily carried out, and the differentiation with respect to θ can be eliminated by integrating by parts. This gives

$$\Gamma(\gamma) = \frac{2}{15\gamma^{1/2}} \int_0^{\pi/2} \frac{(\gamma\cos^2\theta+\sin^2\theta)(1-3\cos^2\theta)+(\gamma-1)\sin^2\theta\cos^2\theta}{(\gamma\cos^2\theta+\sin^2\theta)^{5/2}} \sin\theta d\theta . \quad (129)$$

Let $x = (\gamma-1)^{1/2}\cos\theta$, to get

$$\Gamma(\gamma) = \frac{2}{15\gamma^{1/2}(\gamma-1)^{5/2}} \int_0^{(\gamma-1)^{1/2}} \frac{(x^2+1)(\gamma-1-3x^2)+x^2(\gamma-1-x^2)}{(x^2+1)^{5/2}} dx . \quad (130)$$

This gives equation (91).

POLARIZATION OF STELLAR RADIATION. III. THE POLARIZATION OF 841 STARS*

W. A. HILTNER
Yerkes and McDonald Observatories
Received April 17, 1951

ABSTRACT

The polarization of 841 stars is given in Table 2. The probable error of a single observation is 0.0022 mag.

During the last one and one-half years a large number of stars have been observed for interstellar polarization. In general, only stars of high luminosity were included in the observing program. Many of the stars in the finding list of O and B stars of high luminosity published by Nassau and Morgan,[1] cepheids, long-period variables, Wolf-Rayet stars, eclipsing variables, and one planetary nebula were in the program. Since the list includes over 600 stars not previously observed and since a new technique has been developed that promises even higher accuracy than that obtained with the present equipment,[2] it seems appropriate to publish the available observations at this time.

The photometric equipment employed in the present investigation consisted of the regular photoelectric photometer attached to the Cassegrain focus of the 82-inch reflector of the McDonald Observatory. For an analyzer, a piece of high-quality Polaroid, cemented between two glass plates, was placed in the $f/14$ convergent bundle, 8 inches in front of the focus of the telescope. This Polaroid occupied either of two angular positions 90° apart with respect to the photometer. The apparatus as a whole (Polaroid and photometer) could be rotated on the optical axis of the telescope to any desired position angle. In order to determine the polarization of a star, the following observing procedure was adopted. The photometer and Polaroid were set at some selected position angle. Three deflections were then made, the first and third at the same position of the Polaroid and the second with the Polaroid rotated by 90° from the other position. The photometer and Polaroid were then set at another position angle, 30° from the first. The three deflections were again repeated. If the star was polarized by 0.02 mag. or more, an estimate was made as to the position angle of the plane of vibration. Three observations were then made. One observation (with a total of five instead of three deflections) was made with the Polaroid approximately in the plane of vibration at one of its two positions. This observation determined the amount of polarization. The other two sets of observations were made in order to determine the position angle of the plane of vibration with maximum accuracy. This was done by setting the photometer at a position angle of 45° on either side of the estimated plane of vibration and obtaining three deflections at either position. When regions were observed in which the plane of vibration is relatively con-

* *Contributions from the McDonald Observatory, University of Texas*, No. 201.

[1] *Ap. J.*, 113, 141, 1951. I am grateful to Drs. Nassau and Morgan for permission to use this list in advance of publication.

[2] It is well known that seeing noise limits the accuracy of photoelectric photometry. In some types of observations where the star is compared with itself, there is an opportunity to eliminate the seeing fluctuations. One example is in spectrophotometry, when a narrow spectral region is compared with a broader one (W. A. Hiltner and A. D. Code, *J. Opt. Soc. America*, 40, 149, 1950). A second opportunity is in polarization observations, when one plane of vibration is compared to the perpendicular plane. The seeing fluctuations can be eliminated if the seeing for all perpendicular planes of vibration is coherent. From tests at the 12-inch telescope at Yerkes Observatory and the 82-inch reflector at McDonald, it appears that the seeing is coherent and that a factor of approximately 10 in accuracy can be realized.

stant, such as in Perseus, the two preliminary observations were deleted. When the star showed only slight polarization, a series of observations was made with the photometer and Polaroid set at intervals of 15°–30° in position angle. A complete set of observations of one star required from 12 to 20 minutes. Frequently, from 40 to 55 stars were observed in one night. The spectral region was limited by a Corning No. 3385 filter. The effective wave length is near λ 5400.

The resulting observations were plotted (after any necessary systematic corrections, to be discussed shortly, had been made) with the difference in magnitude of the deflections when the Polaroid was rotated 90° against position angle. The plotted observations were then compared with a series of master sine-curves. The amount of polarization and the position angle were determined by the master-curve that best fitted the observations. Master-curves were available in steps of 0.005 mag.

The internal agreement of photoelectric observations of polarization of stars should be similar to that normally found in stellar photoelectric photometry. Under average conditions the probable error of a single observation is near ±0.003 mag. However, since differential extinction is of no consequence in the observations under consideration, a slight improvement would not be unexpected. The internal agreement was investigated from duplicate observations of 36 stars, with the observed amount of polarization varying from 0.008 to 0.154 mag. The duplicate observations are listed in Table 1 and are plotted in Figure 1. The observations were plotted in the following manner. For alternate stars the first observation was plotted as abscissa and the second as ordinate. The remaining stars were plotted with the first observation as ordinate and the second as abscissa. This procedure removed any possible systematic effects with time, with a resulting false impression of the true accuracy. One characteristic of the present observations is immediately apparent. The probable error of a single observation remains sensibly constant for all values of the observed polarization. This, of course, is expected but is in contrast to the observations made at the U.S. Naval Observatory by the "flicker method," where the probable error of a single observation increases with the measured value of the polarization.[3] The probable error of a single observation of Table 1 and Figure 1 is 0.0022 mag.

Since the error of the position angle of the plane of vibration obviously depends upon the amount of polarization of the star, no value for the probable error can be strictly given without reservation. In order to give a graphic representation of the internal accuracy of a position angle, duplicate observations of Table 1 are plotted in Figure 2. The amount of polarization is plotted along the abscissa and half the difference of the two measures of position angle is plotted as ordinate. With few exceptions, the two measured position angles do not differ from the mean by more than 1°. If we treat all the measures of position angle homogeneously, regardless of the amount of polarization, we have a probable error of 0°.86.

Systematic errors in the observed amount of polarization were investigated by observing near-by stars of no assumed polarization. Normally, HD 166620 ($\pi = 0''.097$), HD 13403 ($\pi = 0''.135$), and, to a much lesser extent, HD 13137 ($\pi = 0''.006$) were observed for these purposes. The largest systematic error observed at any position angle was 0.005 mag. except for a few observations made in October, 1949, where the systematic error was as great as 0.012 mag. These systematic errors, which were usually less than 0.002 mag., were constant for each observing period with the telescope. However, one or more of the above stars were observed on each night, usually near the beginning and end of the night. Consequently, the systematic errors were known with high precision and were applied. Hence no systematic error greater than 0.001 mag. should be present in the final value for the polarization. The scale of polarization was obtained from the linearity of the amplifier.

[3] J. S. Hall and A. H. Mikesell, *Pub. U.S. Naval Obs.*, 17, 16, 1950.

TABLE 1

Duplicate Polarization Observations of 56 Stars

Star	Date	δ (Mag.)	θ	Star	Date	δ (Mag.)	θ
+60°2668.....	1950 Sept. 30	0.054	84	169054.....	1950 June 29	0.045	63
	1950 Oct. 7	0.062	82		1950 Sept. 2	0.040	66
108.....	1949 Oct. 12	0.081	80	185145.....	1950 June 15	0.136	180
	1950 Oct. 19	0.089	82		1950 Sept. 9	0.135	178
+62°79.....	1950 Oct. 9	0.064	73	187459.....	1950 June 29	0.056	33
	1950 Oct. 10	0.061	74		1950 Sept. 2	0.067	32
4841.....	1949 Oct 13	0.091	99	193237.....	1950 Sept. 12	0.024	35
	1949 Oct. 19	0.099	98		1950 Oct. 19	0.024	41
+63°102.....	1950 Oct. 9	0.157	102	E228841.....	1950 Sept. 12	0.030	174
	1950 Oct. 10	0.150	102		1950 Oct. 14	0.025	178
6675.....	1950 Sept. 29	0.084	124	E229221.....	1950 June 25	0.033	65
	1950 Oct. 13	0.088	122		1950 Oct. 14	0.034	67
9105.....	1950 Sept. 2	0.070	104	198478.....	1950 Sept. 11	0.062	5
	1950 Oct. 19	0.074	103		1950 Oct. 19	0.061	4
12801.....	1949 Oct. 13	0.055	112	198479.....	1950 Sept. 10	0.056	16
	1950 Oct. 12	0.047	107		1950 Oct. 19	0.057	15
14010.....	1949 Oct. 12	0.090	115	208938.....	1950 June 28	0.030	158
	1950 Oct. 19	0.095	112		1950 Sept. 2	0.030	161
14143.....	1950 Oct. 6	0.085	117	210221.....	1950 Sept. 8	0.041	44
	1950 Oct. 7	0.088	117		1950 Oct. 19	0.039	45
14322.....	1949 Oct. 11	0.065	113	211853.....	1950 June 15	0.086	45
	1950 Oct. 11	0.067	113		1950 Oct. 9	0.090	45
					1950 Oct. 10	0.088	43
14469.....	1949 Oct. 11	0.045	115				
	1950 Oct. 11	0.049	114	212466.....	1950 Sept. 2	0.055	48
					1950 Sept. 8	0.058	49
+56°595.....	1950 Sept. 30	0.076	111				
	1950 Oct. 6	0.080	114	E239994.....	1950 Sept. 8	0.054	58
					1950 Oct. 9	0.052	59
14818.....	1950 Sept. 29	0.080	114				
	1950 Oct. 11	0.084	114	223385.....	1950 June 29	0.031	55
	1950 Oct. 14	0.080	113		1950 Sept. 2	0.022	58
16779.....	1950 Oct. 6	0.105	114	223960.....	1950 June 28	0.066	79
	1950 Oct. 11	0.103	116		1950 Sept. 2	0.068	80
E237056.....	1950 Oct. 9	0.130	124	224055.....	1950 June 28	0.089	67
	1950 Oct. 10	0.126	125		1950 Sept. 2	0.086	67
20756.....	1950 Oct. 13	0.007	175	225094.....	1950 June 29	0.046	76
	1950 Oct. 14	0.008	167		1950 Sept. 2	0.054	75
21291.....	1950 Sept. 15	0.076	118	225146.....	1950 June 16	0.067	71
	1950 Sept. 29	0.074	117		1950 Oct. 19	0.068	73

All the measures of polarization made in October, 1949, and June, September, and October, 1950, are collected in Table 2.

The first, second, and third columns give the *Henry Draper Catalogue* number, the *Bonner Durchmusterung* number, and "Other Designation," respectively.

The fourth and fifth columns give the 1900 position, taken from the *Henry Draper Catalogue* where possible. Otherwise the positions were computed from the *Bonner Durchmusterung* 1855 position.

The magnitude in the sixth column was also taken from the *Henry Draper Catalogue* for all stars in this catalogue. For those stars in the *Bonner Durchmusterung* only, the magnitudes recorded in this catalogue are given in the column.

The spectral types in the seventh column were, in general, obtained from the *Henry*

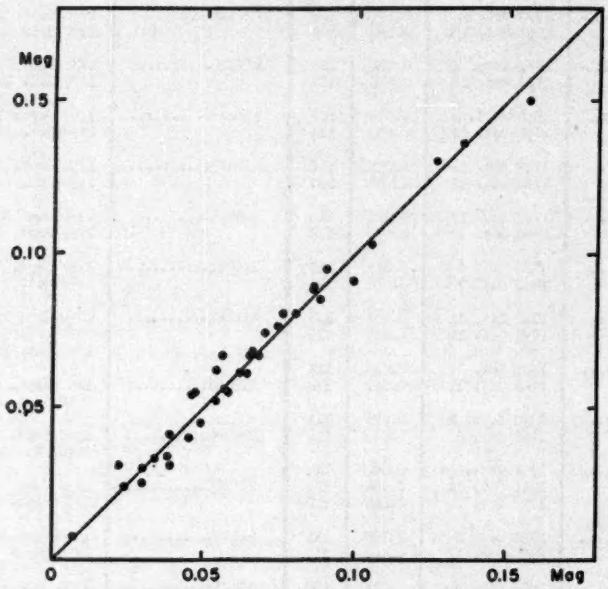

FIG. 1.—Duplicate observations of polarization

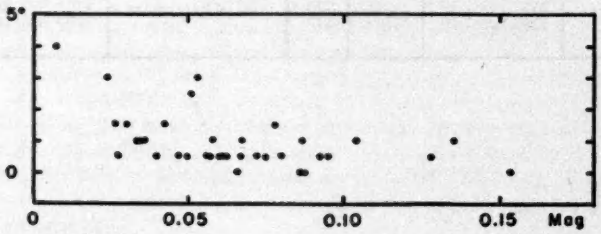

FIG. 2.—Duplicate observations of the plane of vibration. The amount of polarization is plotted along the abscissa, and half the difference of the two measures of position angle is plotted as ordinate.

TABLE 2

Polarization Observations of 841 Stars

HD	BD	Other Designation	α 1900	δ 1900	Mag	Sp	l	b	φ	δ Mag	δ %	θ	θ'	E_1
	+60° 2668		0h 0m	+60°19'	8.8		85.2	- 1.3	8.6	0.060	2.8	83°	92°	
108	+62 2368	MWC 1	0 0.9	+63 7	7.36	O8fp	85.6	+ 1.4	8.6	0.055	1.6	81	90	+0.23
	+59 2829		0 1.5	+60 4	9.5		85.2	- 1.6	8.5	0.081	1.4	75	83	
598	+58 11		0 5.3	+59 6	6.70	B3	85.6	- 2.6	7.7	0.023	1.1	60	68	+0.06
E232121	+54 7	SX Cas	0 5.4	+54 20	var.	A7	84.9	- 7.3	7.7	0.010	0.5	39	47	
698	+57 28	MWC 4	0 6.3	+57 39	7.08	B5	85.5	- 4.1	7.4	0.030	1.4	68	70	+0.13
		SY Cas	0 9.8	+57 52	var.		86.0	- 3.9	6.7	0.010	0.5	36	43	
1070	+58 18		0 9.9	+59 15	8.2	A2	86.2	- 2.5	6.6	0.026	1.2	71	78	
1385	+60 25		0 12.9	+61 10	7.9	B1	86.7	- 0.7	6.0	0.029	1.3	81	87	+0.20
	+62 49		0 13.4	+63 1	8.7		87.0	+ 1.2	5.9	0.067	3.1	81	87	
1544	+61 38		0 14.6	+61 31	8.0	B0	87.0	- 0.3	5.6	0.040	1.8	89	95	+0.14
	+61 39	MWC 5	0 14.8	+61 54	8.9		87.0	0.0	5.6	0.059	2.7	91	97	
	+63 33		0 16.2	+64 3	9.1		87.4	+ 2.2	5.3	0.084	3.9	103	108	
	+60 39		0 16.2	+61 10	9.1		87.1	- 0.7	5.3	0.030	1.4	85	90	
1745	+61 48		0 16.6	+61 38	8.4	B0	87.2	- 0.2	5.2	0.040	1.8	83	88	+0.19
1810	+61 50		0 17.4	+61 41	8.2	B0.5	87.3	- 0.2	5.0	0.037	1.7	78	83	+0.14
1976	+51 62		0 18.9	+51 28	5.36	B3	86.6	-10.4	4.7	.....	...	....	....	+0.02
2083	+71 16		0 20.0	+71 15	6.94	B2	88.4	+ 9.3	4.5	0.035	1.6	95	99	+0.10
	+61 74		0 20.4	+62 0	9.3		87.7	+ 0.1	4.3	0.040	1.8	92	96	
	+62 79		0 20.9	+62 53	9.0		87.8	+ 1.0	4.2	0.062	2.8	73	77	
	+63 48	MWC 669	0 21.0	+63 52	9.0		87.9	+ 1.9	4.2	0.119	5.5	109	113	
	+60 51		0 21.0	+60 52	9.3		87.7	- 1.0	4.2	0.068	2.9	63	67	
2329	+57 85		0 22.1	+58 0	7.24	B3	87.6	- 3.9	4.0	0.025	1.2	65	69	+0.15
E256419	+59 61		0 22.3	+60 4	9.0	B2	87.8	- 1.8	3.9	0.047	2.2	81	85	
	+55 81		0 22.7	+55 51	9.5		87.6	- 6.1	3.8	0.037	1.7	68	72	
2451	+61 92		0 23.2	+61 57	8.6	B	88.0	0.0	3.7	0.041	1.9	84	88	+0.09
2619	+64 52		0 24.7	+64 43	8.2	B	88.4	+ 2.8	3.4	0.100	4.6	99	102	
2654	+61 101		0 25.1	+61 48	7.31	B3	88.2	- 0.2	3.3	0.018	0.8	69	72	+0.11
	+61 105		0 25.6	+61 53	8.8		88.3	- 0.1	3.2	0.074	3.4	81	84	
2789	+66 35	MWC 6	0 26.3	+66 36	8.2	B2e	88.6	+ 4.6	3.0	0.070	3.2	114	117	+0.25
2905	+62 102	K Cas	0 27.3	+62 23	4.24	B1 Ia	88.5	+ 0.4	2.8	0.032	1.5	83	86	+0.13
	+63 61		0 27.6	+63 27	9.8		88.6	+ 1.5	2.7	0.150	6.9	94	97	
2928	+61 113		0 27.5	+61 59	8.7	G	88.5	0.0	2.8	0.070	3.2	67	70	
3191	+60 71		0 30.1	+60 55	8.6	B1	88.8	- 1.1	2.2	0.055	2.5	53	55	+0.23
	+60 78		0 31.3	+60 49	9.4		88.9	- 1.3	1.9	0.086	4.0	60	62	
		No. 1	0 34.0	+60 25			89.3	- 1.6	1.8	0.054	2.5	72	73	
	+63 70		0 34.9	+63 22	9.0		89.4	+ 1.4	1.1	0.105	4.8	105	106	
3940	+63 81		0 36.9	+63 45	7.40	A1	89.7	+ 1.8	0.7	0.106	5.0	100	101	+0.40
3950	+51 133		0 37.0	+51 48	6.93	B3	89.4	-10.2	0.7	0.023	1.1	85	86	+0.14
	+61 153		0 37.1	+61 41	9.2		89.7	- 0.3	0.6	0.010	0.5	105	106	
	+64 76		0 38.9	+64 43	9.2		89.9	+ 2.7	0.2	0.148	6.8	94	94	
4362	+58 101	HR 207	0 40.9	+59 2	6.49	G0 Ib	90.1	- 3.0	359.8	0.024	1.1	67	67	
4613	+64 83		0 45.0	+65 2	8.9	F5	90.3	+ 3.0	359.3	0.110	5.1	96	95	
		No. 2	0 45.8	+60 27	9.0	B2	90.5	- 1.6	359.2	0.048	2.2	74	73	
4694	+63 97		0 45.9	+64 5	8.4		90.4	+ 2.1	359.1	0.148	6.8	90	97	
		XY Cas	0 44.1	+59 34	var.		90.5	- 2.4	359.1	0.041	1.9	82	81	
4717	+62 155		0 44.2	+62 37	8.8	A0	90.5	+ 0.6	359.1	0.100	4.6	103	102	+0.26
	+60 114	MWC 679	0 44.3	+60 22	9.5		90.5	- 1.6	359.0	0.035	1.6	78	77	
	+61 175		0 44.5	+61 50	9.1		90.5	- 0.2	359.0	0.063	2.9	76	75	
4768	+58 119		0 44.6	+59 7	8.0	B5	90.6	- 2.9	359.0	0.049	2.2	82	81	+0.25
4841	+62 160		0 45.4	+63 14	7.06	B5	90.6	+ 1.2	358.8	0.095	4.4	98	97	+0.31
4842	+62 161	VY Cas	0 45.4	+62 23	var.	Mb	90.6	+ 0.4	358.8	0.033	1.5	100	99	
	+63 102		0 46.1	+64 8	9.5		90.7	+ 2.1	358.6	0.155	7.1	102	101	
5005	+55 191		0 47.0	+56 5	7.7	B2	91.0	- 5.9	358.4	0.039	1.8	77	75	+0.11
5015	+60 124	HR 244	0 47.1	+60 34	4.93	F8	90.9	- 1.4	358.4	.....	...	....	....	

TABLE 2 (Cont'd)

HD	BD	Other Designation	α 1900	δ 1900	Mag	Sp	l	b	ϕ	δ Mag	δ %	θ	θ'	E_1
		No. 3	$0^h 47.6$	$+60°16'$			90.9	- 1.7	358.3	0.068	2.9	78°	76°	
	+63° 110	BH Cas	0 48.5	+63 32	var.		91.0	+ 1.6	358.1	0.123	5.7	97	95	
5235	+57 165	W Cas	0 49.0	+58 1	var.	Ce	91.2	- 4.0	358.0	0.050	2.3	96	94	
5458	+61 185		0 51.3	+62 1	8.6	B5p	91.3	0.0	357.5	0.051	2.4	101	99	+0.17
E236589	+55 215		0 52.1	+55 54	9.0	B0	91.7	- 6.1	357.3	0.033	1.5	82	79	
5551	+62 175		0 52.2	+63 11	7.7	B2	91.4	+ 1.2	357.3	0.085	3.9	93	90	+0.34
5552	+61 187		0 52.2	+61 24	9.0	B	91.5	- 0.6	357.3	0.068	3.1	101	98	
5689	+62 178		0 53.5	+63 5	9.2	B	91.5	+ 1.1	357.0	0.087	4.0	96	93	+0.16
5776	+62 181		0 54.3	+62 30	8.4	B6	91.6	+ 0.6	356.8	0.113	5.2	93	90	
	+62 183		0 54.9	+62.54	9.2		91.7	+ 1.0	356.7	0.119	5.5	92	89	
6048	+59 169		0 56.7	+59 36	9.2	B9	92.1	- 2.3	356.3	0.075	3.4	88	84	+0.09
6182	+61 200		0 57.8	+61 18	8.6	B0	92.1	- 0.6	356.1	0.084	3.9	100	96	+0.26
6827			0 59.2	+59 53		WR	92.4	- 2.0	355.8	0.067	3.1	91	87	
6843	+65 129	MWC 10	0 59.4	+65 26	7.10	B8	92.0	+ 3.5	355.7	0.038	1.8	96	94	+0.14
6675	+68 74		1 2.4	+69 10	7.1	B0.5 Ib	92.0	+ 7.3	355.0	0.036	1.7	128	118	+0.16
	+60 180	MWC 11	1 5.8	+60 47	9.4		93.2	- 1.1	354.3	0.092	4.2	89	83	
7108	+61 223		1 6.2	+61 21	8.6	B3	93.1	- 0.5	354.2	0.071	3.3	84	78	+0.34
E236664	+58 195		1 7.5	+58 33	9.4	B	93.5	- 3.3	353.9	0.053	2.4	96	92	
7252	+60 188		1 7.7	+60 21	7.26	B1	93.4	- 1.5	353.9	0.078	3.6	99	93	+0.10
E236689	+57 240		1 12.3	+57 51	9.0	B0	94.3	- 3.9	352.9	0.059	2.7	91	84	
	+57 243		1 12.5	+57 41	9.3		94.4	- 4.0	352.8	0.096	4.4	94	87	
	+61 242	AQ Cas	1 12.6	+61 51	var.		93.8	+ 0.1	352.8	0.107	4.9	110	103	
7661	+55 290	AA Cas	1 13.2	+55 48	var.	Mb	94.7	- 5.9	352.6	0.028	1.3	77	70	
	+57 252		1 13.2	+57 44	9.2		94.4	- 4.0	352.7	0.057	2.6	98	91	
7902	+57 257		1 13.6	+57 40	7.9	B6.5	94.5	- 4.0	352.6	0.065	3.0	95	88	+0.20
7927	+57 260	ϕ Cas	1 13.8	+57 42	5.25	F0 Ia	94.0	- 4.0	352.5	0.074	3.4	93	86	
	+60 219	XZ Cas	1 16.4	+60 39	var.		94.4	- 1.0	352.0	0.082	3.8	110	102	
	+64 156		1 16.9	+65 6	9.2		94.0	+ 3.3	351.8	0.116	5.3	103	95	
	+62 246		1 18.0	+62 16	8.8		94.4	+ 0.6	351.6	0.118	5.4	115	107	
E236740	+59 251		1 20.1	+59 46	8.3	B3	95.0	- 1.8	351.2	0.071	3.3	104	95	
8768	+62 254		1 21.4	+62 45	8.0	B	94.7	+ 1.1	350.9	0.085	3.9	100	91	+0.21
	+60 246	XX Cas	1 22.9	+60 27	var.		95.3	- 1.1	350.5	0.071	3.3	105	95	
8965	+59 290		1 23.3	+59 44	7.26	B5	95.4	- 1.8	350.4	0.062	2.8	103	98	+0.16
	+61 277		1 23.7	+62 13	9.3		95.1	+ 0.6	350.4	0.116	5.3	112	102	
E236762	+58 252		1 24.5	+59 13	9.3	B2	95.7	- 2.3	350.2	0.075	3.4	101	91	
9105	+62 259		1 24.6	+62 51	7.46	B5	95.1	+ 1.3	350.2	0.072	3.3	104	94	+0.33
E236768	+58 256		1 25.2	+58 52	9.0	B2	95.9	- 2.6	350.0	0.073	3.4	104	94	
	+60 261		1 25.9	+60 37	8.7		95.6	- 0.9	349.9	0.080	3.7	111	101	
9311	+59 271		1 26.6	+60 10	7.26	B5	95.8	- 1.3	349.7	0.072	3.3	100	90	+0.24
	+59 273		1 26.7	+60 7	8.5		95.8	- 1.4	349.7	0.080	3.7	105	95	
	+60 279		1 29.7	+60 28	8.5		96.1	- 1.0	349.0	0.070	3.2	104	93	
	+59 286		1 30.2	+59 26	9.0		96.4	- 2.0	348.9	0.083	3.8	102	91	
		RW Cas	1 30.7	+57 15	var.		96.8	- 4.1	348.8	0.062	2.8	89	78	
E236810	+59 296		1 31.8	+60 4	8.7	B3	96.4	- 1.3	348.6	0.081	3.7	97	86	
		No. 4	1 32.5	+57 39			97.0	- 3.6	348.4	0.059	2.7	95	83	
E236815	+59 297		1 32.8	+59 54	8.5	B3	96.6	- 1.4	348.4	0.062	2.8	98	86	
	+57 359		1 33.0	+57 20	9.4		97.1	- 3.9	348.3	0.067	3.1	92	80	
10063	+55 375		1 33.3	+55 17	7.61	B8	97.6	- 5.9	348.2	0.048	2.2	92	80	
10107	+58 273		1 33.8	+58 33	6.88	B9	97.0	- 2.7	348.1	0.015	0.7	99	87	
10125	+63 218		1 33.9	+63 40	8.0	B	95.9	+ 2.3	348.1	0.078	3.6	101	89	+0.16
10362	+60 312		1 36.1	+60 55	6.46	B8	96.8	- 0.4	347.6	0.028	1.3	91	79	
	+61 312		1 36.3	+61 57	8.9		96.6	+ 0.7	347.6	0.112	5.2	110	98	
	+62 297		1 36.4	+63 5	9.2		96.3	+ 1.8	347.6	0.103	4.7	100	88	
	+55 393		1 37.6	+55 40	9.5		98.1	- 5.4	347.3	0.050	2.3	106	93	
	+60 331		1 39.0	+60 44	9.0		97.2	- 0.4	347.0	0.115	5.3	98	85	
	+60 333		1 39.2	+60 44	9.0		97.2	- 0.4	347.0	0.110	5.1	100	87	
	+60 339		1 39.5	+60 45	8.8		97.2	- 0.4	346.9	0.105	4.8	99	86	
	+60 343		1 39.6	+60 45	9.1		97.2	- 0.4	346.9	0.130	6.0	103	90	
E232522	+54 372		1 39.6	+54 51	8.6	B0	98.6	- 6.2	346.8	0.035	1.6	103	90	
10756	+59 318		1 40.1	+60 10	7.71	B8	97.4	- 1.0	346.8	0.070	3.2	100	87	

TABLE 2 (Cont'd)

HD	BD	Other Designation	α 1900	δ 1900	Mag	Sp	l	b	φ	δ Mag	δ %	θ	θ'	E_1
10898	+57° 399		1h 41m9	+57°58'	8.2	B2	98.2	- 3.1	346.4	0.085	3.9	95°	81°	+0.21
	+63 247		1 42.3	+63 50	9.5		96.8	+ 2.7	346.3	0.102	4.7	103	89	
	+59 385	VV Cas	1 44.2	+59 24	var.		98.1	- 1.6	345.9	0.090	4.1	94	80	
	+54 395		1 45.2	+54 58	9.5		99.3	- 5.8	345.6	0.045	2.1	102	88	
E236894	+57 409		1 45.4	+57 57	8.7	BO	98.6	- 3.0	345.6	0.085	3.9	96	82	
E232552	+54 398	MWC 19	1 45.8	+54 51	7.6	BO	99.4	- 6.0	345.4	0.047	2.2	115	100	
	+63 253		1 46.1	+63 42	9.1		97.2	+ 2.6	345.4	0.091	4.2	106	91	
	+54 404		1 46.5	+54 38	9.5		99.6	- 6.1	345.2	0.046	2.1	119	104	
11554	+57 425	MWC 20	1 46.4	+57 24	9.2	B	99.2	- 3.4	344.9	0.092	4.2	96	81	+0.19
11606	+58 351	MWC 21	1 48.8	+58 47	7.04	B3	98.8	- 2.0	344.9	0.065	2.9	96	81	+0.09
	+55 441	MWC 431	1 49.4	+56 4	9.4		99.6	- 4.6	344.7	0.060	2.8	100	85	
	+58 334	X Cas	1 49.6	+58 42	var.		98.9	- 2.0	344.7	0.085	3.9	105	90	
	+63 261	MWC 22	1 50.0	+63 33	9.1		97.7	+ 2.6	344.6	0.089	4.1	103	88	
		IC 1747	1 50.2	+62 23			98.1	+ 1.5	344.6	0.086	4.0	96	81	
	+58 343		1 52.1	+58 27	9.4		99.3	- 2.3	344.1	0.075	3.4	94	78	
11831	+59 364		1 51.1	+59 54	8.0	A3	98.8	- 0.9	344.4	0.113	5.2	97	81	
11857	+60 398	HR 561	1 51.4	+61 12	6.05	B8	98.5	+ 0.4	344.3	0.023	1.1	106	90	
	+58 351		1 53.7	+58 29	9.5		99.4	- 2.2	343.8	0.100	4.6	98	82	
12301	+63 274	53 Cas	1 55.6	+63 54	5.62	B8 Ib	98.2	+ 3.1	343.4	0.051	2.4	110	93	+0.18
12302	+58 356	MWC 23	1 55.6	+59 12	8.2	B3	99.6	- 1.4	343.4	0.044	2.0	88	71	+0.14
12323	+54 441		1 55.8	+55 8	8.96	B9	100.7	- 5.3	343.3	0.033	1.5	102	85	
12365	+60 423		1 56.1	+60 13	7.41	A0	99.3	- 0.4	343.3	0.025	1.2	103	86	
E232588	+54 448		1 57.1	+54 38	8.5	A7	101.1	- 5.7	343.0	0.058	2.7	109	92	
E236935	+57 469	MWC 24	1 57.2	+58 0	9.1	B2	100.1	- 2.5	343.0	0.093	4.3	91	74	
12509	+68 261		1 57.6	+68 54	8.0	B3	98.4	+ 3.2	342.9	0.074	3.4	113	96	
12567	+63 287		1 58.1	+63 49	8.8	B	98.5	+ 3.1	342.8	0.094	4.3	107	90	
12727	+56 425		1 59.6	+56 34	8.8	B8	100.8	- 3.8	342.5	0.075	3.4	105	87	
12740	+48 600		1 59.8	+48 41	8.0	B2	103.2	-11.3	342.1	0.032	1.5	107	89	+0.07
12856	+56 429	MWC 25	2 0.9	+56 38	8.4	B2	101.0	- 3.6	342.2	0.029	1.3	107	89	+0.14
12867	+57 492		2 1.0	+57 14	9.2	B3	100.8	- 3.1	342.2	0.076	3.5	101	83	
12882	+64 295	MWC 26	2 1.1	+64 33	7.54	B3	98.6	+ 3.9	342.1	0.064	2.9	109	91	+0.19
12953	+57 494	MWC 436	2 1.7	+57 57	5.90	A1 Ia	100.7	- 2.4	342.0	0.074	3.4	108	90	+0.11
12993	+57 498		2 2.1	+57 27	8.6	B3	100.9	- 2.8	341.9	0.089	4.1	109	91	
13051	+56 432	MWC 27	2 2.6	+56 31	8.0	BO	101.2	- 3.7	341.8	0.048	2.2	100	82	+0.15
	+63 300	MWC 703	2 2.9	+63 36	9.4		99.1	+ 3.1	341.8	0.106	4.9	108	90	
13136	+55 529		2 3.4	+56 5	7.7	K5	101.5	- 4.1	341.6	0.068	3.1	110	92	
13267	+56 438	5 Per	2 4.6	+57 11	6.36	B5 Ia	101.3	- 3.0	341.4	0.088	4.0	107	88	+0.12
13268	+55 534		2 4.6	+55 41	8.2	BO	101.8	- 4.4	341.4	0.060	2.8	110	91	+0.10
13388	+57 512		2 5.3	+57 28	9.2	B9	101.3	- 2.7	341.2	0.085	3.9	111	92	
	+57 513		2 5.5	+57 38	9.2		101.3	- 2.5	341.2	0.085	3.9	110	91	
	+57 515	MWC 28	2 5.7	+57 13	9.3		101.4	- 2.9	341.2	0.093	4.3	111	92	
13402	+58 396		2 5.9	+59 4	8.2	B0.5	100.8	- 1.1	341.1	0.116	5.3	104	85	
13476	+57 519	HR 641	2 6.6	+58 6	6.50	A3 Ib	101.2	- 2.0	341.0	0.090	4.1	109	90	+0.26
13494	+55 543		2 6.7	+56 6	9.2	B8	101.9	- 3.9	340.9	0.055	2.5	109	90	
13514	+58 480		2 7.1	+58 27	9.0	B	102.8	- 6.4	340.8	0.049	2.2	106	87	
13561	+55 547		2 7.3	+56 2	9.0	B8	102.0	- 3.9	340.8	0.066	3.0	110	91	
	+54 490		2 7.4	+54 35	9.2		102.5	- 5.3	340.7	0.069	3.2	110	91	
13590	+63 310	MWC 706	2 7.6	+63 34	8.0	B5p	99.6	+ 3.2	340.7	0.096	4.4	118	89	+0.19
13621	+54 494		2 7.8	+54 51	8.06	B1	102.5	- 5.0	340.6	0.050	2.3	107	88	
13659	+56 462		2 8.1	+56 28	8.9	B9	102.0	- 3.5	340.6	0.080	3.7	104	85	
13716	+57 525		2 8.6	+57 18	8.5	B1	101.8	- 2.7	340.5	0.088	4.0	112	92	+0.15
13744	+57 526		2 8.9	+57 50	7.8	A0	101.6	- 2.2	340.5	0.092	4.2	109	89	+0.30
13745	+55 554		2 8.9	+55 32	7.96	BO	102.4	- 4.3	340.4	0.063	2.9	110	90	+0.12
13758	+57 527		2 9.0	+57 17	8.9	B8	101.8	- 2.7	340.4	0.100	4.6	108	88	
13831	+56 469		2 9.7	+56 17	8.6	BO	102.2	- 3.6	340.3	0.066	3.0	105	85	+0.08
13841	+56 470		2 9.8	+56 34	7.21	B2	102.2	- 3.3	340.3	0.073	3.4	111	91	+0.13
13854	+56 471	MWC 31	2 9.9	+56 36	6.42	B1	102.2	- 3.3	340.2	0.083	3.8	112	92	+0.17
	+56 473	MWC 441	2 9.9	+56 40	8.7		102.1	- 3.2	340.2	0.095	4.4	111	91	
13866	+56 475		2 10.0	+56 15	7.7	B2	102.3	- 3.6	340.2	0.078	3.4	115	95	+0.14
13890	+56 478	MWC 443	2 10.2	+56 19	8.9	B8	102.3	- 3.5	340.2	0.075	3.4	107	87	

TABLE 2 (Cont'd)

HD	BD	Other Designation	α 1900	δ 1900	Mag	Sp	l	b	φ	δ Mag	δ %	θ	θ'	E_1
13900	+56° 479		2h 10m3	+56°26'	9.0	B5	102.3	- 3.4	340.2	0.075	3.4	116°	96°	
	+56 482		2 10.6	+56 44	8.9		102.2	- 3.1	340.1	0.104	4.8	116	96	
	+56 484	MWC 444	2 10.7	+56 26	9.1		102.3	- 3.4	340.1	0.075	3.4	124	104	
13969	+56 485		2 10.8	+56 38	8.8	B2	102.3	- 3.2	340.0	0.096	4.4	114	94	+0.12
13970	+55 564		2 10.8	+56 11	8.6	B5	102.4	- 3.6	340.0	0.075	3.4	123	103	+0.10
14010	+63 315		2 11.1	+63 58	7.05	B9	99.8	+ 3.7	340.0	0.092	4.2	112	92	+0.23
14014	+55 567		2 11.1	+55 46	9.0	B9	102.6	- 4.0	340.0	0.056	2.6	114	94	
	+56 493		2 11.3	+56 24	9.3		102.4	- 3.4	339.9	0.079	3.6	126	106	
14052	+56 500		2 11.4	+56 45	8.6	B1	102.3	- 3.1	339.9	0.088	4.0	116	96	
14053	+56 498		2 11.4	+56 33	8.7	B2	102.4	- 3.2	339.9	0.065	3.0	115	95	+0.15
14092	+56 507		2 11.7	+56 18	9.5	B8	102.5	- 3.5	339.8	0.091	4.2	120	100	
	+56 512	BU Per	2 11.7	+56 58	var.	cM	102.3	- 2.8	339.9	0.086	4.0	114	94	
14134	+56 522	MWC 32	2 12.1	+56 40	6.66	B5 Ia	102.4	- 3.1	339.8	0.084	3.9	114	94	+0.22
14142	+58 459	T Per	2 12.2	+58 30	var.	cM	101.8	- 1.4	339.8	0.090	4.1	110	90	
14143	+56 530		2 12.2	+56 43	6.66	B2	102.4	- 3.0	339.7	0.086	4.0	117	97	+0.27
14162	+56 535		2 12.4	+56 41	9.4	B	102.5	- 3.1	339.7	0.091	4.2	115	95	
14250	+56 545		2 13.2	+56 39	8.6	B5	102.6	- 3.1	339.5	0.079	3.6	109	89	
14270	+56 547	AD Per	2 13.4	+56 32	var.	cM	102.6	- 3.2	339.5	0.077	3.6	119	99	
14302	+55 587		2 13.6	+55 52	8.8	B2	102.9	- 3.8	339.4	0.068	3.1	115	94	+0.16
14322	+55 588		2 13.8	+55 27	6.84	B8 Ia	103.1	- 4.2	339.4	0.066	3.0	115	92	+0.12
14330	+56 551	FZ Per	2 13.9	+56 42	var.	cM	102.6	- 3.0	339.4	0.084	3.9	115	94	
14331	+55 590		2 13.9	+55 22	8.81	B9	103.1	- 4.4	339.4	0.060	2.8	108	87	
14357	+56 555		2 14.1	+56 25	8.9	B5	102.8	- 3.2	339.3	0.096	4.4	113	92	
14404	+57 550		2 14.5	+57 24	8.6	cM	102.5	- 2.3	339.3	0.070	3.2	112	91	
14422	+56 565	MWC 37	2 14.7	+56 56	9.4	Bp	102.7	- 2.7	339.2	0.067	3.1	117	96	
14433	+56 568		2 14.8	+56 47	6.54	A1 Ia	102.7	- 2.9	339.2	0.086	4.0	112	92	+0.18
14434	+56 567		2 14.8	+56 27	8.5	B2	102.8	- 3.2	339.2	0.084	3.9	116	95	+0.11
14442	+58 455		2 14.9	+59 6	9.2	B0	101.9	- 0.7	339.2	0.090	4.1	113	92	+0.26
14443	+56 570		2 14.9	+56 42	8.6	B	102.8	- 3.0	339.2	0.082	3.8	117	96	
14469	+55 597	SU Per	2 15.1	+56 9	var.	cM	103.1	- 3.4	339.1	0.065	3.0	110	89	
14476	+56 577		2 15.2	+56 49	9.0	B0	102.8	- 2.8	339.1	0.076	3.6	113	92	+0.22
14488	+56 583	RS Per	2 15.3	+56 39	var.	cM	102.8	- 3.0	339.1	0.076	3.5	124	103	
14489	+55 598	9 Per	2 15.3	+55 23	5.22	A2 Ib	103.3	- 4.2	339.0	0.049	2.2	114	93	+0.09
14501	+57 551		2 15.4	+57 42	9.5	B5	102.5	- 2.0	339.1	0.080	3.7	111	90	
14520	+56 588		2 15.6	+56 38	9.2	B9	102.9	- 3.0	339.0	0.087	4.0	115	94	
	+56 589		2 15.6	+57 3	9.1		102.7	- 2.6	339.0	0.080	3.7	117	96	
14528	+57 552	S Per	2 15.7	+58 8	var.	cMe	102.4	- 1.6	339.0	0.108	5.0	133	112	
14535	+56 591		2 15.8	+56 47	7.46	A1	102.9	- 2.8	339.0	0.077	3.6	111	90	+0.26
14542	+56 593		2 15.9	+56 56	6.95	B8 Ia	102.8	- 2.7	339.0	0.067	3.1	116	95	+0.29
	+56 595		2 16.0	+56 45			102.9	- 2.8	338.9	0.079	3.6	113	92	
14580	+56 597		2 16.3	+56 46	var.	cM	102.9	- 2.8	338.9	0.090	4.1	114	93	
14605	+55 605	MWC 44	2 16.5	+56 8	9.7	Oe5	103.2	- 3.4	338.8	0.089	4.1	116	95	+0.35
14622	+40 500		2 16.6	+40 57	5.87	F	108.9	-17.5	337.7	.....	...	....	....	
14633	+40 501		2 16.7	+41 2	7.7	O9	108.9	-17.4	337.8	0.010	0.5	103	81	-0.07
		No. 5	2 16.7	+57 53			102.6	- 1.8	338.8	0.085	3.9	109	88	
14662	+54 535	HR 690	2 16.9	+54 55	6.46	F7 Ib	103.7	- 4.5	338.7	0.068	2.9	111	90	
	+56 606		2 17.7	+57 2	9.0		103.0	- 2.5	338.6	0.085	3.9	111	90	
14818	+55 612	10 Per	2 18.2	+56 10	6.24	B2 Ia	103.4	- 3.3	338.4	0.081	3.7	114	92	+0.27
14826	+56 609		2 18.3	+57 0	8.5	cM	103.1	- 2.5	338.4	0.091	4.2	116	94	
14871	+55 616	DM Per	2 18.9	+55 38	var.	B9	103.7	- 3.7	338.3	0.050	2.3	117	95	
14899	+56 621		2 19.2	+56 47	7.42	B8	103.3	- 2.6	338.2	0.070	3.2	116	94	
14947	+58 467		2 19.5	+58 25	8.04	O5f	102.7	- 1.1	338.2	0.100	4.6	122	100	
14956	+57 568		2 19.6	+57 14	7.32	B2	103.2	- 2.2	338.2	0.076	3.6	117	95	+0.37
		SZ Cas	2 19.9	+59 1	var.		102.6	- 0.5	338.1	0.093	4.3	120	98	
15316	+57 576		2 22.8	+57 22	7.30	A2	103.5	- 1.9	337.4	0.100	4.6	110	87	+0.35
15325	+56 635		2 22.9	+56 48	8.5	B5	103.8	- 2.4	337.4	0.115	5.3	113	90	
	+60 493		2 23.2	+60 44	8.4		102.3	+ 1.2	337.4	0.099	4.6	113	90	
	+62 411		2 23.9	+62 56	8.0		101.5	+ 2.3	337.2	0.083	3.8	113	90	
15450	+56 642	MWC 48	2 24.2	+56 27	8.7	B0p	104.1	- 2.7	337.2	0.086	4.0	121	98	+0.21
	+60 497		2 24.2	+61 11	8.6		102.2	+ 1.7	337.2	0.125	5.8	116	93	

TABLE 2 (Cont'd)

HD	BD	Other Designation	α 1900	δ 1900	Mag	Sp	l	b	φ	δ Mag	δ %	θ	θ'	E_1
	+60° 498		2h 24.5	+61° 7'	9.5		102.3	+ 1.6	337.1	0.134	6.2	125°	100°	
15497	+57 582		2 24.6	+57 15	7.20	B6 Ia	103.8	- 2.0	337.1	0.096	4.4	109	86	+0.40
15548	+56 647		2 25.0	+56 13	8.9	B8	104.2	- 2.9	337.0	0.108	5.0	125	102	
	+60 501		2 25.0	+61 2	9.2		102.4	+ 1.6	337.0	0.120	5.5	122	99	
15558	+60 502		2 25.1	+61 1	7.82	O6	102.4	+ 1.6	337.0	0.110	5.1	120	97	+0.31
15570	+60 504		2 25.2	+60 56	8.0	O5f	102.4	+ 1.5	337.0	0.131	6.0	117	94	+0.39
15571	+56 648		2 25.2	+56 59	8.0	B	104.0	- 2.2	337.0	0.098	4.3	124	101	+0.21
	+56 649		2 25.3	+56 15			104.3	- 2.8	336.9	0.080	3.7	126	103	
15620	+57 584		2 25.6	+57 31	8.2	B8	103.6	- 1.6	336.9	0.111	5.1	111	88	
15629	+60 507		2 25.7	+61 5	8.4	B	102.4	+ 1.6	336.9	0.109	5.0	120	96	
15642	+54 569		2 25.8	+54 54	8.0	B2	104.9	- 4.0	336.8	0.065	3.0	115	92	+0.02
15690	+56 656		2 26.3	+57 5	7.7	B2	104.1	- 2.0	336.7	0.116	5.3	112	89	+0.37
	+60 512		2 26.4	+60 57	9.5		102.6	+ 1.6	336.7	0.028	1.3	107	84	
15752	+57 589		2 26.8	+57 58	8.8	B0.5	103.8	- 1.2	336.6	0.112	5.2	121	98	+0.31
15785	+59 515		2 27.2	+60 6	8.41	B	103.0	+ 0.8	336.5	0.104	4.8	121	97	+0.28
	+62 419		2 27.2	+63 9	9.2		101.8	+ 3.6	336.5	0.100	4.6	114	90	
	+62 424		2 28.4	+62 31	8.5		102.2	+ 3.1	336.2	0.060	2.7	112	88	
E236979	+56 673	YZ Per	2 31.1	+56 37	var.	cM	104.9	- 2.2	335.7	0.053	2.4	124	100	
16243	+57 602		2 31.3	+57 23	8.5	B2	104.6	- 1.5	335.7	0.079	3.6	117	93	+0.31
16810	+58 498		2 32.0	+58 38	8.4	B0.5	104.1	- 0.3	335.5	0.112	5.2	122	98	
16429	+60 541		2 33.1	+60 51	7.8	F0	103.3	+ 1.8	335.3	0.049	2.2	128	103	
16523	+56 686		2 33.9	+56 18	9.98	Oa	105.4	- 2.3	335.1	0.071	3.3	117	92	
16524	+55 689		2 33.9	+55 51	7.49	B9	105.5	- 2.7	335.1	0.015	0.7	116	91	
16691	+56 693		2 35.5	+56 28	8.4	Oe	105.5	- 2.0	334.8	0.078	3.6	118	93	
16778	+59 535		2 36.3	+59 24	7.71	A2 Ia	104.3	+ 0.6	334.6	0.114	5.2	121	96	+0.51
16779	+57 620		2 36.3	+57 24	8.6	B	105.2	- 1.2	334.6	0.104	4.8	115	90	
16808	+57 622		2 36.7	+57 53	8.9	B	105.0	- 0.6	334.5	0.105	4.7	123	97	
16832	+56 703		2 36.9	+56 14	9.0	B	105.8	- 2.2	334.4	0.101	4.6	118	92	
17088	+57 652		2 39.5	+57 19	7.54	B9	105.6	- 1.0	333.9	0.085	3.9	116	90	+0.45
17114	+58 518		2 39.7	+58 55	9.2	B	104.9	+ 0.4	333.9	0.110	5.1	113	87	
17145	+57 634		2 40.0	+57 15	8.0	B6.5	105.7	- 1.1	333.8	0.096	4.4	116	90	+0.47
17378	+56 718	HR 825	2 42.2	+56 40	6.53	A5 Ia	106.2	- 1.5	333.3	0.102	4.7	120	93	
E237007	+59 549		2 42.7	+59 59	9.2	B	104.8	+ 1.5	333.2	0.075	3.4	113	86	
17468	+68 200	SU Cas	2 43.0	+68 28	var.	F5	101.0	+ 9.1	332.8	0.041	1.9	130	105	
17505	+59 552		2 43.4	+60 1	7.11	O7	104.8	+ 1.6	333.1	0.075	3.4	109	82	+0.24
17506	+55 714	η Per	2 43.4	+55 29	3.95	K3 Ib	106.9	- 2.4	333.0	0.020	0.9	118	91	
17520	+59 558		2 43.5	+59 59	8.7	B	104.9	+ 1.6	333.1	0.071	3.3	111	84	
		TX Cas	2 44.2	+62 22	var.		103.9	+ 3.7	332.8	0.077	3.6	120	93	
17603	+56 728		2 44.4	+56 38	8.6	B	106.5	- 1.4	332.9	0.106	4.9	114	87	
	+59 562		2 45.6	+60 3	9.5		105.1	+ 1.7	332.6	0.077	3.6	115	86	
	+60 586		2 46.4	+60 14	8.3		105.1	+ 2.0	332.4	0.053	2.4	114	86	
17857	+63 367		2 47.0	+63 43	7.78	B8	103.5	+ 5.1	332.2	0.102	4.7	112	84	+0.35
	+60 594		2 49.1	+61 1	9.1		105.0	+ 2.8	331.8	0.086	4.0	121	93	
18076	+58 534		2 49.2	+58 41	9.0	B	106.1	+ 0.8	331.8	0.130	6.0	112	84	
	+60 596		2 49.3	+60 16	9.3		105.4	+ 2.2	331.8	0.086	4.0	115	87	
	+51 659		2 51.6	+51 42	9.1		109.8	- 5.2	331.2	0.078	3.6	103	74	
18326	+59 578		2 51.6	+60 10	7.91	O8	105.7	+ 2.2	331.3	0.070	3.2	117	88	+0.24
18352	+60 608		2 51.9	+60 53	7.00	B2	105.4	+ 2.8	331.2	0.077	3.6	115	86	+0.12
18409	+62 504		2 52.4	+62 19	8.0	B	104.7	+ 4.1	331.1	0.093	4.3	115	86	+0.19
E237056	+57 681	MWC 720	2 55.0	+57 13	8.7	Oe5	107.5	- 0.2	330.6	0.128	5.9	125	96	
	+58 561	BSD9-57	3 0.4	+58 48	10.79	B6	107.3	+ 1.6	329.5	0.082	3.8	119	89	(+0.37)
19243	+61 525	MWC 61	3 0.7	+62 0	6.54	B2e	105.7	+ 4.3	329.3	0.050	2.3	130	99	+0.26
		BSD9-61	3 0.9	+58 48	12.40	B5	107.4	+ 1.6	329.4	0.131	6.0	102	71	(+0.81)
		BSD9-64	3 1.0	+58 54	12.28	B5	107.4	+ 1.7	329.4	0.084	3.9	101	70	
19341	+58 568	BSD9-73	3 1.5	+58 58	7.79	B9	107.4	+ 1.8	329.2	0.044	2.0	124	93	(+0.10)
19441	+58 567	BSD9-485	3 2.5	+59 9	7.68	B5	107.4	+ 2.0	329.0	0.100	4.6	116	85	(+0.33)
E237080	+58 568	BSD9-496	3 3.1	+59 11	9.14	B7	107.4	+ 2.1	328.9	0.085	3.9	116	85	(+0.31)
19644	+59 607	BSD9-524	3 4.6	+59 33	8.05	B8	107.4	+ 2.5	328.6	0.064	2.9	115	84	(+0.28)
	+58 574	BSD9-106	3 5.2	+58 34	10.68	B5	106.0	+ 1.7	328.5	0.105	4.8	112	80	
	+59 608	BSD9-555	3 6.0	+59 28	10.30	B7	107.6	+ 2.5	328.3	0.097	4.5	106	74	(+0.33)

TABLE 2 (Cont'd)

HD	BD	Other Designation	α 1900	δ 1900	Mag	Sp	l	b	φ	δ Mag	δ %	θ	θ'	E_1
19820	+59° 609	CC Cas	sh 6m2	+59°11'	var.	O8	107.8	+ 2.3	328.2	0.105	4.8	114°	82°	+0.32
	+58 578	BSD9-123	3 7.0	+58 44	9.95	B5	108.1	+ 2.0	328.1	0.076	3.5	102	70	(+0.35)
E257090	+59 611	BSD9-579	3 7.2	+59 33	9.32	B5	107.7	+ 2.7	328.0	0.111	5.1	104	72	(+0.39)
E257091	+59 612	BSD9-586	3 7.3	+59 33	9.12	B5	107.7	+ 2.7	328.0	0.105	4.8	112	80	(+0.49)
20041	+56 798	HR 964	3 8.2	+56 45	5.92	A0 Ia	109.3	+ 0.4	327.9	0.060	2.8	116	84	+0.28
	+59 624	BSD9-633	3 8.9	+59 37	10.81	B8	107.8	+ 2.8	327.7	0.066	3.0	116	84	(+0.21)
		BSD9-146	3 9.0	+58 49	12.79	F5	108.3	+ 2.2	327.7	0.051	2.4	120	88	
20134	+59 625	MWC 64	3 9.1	+59 41	7.41	B5	107.8	+ 2.9	327.6	0.087	1.7	110	78	(+0.17)
	+51 704		3 9.1	+51 38	9.5		112.1	- 3.9	327.6	0.066	3.0	115	83	
		BSD9-638	3 9.1	+59 34	11.3	B9	107.9	+ 2.8	327.6	0.060	2.8	117	85	(+0.25)
		BSD9-156	3 10.2	+58 50	11.48	B6	108.4	+ 2.3	327.4	0.078	3.6	108	75	(+0.40)
20295	+59 630	BSD9-671	3 10.8	+59 17	8.5	B7	108.2	+ 2.7	327.3	0.055	2.5	106	73	(+0.17)
	+51 710		3 11.6	+51 40	9.4		112.4	- 3.7	327.1	0.095	4.4	107	74	
E237121	+58 587		3 12.7	+58 30	8.3	B2	108.9	+ 2.2	326.9	0.107	4.9	110	77	
20756	+20 543	T Ari	3 15.5	+20 47	5.17	B5	131.9	-28.4	321.0	0.008	0.4	171	132	0.00
	+49 916		3 17.1	+49 18	8.9		114.5	- 5.2	325.9	0.046	2.1	130	96	
20898	+59 648		3 17.1	+60 8	7.66	B8	108.4	+ 3.8	325.9	0.047	2.2	108	74	
20959	+58 600		3 17.8	+59 5	8.2	B5	109.1	+ 3.0	325.8	0.095	4.4	120	86	
21212	+61 587	MWC 667	3 20.3	+62 9	8.7	B2e	107.6	+ 5.7	325.2	0.088	4.0	135	100	+0.31
21278	+48 920	HR 1034	3 20.9	+48 48	4.94	B5	115.3	- 5.3	325.1	0.017	0.8	128	93	
21291	+59 660	HR 1035	3 21.0	+59 36	4.42	B9 Ia	109.1	+ 3.7	325.1	0.075	3.4	117	82	+0.18
21389	+58 607	MWC 461	3 21.9	+58 32	4.76	A0 Ia	109.6	+ 2.9	325.0	0.075	3.4	121	86	+0.23
21483	+29 566		3 22.7	+30 2	7.06	B3	127.0	-20.2	322.2	0.030	1.4	176	138	+0.30
22253	+56 824		3 29.9	+56 23	6.79	B0.5	112.0	+ 1.8	323.4	0.040	1.8	127	90	+0.17
23193	+36 742	HR 1133	3 38.1	+36 9	5.57	A2	125.6	-13.4	320.5	.....	...	....	....	-0.01
	+31 643		3 38.3	+31 51			128.5	-16.6	319.7	0.035	1.6	146	106	
23675	+52 714		3 41.9	+52 21	6.76	B0.5	115.8	- 0.4	321.0	0.067	3.1	133	94	+0.30
23800	+52 715		3 42.9	+52 11	6.87	B2	116.0	- 0.4	320.8	0.058	2.7	125	84	+0.21
		No. 6	3 46.7	+46 35			120.1	- 4.3	319.9	0.041	1.9	145	105	
24431	+52 726		3 48.1	+52 21	6.70	O8	116.6	+ 0.2	319.8	0.041	1.9	118	78	+0.23
24432	+48 1019		3 48.1	+48 45	7.02	B5	118.9	- 2.5	319.7	0.056	2.6	135	95	+0.26
	+55 857		3 50.0	+55 38	9.2		114.6	+ 2.9	319.3	0.110	5.1	133	92	
		No.7	3 51.0	+56 55			113.9	+ 4.0	319.1	0.067	3.1	134	93	
	+56 864		3 51.1	+56 56	9.2		113.9	+ 4.0	319.0	0.084	3.9	136	95	
			3 51.1	+56 56			113.9	+ 4.0	319.0	0.077	3.6	138	97	
	+56 866		3 51.4	+56 49	9.5		114.0	+ 3.9	319.0	0.097	4.5	136	95	
E237204	+56 868		3 52.4	+56 37	9.0	B3	114.2	+ 3.9	318.8	0.082	3.8	134	93	
	+55 858		3 52.8	+55 13	9.2		115.2	+ 2.9	318.8	0.097	4.5	133	92	
25090	+62 643		3 54.1	+62 9	7.28	B1	110.7	+ 8.2	318.1	0.130	6.0	136	94	+0.25
E232874	+58 725		3 54.5	+58 27	8.5	B3	116.6	+ 1.7	318.5	0.011	0.5	95	58	
E237211	+56 873		3 55.3	+56 15	8.9	B5	114.8	+ 3.9	318.2	0.075	3.4	139	97	
E237213	+55 845		3 56.5	+55 43	8.7	B	115.2	+ 3.6	318.0	0.079	3.6	138	96	
25348	+52 752	MWC 80	3 56.6	+53 3	8.2	B	117.1	+ 1.6	318.2	0.030	1.4	122	80	+0.17
25443	+61 669		3 57.4	+61 48	6.75	B0.5	111.2	+ 8.2	317.4	0.115	5.3	136	93	+0.24
25517	+43 886		3 58.1	+44 0	8.9	B2	123.3	- 4.9	317.6	0.055	2.5	160	118	+0.19
25787	+51 861		4 0.2	+51 11	7.49	B3	118.7	+ 0.6	317.4	0.040	1.8	141	98	+0.08
25914	+56 884		4 1.2	+56 50	8.1	B5	115.0	+ 4.8	317.0	0.102	4.7	141	98	+0.32
26630	+48 1065	μ Per	4 7.6	+48 9	4.28	G0 Ib	121.7	- 0.8	316.0	0.024	1.1	147	103	
E232947	+53 765		4 17.6	+53 11	9.0	B	119.2	+ 3.9	314.0	0.137	6.3	149	103	
	+51 921		4 17.7	+51 48	9.1		120.2	+ 2.9	314.0	0.097	4.5	140	94	
27795	+45 951		4 18.2	+45 56	7.16	B2	124.5	- 1.1	314.0	0.052	2.4	132	86	+0.21
281A9	+22 699	72 Tau	4 21.3	+22 46	5.41	B5	142.2	-16.4	310.8	.....	...	....	....	0.00
28446	+53 779	1 Cam	4 24.1	+53 42	5.42	B1	119.5	+ 5.0	312.7	0.050	2.3	151	104	+0.14
E237299	+57 851	MWC 87	4 32.9	+57 43	8.8	B2	117.3	+ 8.5	310.6	0.051	2.4	151	102	+0.22
E232999	+50 1043		4 37.0	+50 23	8.6	B	123.3	+ 4.2	310.5	0.082	3.8	158	108	
30353	+43 1069	MWC 758	4 41.8	+43 6	7.7	Ape	129.4	+ 0.2	309.8	0.050	2.3	149	99	
	+41 974	MWC 91	4 43.2	+41 30			130.8	- 0.7	309.6	0.026	1.2	159	109	
31327	+35 930	HR 1575	4 49.7	+36 1	6.18	B2	135.9	- 3.1	308.4	0.010	0.5	102	50	+0.28
	+30 748		4 52.1	+30 33	9.0		140.5	- 6.1	307.7	.....	...	....	....	
31617	+43 1147		4 52.2	+43 11	7.34	B2	130.6	+ 1.7	308.1	0.040	1.8	168	111	+0.10

TABLE 2 (Cont'd)

HD	BD	Other Designation	α 1900	δ 1900	Mag	Sp	l	b	φ	δ Mag	δ %	θ	θ'	E_1
	+43° 1168		4h 55m.0	+43°42'	9.0		130.5	+ 2.4	307.6	0.124	5.7	137°	85°	
32446	+44 1088		4 58.2	+44 55	7.97	B5	129.8	+ 3.6	307.0	0.050	1.4	147	94	+0.15
	+40 1189		5 3.3	+40 32	8.4		133.9	+ 1.7	306.3	0.043	2.0	160	106	
33357	+41 1101		5 4.6	+42 2	var.	A3	132.9	+ 2.8	306.0	0.047	2.2	154	100	
33461	+41 1106	MWC 101	5 5.3	+41 6	8.0	B3	133.7	+ 2.4	306.0	0.057	1.7	167	113	+0.16
33604	+40 1213	MWC 103	5 6.3	+40 5	7.32	B3	134.6	+ 1.9	305.8	0.026	1.2	165	111	+0.07
34626	+36 1090		5 13.8	+36 32	8.2	B2	136.4	+ 1.1	304.8	0.048	2.2	157	102	+0.09
34656	+37 1146		5 14.0	+37 20	6.71	O7	137.7	+ 1.6	304.7	0.057	2.6	167	112	+0.17
	+39 1264		5 14.1	+39 13	9.4		136.2	+ 2.7	304.7	0.062	2.8	156	101	
34921	+37 1160	MWC 107	5 15.8	+37 35	7.39	B0	137.7	+ 2.0	304.5	0.079	3.6	147	91	+0.21
E242908	+33 1023		5 16.0	+33 25	8.7	B0	141.2	- 0.3	304.5	0.054	2.5	151	95	
E242926	+33 1024		5 16.1	+33 13	9.5	B0	141.4	- 0.4	304.5	0.042	1.9	146	90	
E242935	+33 1026		5 16.2	+33 19	9.6	B3	141.3	- 0.4	304.4	0.065	3.0	163	107	
35215	+30 873		5 18.1	+30 6	9.11	F5	144.2	- 1.8	304.2	0.022	1.0	122	66	
35547	+29 886	MWC 494	5 19.0	+29 32	8.5	Pec.	144.8	- 2.0	304.0	0.024	1.1	135	79	
	+42 1286		5 19.4	+42 56	9.4		133.6	+ 5.6	303.6	0.079	3.6	143	87	
	+42 1288		5 20.1	+42 12	9.0		134.4	+ 5.3	303.6	0.090	4.1	162	106	
35619	+34 1046		5 21.0	+34 41	9.0	B0	140.7	+ 1.2	303.8	0.048	2.2	170	114	+0.20
35683	+34 1049		5 21.1	+34 27	8.6	B0	140.9	+ 1.1	303.8	0.023	1.1	172	116	+0.21
35658	+33 1049		5 21.2	+33 52	7.50	B1	141.4	+ 0.8	303.8	0.045	2.1	162	106	+0.17
	+34 1058		5 22.0	+34 35	8.8		140.9	+ 1.4	303.6	0.063	2.9	160	104	
35921	+35 1137		5 23.0	+35 18	6.71	O9.5	140.4	+ 1.9	303.5	0.043	2.0	143	87	+0.21
35952	+35 1139		5 23.2	+35 53	8.7	B8	140.0	+ 2.3	303.4	0.033	1.5	133	76	
	+35 1141		5 23.3	+35 7	9.1		140.6	+ 1.9	303.4	0.031	1.4	152	95	
36212	+34 1077		5 25.1	+34 48	8.0	B5	141.1	+ 2.0	303.2	0.044	2.0	163	106	
	+39 1328		5 25.2	+39 59	9.2		136.6	+ 4.9	302.9	0.096	4.4	163	106	
36280	+34 1079		5 25.5	+34 52	9.4	B	141.1	+ 2.1	303.1	0.027	1.2	154	97	+0.07
36389	+18 875	119 Tau	5 26.3	+18 32	4.75	M2 Ib	154.9	- 6.6	302.5	0.021	1.0	8	181	
36485	+36 1177		5 26.9	+36 24	7.7	B1	140.0	+ 3.2	302.9	0.068	3.8	149	92	+0.25
36547	+23 942		5 27.4	+23 16	8.8	B2	151.0	- 3.9	302.8	0.037	1.7	144	87	+0.20
	+35 1169	MWC 500	5 27.6	+35 45	8.4		140.6	+ 3.0	302.9	0.036	1.7	133	76	
36879	+21 899		5 29.7	+21 20	7.8	B2	153.0	- 4.4	302.4	0.045	2.1	152	94	+0.14
E245510	+21 901	MWC 505	5 30.4	+21 8	10.6	B	153.2	- 4.4	302.3	0.085	3.9	146	88	
37032	+34 1118		5 30.5	+34 45	8.1	B5	141.7	+ 2.9	302.5	0.030	1.4	169	111	
E245493	+33 1103	MWC 764	5 31.2	+33 54	8.5	B8	142.5	+ 2.6	302.4	0.024	1.1	165	107	
37614	+38 1250		5 34.7	+38 8	8.0	A	139.3	+ 5.4	301.7	0.044	2.0	170	112	
37737	+36 1233		5 35.7	+36 9	8.0	B3	141.1	+ 4.6	301.7	0.021	1.0	133	75	
37767	+36 1236		5 35.9	+36 6	8.4	B5	141.2	+ 4.6	301.6	0.019	0.9	7	129	
	+37 1292		5 35.9	+37 56	8.7		139.6	+ 5.5	301.5	0.025	1.2	5	127	
	+34 1150		5 36.4	+34 18	9.0		142.8	+ 3.7	301.7	0.016	0.7	41	163	
38017	+30 992		5 37.6	+30 53	8.1	B8	145.8	+ 2.1	301.6	0.047	2.2	13	135	
E246901	+33 1138		5 38.3	+33 29	8.9	B	143.7	+ 3.6	301.5	0.028	1.3	158	100	
38131	+35 1223		5 38.4	+35 8	8.12	B9	142.3	+ 4.5	301.4	0.018	0.8	169	110	
	+34 1162		5 38.6	+34 3	9.0		143.2	+ 4.0	301.4	0.024	1.1	176	117	
38191	+21 958		5 38.9	+21 25	9.5	B	154.0	- 2.6	301.5	0.040	1.8	152	94	+0.14
	+36 1261		5 41.7	+36 12	8.2		141.7	+ 5.6	300.8	0.025	1.2	169	110	
38658	+28 902		5 42.3	+28 17	8.5	B8	148.6	+ 1.6	301.2	0.021	1.0	0	121	
38708	+29 1005		5 42.6	+29 6	8.2	A2	147.9	+ 2.1	301.1	0.025	1.2	167	108	
38909	+31 1115		5 44.0	+31 2	8.0	B5	146.4	+ 3.4	300.9	0.025	1.2	152	93	
E248587	+19 1111		5 46.5	+19 7	8.9	A5	156.9	- 2.2	300.7	0.054	2.5	146	87	
E248758	+25 1019		5 47.3	+25 43	8.4	B0	151.3	+ 1.3	300.6	0.047	2.2	141	82	+0.16
E248898	+22 1090		5 48.0	+22 6	10.0	B	154.5	- 0.4	300.6	0.075	3.4	155	96	
E248894	+20 1158		5 48.0	+20 51	9.2	B	155.6	- 1.1	300.6	0.049	2.2	146	87	
39680	+13 1026	MWC 783	5 49.0	+13 49	7.9	B	161.8	- 4.4	300.2	0.014	0.6	143	83	
39746	+27 914		5 49.4	+27 42	7.7	B2	149.9	+ 2.7	300.4	0.040	1.8	178	118	+0.14
39970	+24 1033	HR 2074	5 50.9	+24 14	6.02	B5	153.0	+ 1.2	300.4	0.035	1.6	161	101	+0.18
40005	+23 1119		5 51.1	+23 25	8.6	F8	153.8	+ 0.9	300.3	0.062	2.8	167	107	
40111	+25 1052	139 Tau	5 51.8	+25 57	4.90	B0.5	151.6	+ 2.3	300.2	0.023	1.1	164	104	+0.06
E249695	+30 1071	MWC 785	5 52.2	+30 12	8.9	B0	148.0	+ 4.5	300.0	0.024	1.1	174	114	
E249845	+32 1146		5 53.0	+32 58	8.8	B5	145.8	+ 6.0	299.6	.....	...	....	....	

TABLE 2 (Cont'd)

HD	BD	Other Designation	α 1900	δ 1900	Mag	Sp	l	b	φ	δ Mag	δ %	θ	θ'	E_1
E250028	+25 1065	MWC 786	5h 55m8	+25° 6'	8.9	B2	152.6	+ 2.2	300.0	0.093	4.3	164°	104°	
E250165	+19 1166	MWC 517	5 54.4	+19 11	10.2	B0	157.8	- 0.6	300.0	0.036	1.7	136	76	
40589	+27 945	HR 2111	5 54.7	+27 35	6.08	B8p	150.6	+ 3.6	299.8	0.015	0.7	158	98	
E250289	+23 1148		5 55.0	+23 20	9.2	B	154.3	+ 1.6	300.0	0.064	2.9	162	102	
E250290	+23 1149		5 55.0	+23 18	8.6	B	154.3	+ 1.6	300.0	0.073	3.4	168	108	
E251117	+28 1001		5 58.7	+28 46	9.0	B0	150.0	+ 5.0	299.3	0.033	1.5	161	100	
E251511	+25 1185		5 59.4	+25 1	8.8	B0	155.1	+ 2.3	299.6	0.048	2.2	0	120	
41398	+28 1008		5 59.8	+28 56	7.45	B2	149.9	+ 5.3	299.2	0.048	2.2	166	105	+0.20
E251726	+19 1210		6 1.0	+19 2	10.0	F5	158.7	+ 0.7	299.5	0.069	3.2	171	111	
41690	+21 1120		6 1.6	+21 58	8.0	B2	156.3	+ 2.2	299.4	0.058	2.7	177	116	+0.16
41997	+15 1079		6 3.2	+15 44	8.5	B	161.8	- 0.5	299.4	0.070	3.2	159	98	
42087	+23 1226	MWC 520	6 3.7	+23 8	5.76	B2.5	155.4	+ 3.2	299.2	0.043	2.0	172	111	+0.15
42088	+20 1284		6 3.7	+20 31	7.40	O6	157.7	+ 2.0	299.3	0.052	2.4	176	117	+0.10
42379	+21 1145		6 5.3	+21 36	7.8	B2	157.0	+ 2.8	299.1	0.060	2.8	170	109	+0.20
42400	+20 1302		6 5.4	+20 56	6.86	B5	157.6	+ 2.5	299.1	0.047	2.2	169	108	+0.10
E253049	+20 1305		6 5.8	+20 10	9.4	B8	158.3	+ 2.2	299.1	0.040	1.8	176	115	
42475	+21 1146	TV Gem	6 5.8	+21 54	var.	cM	156.8	+ 3.0	299.0	0.065	3.0	172	111	
42543	+22 1220	6 Gem	6 6.2	+22 56	6.30	M1 Ia	155.9	+ 3.6	298.9	0.046	2.1	174	113	
E253214	+20 1309	MWC 135	6 6.4	+20 7	9.4	B0	158.4	+ 2.3	299.1	0.060	2.8	173	112	+0.24
E253247	+18 1128		6 6.5	+18 3	10.0	B2	160.2	+ 1.3	299.1	0.031	1.4	4	123	
E253659	+16 1046	MWC 796	6 8.1	+16 33	9.7	B0	161.7	+ 0.9	299.0	0.050	2.3	0	119	
42896	+20 1322		6 8.2	+20 13	9.0	B5	158.5	+ 2.7	298.9	0.018	0.8	7	126	
43078	+22 1243		6 9.2	+22 20	8.6	B0	156.8	+ 4.0	298.7	0.070	3.2	165	104	+0.25
E254042	+24 1176		6 9.8	+24 6	8.8	B0	155.3	+ 4.9	298.5	0.085	3.9	173	111	
43384	+25 1275	9 Gem	6 10.8	+25 46	6.26	B3 Ib	155.7	+ 5.0	298.5	0.062	2.8	170	108	+0.20
43582	+22 1267		6 11.9	+22 41	9.0	B6	156.8	+ 4.7	298.4	0.028	1.3	8	126	
E254699	+23 1286		6 12.3	+23 36	9.3	B5	156.0	+ 5.2	298.3	0.074	3.4	176	114	
E254755	+22 1275		6 12.5	+22 43	9.0	B0	156.8	+ 4.8	298.4	0.039	1.8	8	126	
43703	+23 1289	MWC 799	6 12.6	+23 3	8.7	B2	156.5	+ 5.0	298.4	0.037	1.7	143	81	+0.24
43753	+23 1297		6 12.9	+23 2	8.1	B1	156.6	+ 5.0	298.3	0.059	2.7	161	99	+0.18
43818	+23 1300		6 13.2	+23 30	7.03	B0.5	156.2	+ 5.3	298.3	0.043	2.0	177	115	+0.22
43836	+23 1301		6 13.3	+23 19	7.03	B9	156.3	+ 5.2	298.3	0.012	0.6	149	87	+0.23
43837	+20 1369		6 13.3	+20 37	8.4	B	158.7	+ 4.0	298.5	0.054	2.5	150	88	
E255055	+23 1304		6 13.6	+23 20	9.1	B0	156.4	+ 5.3	298.2	0.019	0.9	168	101	
43907	+22 1260		6 13.7	+22 9	8.8	B8	157.4	+ 4.8	298.3	0.031	1.4	16	134	
44139	+22 1291		6 15.1	+22 13	8.8	B9	157.5	+ 5.1	298.2	0.046	2.1	2	120	
44597	+20 1399		6 17.5	+20 27	9.0	B	159.3	+ 4.8	298.1	0.047	2.2	170	108	
E256276	+22 1311		6 17.7	+22 27	9.1	B8	157.6	+ 5.7	298.0	0.033	1.5	9	127	
E256413	+19 1351		6 18.1	+19 58	8.9	B3	159.8	+ 4.7	298.1	0.054	2.5	168	106	
44811	+19 1335		6 18.8	+19 45	8.7	B5	160.1	+ 4.7	298.1	0.035	1.6	172	110	
	+50 1309		6 20.6	+50 20			132.1	+18.3	292.1	.....	...	....	....	
45166	+ 8 1332		6 20.8	+ 8 3	9.6	Oe	170.6	- 0.4	298.4	0.018	0.8	162	100	+0.08
E257971	+11 1191		6 23.1	+11 22	8.9	B3	168.0	+ 1.6	298.2	.....	...	....	....	
46056	+ 4 1291	MWC 808	6 26.0	+ 4 54	7.96	O8	174.0	- 0.8	298.2	0.025	1.2	154	92	+0.17
46149	+ 5 1282		6 26.6	+ 5 6	7.66	O8	173.9	- 0.6	298.2	.....	...	....	....	+0.14
46150	+ 5 1285		6 26.6	+ 5 0	6.80	B2	174.0	- 0.6	298.2	0.016	0.7	7	125	+0.19
46225	+ 4 1302		6 27.0	+ 4 53	7.14	B2	174.2	- 0.6	298.2	0.030	1.4	169	107	+0.19
46300	+ 7 1337	13 Mon	6 27.5	+ 7 24	4.50	A0 Ib	172.0	+ 0.7	298.2	.....	...	....	....	-0.03
E259431	+10 1172	MWC 147	6 27.6	+10 24	9.0	B3	169.4	+ 2.2	298.1	0.017	0.8	106	44	+0.09
E259440	+ 5 1291	MWC 148	6 27.6	+ 5 52	9.6	B0	173.4	+ 0.1	298.2	0.088	4.0	164	102	
47240	+ 5 1334	HR 2452	6 32.5	+ 5 3	6.16	B1	174.7	+ 0.7	298.0	0.023	1.1	173	111	
47359	+ 5 1340	MWC 815	6 33.1	+ 4 58	8.81	B	174.8	+ 0.8	298.0	0.022	1.0	8	126	
47761	- 4 1607	MWC 551	6 35.1	- 4 36	8.5	B0	185.5	- 3.2	297.8	0.048	2.2	169	107	+0.16
48279	+ 1 1472		6 37.5	+ 1 49	7.8	O8	178.1	+ 0.3	298.0	0.029	1.3	155	93	+0.21
	+ 0 1576		6 39.7	+ 0 43	9.2		179.3	+ 0.3	298.0	0.050	2.3	146	84	
49340	+69 394	43 Cam	6 42.9	+69 0	5.13	B5	113.6	+26.2	280.1	0.010	0.5	148	68	-0.02
53428	- 8 1729		6 59.9	- 8 42	7.9	B2	190.0	+ 0.3	298.4	0.015	0.7	117	55	+0.24
53649	- 8 1733		7 0.7	- 8 52	9.1	B	190.2	+ 0.4	298.4	0.029	1.3	114	52	
53667	- 8 1734	MWC 885	7 0.8	- 8 34	7.8	Oe5	190.0	+ 0.5	298.4	0.025	1.2	127	65	+0.17
53754	- 8 1737		7 1.1	- 8 39	8.4	B5	190.1	+ 0.6	298.5	0.032	1.5	129	67	

TABLE 2 (Cont'd)

HD	BD	Other Designation	α 1900	δ 1900	Mag	Sp	l	b	φ	δ Mag	δ %	θ	θ'	E_1
56847	-15° 1748		7h 15.6	-15°27'	8.7	B2	197.5	0.0	299.1	0.015	0.7	97°	86°	+0.19
153764	- 8 4010	HR 6780	15 29.0	- 8 51	5.15	B5	324.2	+35.0	46.4	0.008	0.4	75	121	-0.01
147888	-23 12860		16 19.4	-23 14	6.56	B5	321.5	+16.4	48.8	0.065	3.0	53	102	+0.20
147889	-24 12684		16 19.4	-24 14	8.0	B2	320.8	+15.7	48.6	0.069	3.2	179	48	+0.50
149368	- 5 4518		16 29.1	- 5 56	8.0	B0.5	337.7	+25.2	55.2	0.028	1.3	79	134	+0.09
152516	-21 4443		16 48.7	-21 43	8.08	B5	327.2	+12.1	53.0	0.065	3.0	52	105	+0.10
153855	-31 13502		16 56.8	-31 28	6.88	B2	320.4	+ 4.7	52.9	0.023	1.1	25	78	+0.07
153977	-24 13055	MWC 867	16 57.6	-24 41	9.8	B3	326.0	+ 8.7	53.6	0.025	1.2	35	89	+0.09
154040	-39 11086	MWC 868	16 57.9	-39 11	9.5	B2	314.4	- 0.1	52.8	0.055	2.5	58	111	+0.47
154090	-33 11706	MWC 589	16 58.2	-33 59	4.87	B1p	318.6	+ 3.0	53.0	.....	...	....	....	+0.20
154204	-20 4627	HR 6340	16 58.9	-20 21	6.17	B3	329.7	+11.0	54.4	0.037	1.7	58	112	+0.07
154445	- 0 5224	HR 6353	17 0.4	- 0 45	5.62	B2	347.0	+21.4	59.4	0.078	3.4	91	150	+0.08
158661	-17 4834		17 25.4	-17 3	8.2	B0.5	336.0	+ 7.6	57.6	0.012	0.6	58	116	+0.16
158705	-31 14176		17 25.6	-31 28	7.81	B0	323.9	- 0.3	56.8	0.038	1.8	124	1	+0.44
159176	-32 12955	HR 6535	17 28.1	-32 31	5.71	O=5	323.3	- 1.3	57.2	0.036	1.7	166	45	+0.13
160529	-33 12361	MWC 266	17 35.8	-33 27	6.68	cAlpe	323.4	- 3.1	58.1	0.150	6.9	20	78	+0.46
160704	-23 13515		17 36.3	-23 41	9.5	B2	331.8	+ 1.9	58.2	0.086	4.0	7	65	+0.42
160730	-24 13435		17 36.4	-24 15	10.2	B	331.3	+ 1.6	58.2	0.078	3.6	2	60	+0.40
161108	-27 11872	MWC 268	17 38.5	-27 12	7.9	B0	329.0	+ 0.4	58.4	0.108	5.0	172	50	+0.26
162064	-19 4713		17 44.0	-19 52	8.98	B	336.0	+ 2.4	59.0	0.082	1.5	53	112	+0.35
162168	-32 13411		17 44.5	-32 58	8.0	B0	324.8	- 4.5	59.3	0.050	2.3	161	40	+0.37
162717	-24 13584		17 47.3	-24 15	9.5	B3	332.6	- 0.5	59.3	0.067	3.1	179	58	+0.36
162718	-24 13585	MWC 278	17 47.3	-24 45	9.0	B0	332.2	- 0.8	59.3	0.077	3.6	7	66	+0.42
162978	-24 13615	HR 6672	17 48.7	-24 52	6.13	B2	332.2	- 1.1	59.4	0.027	1.2	179	58	+0.08
163777	-25 12523		17 52.8	-25 10	9.5	B	332.4	- 2.1	59.9	0.019	0.9	168	43	+0.26
164018	-25 13741		17 54.0	-25 7	10.0	B	334.4	- 1.3	59.9	0.029	1.3	132	12	+0.38
164103	-14 4842		17 54.5	-14 47	8.04	B5	341.6	+ 2.8	60.1	0.014	0.6	38	98	+0.24
164359	-22 4500		17 55.6	-22 7	8.2	B0	335.4	- 1.1	60.1	0.014	0.6	5	65	+0.04
164384	-25 13789		17 55.7	-25 10	8.5	B5	334.5	- 1.6	60.1	.....	...	....	....	+0.03
164402	-22 4505	HR 6716	17 55.8	-22 46	5.73	O9.5	334.9	- 1.5	60.1	0.014	0.6	7	67	+0.06
164432	+ 6 3597	HR 6719	17 56.0	+ 6 16	6.18	B3	0.4	+12.6	62.6	0.013	0.6	88	151	+0.05
164438	-19 4800		17 56.0	-19 6	7.28	B3	338.1	+ 0.3	60.1	0.028	1.3	73	133	+0.21
164492	-23 13804		17 56.3	-23 1	6.91	O8	334.7	- 1.7	60.2	.....	...	....	....	+0.26
164536	-24 13783		17 56.5	-24 15	6.87	B3	333.7	- 2.4	60.2	0.009	0.4	29	89	+0.03
164738	-17 5001		17 57.5	-17 36	7.10	B5	339.5	+ 0.8	60.2	0.024	1.1	27	87	+0.13
164852	+20 3649	96 Her	17 58.1	+20 50	5.09	B3	14.3	+18.5	66.3	0.018	0.8	178	64	+0.02
164865	-24 13826		17 58.1	-24 11	8.3	B	333.9	- 2.6	60.4	0.020	0.9	34	94	+0.30
165049	-15 4803		17 59.0	-15 22	8.07	B2	341.7	+ 1.6	60.4	0.015	0.7	49	109	+0.28
165052	-24 13864		17 59.0	-24 24	6.79	O=5	333.8	- 2.9	60.5	.....	...	....	....	+0.14
165319	-14 4880		18 0.3	-14 12	8.1	B0	342.8	+ 1.9	60.5	0.029	1.3	58	119	+0.38
165768	-21 4864		18 2.5	-21 16	7.82	O=	336.9	- 2.1	60.7	.....	...	....	....	
166286	-16 4756		18 4.8	-16 46	7.58	B1	341.1	- 0.4	60.7	0.020	0.9	11	72	+0.21
166504	-16 4759		18 4.9	-16 44	9.7	B5	341.2	- 0.4	60.7	0.029	1.3	53	114	+0.18
	+38 3095		18 6.3	+38 29			52.6	+23.3	71.8	.....	...	....	....	
166628	-19 4895		18 6.4	-19 28	7.14	B3	339.0	- 2.0	60.9	0.010	0.5	155	36	+0.36
166734	-10 4625	MWC 286	18 6.9	-10 46	8.3	B0	346.6	+ 2.1	61.0	0.070	3.2	65	125	+0.61
167268	-20 5055	16 Sgr	18 9.3	-20 25	6.02	O9 II	338.4	- 3.0	61.2	.....	...	....	....	+0.07
167264	-20 5054	15 Sgr	18 9.3	-20 46	5.42	B0 Ia	338.2	- 3.2	61.2	.....	...	....	....	+0.09
167330	-12 4954		18 9.6	-12 34	8.1	B0	345.4	+ 0.7	61.0	0.040	1.8	74	135	+0.35
167451	-13 4897		18 10.2	-13 36	7.9	B2	344.5	0.0	61.1	0.021	1.0	37	98	+0.39
167543	-14 4959		18 10.6	-14 40	8.8	B2	343.6	- 0.6	61.1	0.052	2.4	122	3	+0.26
167838	-15 4911		18 11.9	-15 28	6.64	B5 Ia	343.1	- 1.2	61.2	.....	...	....	....	+0.30
167971	-12 4980		18 12.5	-12 17	7.34	O8f	346.0	+ 0.2	61.2	0.028	1.3	150	31	+0.46
168112	-12 4988		18 13.1	-12 8	8.7	B0	346.2	+ 0.1	61.3	0.025	1.2	127	8	+0.41
168206	-11 4598		18 13.5	-11 40	8.87	WC7	346.6	+ 0.3	61.3	0.053	2.4	92	158	
168302	-16 4812		18 13.9	-16 3	9.9	B5	342.8	- 1.9	61.4	0.020	0.9	76	137	+0.41
168571	-17 5151		18 15.3	-17 26	8.3	B2	341.8	- 2.9	61.5	0.023	1.1	92	153	+0.33
168607	-16 4829	MWC 291	18 15.5	-16 25	8.9	B8	342.7	- 2.4	61.5	0.046	2.1	20	81	
168625	-16 4830		18 15.6	-16 25	9.2	B2	342.7	- 2.4	61.5	0.095	4.4	13	75	
169034	-13 4958		18 17.6	-13 39	8.3	B3 Ia	345.4	- 1.6	61.5	0.042	1.9	66	127	+0.67

TABLE 2 (Cont'd)

HD	BD	Other Designation	α 1900	δ 1900	Mag	Sp	l	b	φ	δ Mag	δ %	θ	θ'	E_1
169454	-14° 5089	MWC 294	18h 19m6	-14° 2'	6.84	B1 Ia	345.2	- 2.2	61.6	0.046	2.1	-12°	74°	+0.51
169754	-11 4681		18 21.1	-11 25	8.1	B2	347.7	- 1.2	61.7	0.015	0.7	44	106	+0.56
170159	-13 4992		18 22.9	-13 4	8.7	BO	346.5	- 2.4	61.8	0.025	1.2	117	179	+0.33
170938	-15 5004		18 26.9	-15 46	8.7	B1	344.5	- 4.5	69.2	0.076	3.6	119	8	+0.50
172252	-12 5152	MWC 947	18 34.1	-11 58	8.7	BO	348.7	- 4.3	62.3	0.104	4.8	147	29	+0.43
172567	- 7 4650		18 34.7	- 7 20	9.7	BO	352.9	- 2.3	62.0	0.035	1.6	11	78	+0.28
173438	- 4 4575		18 40.2	- 4 42	8.1	BO	355.9	- 2.2	62.1	0.057	2.6	58	115	+0.42
173687	- 8 4702	MWC 607	18 41.2	- 8 2	9.2	BO	353.0	- 4.0	62.3	0.025	1.2	87	149	+0.23
174261	+21 3560		18 44.6	+21 3	6.93	B3	19.3	+ 8.8	63.3	.....	...	....	....	+0.03
174391	+15 3583		18 45.2	+15 49	6.54	B3	14.6	+ 6.2	62.6	.....	...	....	....	+0.02
174571	+ 8 3866	MWC 610	18 46.0	+ 8 35	8.4	B2	8.3	+ 2.7	62.1	0.066	3.0	80	142	+0.28
175514	+ 9 3928		18 50.6	+ 9 13	8.5	BO	9.4	+ 2.0	62.0	0.045	2.1	106	168	+0.30
175544	+ 0 4055		18 50.7	+ 0 8	7.73	B3	1.4	- 2.3	62.0	.....	...	....	....	+0.14
175803	+19 3848		18 52.0	+19 43	7.97	B3	18.9	+ 6.6	62.6	0.015	0.7	26	89	+0.13
177812	+ 3 3893		19 1.1	+ 3 6	8.9	B2	5.2	- 3.2	61.7	0.030	1.4	65	127	+0.34
178129	+ 3 3902		19 2.3	+ 3 17	8.0	B5	5.5	- 3.4	61.7	0.010	0.5	48	110	+0.26
180126	+ 9 4037		19 10.2	+ 9 37	7.9	B3p	12.0	- 2.1	61.2	0.008	0.4	27	88	+0.15
180398	+12 3861	MWC 512	19 11.3	+12 56	7.7	B9	15.1	- 0.7	61.0	.....	...	....	....	+0.12
180968	+22 3648	2 Vul	19 13.5	+22 51	5.40	B0.5	24.0	+ 3.7	61.1	0.015	0.7	18	79	+0.10
183143	+18 4085	MWC 517	19 25.0	+18 5	6.93	B7 Ia	20.9	- 0.6	60.2	0.135	6.2	179	59	+0.50
183561	+26 3566		19 25.1	+26 30	8.0	B8	28.5	+ 3.2	60.1	0.024	1.1	178	58	
184279	+ 3 4065	MWC 519	19 28.6	+ 3 54	6.78	BO.5	8.9	- 9.0	60.9	.....	...	....	....	+0.01
185418	+16 3928		19 33.9	+17 2	7.42	B3	21.6	- 3.4	59.3	0.015	0.7	13	72	+0.09
185780	+40 3824		19 35.7	+40 24	7.47	B2	41.7	+ 8.2	60.0	0.014	0.6	99	159	+0.08
185859	+20 4218	HR 7482	19 36.1	+20 15	6.44	BO.5 Ib	24.4	- 2.2	59.0	0.040	1.8	8	67	+0.26
186746	+23 3760		19 41.2	+23 41	7.01	B8p	27.9	- 1.4	58.4	0.040	1.8	25	83	
186841	+23 3767		19 41.7	+23 50	8.2	O5	28.1	- 1.4	58.4	0.056	2.6	27	85	
186943			19 42.2	+28 1	9.98	WN5	31.7	+ 0.7	58.3	0.021	1.0	18	76	
187282			19 44.1	+17 57		WN5	25.4	- 5.0	58.4	0.026	1.2	4	62	
187459	+33 3602	HR 7551	19 45.0	+33 12	6.35	BO.5 II	36.4	+ 2.9	58.1	0.062	2.8	33	91	+0.16
187983	+24 3914	HR 7575	19 47.8	+24 44	5.67	A2 Ia	29.6	- 2.1	57.8	0.019	0.9	159	37	
189066	+35 3878	HR 7620	19 53.1	+35 59	6.04	B5	39.7	+ 3.0	57.1	0.008	0.4	88	145	+0.01
189779	+29 3844		19 56.6	+29 37	8.2	B9	34.8	- 1.1	56.5	0.018	0.8	63	119	
190066	+21 4027		19 58.1	+21 52	6.55	BO.5	28.5	- 5.7	56.8	0.030	1.4	33	90	+0.16
190467	+36 3841	MWC 1000	20 0.0	+36 8	8.0	B2	40.6	+ 1.9	56.1	0.010	0.5	153	29	+0.16
190603	+31 3925	MWC 326	20 0.7	+31 56	5.69	B1.5	37.2	- 0.6	56.0	0.018	0.8	76	132	+0.35
190864	+35 3949		20 1.9	+35 19	8.2	O6	40.1	+ 1.2	55.8	0.020	0.9	168	44	+0.16
190967	+34 3871		20 2.4	+35 6	7.92	B3	40.0	+ 0.9	55.8	0.022	1.0	104	160	+0.18
191611	+36 3906		20 5.7	+36 12	8.6	B	41.3	+ 1.0	55.3	.....	...	....	....	
191781	+44 3865		20 6.6	+45 6	9.25	B	48.8	+ 5.9	55.6	0.015	0.7	17	78	
192103	+35 4013		20 8.1	+35 54	7.94	WC7	41.3	+ 0.4	54.9	.....	...	....	....	
192281	+39 4082		20 9.0	+39 58	7.47	O5f	44.8	+ 2.6	54.9	0.015	0.7	9	64	+0.30
192422	+38 3956		20 9.7	+38 28	7.10	BO.5	43.6	+ 1.6	54.7	0.034	1.6	11	66	+0.27
192539	+31 4001		20 10.3	+31 41	7.38	B5	38.1	- 2.4	54.7	0.025	1.2	177	52	+0.16
192659	+36 3958		20 10.8	+37 3	7.02	O8f	42.6	+ 0.6	54.6	.....	...	....	....	+0.26
192641	+36 3956		20 10.8	+36 21	7.94	WN	42.0	+ 0.2	54.5	0.025	1.2	168	43	
192660	+39 4096		20 10.9	+40 1	7.72	B3	45.0	+ 2.3	54.6	0.022	1.0	140	16	
192832	+41 3675		20 11.9	+42 6	8.5	B	46.8	+ 3.4	54.5	0.025	1.2	63	117	
193032	+38 3980		20 13.0	+38 35	8.1	B	44.1	+ 1.2	54.2	0.035	1.6	38	92	
193076	+37 3866		20 13.3	+37 22	8.0	B	43.1	+ 0.4	54.2	0.010	0.5	96	150	
193077	+36 3987		20 13.3	+37 7	7.97	WN5.5	42.9	+ 0.3	54.2	0.015	0.7	103	157	
193117	+40 4090		20 13.5	+40 32	9.0	B	45.7	+ 2.2	54.2	0.033	1.5	10	64	
193182	+39 4115	MWC 652	20 13.8	+39 16	6.56	Ape	44.7	+ 1.4	54.1	0.014	0.6	134	8	
E228766	+36 3991	MWC 1010	20 13.8	+37 0	9.8	WN7	42.9	+ 0.1	54.1	0.025	1.2	112	166	
193237	+37 3871	MWC 338	20 14.1	+37 43	4.88	Bp	43.5	+ 0.5	54.1	0.023	1.1	37	91	
E228841	+38 4000		20 14.8	+38 54	8.7	BO	44.3	+ 0.9	54.0	0.028	1.3	174	48	+0.32
193370	+34 3967	55 Cyg	20 14.8	+34 40	5.18	F5p	41.1	- 1.4	54.0	.....	...	....	....	
193514	+38 4006		20 15.5	+38 57	7.29	O8f	44.7	+ 1.0	53.9	0.030	1.4	48	102	+0.38
193576	+38 4010		20 15.8	+38 25	8.04	WN6	44.3	+ 0.6	53.8	0.015	0.7	150	24	
E228943	+38 4016		20 16.1	+38 17	10.0	B	44.2	+ 0.5	53.8	0.025	1.2	14	68	

TABLE 2 (Cont'd)

HD	BD	Other Designation	α 1900	δ 1900	Mag	Sp	l	b	φ	δ Mag	δ %	θ	θ'	E_{B-V}
193928	+36° 4028		20h 17m8	+36°36'	9.43	WN6	43.0	- 0.8	53.5	0.026	1.8	68°	121°	
E229153	+37 3910		20 19.0	+37 39	10.1	B	44.0	- 0.3	53.6	0.022	1.0	169	42	
E229159	+38 4050		20 19.2	+38 53	9.4	B	45.0	+ 0.4	53.3	0.035	1.6	79	132	
E229171	+37 3913		20 19.4	+38 8	9.9	B	44.5	- 0.1	53.3	0.017	0.8	20	73	
194279	+40 4150	MWC 654	20 19.7	+40 26	7.05	B2	46.3	+ 1.2	53.3	0.061	2.8	177	50	+0.54
	+36 4048		20 19.8	+36 59	9.4		43.6	- 0.9	53.2	0.068	2.9	54	107	
E229221	+38 4062	MWC 344	20 20.1	+38 11	10.0	B	44.6	- 0.3	53.1	0.034	1.6	66	119	+0.50
E229227	+38 4065		20 20.2	+38 8	10.1	B	44.6	- 0.3	53.1	0.019	0.9	63	116	
E229282	+38 4070		20 20.3	+38 47	10.3	B	45.1	+ 0.1	53.1	0.091	4.2	67	120	
E229284	+38 4069		20 20.3	+38 12	9.3	B	44.6	- 0.2	53.1	0.027	1.2	93	146	
E229288	+38 4071		20 20.4	+38 13	9.5	B	44.6	- 0.2	53.1	0.030	1.4	86	139	
E229289	+38 4072	MWC 1016	20 20.4	+38 11	9.6	B	44.6	- 0.2	53.1	0.041	1.9	99	152	
194779	+40 4164		20 22.4	+41 1	7.66	B	47.1	+ 1.2	52.8	0.010	0.5	57	110	+0.19
	+39 4189		20 22.7	+39 20	9.3		45.8	+ 0.1	52.7	0.060	2.8	14	67	
194889	+40 4165	MWC 1017	20 22.8	+41 3	7.45	BO Ia	47.2	+ 1.1	52.7	0.026	1.2	171	44	+0.54
	+38 4098		20 23.8	+38 26	9.1		45.2	- 0.6	52.6	0.048	2.2	68	121	
	+37 3945		20 24.5	+38 2	9.4		45.0	- 1.0	52.4	0.067	3.1	64	116	
	+40 4185		20 24.5	+40 18	9.4		46.8	+ 0.4	52.4	0.015	0.7	158	30	
195407	+36 4095	MWC 346	20 26.0	+36 39	7.72	B5	44.1	- 2.0	52.3	0.035	1.6	48	100	+0.19
195592	+43 3680	MWC 347	20 27.2	+43 59	7.15	O9 I	50.0	+ 2.3	52.1	0.027	1.2	117	169	+0.52
195593	+36 4105	44 Cyg	20 27.2	+36 36	6.30	F5 Ia	44.2	- 2.3	52.1	0.048	2.2	65	117	
195965	+47 3136		20 29.3	+47 53	6.82	B2	53.3	+ 4.4	51.9	0.020	0.9	35	87	+0.05
	+37 3976		20 30.0	+37 56	9.4		45.6	- 1.9	51.6	0.051	2.4	167	39	
	+36 4145		20 32.5	+37 4	8.5		45.2	- 2.8	51.2	0.038	1.8	38	89	
196604	+44 3519		20 33.4	+44 34	6.3	A3	51.2	+ 1.8	51.0	.....	...	....	....	
197406	+52 2777		20 38.4	+52 14	10.3	Ma	57.6	+ 6.0	50.5	0.020	0.9	101	151	
	+42 3835		20 38.5	+42 49	8.9		50.4	- 0.1	50.1	0.029	1.3	16	66	
197460	+35 4229		20 38.8	+36 2	8.6	WN	45.2	- 4.4	50.3	0.032	1.5	3	53	+0.21
197770	+56 2477	HR 7940	20 40.7	+56 46	6.36	B2	61.4	+ 8.6	50.5	0.088	4.0	130	1	+0.23
	+35 4258		20 42.2	+35 11	9.1		45.0	- 5.5	49.8	0.011	0.5	7	57	
E235350	+50 3189		20 42.3	+50 49	9.0	BO	56.9	+ 4.6	49.7	.....	...	....	....	
198478	+45 3291	MWC 353	20 45.5	+45 45	4.89	B8 Ia	53.4	+ 0.9	48.9	0.061	2.8	5	54	+0.25
198479	+45 3290		20 45.5	+45 16	8.52	B5	53.1	+ 0.6	48.9	0.057	2.6	15	64	
198512	+53 2495	MWC 354	20 45.7	+53 32	7.95	Pec.	59.4	+ 6.0	49.2	0.041	1.9	128	177	+0.16
	+44 3594	MWC 1051	20 45.7	+45 3	9.4		52.9	+ 0.4	48.9	0.044	2.0	12	61	
198781	+63 1668	HR 7993	20 47.6	+63 40	6.38	BO	67.3	+12.3	50.1	0.030	1.4	157	27	+0.07
198895	+54 2429	MWC 355	20 48.4	+55 7	6.26	B3	60.8	+ 6.7	48.9	0.119	5.5	149	18	+0.34
198931	+43 3747	MWC 1052	20 48.6	+44 3	9.0	B8	52.5	- 0.6	48.4	0.096	4.4	146	14	
	+37 4092		20 49.8	+37 48	9.2		48.0	- 5.0	48.4	0.028	1.3	172	40	
199216	+48 3242		20 50.7	+49 9	7.13	B1	56.6	+ 2.5	48.1	0.040	1.8	135	3	+0.32
199308	+55 2486		20 51.3	+55 58	7.61	B3	61.7	+ 7.0	48.4	0.042	1.9	162	30	+0.12
199356	+39 4368	MWC 357	20 51.6	+39 55	7.02	BOp	49.8	- 3.8	48.0	0.058	2.7	151	19	+0.16
199478	+46 3111	MWC 358	20 52.4	+47 2	5.76	B8	55.2	+ 0.8	47.7	0.040	1.8	11	59	+0.22
	+42 3914		20 52.7	+42 44	8.3		52.0	- 2.1	47.7	0.100	4.6	150	18	
199579	+44 3689	HR 8028	20 53.1	+44 33	6.01	O6	53.4	- 0.9	47.6	0.020	0.9	55	108	+0.11
	+45 3341		20 53.6	+46 9	9.0		54.7	+ 0.1	47.5	0.068	3.1	50	98	
	+44 3655		20 54.8	+44 45	9.3		53.8	- 1.0	47.3	0.048	2.2	42	89	
	+45 3360		20 57.0	+45 51	9.5		54.8	- 0.5	46.9	0.030	1.4	25	72	
200776	+45 3384		21 0.4	+45 56	8.1	B8	55.3	- 0.9	46.3	0.010	0.5	31	77	
200857	+54 2470		21 1.0	+54 51	7.16	B3	61.8	+ 5.2	46.4	0.036	1.7	155	21	+0.36
202124	+43 3842		21 8.8	+44 7	7.83	B	55.0	- 3.2	44.8	0.011	0.5	90	135	+0.14
202214	+59 2334	HR 8119	21 9.3	+59 35	5.65	B1	66.0	+ 7.7	45.1	0.017	0.8	143	8	+0.15
202258	+43 3850		21 9.5	+43 28	7.70	B3	54.7	- 3.8	44.7	0.015	0.7	50	95	+0.13
	+41 4064		21 12.3	+42 7	8.6		54.1	- 5.1	44.2	0.052	2.4	53	97	
203025	+57 2309	MWC 365	21 14.6	+58 10	6.41	B3	65.5	+ 6.2	43.9	.....	...	....	....	+0.17
203938	+46 3294		21 20.2	+46 44	7.10	B1	58.3	- 2.7	42.6	0.030	1.4	160	25	+0.33
	+43 3913	MWC 640	21 21.3	+44 1	8.4		56.6	- 4.9	42.5	0.050	2.3	42	84	
204710	+44 3832		21 25.4	+44 29	6.90	B8	57.5	- 5.0	41.7	0.050	2.3	36	78	
204722	+43 3941	MWC 370	21 25.5	+43 54	7.52	B2	57.1	- 5.4	41.7	0.025	1.2	10	52	+0.09
204827	+58 2272		21 26.1	+58 18	7.8	BO	66.7	+ 5.3	41.6	0.122	5.6	59	101	+0.34

TABLE 2 (Cont'd)

HD	BD	Other Designation	α 1900	δ 1900	Mag	Sp	l	b	φ	δ Mag	δ %	θ	θ'	E_1
205196	+56° 2589		21h 26m	+57° 4'	7.56	BO Ib	66.2	+ 4.1	41.0	0.062	2.8	79°	120°	+0.37
	+47 3487	MWC 374	21 32.1	+47 28	9.1		60.3	- 3.5	40.3	.....	...	....	....	
	+37 4368		21 32.6	+37 49	9.5		54.0	-10.9	41.0	.....	...	....	....	
	+48 3437		21 32.6	+48 54	8.5		61.3	- 2.5	40.2	0.026	1.5	179	38	
206183	+56 2614		21 35.3	+56 32	8.1	09	66.5	+ 3.1	39.6	0.015	0.7	46	86	+0.11
206259	+51 3112		21 35.8	+51 54	7.48	A0	63.3	- 0.5	39.5	0.017	0.8	29	69	
	+49 3591		21 36.7	+50 3	9.5		62.6	- 2.0	39.3	.....	...	....	....	
206773	+57 2374	MWC 376	21 39.3	+57 17	6.98	BOp	67.4	+ 3.4	38.8	0.039	1.8	170	29	+0.17
206936	+58 2516	μ Cep	21 40.4	+58 19	var.	k2 Ia	68.2	+ 4.1	38.7	0.035	1.6	38	77	
B259758	+58 2520		21 41.8	+58 36	9.0	BO	68.5	+ 4.2	38.4	0.046	2.1	51	89	
	+49 3615	MWC 1050	21 42.2	+49 50	8.8		63.1	- 2.7	38.2	0.082	3.8	9	47	
207260	+60 2288	υ Cep	21 42.6	+60 40	4.46	A2 Ia	69.9	+ 5.7	38.3	0.057	1.7	46	84	+0.20
207329	+51 3144	MWC 378	21 43.1	+51 39	7.45	B2	64.4	- 1.4	38.0	0.036	1.8	1	39	+0.23
207538	+59 2420		21 44.6	+59 14	7.08	BO	69.2	+ 4.4	37.8	0.046	2.1	61	99	+0.26
207673	+40 4648	HR 8345	21 45.6	+40 40	6.49	A2 Ib	57.9	-10.3	38.2	.....	...	....	....	+0.23
207795	+52 3043		21 46.5	+52 14	6.56	B2	65.1	- 1.2	37.3	0.017	0.8	6	43	+0.26
	+47 3588		21 48.9	+47 33	8.8		62.6	- 5.2	37.0	.....	...	....	....	
208501	+55 2644	13 Cep	21 51.5	+56 8	6.01	B8 Ib	68.0	+ 1.4	36.3	0.035	1.6	43	79	+0.39
208816	+62 2007	VV Cep	21 53.8	+63 9	var.	cMep	72.4	+ 6.9	36.2	0.052	1.5	39	75	
B259673	+52 3071		21 54.1	+52 19	9.0	BO	66.1	- 1.9	35.8	0.052	2.4	28	64	
208905	+60 2520		21 54.3	+60 49	6.90	B3	71.1	+ 5.0	35.9	0.018	0.8	39	75	+0.13
B259679	+53 2749	MWC 647	21 55.0	+53 59	8.8	B2	67.2	- 0.6	35.6	0.038	1.8	51	87	
209145	+59 2443		21 56.1	+59 50	7.96	B8	70.7	+ 4.1	35.5	.....	...	....	....	
209296	+56 2676	MWC 383	21 57.2	+56 14	8.1	A0	68.8	+ 1.0	35.2	0.020	0.9	24	59	+0.17
209676	+52 3068		22 0.1	+52 43	8.4	B	67.1	- 2.1	34.6	0.066	3.0	33	68	
	+51 3239		22 0.3	+51 37	9.2		66.5	- 3.0	34.6	0.045	2.1	80	65	
209900	+52 3095		22 1.6	+53 1	8.9	A	67.4	- 2.0	34.3	0.048	2.2	89	75	
209975	+61 2246	19 Cep	22 2.1	+61 48	5.17	09.5 Ib	72.4	+ 5.3	34.3	0.023	1.1	68	102	+0.11
	+49 3735		22 2.2	+49 25	9.0		65.5	- 5.0	34.3	0.036	1.7	35	69	
210072	+54 2683		22 2.7	+54 46	8.0	B8	68.6	- 0.6	34.0	0.015	0.7	47	81	
210221	+52 3114	HR 8443	22 3.8	+52 49	6.50	A3 Ib	67.6	- 2.3	33.8	0.041	1.9	45	79	
210334	+45 3813	AR Lac	22 4.6	+45 15	var.	G5	63.5	- 8.7	34.1	.....	...	....	....	
	+52 3122		22 5.0	+52 28	9.2		67.6	- 2.7	33.6	0.037	1.7	49	85	
B255739	+50 3581	Y Lac	22 5.2	+50 33	var.	F8	66.5	- 4.3	33.6	0.026	1.2	40	74	
210478	+60 2348		22 5.6	+60 30	7.26	B8	72.1	+ 4.0	33.5	0.018	0.8	49	83	
		CX Cep	22 6.1	+57 13	var.	WN5	70.3	+ 1.2	33.3	0.144	6.6	45	78	
210628	+55 2695		22 6.6	+55 36	6.87	B3	69.5	- 0.2	33.2	0.027	1.2	59	92	+0.15
210809	+51 3281		22 7.9	+51 56	7.7	09.5	67.7	- 3.4	33.0	0.033	1.5	49	82	+0.17
210839	+58 2402	λ Cep	22 8.1	+58 56	5.19	06f	71.5	+ 2.5	32.9	0.024	1.1	59	92	+0.19
	+52 3135		22 8.4	+53 12	9.1		68.4	- 2.4	32.9	0.043	2.0	40	73	
B259886	+56 2733		22 8.9	+56 46	8.6	BO	70.4	+ 0.6	32.7	0.110	5.1	49	82	
B259895	+56 2735		22 9.8	+57 10	8.7	B2	70.7	+ 0.8	32.6	0.066	3.0	51	84	
	+53 2838		22 12.4	+53 40	9.5		69.1	- 2.3	32.0	0.052	2.4	50	82	
	+54 2726		22 13.0	+54 59	9.1		69.9	- 1.2	31.9	0.085	3.9	54	86	
B255761	+52 3167		22 13.2	+53 13	8.4	B1	69.0	- 2.8	31.9	0.042	1.9	29	61	
211604	+55 2713		22 13.2	+55 39	8.5	A5	70.3	- 0.7	31.8	.....	...	....	....	
	+53 2837		22 13.3	+53 42	9.4		69.8	- 2.4	31.9	0.040	1.8	45	77	
B255763	+53 2838		22 13.4	+53 59	8.8	B3	69.4	- 2.1	31.8	0.047	2.2	55	87	
211775	+55 2716		22 14.4	+55 38	8.8	G0	70.4	- 0.8	31.6	.....	...	....	....	
211820	+55 2720		22 14.8	+55 41	8.6	F2 Ib	70.5	- 0.8	31.5	0.068	3.1	55	87	
	+53 2843		22 14.9	+53 46	9.3		69.5	- 2.4	31.5	0.056	2.7	51	83	
211853	+55 2721		22 15.0	+55 37	9.0	WN5.5	70.5	- 0.8	31.5	0.089	4.1	44	76	
211880	+62 2061		22 15.2	+62 43	8.5	B8	74.2	+ 5.2	31.6	0.010	0.5	52	84	
B255795	+51 3330	MWC 1057	22 15.2	+51 37	8.6	B2	68.4	- 4.3	31.5	0.019	0.9	40	72	
211905	+55 2723		22 15.4	+55 47	8.9	A0	70.6	- 0.7	31.4	0.045	2.1	44	75	
211971	+59 2506		22 15.9	+59 38	7.16	B8	72.7	+ 2.5	31.3	0.014	0.6	87	118	
212043	+56 2755		22 16.4	+56 25	6.54	B8	71.1	- 0.3	31.12	.....	...	....	....	
212044	+51 3341	MWC 386	22 16.4	+51 21	7.08	B2p	68.4	- 4.6	31.3	0.028	1.3	49	80	+0.04
212188	+55 2729		22 17.3	+55 30	7.89	B9 III-IV	70.7	- 1.1	31.0	.....	...	....	....	
212312	+54 2750		22 18.3	+55 6	8.41	F2 Ib	70.6	- 1.5	30.8	0.064	2.9	48	79	

TABLE 2 (Cont'd)

HD	BD	Other Designation	α 1900	δ 1900	Mag	Sp	l	b	φ	δ Mag	δ %	θ	θ'	E_1
E235813	+54° 2751		22h 18m5	+54°18'	8.7		70.2	- 2.2	30.8	0.056	2.7	43°	74°	
212455	+54 2756		22 19.3	+54 44	8.4	B6	70.6	- 1.9	30.6	0.058	2.7	49	80	+0.28
212466	+55 2737	Rw Cep	22 19.4	+55 28	var.	G8 Ia	41.0	- 1.3	30.6	0.057	2.6	48	79	
E235825	+54 2758		22 19.6	+54 44	9.1	B2	70.6	- 1.9	30.5	0.071	3.3	54	85	
	+54 2764		22 20.1	+54 53	9.4		70.7	- 1.8	30.4	0.065	3.0	46	76	
212827	+53 2877		22 22.0	+53 16	8.1	A2	70.2	- 3.4	30.1	0.041	1.9	44	74	
	+54 2775		22 22.2	+54 57	9.3		71.0	- 1.9	30.0	0.062	2.8	53	83	
	+52 3210		22 23.0	+53 8	9.4		70.2	- 3.6	29.9	0.040	1.8	54	84	
	+53 2885		22 23.2	+53 40	9.5		70.5	- 3.1	29.8	0.026	1.2	53	83	
213087	+64 1664	26 Cep	22 23.9	+64 37	5.66	B0	76.0	+ 6.4	29.8	0.017	0.8	33	63	+0.22
213225	+56 2785		22 24.8	+56 25	8.0	K0	72.1	- 0.8	29.4	.....	...	....	....	
E239967	+55 2756		22 25.1	+56 5	9.1	B2	72.0	- 1.1	29.4	0.067	3.1	47	76	
213306	+57 2548	δ Cep	22 25.4	+57 54	var.	G0	72.9	+ 0.4	29.3	0.012	0.6	49	78	
213405	+64 1672		22 26.0	+64 36	8.4	B0	76.2	+ 6.2	29.4	0.013	0.6	9	38	+0.18
	+54 2790		22 26.2	+54 17	9.3		71.2	- 2.8	29.2	0.052	2.4	55	84	
	+56 2795	ST Cep	22 26.4	+56 29	var.		72.3	- 0.9	29.1	0.033	1.5	44	73	
213470	+56 2794		22 26.5	+56 43	6.73	A3 Ia	72.4	- 0.7	29.1	0.067	3.1	56	85	
		TW Lac	22 26.5	+54 7	var.		71.2	- 3.0	29.1	0.008	0.4	43	72	
213482	+56 2795		22 26.6	+56 20	6.6	F8 Ib	72.2	- 1.0	29.0	0.034	1.6	43	73	
E235870	+54 2794		22 27.7	+54 44	8.6	G8 II	71.6	- 2.5	28.8	0.027	1.2	57	86	
E235874	+50 3748		22 28.9	+50 42	9.0	B0	69.6	- 6.1	28.7	0.029	1.3	42	71	
E239994	+56 2806		22 29.8	+56 49	9.0	F8 Ib	72.9	- 0.8	28.4	0.053	2.4	56	84	
214369	+57 2568	W Cep	22 32.6	+57 54	var.	cMe	73.7	0.0	27.8	0.058	2.7	66	94	
214419	+56 2818	CQ Cep	22 32.9	+56 25	var.	WN6	73.0	- 1.4	27.7	0.113	5.2	65	93	
		No. 19	22 34.0	+54 47			72.4	- 2.9	27.5	0.043	2.0	52	80	
E240010	+55 2783	LMC 655	22 34.6	+55 19	9.3	B	72.8	- 2.5	27.4	0.079	3.6	76	108	
214975	+56 2829	Z Lac	22 36.9	+56 19	var.	F5	73.5	- 1.8	26.9	0.050	2.3	61	88	
E240024	+55 2789	RR Lac	22 37.5	+55 55	var.	G5	73.4	- 2.1	26.8	0.057	2.6	59	86	
		No. 20	22 38.5	+56 12			73.6	- 1.9	26.5	0.050	2.3	51	78	
	+55 2795		22 38.7	+55 50	9.4		73.5	- 2.3	26.5	0.050	2.3	49	75	
	+53 2964	LMC 1067	22 39.2	+53 33	9.4		72.6	- 4.3	26.4	0.025	1.2	61	87	
	+54 2847		22 40.3	+55 23	9.5		73.5	- 2.8	26.2	0.078	3.4	51	77	
215605	+57 2597	LMC 658	22 41.3	+57 20	9.5	B	74.5	- 1.1	25.9	0.031	1.4	40	66	
E240047	+56 2852		22 41.4	+56 55	9.2	B	74.3	- 1.5	25.9	0.046	2.2	62	88	
	+55 2808		22 42.3	+55 48	9.5		74.0	- 2.5	25.7	0.060	2.8	51	77	
215806	+57 2606		22 42.7	+57 46	9.4	B	74.9	- 0.8	25.6	0.040	1.8	71	97	
215835	+57 2607		22 42.9	+57 33	8.6	B	74.8	- 1.0	25.6	0.060	2.8	63	89	
215836	+55 2809		22 42.9	+55 54	9.2	B	74.1	- 2.5	25.6	0.073	3.4	56	82	
216014	+64 1717	AH Cep	22 44.2	+64 32	var.	B0	77.9	+ 5.3	25.4	0.035	1.6	58	83	+0.27
E240073	+55 2815	V Lac	22 44.5	+55 47	var.	G5	74.2	- 2.7	25.3	0.053	2.4	55	80	
216044	+54 2865		22 44.5	+54 36	8.6	B2	73.7	- 3.7	25.3	0.023	1.1	64	89	+0.12
216105	+55 2817	X Lac	22 45.0	+55 54	var.	G5	74.3	- 2.6	25.2	0.048	2.2	64	89	
216206	+49 3954	HR 8692	22 45.9	+50 9	6.43	G4 Ib	72.0	- 7.9	25.2	0.025	1.2	62	87	
216248	+57 2625		22 46.3	+58 8	9.9	B	75.4	- 0.6	24.8	0.031	1.4	54	79	+0.19
216411	+58 2492	LMC 1074	22 47.6	+58 28	7.16	B1 Ia	75.7	- 0.4	24.6	0.059	2.7	46	71	+0.37
216438	+52 3315		22 47.8	+53 11	8.4	B2	73.6	- 5.2	24.6	0.031	1.4	56	81	+0.07
216532	+61 2356		22 48.6	+61 54	8.0	B3	77.3	+ 2.6	24.4	0.044	2.0	71	95	+0.13
216629	+61 2361	LMC 1075	22 49.4	+61 36	9.2	B	77.2	+ 2.4	24.2	0.111	5.1	105	129	+0.44
216658	+61 2363		22 49.6	+61 36	8.6	B	77.3	+ 2.3	24.2	0.091	4.2	101	125	+0.38
216711	+61 2364		22 50.0	+62 4	9.4	B	77.5	+ 2.7	24.1	0.047	2.2	86	110	+0.35
	+55 2840		22 50.9	+55 51	9.4		75.1	- 3.0	23.9	0.064	2.9	46	70	
	+56 2903		22 51.6	+57 4	9.4		75.7	- 1.9	23.7	0.068	2.9	59	83	
216896	+61 2370		22 51.8	+61 46	8.0	O8	77.6	+ 2.4	23.7	0.085	3.9	85	109	+0.29
216927	+58 2511		22 52.0	+58 22	8.0	B9	76.2	- 0.7	23.6	0.040	1.8	39	63	+0.45
	+63 1907		22 52.4	+63 56	9.0		78.5	+ 4.3	23.6	0.080	3.7	40	64	
217035	+62 2136		22 52.6	+62 19	7.76	B5	77.9	+ 2.8	23.5	0.037	1.7	91	115	+0.22
217061	+61 2372		22 52.8	+62 5	8.4	B	77.8	+ 2.6	23.5	0.080	1.4	87	111	+0.38
217086	+61 2373		22 53.0	+62 12	7.70	B0	77.9	+ 2.8	23.4	0.024	1.1	93	116	
217312	+62 2147		22 54.8	+62 32	7.7	B8	76.2	+ 3.0	23.1	0.028	1.3	80	103	
		No. 21	22 55.1	+57 11			76.1	- 2.0	23.0	0.058	2.7	58	81	

TABLE 2 (Cont'd)

HD	BD	Other Designation	α 1900	δ 1900	Mag	Sp	l	b	φ	Mag	%	θ	θ'	E_1
217465	+62° 2152		22h 55.8	+62°14'	8.9	B2	76.2	+ 2.6	22.8	0.016	0.7	93°	116°	+0.31
217476	+56 2923	HR 8752	22 55.9	+56 24	5.48	G0 Ia	75.9	- 2.8	22.8	0.064	2.9	70	93	
217490	+58 2521		22 56.0	+59 5	8.6	B	77.0	- 0.3	22.8	0.074	3.4	51	74	
E240160	+56 2928		22 57.4	+56 27	9.3	B	76.2	- 2.8	22.5	0.058	2.7	75	97	
	+56 2929		22 57.5	+56 30	9.4		76.2	- 2.8	22.5	0.049	2.2	63	85	
	+56 2930		22 57.8	+57 0	9.3		76.4	- 2.3	22.4	0.080	3.7	76	98	
E240165	+56 2931		22 58.0	+56 39	9.5	B	76.3	- 2.6	22.4	0.061	2.8	78	100	
E240168	+55 2878		22 58.2	+56 4	8.9	B0	76.1	- 3.2	22.3	0.037	1.7	37	59	
E240171	+56 2934		22 58.5	+56 36	9.1	B	76.3	- 2.7	22.3	0.045	2.1	66	88	
217919	+62 2161		22 59.0	+63 10	7.8	B	78.9	+ 3.3	22.2	0.015	0.7	64	86	
218066	+62 2163		23 0.0	+62 51	7.8	B5	78.9	+ 3.0	21.9	0.015	0.7	37	59	
218195	+57 2689		23 1.0	+57 43	8.1	B3	77.1	- 1.8	21.7	0.055	2.5	70	92	
218323	+63 1928		23 2.0	+63 46	7.8	B	79.4	+ 3.8	21.5	0.041	1.9	68	90	
218342	+62 2170		23 2.1	+62 41	7.46	B0	79.0	+ 2.8	21.5	0.041	1.9	58	79	+0.30
218376	+58 2545	1 Cas	23 2.4	+58 53	4.93	B1	77.7	- 0.8	21.4	0.019	0.9	71	92	+0.03
	+55 2899		23 2.7	+55 28	9.4		76.5	- 4.0	21.4	0.027	1.2	63	84	
E236044	+53 3076		23 2.7	+54 13	9.0	B0	76.0	- 5.1	21.4	0.035	1.6	64	85	
		SW Cas	23 2.9	+58 1	var.		77.4	- 1.6	21.3	0.055	2.5	66	89	
218915	+52 3383		23 6.7	+52 31	7.06	O9 I	76.0	- 6.9	20.6	0.025	1.2	53	74	+0.13
218997	+58 2560	V Cas	23 7.4	+59 8	var.	Md	78.4	- 0.8	20.3	0.034	1.6	83	103	
219287	+58 2565		23 9.6	+58 51	8.5	B	78.5	- 1.1	19.8	0.023	1.1	61	81	
219460	+59 2685		23 10.8	+59 55	9.2	WN5	79.0	- 0.2	19.6	0.055	2.5	74	94	
E236083	+54 2943		23 12.7	+54 57	9.2	A5	77.6	- 5.0	19.2	0.010	0.5	87	106	
	+63 1962		23 12.8	+63 15	8.3		80.4	+ 2.9	19.2	0.053	2.4	63	82	
	+63 1964		23 13.1	+63 35	8.3		80.5	+ 3.2	19.1	0.089	4.1	63	82	
E240250	+59 2695		23 13.6	+59 19	8.6	B0	79.2	- 0.9	19.0	0.067	3.1	90	109	
	+62 2210		23 14.3	+62 56	8.5		80.4	+ 2.5	18.8	0.144	6.6	74	93	
220116	+57 2724	NGC 399	23 16.1	+57 43	8.8	B	78.9	- 2.5	18.4	0.090	4.1	81	99	
	+60 2522		23 16.2	+60 38	8.0		79.9	+ 0.3	18.4	0.033	1.5	63	81	
	+60 2525		23 17.3	+60 18	9.3		79.9	- 0.1	18.2	0.029	1.3	62	80	
220770	+60 2539		23 21.4	+60 53	8.2	F5	80.6	+ 0.3	17.3	0.048	2.2	69	86	
	+60 2542		23 22.6	+60 50	8.9		80.7	+ 0.2	17.0	0.039	1.8	67	84	
	+60 2562		23 30.0	+61 5	8.3		81.6	+ 0.2	15.4	0.068	3.1	73	88	
		RS Cas	23 32.6	+61 53	var.		82.2	+ 0.9	14.8	0.109	5.0	75	90	
	+61 2509		23 39.0	+61 36	8.5		82.8	+ 0.4	13.4	0.048	2.2	77	90	
	+60 2615		23 39.9	+61 7	8.9		82.8	0.0	13.2	0.030	1.4	70	83	
	+62 2296		23 42.4	+62 40	6.0		83.4	+ 1.4	12.7	0.057	2.6	115	128	
	+61 2526		23 42.8	+61 29	8.5		83.2	+ 0.2	12.6	0.024	1.1	90	103	
	+62 2299		23 43.1	+62 50	9.2		83.6	+ 1.5	12.5	0.023	1.1	174	7	
	+61 2529		23 43.6	+61 26	8.6		83.2	+ 0.2	12.4	0.034	1.6	88	100	
223385	+61 2533	NGC 663	23 44.0	+61 40	5.61	A2	83.4	+ 0.4	12.3	0.026	1.2	57	69	+0.29
223387	+56 3094	NGC 401	23 44.0	+56 40	9.2	B	82.3	- 4.5	12.4	0.051	2.4	68	80	+0.13
	+60 2629	UU Cas	23 45.7	+60 21	var.		83.3	- 1.0	12.0	0.072	3.3	76	88	
	+62 2313		23 46.9	+62 45	8.5		84.0	+ 1.4	11.7	0.035	1.6	79	91	
		RY Cas	23 47.1	+58 11	var.		83.1	- 3.1	11.7	0.036	1.7	81	93	
	+61 2550		23 47.3	+61 34	9.2		83.8	+ 0.2	11.6	0.029	1.3	62	74	
		TZ Cas	23 47.9	+60 27	var.		83.6	- 0.9	11.5	0.079	3.6	89	101	
223924	+56 3106		23 48.6	+56 16	8.0	B2	82.9	- 5.0	11.4	0.035	1.6	64	75	+0.05
	+61 2559		23 48.6	+61 52	9.2		84.0	+ 0.5	11.3	0.043	2.0	65	76	
223960	+60 2636	NGC 405	23 48.9	+60 18	6.98	B9	83.7	- 1.1	11.3	0.067	3.1	80	91	+0.31
223987	+60 2637		23 49.2	+61 3	7.56	B1	83.9	- 0.4	11.2	0.055	2.5	70	81	+0.30
224014	+56 3111	ρ Cas	23 49.4	+56 57	4.85	F8p	83.1	- 4.4	11.2	0.030	1.4	51	62	
224055	+61 2562	NGC 404	23 49.7	+61 17	7.16	B3	84.0	- 0.1	11.1	0.088	4.0	67	78	+0.39
224151	+56 3115	HR 9052	23 50.5	+56 53	6.05	B0.5	83.3	- 4.5	10.9	0.020	0.9	87	98	+0.15
224257	+55 3051		23 51.3	+55 26	8.5	B	83.1	- 5.9	10.8	0.033	1.5	66	77	
	+66 1661		23 52.4	+67 0	8.7		85.4	+ 5.4	10.5	0.087	4.0	89	99	
224424	+58 2676	NGC 405	23 52.7	+59 9	7.8	B1	84.0	- 2.3	10.4	0.043	2.0	48	58	+0.43
224436	+56 3122		23 52.8	+56 32	8.6	B0	83.5	- 4.9	10.4	.....	...	....	....	
E240464	+59 2799		23 53.7	+59 43	9.2	F5	84.2	- 1.8	10.2	0.032	1.5	78	88	
224599	+59 2801		23 54.1	+59 29	10.2	B	84.2	- 2.0	10.1	0.030	1.4	21	31	+0.15

TABLE 2 (Concluded)

HD	BD	Other Designation	α 1900	δ 1900	Mag	Sp	l	b	ϕ	δ Mag	δ %	θ	θ'	E_1
224855	+59° 2810	WZ Cas	23h 56m2	+59°48'	var.	C9	84.5	- 1.7	9.7	0.010	0.5	49°	59°	
224905	+59 2813	MWC 666	23 56.6	+59 54	9.2	B	84.6	- 1.6	9.6	0.024	1.1	101	111	+0.11
	+66 1675		23 57.1	+66 51	9.0		85.8	+ 5.2	9.5	0.118	5.2	106	115	
225094	+62 2556	MWC 408	23 58.3	+63 5	6.26	B3	85.3	+ 1.4	9.2	0.050	2.3	75	84	+0.22
225146	+60 2663		23 58.8	+60 33	8.6	B0	85.0	- 1.1	9.1	0.068	3.1	72	81	+0.20
225160	+61 2585	MWC 410	23 58.9	+61 40	8.6	O8	85.1	0.0	9.1	0.053	2.4	92	101	+0.19

Draper Catalogue. A few classifications were obtained from the list of supergiants by Morgan and Roman[4] and some from the *Bergedorfer Spectral-Durchmusterung*. W. W. Morgan and W. P. Bidelman kindly supplied some classifications.

The galactic co-ordinates l and b in the eighth and ninth columns were taken from the Lund[5] tables. They refer to the galactic pole with a 1900 position of $\alpha = 12^h40^m$ and $\delta = +28°$.

The tenth column gives the galactic parallactic angle, which is the angle between the galactic latitude circle and the declination circle. This angle was also computed from the Lund tables and is given here to the nearest tenth of a degree.

The eleventh and twelfth columns give the observed polarization in magnitude and per cent, respectively.

The observed position angles of the plane of vibration, θ, are recorded in the thirteenth column, and this same plane of vibration, referred to the galactic co-ordinate system, is recorded in the fourteenth column. It will be noted that these angles differ by 90° from those published by the U.S. Naval Observatory, where the older terminology, "plane of polarization," is employed.[6]

The color excess E_1 in the fifteenth column was taken from the colors of 1332 stars by Stebbins, Huffer, and Whitford.[7] No correction to the color excess was made where the spectral type in the seventh column is different from that originally used to compute the color excess.

In general, only one observation was made of each star, since a second observation would not have added significantly to the data. Care was exercised in the identification. A chart for use at the telescope was made from the *Bonner Durchmusterung* charts if the star appeared in this catalogue. In all cases an appropriate chart was used in the identification of all stars.

There are 228 stars in the present list in common with the 551 stars published by the U.S. Naval Observatory.[3] In order to determine any systematic difference between the two lists of observations, the stars in common are plotted in Figure 3. Although the scatter may be somewhat larger than we should anticipate for two photoelectric systems, there does not appear to be any systematic difference between the two systems. However, this is not the case for the position angles, where, from Figure 4, we see that there is a systematic mean difference between the McDonald position angles and those of the U.S. Naval Observatory of approximately 3°.3, with the McDonald position angles the smaller. Although a search has been made as to the origin of this systematic difference, no explanation has been found.

All the stars in Table 2 whose galactic latitudes lie between −6° and +6° are plotted in Figures 5–12. An inspection of these figures amply confirms the conclusions reached earlier:[8] "Stars of low galactic latitude have a tendency to show polarization in which the electric vector maximum [plane of vibration] is approximately parallel to the galactic plane. This relationship, however, may not hold for all galactic longitudes, for a few scattered observations in Scutum [l = 345°–355°] and Cygnus [l = 35°–65°] indicate that this relationship does not hold at these longitudes." This general trend of the plane of vibration to be parallel to the galactic plane may be a reflection of the galactic rotation. For if the polarization is a consequence of the alignment of elongated interstellar particles by magnetic fields and if these magnetic fields of the order of 10^{-6} gauss have their origin in the stretching of the magnetic lines of force[9] by motion of the material, then it

[4] *Ap. J.*, **112**, 363, 1950.

[5] John Ohlsson, *Ann. Obs. Lund*, No. 3, 1932.

[6] F. A. Jenkins and H. E. White, *Fundamentals of Optics* (New York: McGraw-Hill Book Co., Inc., 1950).

[7] *Ap. J.*, **91**, 20, 1940.

[8] W. A. Hiltner, *Ap. J.*, **109**, 478, 1949.

[9] See, e.g., G. K. Batchelor, *Proc. R. Soc. London, A*, **201**, 405, 1950.

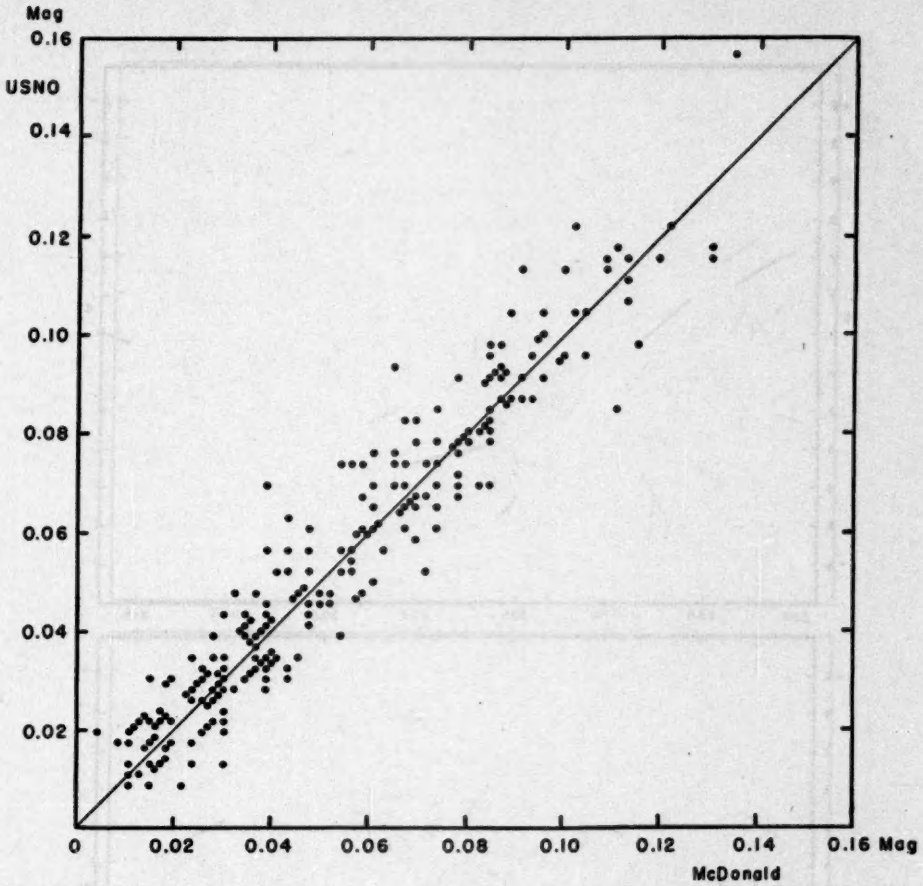

FIG. 3.—Comparison of polarization observations made at McDonald Observatory with those made at the U.S. Naval Observatory.

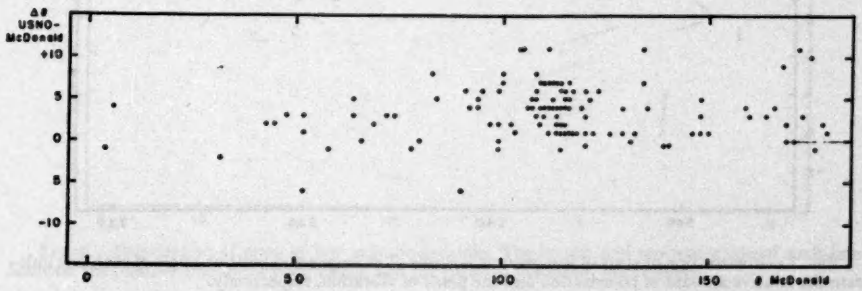

FIG. 4.—Comparison of position-angle observations made at McDonald Observatory with those made at the U.S. Naval Observatory.

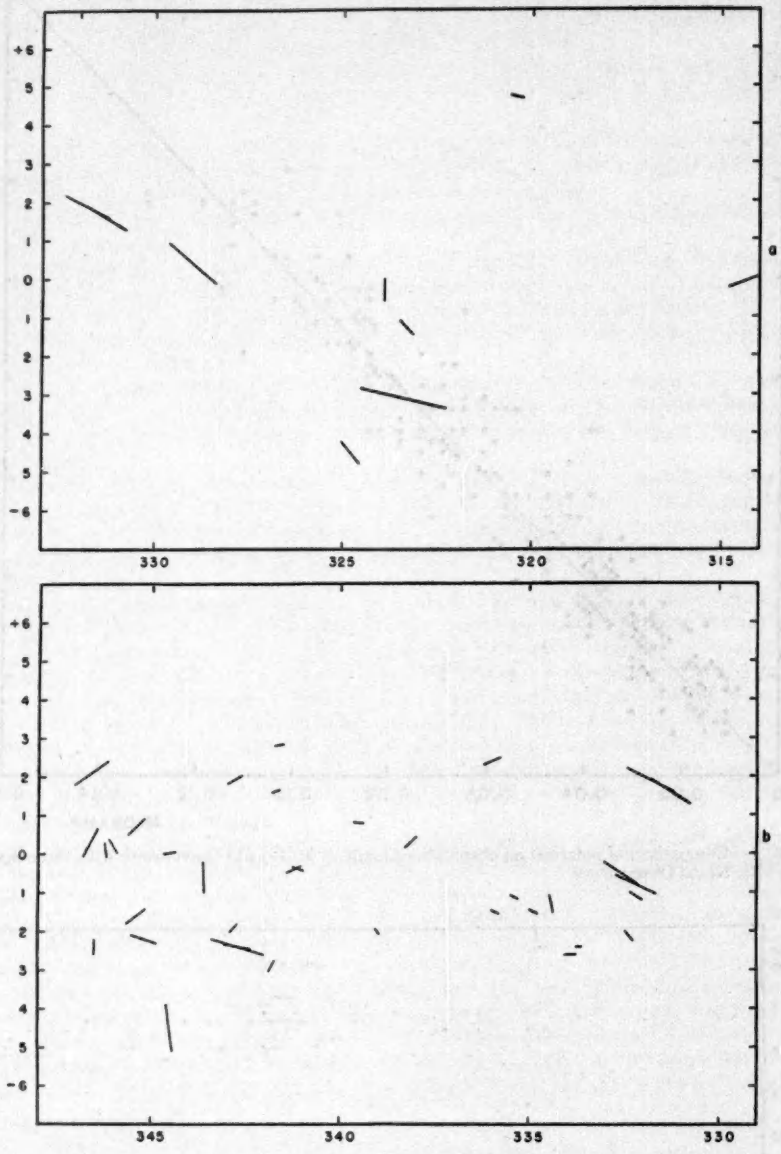

FIG. 5.—Polarization of stars of low galactic latitude. The length and position angle of each line indicate the relative amount of polarization and the plane of vibration, respectively.

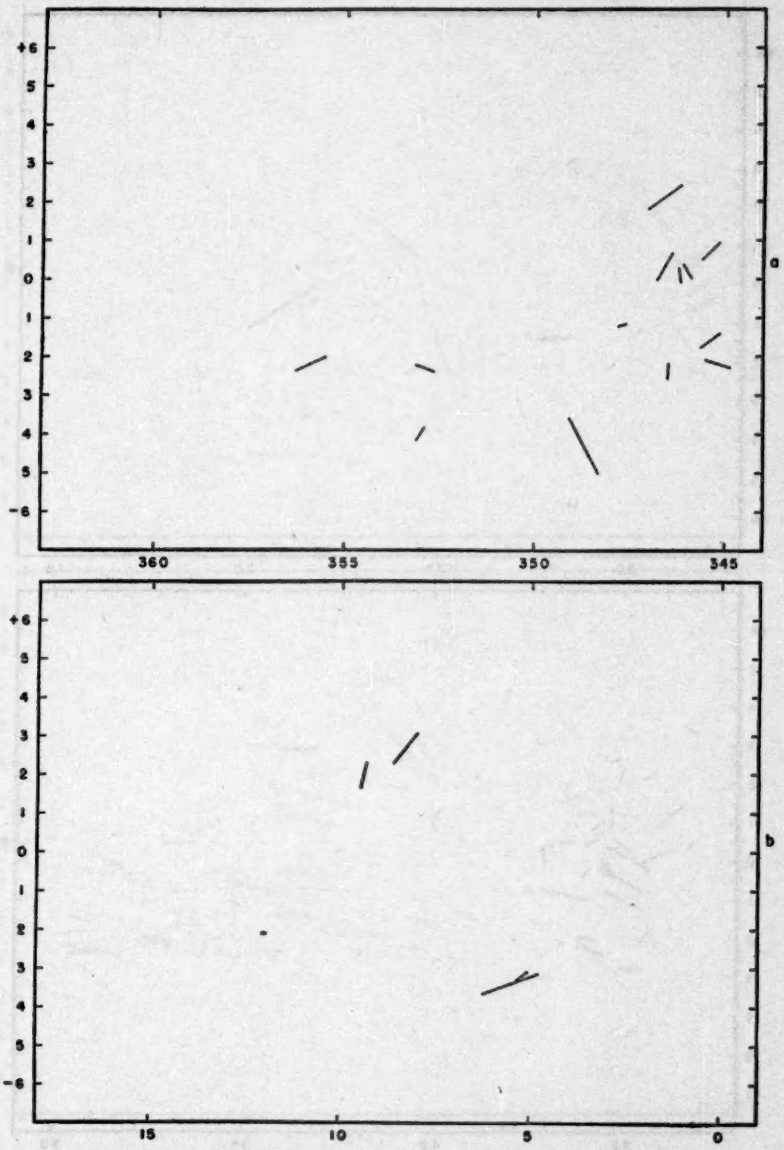

FIG. 6.—Polarization of stars of low galactic latitude. The length and position angle of each line indicate the relative amount of polarization and the plane of vibration, respectively.

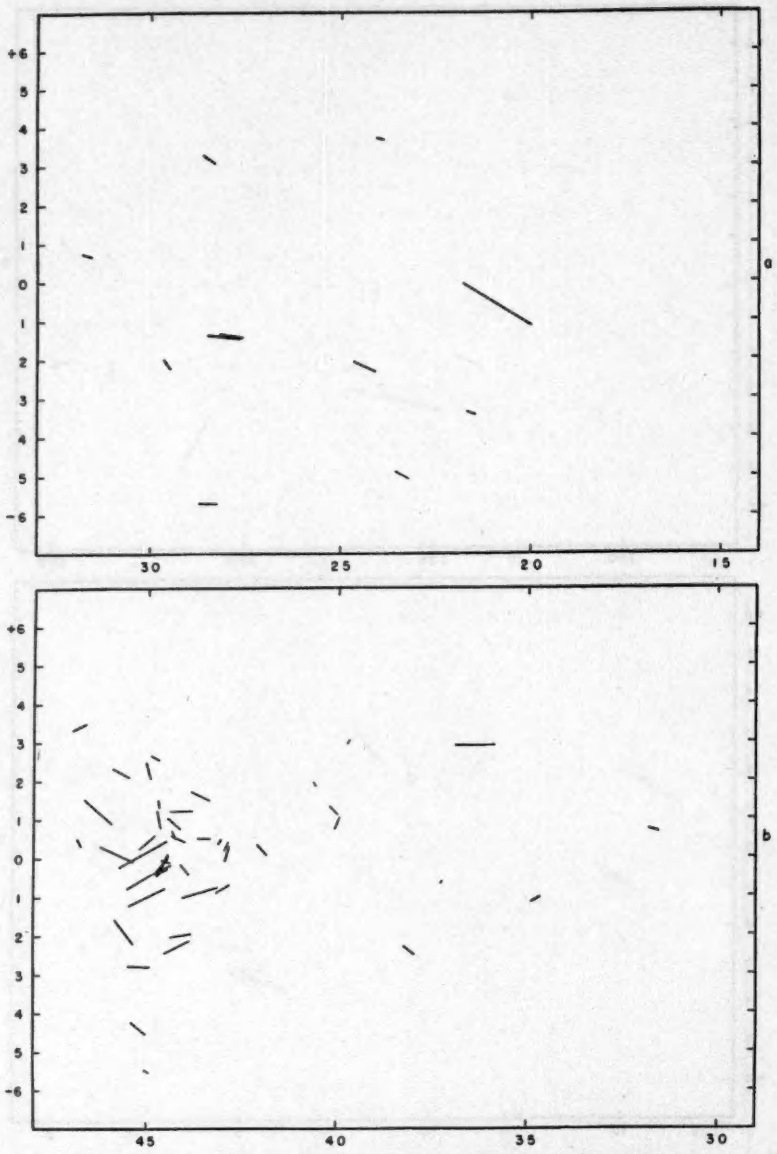

FIG. 7.—Polarization of stars of low galactic latitude. The length and position angle of each line indicate the relative amount of polarization and the plane of vibration, respectively.

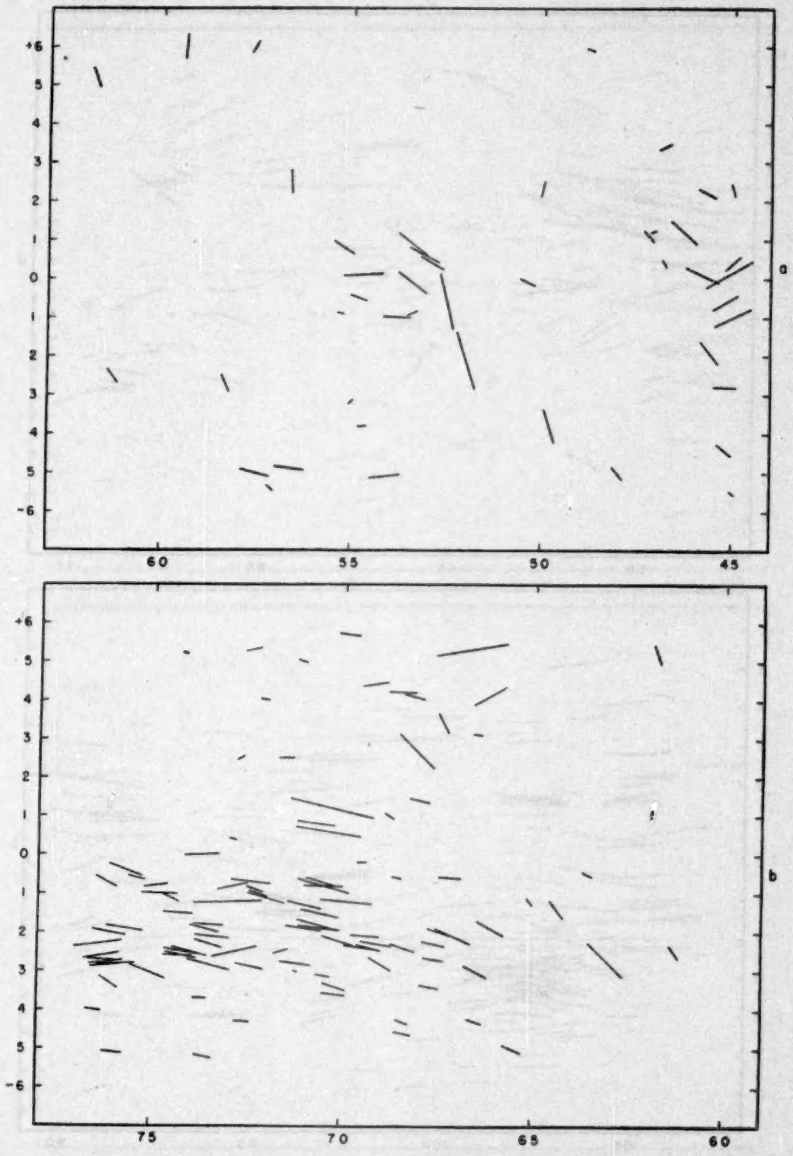

FIG. 8.—Polarization of stars of low galactic latitude. The length and position angle of each line indicate the relative amount of polarization and the plane of vibration, respectively.

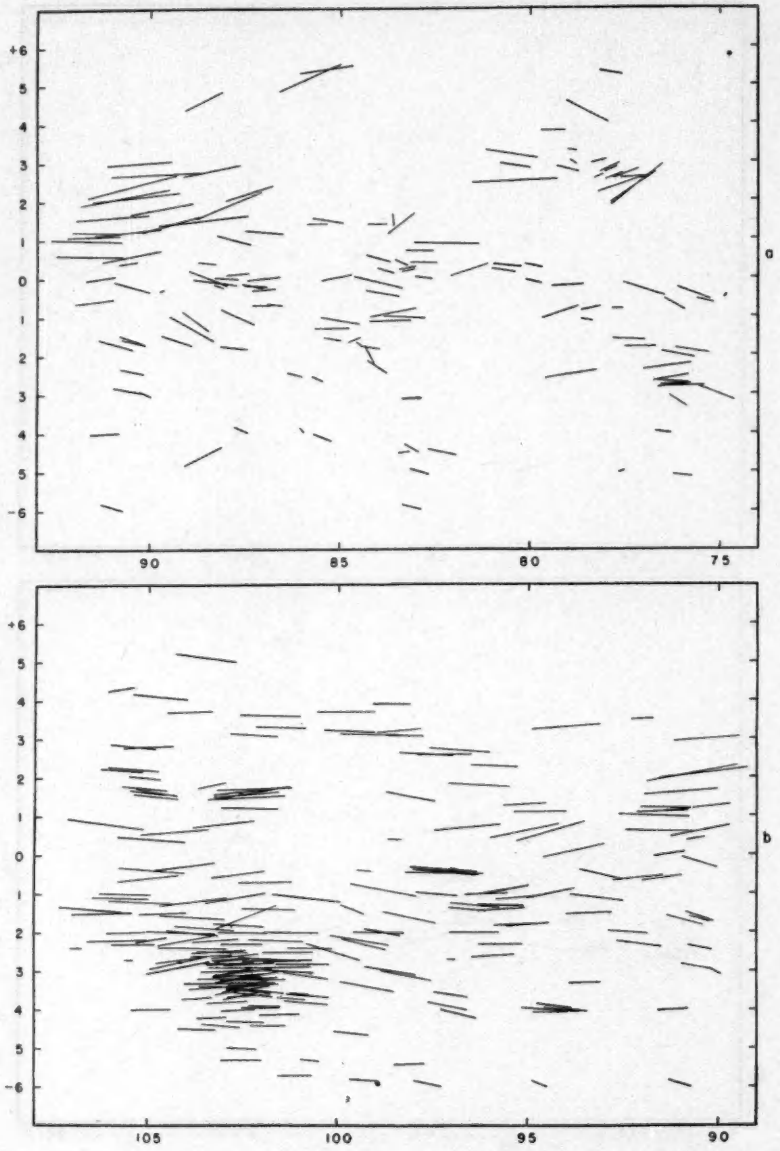

FIG. 9.—Polarization of stars of low galactic latitude. The length and position angle of each line indicate the relative amount of polarization and the plane of vibration, respectively.

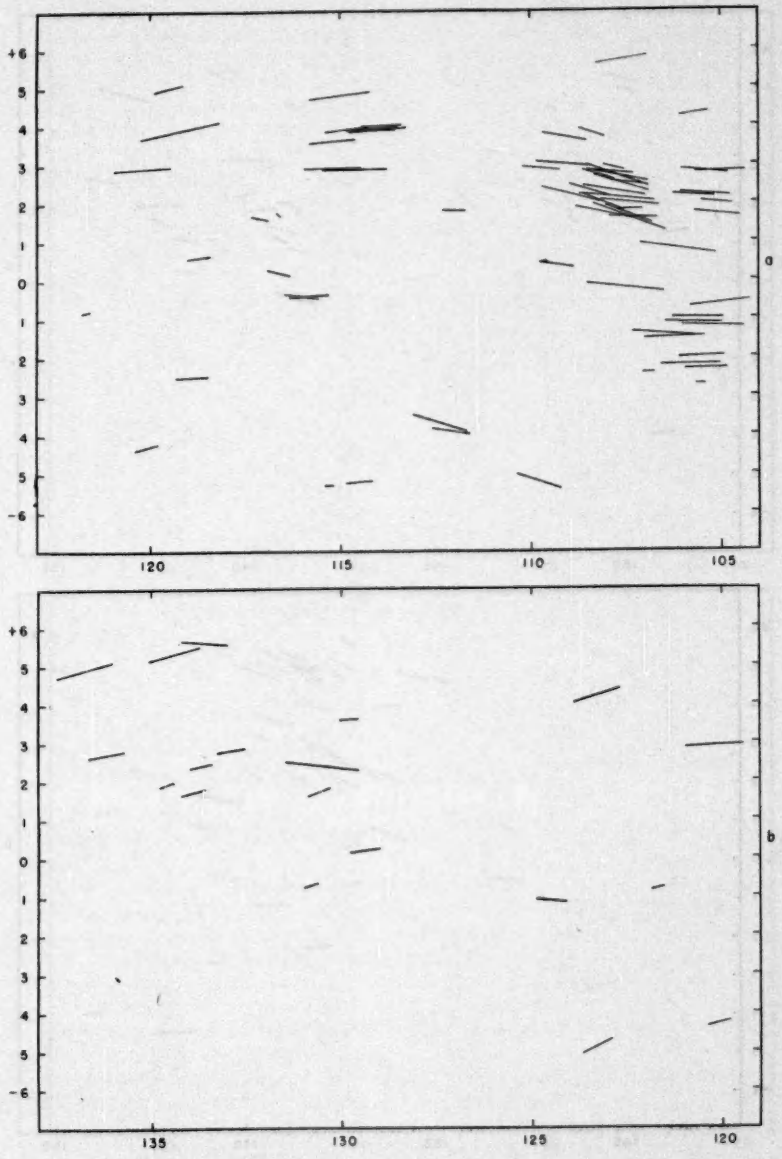

FIG. 10.—Polarization of stars of low galactic latitude. The length and position angle of each line indicate the relative amount of polarization and the plane of vibration, respectively.

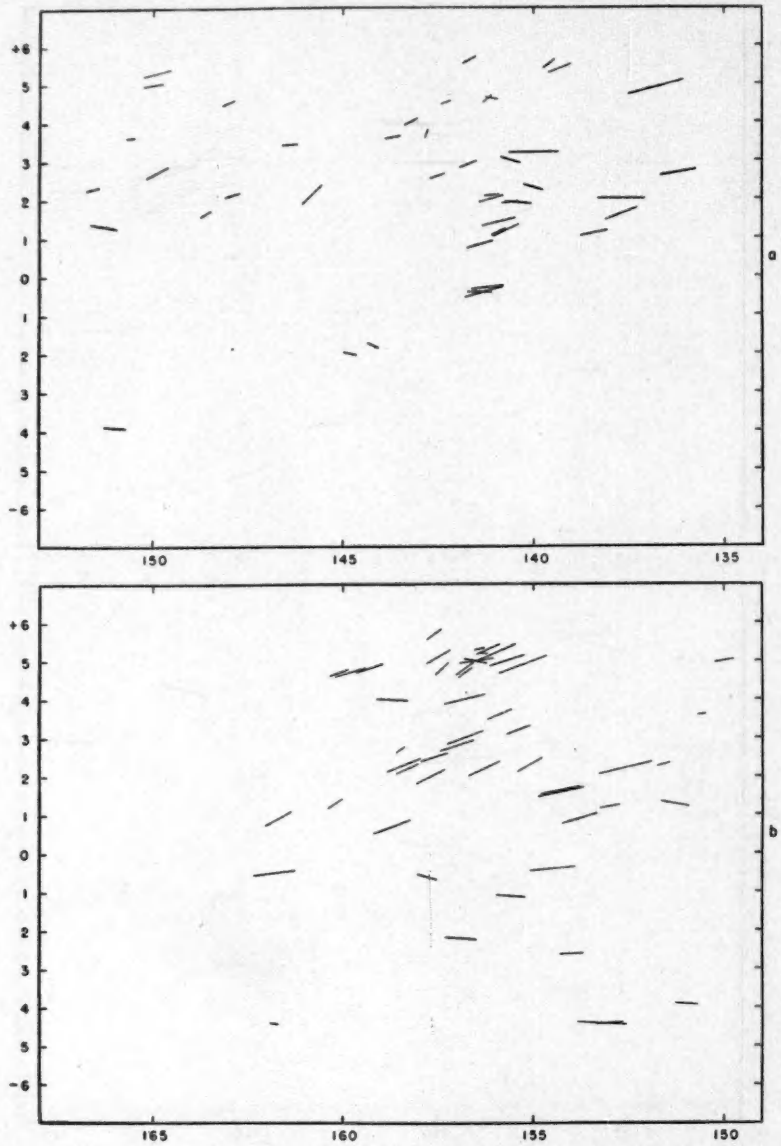

FIG. 11.—Polarization of stars of low galactic latitude. The length and position angle of each line indicate the relative amount of polarization and the plane of vibration, respectively.

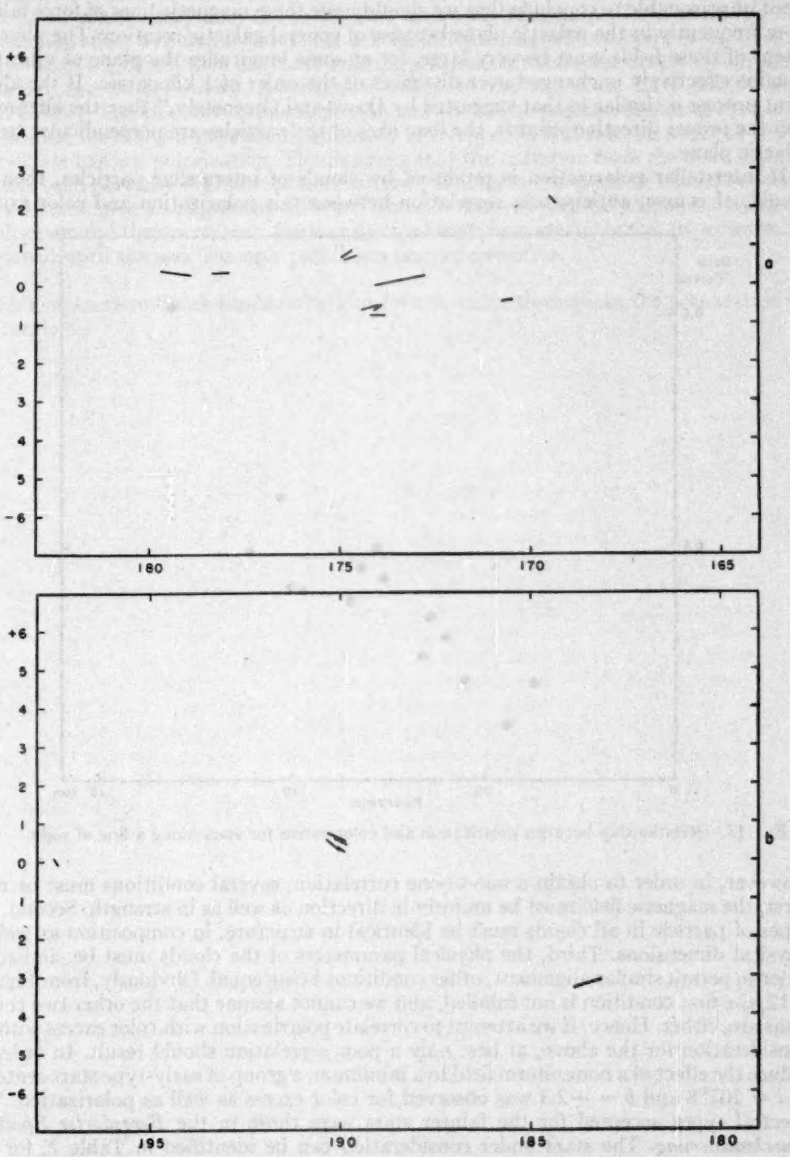

FIG. 12.—Polarization of stars of low galactic latitude. The length and position angle of each line indicate the relative amount of polarization and the plane of vibration, respectively.

is not unreasonable to conclude that we should have these magnetic lines of force falling more frequently in the galactic plane because of general galactic rotation. The physical extent of these fields must be very large, for at some longitudes the plane of vibration remains effectively unchanged over distances of the order of 1 kiloparsec. If the alignment process is similar to that suggested by Davis and Greenstein,[10] then the alignment is in the proper direction; that is, the long axes of the particles are perpendicular to the galactic plane.

If interstellar polarization is produced by clouds of interstellar particles, then we should, of course, anticipate a correlation between this polarization and color excess.

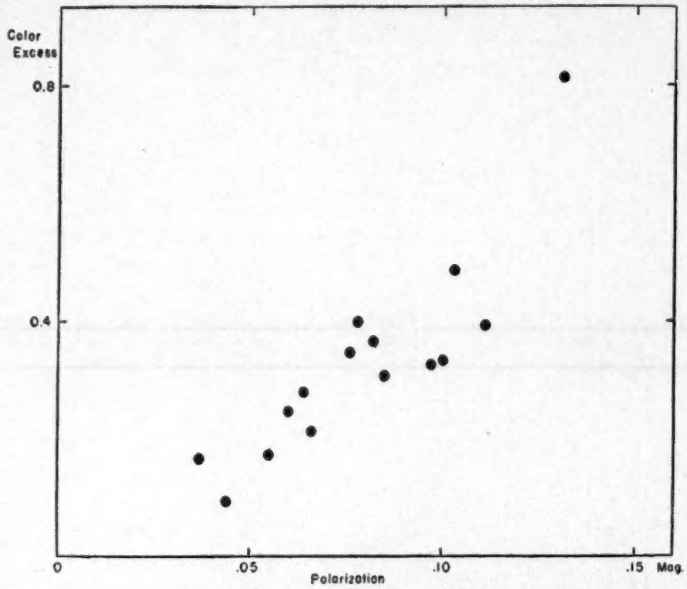

FIG. 13.—Relationship between polarization and color excess for stars along a line of sight

However, in order to obtain a one-to-one correlation, several conditions must be met. First, the magnetic field must be uniform in direction as well as in strength. Second, the types of particle in all clouds must be identical in structure, in composition as well as physical dimensions. Third, the physical parameters of the clouds must be similar, in order to permit similar alignment, other conditions being equal. Obviously, from Figures 5–12, the first condition is not fulfilled, and we cannot assume that the other two conditions are, either. Hence, if we attempt to correlate polarization with color excess without consideration for the above, at best only a poor correlation should result. In order to reduce the effect of a nonuniform field to a minimum, a group of early-type stars centered at $l = 107°.8$ and $b = +2.3$ was observed for color excess as well as polarization. The spectral types accepted for the fainter stars were those in the *Bergedorfer Spectral-Durchmusterung*. The stars under consideration can be identified in Table 2, for the *Bergedorfer Spectral-Durchmusterung* (abbreviated "BSD") numbers are given under "Other Designation" and the color excesses are in parentheses. Figure 13 is a plot of these stars. Some of the scatter is due to observational errors, both in color excess and in

[10] *A.J.*, 55, 71, 1950.

polarization. The correlation between color excess and polarization is reasonably good, but a linear relationship does not exist. This is entirely reasonable, for if there is a depolarization effect by a nonuniform field or a variation in particle structure or in physical conditions of the cloud, then the curve relating polarization and color excess should show a positive second derivative. Attention is called to the two stars HDE 237090 and HDE 237091. The two stars are separated by only 0.'7. The position angles of the plane of vibration for the two stars are significantly different (8°), and the one with the larger color excess has less polarization. This suggests that the radiation from the more distant star has been partially depolarized because the particles in the cloud or clouds between the two stars have an alignment different from the general particle alignment between the observer and the nearer star. Further discussion of the material in this paper must be postponed until the spectroscopic parallaxes become available.

It is a pleasure to thank Barbara Perkins for assistance throughout the preparation of this catalogue.

THE CONDITION FOR TURBULENCE IN ROTATING STARS

T. G. COWLING
Princeton University Observatory
Received June 1, 1951

ABSTRACT

The problem considered is whether stellar rotation has a stabilizing effect capable of preventing convection perpendicular to the axis of rotation. Stability for small displacements is studied. For axially symmetric displacements a stabilizing effect is found, in agreement with the earlier results of Randers and Walén. For nonsymmetric displacements the stabilizing effect is less, and it disappears altogether for particular displacements. For the latter there is instability whenever the temperature gradient exceeds the adiabatic value. With nonuniform angular velocity, the shear may produce instability for slightly smaller temperature gradients. The displacements of maximum instability lead to a considerable convection of energy perpendicular to the axis of rotation, but this convection may possibly be less efficient than convection parallel to the axis.

I. INTRODUCTION

In the past there has been some controversy as to the effect of rotation on turbulence in stars. Certain workers[1] have maintained that rotation has an absolute stabilizing influence, so that turbulence cannot arise or is limited to motion mostly parallel to the axis of rotation, unless the actual temperature gradient considerably exceeds the adiabatic value. Others (myself among them[2]) have suggested that rotation is less important and that the condition for turbulence in a rotating star is much the same as in a nonrotating one.

Those holding the first opinion appeal to a result for an incompressible fluid, first enunciated by Rayleigh,[3] which shows that rotation has a stabilizing influence if the circulation $2\pi R^2\Omega$ increases as R increases (where Ω is the angular velocity at a distance R from the axis of rotation). Rayleigh's argument was very simple. If $R^2\Omega$ increases with R, then, assuming the conservation of angular momentum, an element displaced outward from the axis arrives in its new surroundings with less than the local angular velocity. Hence it is subject to less centrifugal force and tends to fall back. Using a similar argument and assuming uniform rotation, Randers obtained the following instability criterion for radial displacements:

$$\frac{1}{\rho}\frac{\partial p}{\partial r}\left(\frac{1}{T}\frac{\partial T}{\partial r}-\frac{\gamma-1}{\gamma}\frac{1}{p}\frac{\partial p}{\partial r}\right)>4\Omega^2\sin^2\theta\,. \tag{1}$$

Here p is the pressure, T the temperature, ρ the density, γ the ratio of specific heats, r the distance from the center, and θ the angle which r makes with the axis. The expression on the right represents the stabilizing influence of rotation; in its absence equation (1) gives the usual criterion that the actual temperature gradient is greater than the corresponding adiabatic value. For displacements perpendicular to the axis of revolution and a general law of rotation, Walén similarly obtained a criterion which can be put in the following form:

$$\frac{1}{\rho}\frac{\partial p}{\partial R}\left(\frac{1}{T}\frac{\partial T}{\partial R}-\frac{\gamma-1}{\gamma}\frac{1}{p}\frac{\partial p}{\partial R}\right)>\frac{2\Omega}{R}\frac{\partial}{\partial R}(R^2\Omega)\,. \tag{2}$$

[1] See, e.g., Randers, *Ap. J.*, **95**, 454, 1942; Walén, *Ark. f. mat., astr. och fys.*, Vol. **33a**, No. 18, 1946.

[2] *M.N.*, **105**, 166, 1945.

[3] *Proc. R. Soc. London, A.*, **93**, 148, 1916.

Those holding the contrary opinion point out that the above criteria were all derived by considering displacements symmetric about the axis, so that $R^2\Omega$ is constant for any element during its displacement. If more general displacements are considered, azimuthal pressure gradients insure that $R^2\Omega$ does not remain constant; therefore, they suggest that we modify the stability criterion. In particular, they suggest that two columns of moving material, one rising and one falling, may "lean" against each other in such a way that the angular velocity of each hardly differs from the local angular velocity at any level, so that the stabilizing influence is lost. They have, however, given no quantitative estimate of the importance of rotation. This paper is an attempt to supply such a criterion.

Actually, two distinct questions need to be considered. One is whether the condition for the onset of turbulence is altered by the presence of rotation; the second, whether turbulence, once established in a rotating star, is seriously different in its general properties from that in a nonrotating one. The first question alone is considered in what follows, stability for small displacements being studied. The results confirm the criteria of Randers and Walén for the types of displacement which they considered. For more general types of displacement, however, the results are different. For a uniformly rotating star, displacements are found to exist for which the stability criterion is little more restrictive than in a nonrotating star. For nonuniform rotation also, certain displacements exist for which rotation has no stabilizing influence; indeed, by producing a shear, the nonuniform rotation assists instability.

To make the mathematical problem tractable, certain simplifying assumptions are made. First, as far as possible, only the *local* condition for turbulence is investigated; thus the convected elements are assumed to have dimensions small compared with the scale of variation of macroscopic variables like pressure, density, etc. On the other hand, ordinary viscosity (gas and radiative), in general, produces negligible results unless the dimensions of the convected elements are small compared with (say) 1 km. It may therefore also be assumed that the convected elements, though small, are not so small that viscosity needs to be taken into account. Finally, any fluctuations in gravity due to the convection are ignored.

II. UNIFORM ANGULAR VELOCITY; FUNDAMENTAL EQUATIONS

Consider, first, the case of uniform angular velocity, Ω. Take cylindrical polar coordinates R, ϕ, and z with the star's center as pole and its axis of rotation as polar axis; in a small disturbance of the steady rotation let the velocity of a moving element have components u, $R\Omega + v$, and w, respectively, in the directions of R, ϕ, and z increasing. Correct to terms of first order in the small quantities u, v, and w, the equations of motion of the material are

$$-\frac{\partial \delta p}{\partial R} - g \sin \alpha \, \delta \rho = \rho \left(\frac{Du}{Dt} - 2\Omega v \right), \tag{3}$$

$$-\frac{\partial \delta p}{R \partial \phi} = \rho \left(\frac{Dv}{Dt} + 2\Omega u \right), \tag{4}$$

$$-\frac{\partial \delta p}{\partial z} - g \cos \alpha \, \delta \rho = \rho \frac{Dw}{Dt}, \tag{5}$$

where

$$\frac{D}{Dt} = \frac{\partial}{\partial t} + \Omega \frac{\partial}{\partial \phi}. \tag{6}$$

Here g denotes the apparent gravity, which is the resultant of the true gravity and the centrifugal acceleration, and α is the angle (nearly equal to our earlier θ) which g makes

with the polar axis. Also δp and $\delta\rho$ denote the changes in pressure and density at a particular point due to the disturbing motion; p and ρ are used for the undisturbed pressure and density. The terms involving 2Ω in the equations represent the Coriolis force. The operator D/Dt denotes time differentiation following the undisturbed rotation.

To these equations two others are added. The first is the equation of continuity,

$$\frac{D\delta\rho}{Dt}+\frac{\partial}{R\partial R}(R\rho u)+\frac{\partial}{R\partial\phi}(\rho v)+\frac{\partial}{\partial z}(\rho w)=0. \tag{7}$$

The other is found by assuming that the motion during the disturbance is adiabatic; it is

$$\frac{1}{p}\left(\frac{D\delta p}{Dt}+u\frac{\partial p}{\partial R}+w\frac{\partial p}{\partial z}\right)=\frac{\gamma}{\rho}\left(\frac{D\delta\rho}{Dt}+u\frac{\partial\rho}{\partial R}+w\frac{\partial\rho}{\partial z}\right). \tag{8}$$

This equation can be simplified as follows: In uniform rotation the surfaces of constant pressure and density coincide, and the gradients of p and ρ are in the same direction. Hence we may put

$$\frac{\partial p}{\partial R}\Big/\frac{\partial\rho}{\partial R}=\frac{\partial p}{\partial z}\Big/\frac{\partial\rho}{\partial z}=\frac{\Gamma p}{\rho}, \tag{9}$$

so that Γ would be the ratio of specific heats required to make the actual temperature gradient adiabatic. Also

$$\frac{\partial p}{\partial R}=-\rho g\sin\alpha, \qquad \frac{\partial p}{\partial z}=-\rho g\cos\alpha. \tag{10}$$

Thus equation (8) becomes

$$\frac{D\delta p}{Dt}-\gamma gH\frac{D\delta\rho}{Dt}-\rho g\left(1-\frac{\gamma}{\Gamma}\right)(u\sin\alpha+w\cos\alpha)=0, \tag{11}$$

where H is the scale height, defined by

$$H=\frac{p}{\rho g}=\frac{p}{|\text{grad } p|}. \tag{12}$$

III. SOLUTION OF THE EQUATIONS

Equations (3)–(7) and (11) are a set of linear differential equations giving the variation of ρu, ρv, ρw, δp, and $\delta\rho$. In these equations the convected elements are assumed to be small compared with the scale of variation of macroscopic variables. Thus, for example, in the relation

$$\frac{\partial}{R\partial R}(R\rho u)=\frac{\partial}{\partial R}(\rho u)+\frac{\rho u}{R}$$

the second term on the right, arising from differentiating the R, is small compared with the first and can be neglected. Similarly the quantities g, α, H, γ, Γ, and R can be treated as constants wherever they appear as coefficients of ρu, ρv, ρw, δp, and $\delta\rho$ or their derivatives. Hence, in particular, equation (6) can be replaced by

$$\frac{D\delta\rho}{Dt}+\frac{\partial(\rho u)}{\partial R}+\frac{\partial(\rho v)}{R\partial\phi}+\frac{\partial(\rho w)}{\partial z}=0, \tag{13}$$

and equations (3), (4), (5), (13), and (11) can be treated as linear equations with constant coefficients in the variables ρu, ρv, ρw, δp, and $\delta\rho$.

Such equations have solutions proportional to exponential functions (real or complex) of the independent variables. Thus in these equations we put

$$\frac{\partial}{\partial R} = il\,, \qquad \frac{\partial}{R\partial\phi} = im\,, \qquad \frac{\partial}{\partial z} = in\,, \qquad \frac{D}{Dt} = i\sigma\,,$$

where l, m, n, and σ are constants. The equations then become

$$\rho(i\sigma u - 2\Omega v) + il\,\delta p + g\sin\alpha\,\delta\rho = 0\,, \tag{14}$$

$$\rho(i\sigma v + 2\Omega u) + im\,\delta p = 0\,, \tag{15}$$

$$\rho i\sigma w + in\,\delta p + g\cos\alpha\,\delta\rho = 0\,, \tag{16}$$

$$\rho(ilu + im\,v + inw) + i\sigma\,\delta\rho = 0\,, \tag{17}$$

$$-\rho g\left(1 - \frac{\gamma}{\Gamma}\right)(u\sin\alpha + w\cos\alpha) + i\sigma\,\delta p - \gamma g H i\sigma\,\delta\rho = 0\,. \tag{18}$$

In these equations we can make further approximations. The quantities l^{-1} and n^{-1} represent the dimensions of convected elements in the R and z directions and so are negligible in our approximation, compared with the scale height H; also $H\Omega^2$ is comparable with $R\Omega^2$, which is, at most, of the same order as g. In consequence, the solutions of the equations fall into two groups. The first gives sound waves, for which, approximately,

$$\sigma^2 = \gamma g H(l^2 + m^2 + n^2)\,.$$

In these solutions Ω^2/σ^2 is negligible, and the terms in equations (14) and (16) involving $\delta\rho$ and that in equation (18) involving $1 - \gamma/\Gamma$ can be neglected. The other group gives much smaller values of σ^2, comparable, at most, with g/H and Ω^2. In these, all the terms of equations (14), (15), and (16) are, in general, comparable in order of magnitude. Hence in equation (17) the term $i\sigma\delta\rho$ is comparable with $\rho\sigma^2 u/g$, or with $\rho u/H$, and is negligible compared with the other terms in this equation; also in equation (18) the term $i\sigma\delta p$ is comparable with $i\sigma g\delta\rho/l$, and so is negligible compared with the term $\gamma g H i\sigma\delta\rho$. Only the second group of solutions is of interest in considering dynamical stability. Hence in equations (17) and (18), respectively, the terms $i\sigma\delta\rho$ and $i\sigma\delta p$ are neglected, so that these equations become

$$\rho(lu + m\,v + nw) = 0\,, \tag{19}$$

$$\eta\rho(u\sin\alpha + w\cos\alpha) + i\sigma\,\delta\rho = 0\,. \tag{20}$$

Here

$$\eta = \frac{(1 - \gamma/\Gamma)}{\gamma H}\,,$$

or, using equations (9) and (12),

$$\eta = \frac{1}{\gamma p}|\operatorname{grad} p| - \frac{1}{\rho}|\operatorname{grad}\rho|\,. \tag{21}$$

It will be noted that equations (19) and (20) are identical, in our approximation, with the corresponding equations for an incompressible liquid of nonuniform density, $\eta\rho$ corresponding to the density gradient. Eliminating the variables ρu, ρv, ρw, $\delta\rho$, and δp be-

tween equations (14), (15), (16), (19), and (20), we obtain

$$\begin{vmatrix} i\sigma, & -2\Omega, & 0, & il, & g\sin\alpha \\ 2\Omega, & i\sigma, & 0, & im, & 0 \\ 0, & 0, & i\sigma, & in, & g\cos\alpha \\ l, & m, & n, & 0, & 0 \\ \eta\sin\alpha, & 0, & \eta\cos\alpha, & 0, & i\sigma \end{vmatrix} = 0 .$$

Expanding the determinant gives us

$$\sigma\{\sigma^2(l^2+m^2+n^2) - 4\Omega^2n^2 + \eta g[m^2+(l\cos\alpha - n\sin\alpha)^2]\} = 0 . \qquad (22)$$

IV. THE STABILITY CONDITION

Equation (22) can be regarded as an equation to give σ when l, m, and n (representing the dimensions of a disturbance) are given. To give cellular convection, l, m, and n must be real. Actually, the variation of density with height leads to a slow variation of amplitude of the disturbance with height; but the present approximation ignores these variations, and it is accordingly not necessary to give l and n imaginary parts. On the other hand, σ may be real or imaginary; if the latter, one of its values corresponds to a steadily increasing motion, and so to instability. We shall regard l, m, and n as able to take all real values (subject to the limitation imposed by assuming the convected elements to be small). Equation (22) is unaltered if the sign of σ, of m, or of l and n simultaneously, is reversed; hence the real expression for any of the variables ρu, ρv, ρw, $\delta\rho$, and δp must be of the form

$$\text{Const.} \times \cos(lR + nz + \epsilon_1)\cos(mR\phi + \epsilon_2)\cos(\sigma t + \epsilon_3)$$

if σ is real, and

$$\text{Const.} \times \cos(lR + nz + \epsilon_1)\cos(mR\phi + \epsilon_2)\, e^{\pm|\sigma|t}$$

if σ is imaginary. The phases ϵ_1, ϵ_2, and ϵ_3 may be different for the different variables.

One root of equation (22) is $\sigma = 0$, whatever the values of l, m, n, and η. By equation (20) the corresponding motion is horizontal (i.e., normal to g). In the absence of rotation, equilibrium is obviously neutral for horizontal displacements; it is, however, noteworthy that, even when rotation is present, equilibrium is still neutral for certain horizontal displacements, rotation exerting no stabilizing influence.

The remaining roots of equation (22) indicate instability if

$$\eta g[m^2+(l\cos\alpha - n\sin\alpha)^2] > 4\Omega^2n^2 . \qquad (23)$$

In the absence of rotation, this reduces to $\eta > 0$; by equation (21) this gives the usual condition that the actual temperature gradient exceeds the adiabatic. If displacements symmetric about the axis of rotation alone are considered, we must put $m = 0$ in formula (23).

Inequality (23) does not depend on the absolute magnitudes of l, m, and n but only on their ratios; that is, it is independent of the actual dimensions of the moving elements. If $m = 0$, $l\sin\theta + n\cos\theta = 0$ (corresponding to displacements which, apart from the consequences of conservation of angular momentum, would be wholly radial), inequality (23) reduces to

$$\eta g\cos^2(\alpha - \theta) > 4\Omega^2\sin^2\theta ,$$

which is equivalent to Randers' criterion (1), since $\alpha - \theta$ is the small angle between g

and the radial direction. If $m = 0 = l$, formula (23) similarly reduces to Walén's criterion (2) for displacements perpendicular to the axis of rotation. In general, formula (23) indicates that ηg must be comparable with $4\Omega^2$, and so the temperature gradient must exceed the adiabatic by an amount which, though small, is not negligible; this indicates the stabilizing influence of rotation for general displacements.

For certain displacements, however, the adiabatic temperature gradient need be exceeded by only a very small amount to insure instability; these are the displacements in which n is small compared with one or both of l and m. Thus convection must occur whenever the actual temperature gradient exceeds the adiabatic; but it is limited to certain types of motion unless the adiabatic value is markedly exceeded.

By equations (14)–(17), the motion is such that

$$\frac{u \sin \alpha + w \cos \alpha}{i\sigma [m^2 + (l \cos \alpha - n \sin \alpha)^2]} = \frac{v}{2\Omega n (l \cos \alpha - n \sin \alpha) - i\sigma m (l \sin \alpha + n \cos \alpha)} = \frac{u \cos \alpha - w \sin \alpha}{-2\Omega m n - i\sigma (l \sin \alpha + n \cos \alpha)(l \cos \alpha - n \sin \alpha)}. \tag{24}$$

Hence, unless n exactly vanishes, the motion is wholly horizontal ($u \sin \alpha + w \cos \alpha = 0$) at the limit between stability and instability ($\sigma = 0$) and so does not contribute to the outward convection of energy. This is, however, unimportant when n is small; the vertical motion then becomes comparable with the horizontal if the stability limit is slightly exceeded—in fact, if $il\sigma$ or $im\sigma$ becomes comparable with $n\Omega$. For any positive η, however small, it is always possible to choose l/n or m/n so large that this is so.

The motions when n is small can most simply be studied in the limit $n = 0$, which gives instability whenever $\eta > 0$. In this limit equation (24) is replaced by

$$\frac{u}{m^2 \sin \alpha} = \frac{v}{-lm \sin \alpha} = \frac{w}{(l^2 + m^2) \cos \alpha}.$$

The motions are thus of two kinds. The first, given by $m = 0 = n$, is a motion wholly parallel to the axis of rotation. It is no surprise to find that this gives instability whenever $\eta > 0$; it has long been agreed that there is instability for displacements parallel to the axis if the adiabatic temperature gradient is exceeded by an arbitrarily small amount. The second, given by $n = 0$, $m \neq 0$, has not been considered earlier; because $m \neq 0$, it is a motion in which azimuthal pressure gradients are important. It is a whirling motion in "tubes" parallel to the axis of rotation. The axis of the whirling motion does not coincide with the tube axis save in the equatorial plane; elsewhere it is in the vertical plane through the tube axis, its direction being such that the plane of the whirling motion passes within the *acute* angle between the directions of the tube axis and of local gravity. The type of motion in this case is illustrated in Figure 1.

Motion when n is small but not zero may be expected to approximate to that given by $n = 0$. Thus when $m \neq 0$ the motion is neither mainly parallel to the axis of rotation nor (in general) nearly horizontal, and there is instability for such motion when the temperature gradient is only slightly greater than the adiabatic. The motion possesses considerable regularity in this case, so that one can hardly refer to it as turbulence. But it should be able to contribute appreciably to the transport of energy perpendicular to the rotational axis, as well as to that parallel to the axis. Clearly, further investigation is needed before it can confidently be affirmed that rotation does not greatly hamper convective transport perpendicular to the axis; but the above results do at least suggest that such a conclusion is possible.

V. BOUNDARY CONDITIONS

In the above, l, m, and n were assumed to be arbitrary. This is not exactly correct. The problem of free oscillations is an eigen-value problem, and the eigen-values depend

on boundary conditions. In our problem an unstable region can be supposed to be surrounded by stable regions, into which the disturbance hardly penetrates. These provide effective boundaries and so determine the eigen-values.

No serious error is, in fact, involved by assuming that l, m, and n can take all values. The greatest "wave length" permitted for a disturbance is comparable with the dimensions of the unstable region; we are considering wave lengths small compared with this, i.e., "overtones" of high order. Such overtones give a large number of possible wave lengths very close together. The stability condition is virtually the same for all overtones giving much the same ratios $l : m : n$, and accordingly the boundary conditions are unimportant. This is fortunate, but similar good fortune cannot always be expected.

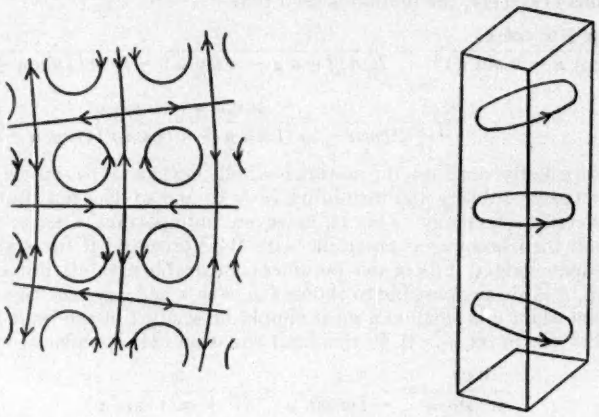

FIG. 1.—Motion in the case $n = 0$, $m \neq 0$. The left-hand diagram shows the motion projected on the equatorial plane: that on the right shows the circulation in a whirl tube and indicates the progressive tilt of the plane of whirling to the equatorial plane on going away from that plane. The axis of rotation is, in either case, supposed to be on the left of the region shown.

In particular, when considering an angular velocity which varies from point to point, boundary conditions have to be taken into consideration before a stability criterion can be obtained.

VI. NONUNIFORM ROTATION: THE EQUATIONS

Consider, now, the case when Ω, the angular velocity in the undisturbed rotation, varies from point to point. In this case the surfaces of equal pressure and equal density in the undisturbed state do not coincide unless Ω depends only on R. Such a dependence of Ω will be assumed; the problem is sufficiently difficult even so, and it is doubtful whether any qualitatively different results would be found for a more general variation of Ω.

With this assumption, equations (3), (5), (6), (7), and (11) remain valid as before, but equation (4) is replaced by

$$-\frac{\partial \delta p}{R\partial \phi} = \rho \left\{ \frac{Dv}{Dt} + \frac{1}{R}\frac{d}{dR}(R^2\Omega)\, u \right\} = \rho \left\{ \frac{Dv}{Dt} + (2\Omega + \Omega_1)\, u \right\}, \tag{25}$$

where

$$\Omega_1 = R\frac{d\Omega}{dR}. \tag{26}$$

In spite of the dependence of Ω on R, it is permissible to treat 2Ω, as it appears explicitly in equations (3) and (25), as a constant. The derivative of Ω, as it appears in Ω_1, must be retained, since Ω_1 may be comparable with Ω; but the variation in 2Ω where it explicitly appears can be neglected, since what is at issue here is the small variation of Ω in a distance comparable with the scale of the convection. The approximation is similar to that made in neglecting the variation of g.

However, the variation of Ω cannot, in general, be ignored where it appears in the relation

$$\frac{D}{Dt}=\frac{\partial}{\partial t}+\Omega\frac{\partial}{\partial\phi}.$$

Here $\partial/\partial\phi$ is, in general, large, and so the small variations in Ω have to be taken into account. For uniform rotation it was found above that $D/Dt(\equiv i\sigma)$ vanishes at the limit of instability; the same may be expected to apply here on a special locus $R=R_0$; but D/Dt is not negligible save on this locus. This fact makes the discussion of instability for nonuniform rotation altogether different from that given for uniform rotation.

Because of the dependence of Ω on R in D/Dt, it is no longer possible to assume an exponential dependence of the variables on R. It will, however, still be assumed that

$$\frac{\partial}{R\partial\phi}=im\,,\qquad\frac{\partial}{\partial z}=in\,,\qquad\frac{D}{Dt}=i\sigma\,;$$

here m and n are still to be treated as constants, but σ is a function of Ω, and so of R. In fact,

$$\frac{\partial}{\partial R}(i\sigma)=\frac{\partial}{\partial R}\left(\frac{\partial}{\partial t}+\Omega\frac{\partial}{\partial\phi}\right)=\frac{d\Omega}{dR}\frac{\partial}{\partial\phi};$$

and so

$$\frac{\partial\sigma}{\partial R}=mR\frac{d\Omega}{dR}=m\Omega_1\,. \tag{27}$$

Again, g, α, H, γ, and R are treated as constants when they appear as coefficients in equations (3), (5), (7), (11), and (25); but since, as mentioned in Section V, it is impossible here to obtain definite results without introducing boundary conditions, Γ and the η defined in equation (21) are supposed to be functions of R. The terms $i\sigma\delta\rho$ and $i\sigma\delta p$ obtained in equations (7) and (11) are neglected, as before. Thus equations (3), (5), (7), (11), and (25) become

$$\begin{aligned}
&-\frac{\partial\,\delta p}{\partial R}-g\sin\alpha\,\delta\rho=\rho(i\sigma u-2\Omega v)\,,\\
&-im\,\delta p=\rho[i\sigma v+(2\Omega+\Omega_1)u]\,,\\
&-in\,\delta p-g\cos\alpha\,\delta\rho=\rho i\sigma w\,,\\
&\frac{\partial}{\partial R}(\rho u)+im\rho v+in\rho w=0\,,\\
&\eta\rho(u\sin\alpha+w\cos\alpha)+i\sigma\,\delta\rho=0\,.
\end{aligned} \tag{28}$$

Solving the second, third, and last of these equations for ρv, ρw, and $\delta\rho$ and substitut-

ing in the others, we find

$$(\sigma^2+\eta g\cos^2\alpha)\,(i\sigma\frac{\partial\delta p}{\partial R}+2\Omega im\,\delta p)+ng\eta\sigma\sin\alpha\cos\alpha\,\delta p$$
$$-U\{(\sigma^2+\eta g\cos^2\alpha)\,(\sigma^2-2\Omega[2\Omega+\Omega_1])+\eta g\sigma^2\sin^2\alpha\}=0\,,$$

$$(\sigma^2+\eta g\cos^2\alpha)\,(\sigma\frac{\partial U}{\partial R}-m[2\Omega+\Omega_1]\,U)-ing\eta\sigma U\sin\alpha\cos\alpha$$
$$-i\delta p\{\sigma^2(m^2+n^2)+\eta gm^2\cos^2\alpha\}=0\,,$$

where U is written for ρu. Substitute for δp from the second of these equations in the first; then, after dividing by $\sigma^2+\eta g\cos^2\alpha$, we have

$$\sigma\frac{\partial}{\partial R}[\Lambda^{-1}\{(\sigma^2+\eta g\cos^2\alpha)\,(\sigma U'-mU[2\Omega+\Omega_1])-ing\eta\sigma U\sin\alpha\cos\alpha\}]$$
$$-i\Lambda^{-1}[(\sigma^2+\eta g\cos^2\alpha)\,2\Omega im\sigma U'+ng\eta\sigma\sin\alpha\cos\alpha\,(\sigma U'-m\Omega_1U) \qquad (29)$$
$$+2\Omega(2\Omega+\Omega_1)\,i\sigma^2n^2U-i\sigma^2U\{\sigma^2(m^2+n^2)+\eta g(m^2+n^2\sin^2\alpha)\}]=0\,,$$

where

$$\Lambda=\sigma^2(m^2+n^2)+\eta gm^2\cos^2\alpha\,, \qquad (30)$$

and the primes denote differentiation with respect to R. Using equation (27) and

$$\Lambda'=2\sigma m\Omega_1(m^2+n^2)+\eta' gm^2\cos^2\alpha$$

and dividing by σ^2/Λ, we reduce equation (29) to

$$(\sigma^2+\eta g\cos^2\alpha)\,U''-2in\eta gU'\sin\alpha\cos\alpha-U[\sigma^2(m^2+n^2)$$
$$+\eta g(m^2+n^2\sin^2\alpha)-2\Omega n^2(2\Omega+\Omega_1)]-n\cos\alpha\Lambda^{-1}g(2m\Omega_1\eta+\sigma\eta') \qquad (31)$$
$$\times\{n\cos\alpha\sigma U'-[mn(2\Omega+\Omega_1)\cos\alpha+i\sigma\sin\alpha(m^2+n^2)]\,U\}=0\,.$$

VII. THE STABILITY CRITERION

Clearly, equation (31) is too complicated for anything like a general solution to be attempted. We therefore concentrate on special cases.

In the special case $m=0$, the quantity σ ceases to depend on R. It is possible in this case to solve the problem without recourse to boundary conditions, treating η as constant. Putting $m=0$, $\eta'=0$, the equation reduces to

$$(\sigma^2+\eta g\cos^2\alpha)\,U''-2in\eta gU'\sin\alpha\cos\alpha$$
$$-Un^2[\sigma^2+\eta g\sin^2\alpha-2\Omega(2\Omega+\Omega_1)]=0\,.$$

As in the case of uniform rotation, a solution now exists such that $U\propto e^{lR}$; it is such that

$$\sigma^2(l^2+n^2)+\eta g(l\cos\alpha-n\sin\alpha)^2-2\Omega(2\Omega+\Omega_1)\,n^2=0\,.$$

The corresponding instability condition is

$$\eta g(l\cos\alpha-n\sin\alpha)^2>2\Omega(2\Omega+\Omega_1)\,n^2\,. \qquad (32)$$

This reduces to Walén's criterion (2) if $l=0$, as, indeed, it should.

Equation (32) indicates that for some displacements nonuniform rotation exerts a stabilizing influence if $\Omega(2\Omega + \Omega_1)$ is positive, i.e., if

$$\Omega \frac{d}{dR}(R^2\Omega) > 0 .$$

Here, however, it is also of interest to know whether such a stabilizing influence is present for all displacements. The results for uniform rotation suggest that the stabilizing influence disappears as n becomes small. We therefore consider the special case $n = 0$.

For this case, equation (31) reduces to the much simpler form,

$$(\sigma^2 + \eta g \cos^2 \alpha) U'' - U m^2 (\sigma^2 + \eta g) = 0 . \tag{33}$$

In this equation Ω does not appear explicitly; it appears implicitly through σ, but essentially this only introduces the derivative $d\Omega/dR$. This can be seen as follows. In uniform rotation, σ vanishes at the limit of stability. By equation (27), σ cannot vanish everywhere for nonuniform rotation, but we can expect that, at the limit of stability, $\sigma = 0$ for one special value of R. Take this value of R as $R = R_0$; then, by equation (27), in our approximation,

$$\sigma = m\Omega_1 (R - R_0) . \tag{34}$$

Equation (34) indicates that, in motion such that $n = 0$, the only influence of the angular velocity is exerted through its inhomogeneity, i.e., through the shear which it produces. Equations (33) and (34) are, in fact, identical with the equations obtained by ignoring curvature and by considering a mass of gas under gravity, moving with a velocity whose gradient Ω_1 makes an angle α with the horizontal. It is well known that a shearing motion tends to destabilize; accordingly, not only has the stabilizing effect of rotation disappeared in the case $n = 0$, but it has been replaced by an actual destabilizing effect.

It is, of course, desirable to derive these results mathematically from equation (33), so as to be satisfied that the special assumptions made in deriving this equation are not themselves inconsistent with the types of motion to whose instability the shear may be expected to lead. It is shown in the appendix to this paper that, for example, equation (33) indicates instability in some cases when $\eta < 0$ (i.e., the temperature gradient is *less* than the adiabatic) everywhere save at one point, where $\eta = 0$. Instability is likely to be found in even less favorable cases; the Richardson criterion indicates that instability occurs if $-\eta g$, though positive, is less than a number comparable with Ω_1^2. For present purposes, however, it is sufficient to have found that nonuniform rotation does not prevent instability any more than uniform rotation does.

The reason for the unimportance of Coriolis forces in the case $n = 0$ can readily be seen from the equations of motion (28). If $n = 0$, the variable δp disappears from the third of these equations, and the fourth becomes

$$\frac{\partial}{\partial R}(\rho u) + im\rho v = 0 .$$

Hence in the first equation the pressure and the Coriolis forces appear in the combination

$$\frac{\partial}{\partial R}(\delta p) - 2\Omega\rho v \equiv \frac{1}{im}\frac{\partial}{\partial R}(im\,\delta p + 2\Omega\rho u) .$$

The second equation also involves the combination $im\delta p + 2\Omega\rho u$; hence it is possible to cancel the Coriolis terms completely from the equations simply by altering the pressure by $2i\Omega\rho u/m$. That is, the Coriolis forces lead to a change in the pressure, but are otherwise unimportant.

The effect of the Coriolis forces, though not negligible, will clearly be small if n is not zero, but small. Thus in this case, too, rotation can exert very little stabilizing influence. As equation (32) indicates, rotation does exert a stabilizing influence for many kinds of displacement. But, at the very least, we can assert that nonuniform rotation, as well as uniform, permits instability as soon as the temperature gradient exceeds the adiabatic.

Nonuniform rotation may, however, hamper the transfer of energy by convection. The flow pattern in the limit of stability, projected on a plane normal to the axis of rotation, is roughly as shown in Figure 2, *a*. The flow indicated is everywhere that relative to the local velocity of rotation; by equation (34) the flow pattern moves with the velocity of undisturbed rotation at $R = R_0$. Well away from $R = R_0$, where the disturbance velocity is small, the variation of angular velocity with R means that a material element is carried past the successive convection cells without the disturbance being able to superpose more than an oscillation on its steady flow; it does not circulate right around a convection

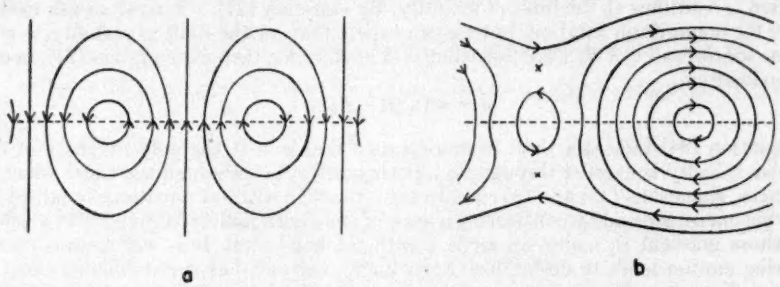

FIG. 2.—Flow at the limit of stability when $\cos a = 0$. The flow is in the equatorial plane: the broken line is $R = R_0$, and R increases perpendicular to this line. *a* gives the flow everywhere relative to the local undisturbed velocity of rotation; *b* that relative to the undisturbed velocity of rotation at $R = R_0$. In *b* the ratio of the disturbance velocity to the undisturbed velocity gradient is arbitrarily adjusted to give zero velocity to the points marked with a cross.

cell. This is illustrated in Figure 2, *b*, which indicates the type of motion of the material elements relative to the undisturbed velocity of rotation at $R = R_0$. It is, of course, incorrect to apply results derived at the limit of instability to a definitely unstable layer without modification. In an unstable layer, convection cells may exist at different heights, and material may pass from one cell to another to continue its upward motion. Nevertheless, the argument certainly suggests that nonuniform rotation may impede energy transport by convection. Equally, convection may operate to destroy the nonuniformity of the rotation.

A last comment should be added. For the sake of mathematical simplicity, the convected elements were assumed to be small compared with the distance within which macroscopic variables alter appreciably. It should be emphasized, however, that the reason for the assumption is purely mathematical convenience. There is, in fact, nothing to show that the general results are not valid when the convected elements are comparable with the scale height or are larger. It is my own belief that in the presence of rotation, as in its absence, the convection cells increase up to sizes comparable with the dimensions of the unstable region.

A large part of the work described in this paper was done while the author was visiting professor at the California Institute of Technology and at Princeton University. The author desires to thank both these institutions for their generous hospitality.

APPENDIX

We wish to show that equation (33) can indicate instability in some cases when $\eta < 0$. The general discussion of this equation is difficult; for example, substituting from equation (34) in equation (33), we find, in general, an equation with singularities, where

$$m\Omega_1 (R - R_0) = \pm \cos \alpha \sqrt{(-\eta g)}.$$

Since $U' = \infty$ at the singularities, it is necessary to take viscosity into account in their vicinity. To avoid such complications, attention is restricted to a special case in which the singularities do not arise. The nonappearance of singularities is of little physical importance; far from always opposing instability in fluid flow, viscosity often assists instability to appear.[4]

The special case considered is that in which $\cos \alpha = 0$ (corresponding to conditions at the equatorial plane) and η has a double zero at $R = R_0$, while remaining negative everywhere else; it is supposed to be an even function of $R - R_0$. At the limit of instability, as has been explained, equation (34) is valid; thus, if $x = R - R_0$, equation (33) becomes

$$U'' - U\left(m^2 + \frac{\eta g}{\Omega_1^2 x^2}\right) = 0,$$

where primes now denote differentiation with respect to x. Put

$$\eta g = -\Omega_1^2 x^2 f(x), \tag{35}$$

where $f(x)$ is a positive even function of x, finite at $x = 0$. Then

$$U'' - U[m^2 - f(x)] = 0. \tag{36}$$

Since η is finite, equation (35) shows that $f(x) \to 0$ as $|x| \to \infty$. Thus, for large positive values of x, equation (36) approximates to $U'' = m^2 U$, and the asymptotic behavior of its solutions is given by

$$U = A_1 e^{|m|x+\kappa_1} + A_2 e^{-|m|x+\kappa_2}, \tag{37}$$

where A_1 and A_2 are constants, and κ_1 and κ_2 vary more slowly, for large values of x than any multiple of x, however small. For large negative values of x there is a similar expression,

$$U = A_3 e^{|m|x+\kappa_3} + A_4 e^{-|m|x+\kappa_4}, \tag{38}$$

where A_3 and A_4 depend linearly on A_1 and A_2.

To insure that U is everywhere finite, A_1 and A_4 must vanish; this imposes boundary conditions on the solution of equation (36). A nonvanishing solution satisfying these boundary conditions can always be found if m^2 is suitably chosen. For some functions f, more than one m^2 can be found to give a solution; in this case we fix attention on the least value of m^2, which gives a solution which is everywhere positive and an even function of x. The flow corresponding to this solution is shown in Figure 2 for the case $f(x) = 1/(x^2 + k^2)$.

The existence of a solution of equation (36) does not suffice by itself to prove that the distribution of η given by equation (35) corresponds to the limit of stability. The period of oscillations relative to the rotating star is everywhere $2\pi/\sigma$; by equation (34), this period is infinite at $R = R_0$, but nowhere else. Thus the motion can be called oscillatory just as fairly as it can be treated as motion at the limit of stability. Indeed, motion which is oscillatory at one level is stationary at a neighboring level; if the period is $2\pi/\sigma_0$ at $R = R_0$, equation (34) is replaced by

$$\sigma = m\Omega_1 (R - R_0) + \sigma_0,$$

which is simply equation (34) with R_0 replaced by $R_0 - \sigma_0/m\Omega_1$. To prove that the limit of sta-

[4] See, e.g., C. C. Lin, *Quart. Appl. Math.*, 3, 117, 218, and 277, 1945. Further references are given in these papers.

bility has actually been reached, it must be shown that, with slightly varied conditions, an oscillation of steadily increasing amplitude can be obtained. It can actually be shown that the only variation of conditions which is required is a slight change of m^2 from the value for which equation (36) is satisfied; no change in $f(x)$ is necessary. That is, the distribution of η given by equation (35) actually corresponds to instability; even in an unstable state some displacements may be neutral, and in the present instance the motion given by equation (36) represents such a neutral motion.

For an oscillation of increasing amplitude, equation (34) is replaced by

$$\sigma = m\Omega_1 (R - R_0 + \epsilon - i\epsilon') , \tag{39}$$

where, if $m\Omega_1 > 0$ (as can be secured by suitable choice of m), ϵ' must be positive. Using this equation and the value of η given by equation (35), we obtain, in place of equation (36),

$$U'' - U\left[m^2 - \frac{x^2 f(x)}{(x+\epsilon-i\epsilon')^2}\right] = 0 . \tag{40}$$

The asymptotic behavior for large x, of the solutions of equation (40) which satisfy the boundary conditions $A_1 = 0 = A_4$ is again given by equations (37) and (38). Assume that m^2 takes a value only slightly different from that for which equation (36) is satisfied. By adjusting the arbitrary constants in the solution of equation (40), we can insure that the solution satisfies the boundary condition at $x = -\infty$ and also (assuming that ϵ and ϵ' are small and that $\epsilon' \neq 0$) that it deviates only slightly from the solution of equation (36), save when x is large and positive. To insure that the solution also satisfies the boundary condition at $x = +\infty$, it is necessary that, in equation (37), the real and imaginary parts of A_1 both vanish. This can be insured by suitable choice of the two constants ϵ and ϵ'. It is necessary only to satisfy ourselves that, with a suitably chosen value of m^2, we get a positive value of ϵ'.

Let U_0 and m_0^2 denote the values of U and m^2 for which equation (36) is satisfied, and let the corresponding values for which equation (40) is satisfied be $U_0 + U_1$ and $m_0^2 + \Delta$. It is assumed that U_1, Δ, ϵ, and ϵ' are so small that their squares and products can be neglected. Then, from equations (36) and (40), we obtain

$$(U_0 + U_1)\{U_0'' - U_0[m_0^2 - f(x)]\}$$
$$= U_0\left(U_0'' + U_1'' - [U_0 + U_1]\left[m_0^2 + \Delta - \frac{x^2 f(x)}{(x+\epsilon-i\epsilon')^2}\right]\right)$$

or

$$U_0 U_1'' - U_1 U_0'' = U_0(U_0 + U_1)\left(\Delta + f[x]\left[1 - \frac{x^2}{(x+\epsilon-i\epsilon')^2}\right]\right).$$

Integrate this relation from $-\infty$ to $+\infty$; then, since U_0, U_1, and their derivatives all vanish at the limits,

$$\int_{-\infty}^{\infty} U_0(U_0 + U_1)\left\{\Delta + f(x)\left(1 - \frac{x^2}{[x+\epsilon-i\epsilon']^2}\right)\right\}dx = 0 ,$$

or, approximately,

$$\Delta\int_{-\infty}^{\infty} U_0^2 dx + \int_{-\infty}^{\infty} U_0(U_0 + U_1) f(x)\left(1 - \frac{x^2}{[x+\epsilon-i\epsilon']^2}\right)dx = 0 . \tag{41}$$

To estimate the second integral, suppose that a positive number N exists which is large compared with ϵ and ϵ' but small compared with the scale within which U_0, U_1, and $f(x)$ vary by an appreciable fraction of themselves. To fix ideas, suppose that N is comparable with $(\epsilon^2 + \epsilon'^2)^{1/4}$; small quantities of order $(\epsilon^2 + \epsilon'^2)^{3/4}$ will be neglected.[5] The range of integration is divided into

[5] It can be verified that, in the argument which follows, the small quantities of order $(\epsilon^2 + \epsilon'^2)^{3/4}$ exactly cancel. However, the argument is easier and perfectly adequate if they are simply neglected.

three parts, from $-\infty$ to $-N$, from $-N$ to N, and from N to ∞. In the first and third parts of the range,

$$\frac{x^2}{(x+\epsilon-i\epsilon')^2} = 1 - \frac{2(\epsilon-i\epsilon')}{x} + \frac{3(\epsilon-i\epsilon')^2}{x^2} - \ldots .$$

Hence the contribution of these parts of the range to the integral is

$$\left\{\int_{-\infty}^{-N} + \int_{N}^{\infty}\right\} U_0(U_0+U_1) f(x) \left\{\frac{2(\epsilon-i\epsilon')}{x} - \frac{3(\epsilon-i\epsilon')^2}{x^2}\right\} dx ,$$

the later terms in the series being neglected because $(\epsilon - i\epsilon')/x$ is, at most, of order $(\epsilon^2+\epsilon'^2)^{1/4}$ in the range of integration. Since U_0 and $f(x)$ are even functions of x, this reduces to

$$2(\epsilon-i\epsilon')\left\{\int_{-\infty}^{-N} + \int_{N}^{\infty}\right\} U_0 U_1 f(x) \frac{dx}{x} + 3(\epsilon-i\epsilon')^2 \left\{\int_{-\infty}^{-N} + \int_{N}^{\infty}\right\} U_0(U_0+U_1) f(x) \frac{dx}{x^2} .$$

Both the terms in this expression are negligibly small: the first term because U_1 is comparable with ϵ and ϵ', and $(\epsilon - i\epsilon')/x$ with $(\epsilon - i\epsilon')/N$, so that the term is of order $(\epsilon^2+\epsilon'^2)^{3/4}$ at most; the second because (as can be seen by integrating by parts) the integral is, at most, of order $1/N$, so that the term is again of order $(\epsilon^2+\epsilon'^2)^{3/4}$.

The contribution to the second integral of equation (41) from the range $(-N, N)$ is

$$\int_{-N}^{N} \chi(x) \left\{\frac{2(\epsilon-i\epsilon')}{x+\epsilon-i\epsilon'} - \frac{(\epsilon-i\epsilon')^2}{(x+\epsilon-i\epsilon')^2}\right\} dx , \tag{42}$$

where

$$\chi(x) = U_0(U_0+U_1) f(x) .$$

In this range we put

$$\chi(x) = \chi(0) + x\chi'(0) .$$

This approximation is sufficient because both x and the range of integration are comparable with N, and so an x^2 term in the expansion of $\chi(x)$ leads to a contribution of order N^3, i.e., of order $(\epsilon^2+\epsilon'^2)^{3/4}$. Thus, substituting and integrating, the expression (42) becomes

$$\{\chi(0) - (\epsilon-i\epsilon')\chi'(0)\}\left\{2(\epsilon-i\epsilon')\log\frac{N+\epsilon-i\epsilon'}{-N+\epsilon-i\epsilon'} - (\epsilon-i\epsilon')^2\frac{2N}{N^2-(\epsilon-i\epsilon')^2}\right\} + \chi'(0)(\epsilon-i\epsilon')^2\left(4N - \log\frac{N+\epsilon-i\epsilon'}{-N+\epsilon-i\epsilon'}\right).$$

Nearly all the terms in this are seen to be negligible; the one exception arises from the product of $\chi(0)$ into the logarithmic term in the second bracket. Correct to our approximation, this yields

$$\pm 2\pi i(\epsilon-i\epsilon')\,[U_0^2]_{x=0} f(0) ,$$

the sign in the $\pm$ being the sign of ϵ'.

Hence equation (41) has now been reduced to

$$\Delta\int_{-\infty}^{\infty} U_0^2 dx \pm 2\pi i(\epsilon-i\epsilon')\,[U_0^2]_{x=0} f(0) = 0 .$$

Taking real and imaginary parts, this gives $\epsilon = 0$ and

$$\Delta \int_{-\infty}^{\infty} U_0^2 dx + 2\pi |\epsilon'| [U_0^2]_{x=0} f(0) = 0 . \tag{43}$$

For this equation to have a solution, Δ must be negative, and so m^2 must be less than m^0. Conversely, by taking m^2 less than m_0^2, it is possible to obtain solutions of equation (40) with ϵ' positive.[6] These solutions correspond to steadily increasing motions; hence it is proved that the distribution of η given by equation (35) corresponds to instability for some displacements.

[6] It might be thought that the presence of $|\epsilon'|$ in eq. (43) implies that damped motions, like the increasing ones, occur only if $m^2 < m_0^2$. This is incorrect; damped motions demand a friction layer where viscosity is important, and this reverses the sign of the $|\epsilon'|$ term (see Lin, *op. cit.*). Equation (43) applies to increasing motions only; thus in eq. (39), if $\epsilon' < 0$, $m\Omega_1$ must be taken to be negative also.

ON THE VARIATION OF TURBULENT VELOCITIES IN STELLAR AND SOLAR ATMOSPHERES

SU-SHU HUANG
Yerkes Observatory
Received January 18, 1951

ABSTRACT

In this paper it is shown that Wright's observed relation between turbulent velocities and excitation potentials can be understood if it is assumed that the mean turbulent velocity in stellar atmospheres decreases exponentially with optical depth in the atmosphere. Theoretical curves between turbulent velocities and excitation potentials derived on this assumption agree well with the observations. Wright's further result that the turbulent velocity is greater for ionized atoms than for the neutral atoms can also be interpreted, as also the variation of turbulent velocity required by Allen's analysis of the spectral lines at different points of the solar disk.

I. INTRODUCTION

Recently several writers[1] have tried to apply to the theory of stellar atmospheres the modern ideas relating to the spectrum of turbulence. In particular, the present author has emphasized[2] that, in dealing with the interpretation of observational data in terms of turbulent motion in the reversing layer, we must distinguish the effects caused by eddies with wave lengths large, respectively small, compared to the thickness of the reversing layer. In Paper II we distinguished these eddies by terming them "large," respectively "small," and showed that, while the velocity of large eddies is reflected only in the broadening of spectral lines, the abnormally high thermal velocity derived for certain stars from the curve of growth is generally attributed to the small eddies. In the following discussion we shall limit ourselves mainly to the analysis of small eddies; the term "turbulent velocity" should always be understood to refer to these small eddies unless it is explicitly stated otherwise.

During the past years K. O. Wright has published a series of papers[3] on the turbulent velocities in the atmospheres of stars by the method of the curve of growth. In his analysis of the observed data he first separates all the measurable spectral lines of neutral iron into groups according to their excitation potentials, and then plots curves of growth for the various groups of lines. Proceeding in this way, he finds that the turbulent velocity varies with the excitation potential of the lower-energy level from which the lines arise. The relation between the turbulent velocity and the excitation potential has the same general behavior in all the stars that he has studied. Accepting Wright's relation as real,[4] we can derive some important phenomenological properties of the "small eddies" in the reversing layers. In fact, we shall show that Wright's relation can be obtained from theoretical considerations if the turbulent velocity in the reversing layer is assumed to

[1] R. S. Richardson and M. Schwarzschild, *Ap. J.*, 111, 351, 1950; M. H. Wrubel, *Ap. J.*, 112, 424, 1950; S. S. Huang, *Ap. J.*, 112, 399, 418, 1950, which will be referred to as "Paper I" and "Paper II," respectively.

[2] As mentioned in Papers I and II, the distinction between large eddies and small eddies was first made by O. Struve and A. Unsöld and has recently been discussed in some detail by several authors, including M. Schwarzschild (*Ap. J.*, 108, 225, 1948), Unsöld and Struve (*Ap. J.*, 110, 455, 1949), and others.

[3] *J.R.A.S. Canada*, 40, 183, 1946; 41, 49, 1947; *Pub. Dom. Ap. Obs. Victoria*, Vol. 8, No. 1, 1948, and No. 9, 1950; R. B. King and K. O. Wright, *Ap. J.*, 106, 224, 1947; K. O. Wright and E. van Dien, *J.R.A.S. Canada*, 43, 15, 1949.

[4] L. Goldberg and K. A. Pierce, O.N.R. Project M720-5, Ann Arbor, October, 1947; D. H. Menzel and B. Bell, O.N.R. Project M720-5, Ann Arbor, June, 1948.

increase exponentially with height in the atmosphere. Theoretical curves derived on this assumption agree very well with the observed curves for all stars except the sun.

Another important result obtained by Wright,[5] namely, that the turbulent velocity is greater for ionized atoms than for neutral ones, can also be accounted for on the assumed variation of the turbulent velocity.[6] Also, C. W. Allen's result that the center-limb observations[7] of the solar lines require a variable turbulent velocity can be understood in terms of the assumed model.

It may be recalled in this connection that in Paper I we showed that the magnitude of the turbulent velocity derived from the curve of growth is uncertain if the exact distribution of turbulent velocities is unknown. But the velocities derived from the observed curves, by comparison with a definite set of theoretical curves, are approximately the same relative to one another, whether these theoretical curves are derived from a Gaussian distribution, from a δ-function distribution, or from any other distribution of turbulent velocities. This can be seen by comparing the two sets of curves derived in Paper I.

II. A DESCRIPTION OF THE METHOD

The equation of radiative transfer for an absorption line in a gas in which the mean atomic-line absorption coefficient is further complicated by the presence of turbulence cannot be easily solved, especially if the turbulent velocity varies with height. Fortunately for practical applications, a rigorous solution is not necessary, and an approximate method usually suffices to account for the observed results.

Consider a semi-infinite plane-parallel atmosphere. In a standard notation[8] the equation of transfer governing the formation of absorption lines can be written in the form

$$\mu \frac{dI(t, \mu)}{dt} = I(t, \mu) - J(t, \mu) , \tag{1}$$

where t is the total optical thickness at the point in the line considered and $J(t, \mu)$ is the source function. The formal solution of this equation is

$$I(0, \mu) = \int_0^\infty J(t, \mu)\, e^{-t/\mu} \frac{dt}{\mu} . \tag{2}$$

Now it is a well-known approximation that, for any slowly varying function $f(x)$,

$$\int_0^\infty e^{-x} f(x)\, dx \simeq f(1) .$$

In this approximation we can write equation (2) in the form

$$I_\nu(0, \mu) \simeq J(t_\nu = \mu, \mu) . \tag{3}$$

Now

$$t_\nu = \int_0^s (\sigma_\nu + l_\nu + r)\, ds = \tau_\nu + \int_0^{\tau_\nu} N(\tau)\, \kappa_\nu d\tau , \tag{4}$$

where σ_ν is the scattering coefficient, l_ν is the line-absorption coefficient, and r is the continuous absorption coefficient; further, in equation (4) τ_ν stands for the optical thickness in the neighboring continuum, and κ_ν stands for the atomic-line absorption coefficient as

[5] *J.R.A.S. Canada*, **40**, 183, 1946.

[6] A detailed discussion on this point will be given in a later paper.

[7] *M.N.*, **109**, 343, 1949.

[8] S. Chandrasekhar, *Radiative Transfer* (London: Oxford University Press, 1950); A. Unsöld, *Physik der Sternatmosphären* (Berlin: J. Springer, 1938).

usually used in the theory of stellar atmospheres, allowing for both scattering and pure absorption. Finally, $N(\tau)$ is the number of effective absorbing atoms contained in a column of unit cross-section and per unit optical depth τ in the continuum. Now N is a function of the temperature T; thus

$$N = N_0 \frac{g_i}{u} e^{-\chi_i/kT}, \tag{5}$$

where

$$T(\tau) = T_e(\tfrac{1}{2} + \tfrac{3}{4}\tau)^{1/4}. \tag{6}$$

We can define $\bar{N}$ as an average value for N, and write equation (4) approximately as

$$I_\nu = \tau_\nu + \bar{N}\bar{\kappa}_\nu \tau_\nu. \tag{7}$$

Returning to equation (3), we observe that the source function is a function of the geometrical depth s and hence of optical depth τ in the continuum. The relation

$$I_\nu = \mu \tag{8}$$

determines a value of τ_ν at which the source function is to be evaluated. Now, according to equations (7) and (8),

$$\tau_\nu = \frac{\mu}{1 + \bar{N}\bar{\kappa}_\nu}. \tag{9}$$

The emergent intensity $I_\nu(0, \mu)$ is therefore determined by the mean atomic-line absorption coefficient $\bar{\kappa}_\nu$ and the mean number of absorbing atoms $\bar{N}$ between the layers $\tau = 0$ and $\tau = \tau_\nu$. But equation (9) gives different values for τ_ν for different points within a line; thus τ_ν will have a minimum at the center of the line and will increase as we go out into the wings.

The real situation is somewhat more involved, since τ_ν is a function of ν and the mean atomic-line absorption coefficient $\bar{\kappa}_\nu$ for absorbing atoms between the layers $\tau = 0$ and $\tau = \tau_\nu$ is not unambiguously defined. But, consistent with the present scheme of approximation, we may choose a mean depth, say τ_0, which corresponds to a frequency ν' between the center and the wing of the line, and regard $\bar{\kappa}_\nu$ as the mean atomic-line absorption coefficient for all absorbing atoms between the layers $\tau = 0$ and $\tau = \tau_0$. For our purpose the frequency ν' may be defined by

$$\bar{\kappa}(\nu') = m\,\bar{\kappa}(\nu_0) = m\,\kappa_0, \tag{10}$$

where m is a constant less than unity and ν_0 is the frequency at the center of the line. Thus, if we consider the linear and the flat portions of the curve of growth which depends on the Doppler broadening, we may expect that $m \sim 0.5$. As we shall see later, our conclusions are not sensitive to the exact value of m. Since (cf. eqs. [9] and [10])

$$\tau_0(\bar{N}, \mu) = \frac{\mu}{1 + \bar{N}\bar{\kappa}(\nu')} = \frac{\mu}{1 + m\bar{N}\bar{\kappa}_0}, \tag{11}$$

we can express the result of the foregoing discussion by stating that the relevant mean value of κ_ν is given by

$$\kappa_\nu = \frac{\int_0^{\tau_0(\bar{N}, \mu)} \kappa_\nu N\, d\tau}{\int_0^{\tau_0(\bar{N}, \mu)} N\, d\tau}. \tag{12}$$

Here N enters as a weighting factor. By writing the integral in equation (12) in terms of τ, we have effectively allowed for the variation of density with depth. Now κ_ν is related to τ in a complicated way; it is a function of temperature T, of turbulent velocity v, of damping constant a, etc.; and T, v, a, etc., are functions of τ. Thus

$$\kappa_\nu = \kappa_\nu (T, v, a, \ldots),$$
$$T = T(\tau), \quad v = v(\tau), \quad a = a(\tau), \quad \text{etc.} \tag{13}$$

Also we have

$$N = N(T). \tag{14}$$

If T, v, a, . . . , are all monotonic functions of τ, we may suppose that, in some approximation,

$$\bar{\kappa}_\nu \simeq \kappa_\nu (\bar{T}, \bar{v}, \bar{a}, \ldots),$$
and
$$\bar{N} \simeq N(\bar{T}), \tag{15}$$

where $\bar{T}$, $\bar{v}$, $\bar{a}$, . . . , are defined as follows:

$$\bar{T}\int_0^{\tau_0} N\,d\tau = \int_0^{\tau_0} T(\tau)\,N\,d\tau,$$
$$\bar{v}^2\int_0^{\tau_0} N\,d\tau = \int_0^{\tau_0} v^2(\tau)\,N\,d\tau, \tag{16}$$
$$\bar{a}\int_0^{\tau_0} N\,d\tau = \int_0^{\tau_0} a(\tau)\,N\,d\tau, \text{ etc.}$$

Equations (15) reduce to identities when τ_0 approaches zero or when T, v, a, . . . , are all constant with depth. Formally, we have shown that $I_\nu(0, \mu)$ is determined by $\bar{N}\bar{\kappa}_\nu$; it follows from equations (15) that the observed line is determined completely by the mean temperature $\bar{T}$, the root-mean-square velocity $\bar{v}$, the mean damping constant $\bar{a}$, etc., between the layers $\tau = 0$ and $\tau = \tau_0$. In other words, the temperature, the velocity, etc., determined from observations of the equivalent widths of spectral lines will be given by equations (16). In the present paper we shall consider only the turbulent velocity. A consideration of the temperature and the damping constant will be given in a later paper.

For convenience, we shall let v denote the combined velocity of thermal and turbulent motions (this agrees with the definition Wright has used in his paper). As the thermal velocity varies only as the square root of the temperature, we can regard the thermal motion as practically constant throughout the layer considered and attribute all the variations to turbulence.

Quite generally, we may write

$$v = v(\tau, \mu). \tag{17}$$

If v is a function of τ only, then the turbulence is isotropic but nonhomogeneous; but, if v is a function of μ only, the turbulence is homogeneous but anisotropic. When model atmospheres for supergiant stars are computed, we can infer from equation (17) the relation between v and the geometrical depth.

We shall presently see that $\bar{v}^2$, as derived from an analysis of the emergent intensity $I_\nu(0, \mu)$, depends on the effective number of absorbing atoms $\bar{N}$; in other words, $\bar{v}^2 \equiv$

$\overline{v^2}(\mu, \overline{N})$. According to equations (16), this last quantity is given by

$$\overline{v^2}(\mu, \overline{N}) = \frac{\int_0^{\tau_0} v^2(\tau, \mu) N(\tau) d\tau}{\int_0^{\tau_0} N(\tau) d\tau}, \tag{18}$$

where the upper limit of integration τ_0 is defined by equation (11). Equation (18) will be true even if the velocities at a definite τ and μ are further distributed in a Gaussian form, provided that $v(\tau, \mu)$ is the most probable velocity of the distribution at each τ and μ. Equation (18) gives a relation between the position μ on the solar disk which we observe and the velocity derived from the observed spectrum, provided that we use the same group of spectral lines (i.e., the same $\overline{N}$ at all μ). Except for the sun, this relation cannot be directly used, because we observe only the emergent flux corresponding to the integrated light from the whole stellar disk. Hence in these latter cases the turbulent velocity observed in a stellar spectrum is a further average of equation (18) over the whole range of μ with a weighting factor which takes into account the different depths we see at different points on the disk. Thus in these cases the observed mean-square velocity $\overline{v^2}(\overline{N})$ is a function of $\overline{N}$ alone and is given by

$$\overline{v^2}(\overline{N}) = \frac{\int_0^1 \mu d\mu \int_0^{\tau_0} v^2(\tau, \mu) N(\tau) d\tau}{\int_0^1 \mu d\mu \int_0^{\tau_0} N(\tau) d\tau}. \tag{19}$$

Equation (19) is a general relation between the velocity derived from the curve of growth plotted for a group of spectral lines and the average number of the absorbing atoms which produce this group of lines. If, following Wright, we limit ourselves to absorption lines formed by a definite species of atoms at a definite stage of ionization (in Wright's case, *Fe* I), equation (19) becomes a relation between v and χ; thus

$$\overline{v^2}(\chi) = \frac{\int_0^1 \mu d\mu \int_0^{\tau_0} v^2(\tau, \mu) e^{-\chi/kT} d\tau}{\int_0^1 \mu d\mu \int_0^{\tau_0} e^{-\chi/kT} d\tau}. \tag{20}$$

It is, of course, evident that the notations $v(\tau, \mu)$, $\overline{v^2}(\mu, \overline{N})$, $\overline{v^2}(\overline{N})$, and $\overline{v^2}(\chi)$ have different physical meanings.

III. COMPARISON WITH OBSERVED RESULTS FOR STARS

Equation (19) or equation (20) is an integral equation for $v(\tau, \mu)$ when the empirical relation $\overline{v^2}(\overline{N})$ or $\overline{v^2}(\chi)$ is given. But this equation is not a simple one, and it cannot easily be inverted. Moreover, the accuracy of empirical results does not justify such an inversion process. The best way is therefore to assume some plausible form for $v(\tau, \mu)$ and then to determine that function which best fits the observed results. When this was done, it was found that neither anisotropy nor a linear decrease with depth of turbulent velocities can account for the velocity–excitation potential relation (or, briefly, the v-χ relation) observed by Wright. It appeared that the turbulent velocity must decrease exponentially as we descend into the reversing layer. Let us assume, then, that

$$v(\tau, \mu) = v_0 e^{-a\tau}, \tag{21}$$

where the parameters v_0 and a are to be determined from a comparison with the observed data.

As $N(\tau)$ is a slowly varying function of τ compared with $e^{-\alpha\tau}$, we shall take the former term outside the integration sign with respect to τ and replace it by its value at $\tau = \tau_0/2$. Equation (19) then simplifies to

$$\overline{v^2}(\overline{N}) = \frac{v_0^2 \int_0^1 \mu\, d\mu\, N(\tfrac{1}{2}\tau_0)\, \tau_0 Y(2\alpha\tau_0)}{\int_0^1 \mu\, d\mu\, N(\tfrac{1}{2}\tau_0)\, \tau_0}, \tag{22}$$

where

$$Y(x) = \frac{1 - e^{-x}}{x}.$$

The stars we shall consider are mostly F supergiants; we shall therefore take $T_e = 6500°$ K.[9] However, the final results will not change appreciably if we take any value for T_e in the range 6000°–7000° K. Expressing χ in electron-volts, we have, from equations (5) and (6),

$$N(\tau) = N_0 \frac{g_i}{u} \exp\left[-1.8\,(\tfrac{1}{2} + \tfrac{3}{4}\tau)^{-1/4}\chi\right]. \tag{23}$$

The value of the atomic-line absorption coefficient κ_0 at the center of the line is

$$\kappa_0 = \frac{\pi^{1/2}e^2}{mc} f \frac{\lambda}{v} = 1.489 \times 10^{-12} f, \tag{24}$$

if we take an average value for λ/v of 10^{-10} seconds. With regard to $\overline{N}$, we may take the average of $N(\tau)$ over τ as given by equation (23). However, it will be more convenient to take $\overline{N}$ to be the value of $N(\tau)$ at a definite depth, say, $\tau = \tau'$, in all our calculations, because it is only in the relative numbers of absorbing atoms for different values of χ that we are interested. It follows from equations (11), (23), and (24) that

$$\tau_0 = \mu\left[1 + 1.5 \times 10^{-12}\left(\frac{g_i}{u} N_0 m f\right) e^{-\chi/kT(\tau')}\right]^{-1}. \tag{25}$$

In our later calculations we shall simply set $\tau' = 0$.

Although $g_i f$ differs for different lines even for the same species of atoms, the determination of velocity by the curve-of-growth method averages out all the difference with respect to individual lines. Hence it is possible for us to take an average value of this quantity for all lines. Moreover, Wright's determinations of the abundance[10] of *Fe* I in the stars he observed do not differ very widely, so we may take $(g_i/u)N_0 mf$ as a constant in the calculations of the velocity determined by *Fe* I lines in all the stars we shall consider. In agreement with the actual determination of N_0, we shall set

$$\frac{g_i}{u} N_0 m f = 2 \times 10^{14}. \tag{26}$$

With the aid of equations (25) and (26), equation (22) was numerically integrated, and the two parameters v_0 and α were determined from the best fit with Wright's observations. The results of this analysis are summarized in Table 1.

Both the computed curve and the observed points are plotted in Figure 1. In some cases Wright gives two sets of values which are the result of comparison of the same observational material with two different theoretical curves of growth based, respec-

[9] G. P. Kuiper, *Ap. J.*, **88**, 429, 1938.

[10] *Pub. Dom. Ap. Obs. Victoria*, Vol. 8, No. 1, 1948.

tively, on the Schuster-Schwarzschild model and the Milne-Eddington model. In Figure 1 Wright's results for the Schuster-Schwarzschild model are plotted. The results derived from the Milne-Eddington model will not appreciably change the derived values of v_0 and a. We see from Figure 1 that the computed curves fit the observed data very well for all the stars considered. For supergiant stars the agreement is especially good. As the theory is only approximate and the observed results are subject to uncertainties,[4] the values of v_0 and a thus determined cannot be taken too seriously. For example, one set of observed results for a Persei gave $v_0 = 6.4$ km/sec and $a = 2.0$ (curve *a*), while another set gave $v_0 = 7.0$ km/sec and $a = 2.7$ (curve *e*). But the present calculation establishes one point quite definitely, i.e., Wright's anomalous curve of growth is a natural consequence if the turbulent velocity is dominant in the higher levels of the reversing layer. Another interesting point is that a has values of the same order of magnitude for all stars studied, except for the peculiar star ϵ Aurigae.[11] One observational point for ϵ Aurigae is too far

TABLE 1

DETERMINED VALUES OF v_0 AND a

Star	Sp. Classification in MKK System*	Reference for Observed Results in *J.R.A.S. Canada*†	v_0 (Km/Sec)	a	Plotted Curve in Fig. 1
a Persei	F5 I*b*	41, 49, Table 1	6.4	2.0	*a*
γ Cygni	F8 I*b*	41, 49, Table 2	7.5	2.3	*b*
a Canis Minoris	F5 IV	41, 49, Table 2	3.5	2.3	*c*
a Carinae	F0 I*b*–II	41, 49, Table 3	3.6	2.0	*d*
δ Canis Majoris	F8 I*a*	41, 49, Table 3	8.5	2.7	*f*
ϵ Aurigae	F2p I*a*	43, 15, Table 1	19.5	50	*g*
a Persei	F5 I*b*	43, 15, Table 1	7.0	2.7	*e*

* W. W. Morgan, P. C. Keenan, and E. Kellman, *An Atlas of Stellar Spectra* (Chicago: University of Chicago Press, 1943); W. W. Morgan and N. G. Roman, *Ap. J.*, **112**, 362, 1950. The spectral class of a Carinae listed here has been recently determined on the basis of the present system by Dr. W. P. Bidelman, and the present author is indebted to him for his kindness.

† By Wright and Wright and van Dien.

away from a smooth curve which joins the other observed points. This irregularity has been discussed by Wright from the point of view of the observational method, and we may refer the reader to his paper.

IV. COMPARISON WITH OBSERVED RESULTS FOR THE SUN

The results obtained by Wright and by King, and Wright[3] for the sun have considerable observational scatter on account of the small turbulent velocity. The results of these authors are plotted in Figure 2, in which the solid dots denote the results from analysis of *Fe* I lines and the crosses those derived from *V* I lines. Three sets of values of turbulent velocities for *V* I lines determined from three different theoretical curves of growth are given in King and Wright's paper. We have plotted the values derived from D. H. Menzel's theoretical curves.[12] The computed curve for *Fe* I is shown as a full-line curve and that for *V* I is shown as a dotted line. Both are plotted for $v_0 = 2.5$ km/sec and $a = 2$. The difference between these two curves is due to the difference between the abundances of the two elements in the solar atmosphere. Also in computing the *V* I curve we have adopted a value for $(g_i/u)N_0 f$ equal to one one-hundredth of the corresponding value for *Fe* I. The agreement is not very good, but it is well within the inaccuracy inherent in the curve-of-growth method.

[11] G. P. Kuiper, O. Struve, and B. Strömgren, *Ap. J.*, **86**, 570, 1937.

[12] *Ap. J.*, **84**, 462, 1936; *Pop. Astr.*, **47**, 66, 1939.

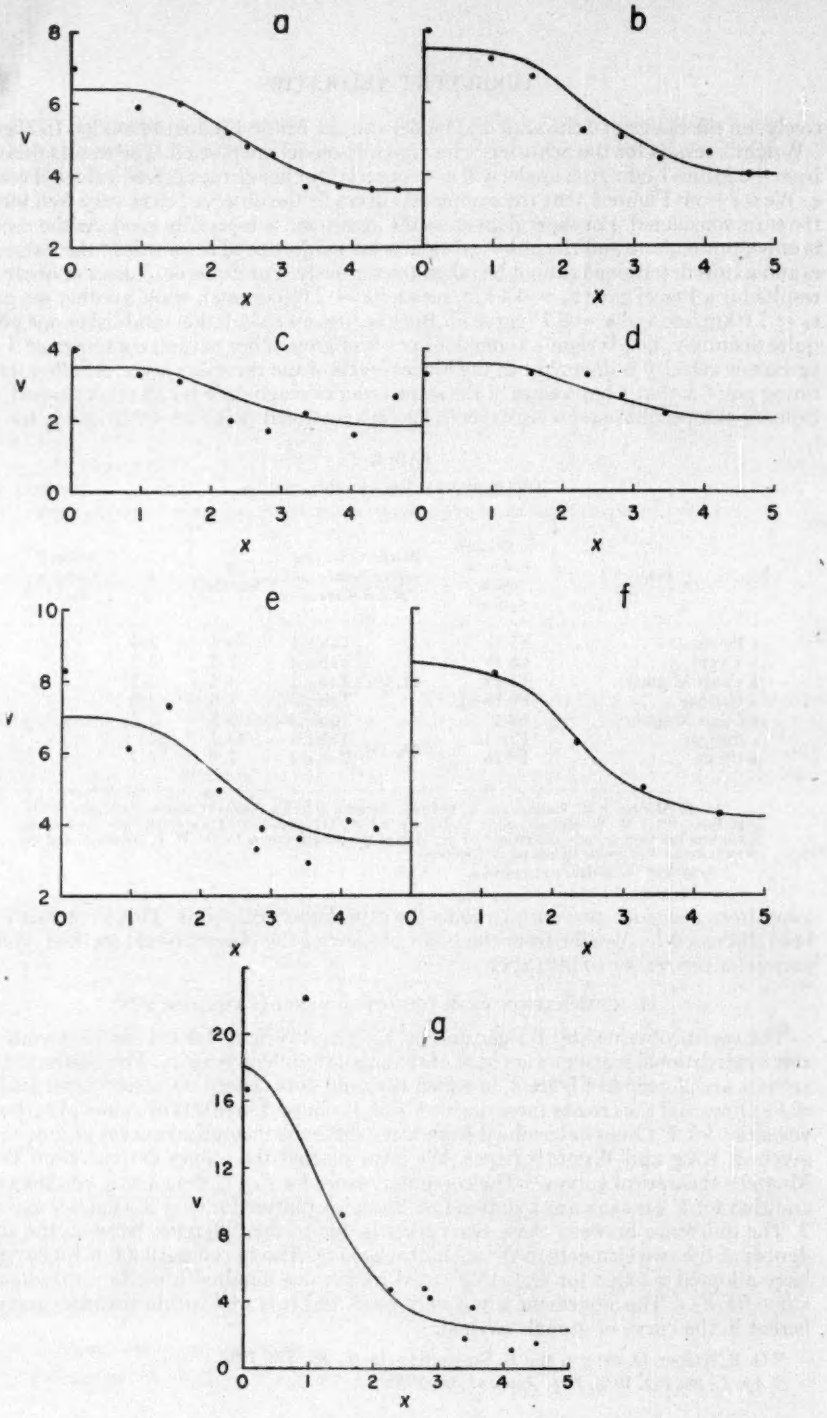

FIG. 1.—The relation between turbulent velocities and excitation potentials as found in *Fe* I lines in certain stars. The curves calculated according to equation (22) are compared with the observed points obtained by K. O. Wright for various stars listed in the following (cf. Table 1): curves *a*, α Persei; *b*, γ Cygni; *c*, α Canis Minonis; *d*, α Carinae; *e*, α Persei; *f*, δ Canis Majoris; *g*, ϵ Aurigae. The velocity is plotted in units of kilometers per second and the excitation potential is in units of electron-volts.

Next we shall consider the center-limb variation of turbulent velocity. From equation (18) it follows that the velocity-direction, (v-μ) relation depends further on the parameter $\bar{N}$ or, if we consider a single species of atoms at a definite stage of ionization, the parameter χ. Hence we shall have a family of curves in the v-μ plane instead of a single curve. We have illustrated these curves in Figure 3, which is plotted for the *Fe* I lines, with $a = 2$. If we now plot the observed points derived from all kinds of lines (including all points on the linear and the flat parts of the curve of growth, but not points on the damping branch) in the same v-μ plane, the points should be scattered in an area bounded by curves *1–7* in Figure 3, instead of lying on a single curve. But if the turbulent velocity does not depend on depth but is anisotropic, then the v-μ relation will be independent of $\bar{N}$ or χ. From a glance at Allen's results[7] it would seem to us that the points are scattered in an area (see Fig. 1 of Allen's paper). His observed points have been reproduced in Figure 3. As he used weak lines, the observed points should be located between curves *4* and *7*, as they are in Figure 3. This supports our assumption regarding the variation of the turbulent velocity with depth. It should be noticed that Allen's graph includes only a

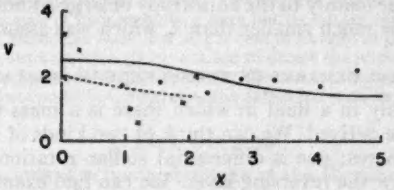

FIG. 2.—The relation between turbulent velocities and excitation potentials as found in the solar atmosphere. The solid curve is calculated for *Fe* I lines and the dotted curve for *V* I lines. The solid dots denote the observed results of *Fe* I lines, while the crosses are the observed points of *V* I lines. The same units have been used here as in Fig. 1.

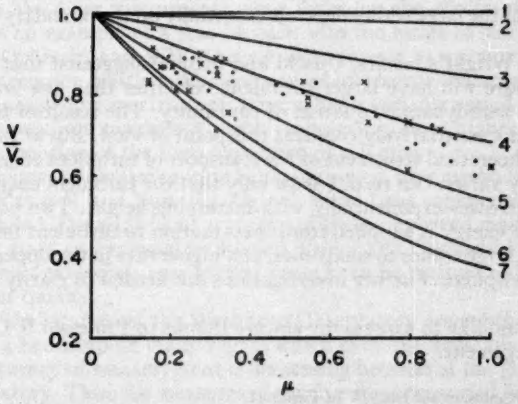

FIG. 3.—The center-limb variation of turbulent velocities. The curves *1–7* between v/v_0 and μ are calculated for *Fe* I lines according to equations (18) and (21) in the following manner: curves *1*, $\chi = 0$; *2*, 1 ev.; *3*, 2 ev.; *4*, 2.5 ev.; *5*, 3 ev.; *6*, 4 ev.; *7*, 5 ev. They illustrate a general feature that, as the abundance of effective absorbing atoms decreases, the (v-μ) relation changes in a sequence from curve *1* to curve *7*. C. W. Allen's results from an analysis of line width have been plotted here for comparison. (Dots and crosses represent results obtained from blue and violet lines, respectively.) All analyzed lines are weak; hence we expect them to scatter in an area between curves *4* and *7* in the figure.

few observations near the center of the disk and no strong lines. Our theory predicts that for strong lines (but still not strong enough to be on the damping part of the curve of growth) the turbulent velocity derived at the center and that at the limb should be comparable. One point we should like to emphasize is that Allen's results for the turbulent velocity derived from line widths depends on effects caused by the large as well as by the small eddies, while our estimate of $v_0 = 2.5$ km/sec based on Wright's results is valid only for the small eddies.[13] The value of v_0 suggested by Allen's determination is 3.6 km/sec. A direct comparison is therefore impossible. An approximate procedure is to compare the ratio v/v_0 of our results with his observations. This we have done in Figure 3.

Allen's v-μ relation can be the result of two effects: i.e., the anisotropy of the large eddies and the variation of small eddies with depth. In the method of comparison adopted, the assumption is implicit that the center-limb variation of velocities of the small eddies will follow the same pattern as that found by Allen. This is not necessarily true, and it can be verified only when the curve-of-growth method is used in the investigation of center-limb variations of velocities. If, on the contrary, the curve-of-growth method shows only slight variation of turbulent velocities from center to limb, Allen's results would then be due mainly to the anisotropy of large eddies, and a in equation (21) for small eddies must be much smaller than 2, which was assumed in the calculations.

V. SOME GENERAL REMARKS ON TURBULENCE IN STELLAR ATMOSPHERES

Turbulence exists only in a fluid in which there is a mass motion from which the turbulent energy can be derived. We can think of two kinds of such mass motions that exist in stellar atmospheres: one is differential stellar rotation, and the other is the convective motion below the reversing layer. We can find examples of both types on a smaller scale in the earth's atmosphere. Hence, if we do not consider radiation pressure, which may be responsible for turbulence in the chromosphere,[14] the properties of turbulence in stellar atmospheres can be suggested by our knowledge of turbulence in the earth's atmosphere. In the earth's atmosphere, a few meters above the ground the fluctuation of turbulent velocities of small eddies is the same in all directions,[15] and we may expect that the same thing is true in stellar atmospheres. But, as has been pointed out previously,[1] the distribution of the large eddies depends essentially on the boundary conditions, which are anisotropic.

In explaining Wright's results, Unsöld and Struve[2] suggested that the higher layers with lower pressure will have larger turbulent velocities than the lower, dense layers, according to the aerodynamic equation of continuity. The result of the calculations of the present paper quantitatively confirms this point of view. But at present there exists no satisfactory theoretical treatment of the transport of turbulent energy in a medium in which the density varies. Our results show only that the turbulent energy of small eddies per unit mass increases exponentially with increasing height. Two possibilities may be suggested: either energy is supplied from mass motion to turbulent motion, or energy is transferred from large eddies to small ones, at a higher rate in the upper atmosphere than in the lower atmosphere. Further investigations are needed to clarify this point.

Finally, I should like to express my sincere thanks to Professor S. Chandrasekhar for his kind encouragement.

[13] For detailed discussion see Sec. IV of Paper II.

[14] L. Goldberg, *Ap. J.*, **89**, 623, 1939.

[15] E.g., O. Sutton, *Atmospheric Turbulence* (London: Methuen, 1949).

PHOTOELECTRIC STUDIES OF FIVE ECLIPSING BINARIES

C. M. HUFFER AND ZDENĚK KOPAL
Washburn Observatory and Massachusetts Institute of Technology
Received June 18, 1951

ABSTRACT

Light-curves of the five eclipsing binaries VV Orionis, RZ Cassiopeiae, U Ophiuchi, WW Aurigae, and TV Cassiopeiae have been completed at the Washburn Observatory. These photoelectric measures were made mostly during 1948 and 1949, with the 1P21 photomultiplier, which has an effective wave length of 4600 A. The computations were made at the Massachusetts Institute of Technology. Kopal's method was used, the numerical computations being performed with electric desk calculators.

The stars U Ophiuchi and WW Aurigae are double-line binaries in which Petrie's line-intensity ratios aid in giving definite solutions from partial eclipses. The brighter star is the larger in each case. TV Cassiopeiae is less certain because of poor secondary lines but its fainter component appears also to be the smaller of the two. RZ Cassiopeiae loses over 80 per cent of its light at primary minimum, when the fainter, larger star is in front; but a search by Struve failed to detect the secondary spectrum. VV Orionis is a case of total and annular eclipses of a single-line binary. Because of the shallow eclipses and the uncertainty of the measures, it was not possible to determine the darkening coefficients from the investigations.

I. INTRODUCTION

Photoelectric observations of eclipsing binaries at the Washburn Observatory, which had been discontinued during the war years, have been resumed, with some changes of technique. The major changes include the introduction of the 1P21 photomultiplier and automatic recording. The former increases the sensitivity of the photometer, and the latter makes possible the reading of an objective, impersonal record at later convenience.

The five stars whose light-curves are discussed in the present report were selected for various reasons. Increased sensitivity permitted observing stars about 2 mag. fainter than was possible with the older instruments, thus widening the choice of eclipsing stars. TV Cassiopeiae is an example of a star brought into the range of sufficiently accurate measurement. U Ophiuchi and WW Aurigae were chosen as examples of double-line spectroscopic binaries for which light-curves of photoelectric accuracy did not exist. RZ Cassiopeiae, a single-line spectroscopic binary, has a variable period which still needs discussion. VV Orionis was considered worth reobserving, since higher precision might give improved information of the limb darkening of a B star.

While the techniques of observing were being improved, new methods of computation were being devised as well, and Russell's original method was superseded by those based on Tsesevich's tables.[1] The additional accuracy of these improved methods of deriving information about stars, as discussed by Russell, Kopal, and Piotrowski in articles in the *Astrophysical Journal* extending over several years,[2] can be realized only from observations of the highest quality.

Unfortunately, the location of the Washburn Observatory among the city lights and smoke introduces a handicap on many nights which even the finest photometer cannot overcome. The accuracy of measurement is decreasing because of the growth of the city west of the observatory. Thus the measures of the five stars presented here are not quite equal in precision to the best obtained photoelectrically at observatories with more transparent skies and a larger number of clear nights per year. But the final results, obtained by photoelectric measures made on the best nights and computed by the modern

[1] *Bull. Astr. Inst. U.S.S.R. Acad. Sci.*, Vols. 45 and 50, 1939–1940.

[2] E.g., Z. Kopal, *Ap. J.*, 94, 145, 1941, and subsequent publications.

methods now available, probably represent the best that has been done with the data from the Madison telescope.

II. OBSERVATIONAL TECHNIQUE

Shortly after the change to the 1P21 multiplier, another improvement was instituted in the form of automatic recording on an Esterline-Angus meter. The amplifier between the multiplier and the meter was originally of the type described by Kron.[3] On November 17, 1949, this was changed to the so-called "MIT" amplifier.[4] Both amplifiers incorporate a large amount of negative feedback and are thus accurately linear and have a gain dependent almost entirely on resistance ratios. The latter amplifier is the only one in which linearity was actually tested, with no departures exceeding the experimental error. Since its gain-stability was considered adequate, steps on a wire-wound attenuator were substituted for the traditional shade glasses used in equalizing variable and comparison star.

The automatic recording not only eliminates the need of an assistant in the dome, but the recordings reveal short-period fluctuations, which immediately show trouble with thin clouds or smoke invisible to the human eye and consequently improve the accuracy of the observations.

After some experimentation, a standard policy of 1-minute exposures on the comparison star and 6 minutes on the variable was adopted. This saved time in moving the telescope and added materially to the number of points on the light-curves. In the case of rapid variations during the primary eclipses, the chart could be read at 1-minute or shorter intervals. The change of intensity of the comparison star, due to change of altitude or change of sensitivity of the photometer with temperature, could be assumed linear over reasonably short intervals and interpolated for the time of observation of the variable star. The long exposures also practically eliminated the pen-drag error in the meter. Tests showed that it could not exceed 0.1 division on the chart.

All observations were made with no color filter, through a diaphragm of such size that the out-of-focus violet image of the refracting telescope had sufficient clearance. The smallest diaphragm was 2.5 mm or 1.4 minutes of arc in diameter.

Differential extinction corrections were applied according to the standard procedures in use for many years at the Washburn Observatory.[5] Seasonal adjustments due to possible changes in the color response of the photocathode proved unnecessary except in the cases of U Ophiuchi and RZ Cassiopeiae. Here the major corrections were due to the change from shade glasses to step ratios. The change from Kunz cells to the 1P21 multiplier required adjustments amounting to about 0.02 mag. in the case of the two stars.

III. OBSERVATIONAL DATA

The variables with their comparison stars are listed in Table 1, the data being taken from the Albany catalogue[6] except for TV Cassiopeiae, data for which are from the *Henry Draper Catalogue*,[7] corrected to 1950.

A single comparison star was used in three cases in which it had been previously tested and found to be constant. For VV Orionis and TV Cassiopeiae two comparison stars were used, since it had not been established that one was invariable. As soon as the constancy

[3] *Electronics*, August, 1948, p. 103.

[4] G. E. Valley and H. Wallman, *Vacuum Tube Amplifiers* ("Radiation Laboratory Series," Vol. 18 [New York: McGraw-Hill Book Co., Inc., 1948]), p. 480.

[5] Stebbins and Huffer, *Pub. Washburn Obs.*, 15, 16, 1928.

[6] Benjamin Boss, *General Catalogue of 33,342 Stars for the Epoch 1950* (Washington: Carnegie Institution of Washington, 1937).

[7] *Harvard Ann.*, Vols. 91–99, 1918.

of both had been demonstrated by repeated intercomparisons, all observations against either *a* or *b* could have been used. However, for these two cases the entries in Table 12 are referred to the mean of the two comparisons; that is, the tabular Δ mag. is the mean of the differences of magnitude (var. − *a*) and (var. − *b*).

VV ORIONIS

The variability of VV Orionis was first pointed out by Miller Barr in 1903, but the period and nature of the variation were not given.[8] It was later found from the investigations of Hertzsprung and Adams and still later by Daniel that the period is about 1.4854 days. Hertzsprung in 1914 recognized that the primary is annular and the secondary total.[9]

Photoelectric observations were made by F. Bradshaw Wood at Tucson, and a solution was included in his thesis.[10] He called attention to the large scatter of the measures

TABLE 1

CATALOGUE DATA

Star	R.A. 1950	Decl. 1950	Mag.	Spec.	BD
VV Orionis.....	5^h31^m0	− 1° 11′	5.3–5.7	B2	− 1°943
a) HD 36591...	30.2	− 1 38	5.30	B2	− 1 935
b) HD 36779...	31.5	− 1 04	6.18	B3	− 1 949
RZ Cassiopeiae...	2 44.4	+69 26	6.3–7.8	A0	+69 179
a) HD 16769...	40.5	+67 37	5.84	A2	+67 224
WW Aurigae.....	6 29.2	+32 30	5.6–6.2	A0	+32 1324
a) HD 46251...	30.4	+33 04	6.38	A0	+33 1356
U Ophiuchi.....	17 14.0	+ 1 16	5.7–6.4	B8	+ 1 3408
a) HD 156208..	13.7	+ 2 14	6.02	A0	+ 2 3283
TV Cassiopeiae...	0 16.6	+58 51	7.4–9.0	B9	+58 30
a) HD 1264....	14.4	+56 38	7.32	A0	+56 31
b) HD 1334....	15.2	+58 47	7.8	B5	+58 24

and hinted that further observations were desirable. The star was therefore reobserved at Madison from 1946 to 1950. Since it is near the celestial equator, observations are limited to a maximum of 6 hours per night and in the direction of the city. During the winter, smoke interferes unless the wind is from the north. The result has been that the observations are less accurate than desired and the secondary minimum is insufficiently observed. We have, therefore, included Wood's observations with ours and have based the solution on the combined observations, thus improving the distribution of the normal points on the curve. The amplitude of the variation being equal in the two sets of observations, the curves have been adjusted to maximum, and Wood's observations were reduced to the Madison observations by subtracting 0.750 mag. from Wood's published magnitudes. The same comparison stars were used by both observers.

Since Wood used a Kunz cell and the Madison observations were made with the 1P21 multiplier, the observations of both observers were plotted and carefully examined. The average deviation of the Madison observations from the normals between minima is ±0.006 mag. from 54 observations; the average deviation of the Tucson observations is ±0.014 mag. from 14 observations. The individual observations are plotted on the light-

[8] Müller and Hartwig, *Geschichte und Literatur des Lichtwechsels*, 1, 149 (Leipzig, 1918).

[9] *A.N.*, 198, 15, 1914.

[10] *Contr. Princeton U. Obs.*, Vol. 21, 1946.

curve (Fig. 1) and are tabulated along with those of the other four stars in Table 12 at the end of the paper.

The period used was 1.4853789 days, as given by Wood. Since the partial phases, before and after minimum, could not be observed on any single night, no attempt was made to determine the times of minimum from the Madison observations. From the light-curve no serious departures from Wood's phases could be detected.

RZ CASSIOPEIAE

The well-known eclipsing binary RZ Cassiopeiae was discovered by Müller in 1906. The first orbit was published by R. S. Dugan[11] in 1916, using observations made visually

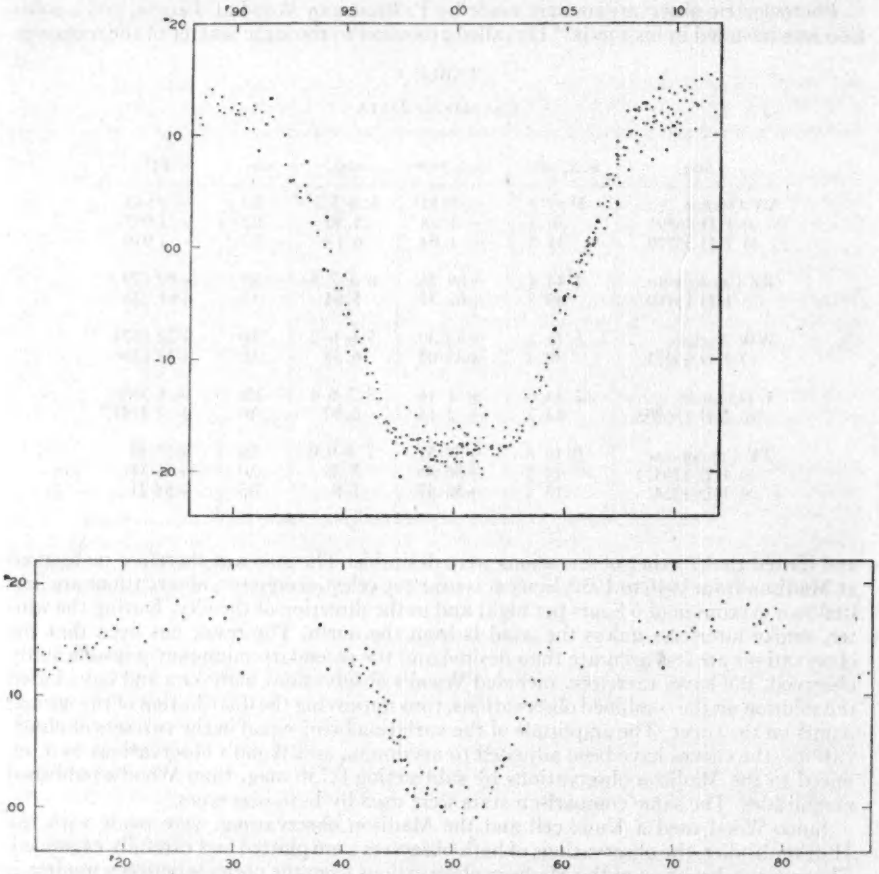

FIG. 1.—Photoelectric measures of VV Orionis. Filled circles are Washburn Observatory observations; open circles, Wood's observations. Upper drawing is primary eclipse; lower drawing, remainder of light-curve. Vertical scales are the same; the upper horizontal scale is double the lower horizontal scale. Both are expressed in decimals of the period.

[11] *Pub. Princeton U. Obs.*, **4**, 24, 1916; *M.N.*, **76**, 729, 1916.

by himself. He also reported the variation of the period, which was confirmed and investigated by A. de Sitter.[12] This variation, also discussed later by S. Gaposchkin and L. E. Erro,[13] was reviewed by Huffer at the New Haven meeting of the American Astronomical Society in 1948.[14] The times of minima observed photoelectrically are not represented by de Sitter's formula, nor can any formula be found which represents all the published minima. An approximate formula,

$$\text{Time of primary minimum} = \text{JD } 2432862.6197 + 1^d.19525189E + 0^d.0041 \sin\left[(E - 195) \cdot \frac{360^\circ}{3230}\right],$$

represents the Washburn Observatory minima fairly well, but the minima published by de Sitter and Gaposchkin very badly. The observed photoelectric minima are given in

TABLE 2

OBSERVED MINIMA OF RZ CASSIOPEIAE

Helioc. JD	E	Phase (P)	O−C (Day)
2429875.6902	10475	+0.0042	+0.0005
2430028.6812	10603	+ .0031	− .0009
0322.7125	10849	+ .0026	− .0013
2085.7011	12324	− .0040	.0000
2115.5827	12349	− .0038	+ .0002
2152.6358	12380	− .0035	+ .0005
2452.6460	12631	− .0019	+ .0012
2820.7853	12939	− .0005	+ .0009
2862.6189	12974	− .0007	+ .0005
3157.8472	13221	+ .0002	− .0006
3169.8005	13231	+ .0009	.0000
3242.7101	13292	+0.0002	−0.0012

Table 2, with O − C computed from the above formula. The epoch E is numbered as in Dugan's and de Sitter's papers.

Phases used in this paper are computed from the nearest minimum listed above, the variation being neglected inside the short intervals. If accurate times of minima between 1933 and 1940 were available, it should prove possible to obtain a more accurate representation of the variation of the period. Figure 2 shows the individual observations.

WW AURIGAE

The variability of WW Aurigae was discovered by Solowiew in 1916 and independently by Schwab in 1918. Various observers[15] have published light-curves and elements, but apparently none was obtained by photoelectric methods. Observations made at the Washburn Observatory extending through the years 1947–1950 are plotted in Figure 3. Table 3 gives the times of observed minima, the dates given as heliocentric Julian days, and the minima computed from the period 2.52501906 days.

[12] *B.A.N.*, **7**, 119, 1933.

[13] *Harvard Bull.*, No. 912, p. 12, 1940.

[14] C. M. Huffer, *A.J.*, **54**, 129, 1949.

[15] R. Prager, *Geschichte und Literatur des Lichtwechsels der veränderlichen Sterne*, Vol. 1, *Veröff. U.-Sternw. Berlin-Babelsberg*, p. 112, 1934.

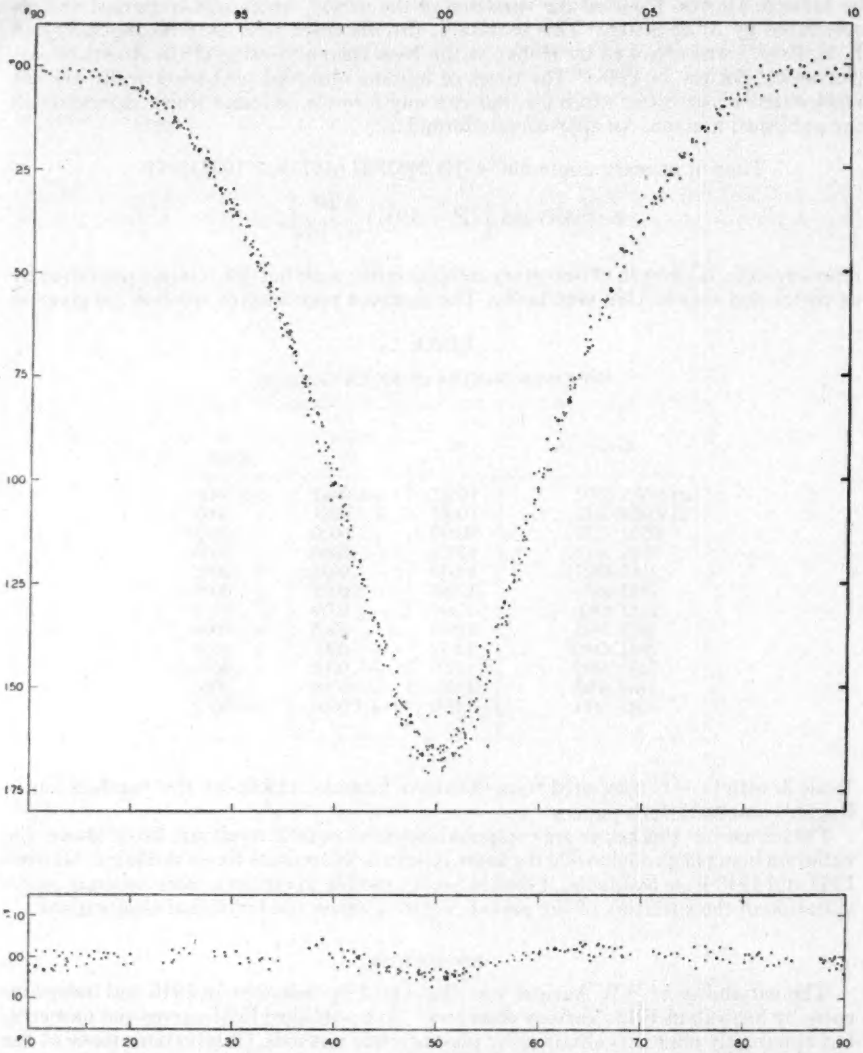

FIG. 2.—Photoelectric measures of RZ Cassiopeiae made at the Washburn Observatory. Upper drawing is primary eclipse; lower drawing remainder of light-curve. The vertical scales are the same; the horizontal scale in the upper drawing is four times the scale of the lower drawing. The secondary eclipse can be seen approximately centered at phase 0P50. The horizontal scale is given in decimals of the period.

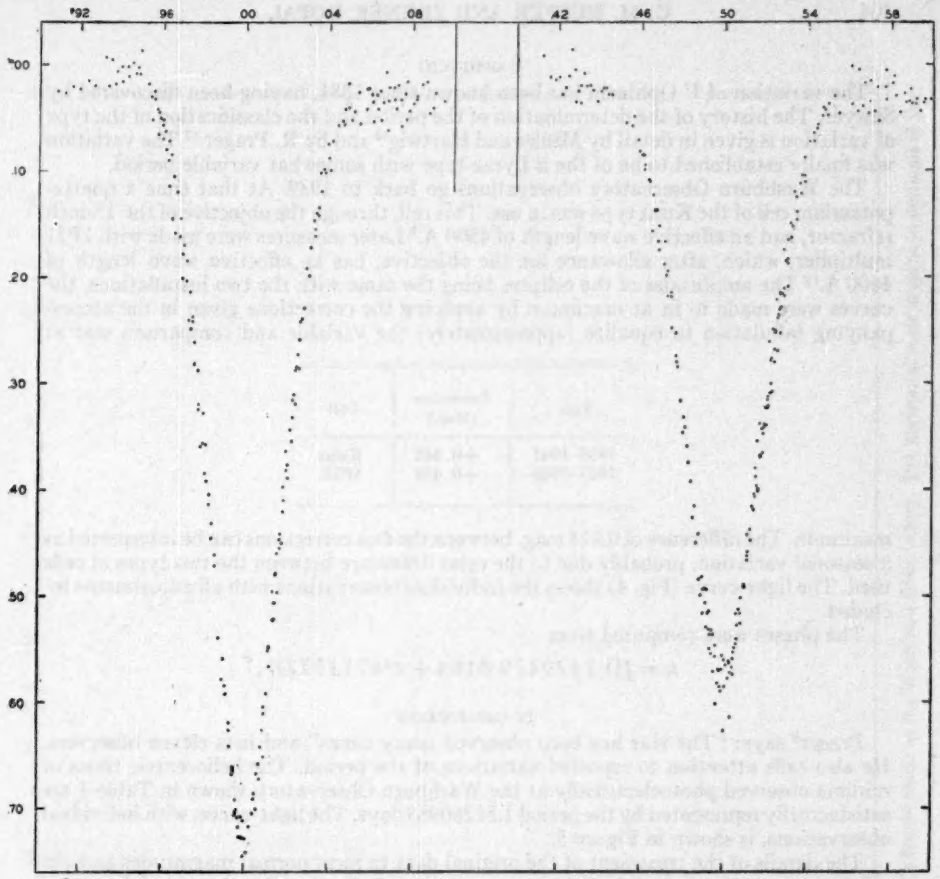

FIG. 3.—Photoelectric measures of WW Aurigae made at the Washburn Observatory. Primary and secondary eclipses only are shown. The horizontal scale is given in decimals of the period.

TABLE 3

OBSERVED MINIMA OF WW AURIGAE

Min.	Heliocentric Date 2430000+	Computed Min. 2430000+	O−C (Day)
II.....	2888.7263	2888.7255	+0.0008
II.....	2936.6998	2936.7009	− .0011
I.....	3225.8159	3225.8156	+ .0003
II.....	3249.8035	3249.8033	+ .0002
I.....	3263.6905	3263.6909	− .0004
II.....	3292.7299	3292.7286	+ .0013
II.....	3297.7776	3297.7786	−0.0010

U OPHIUCHI

The variation of U Ophiuchi has been known since 1881, having been discovered by Sawyer. The history of the determination of the period and the classification of the type of variation is given in detail by Müller and Hartwig[16] and by R. Prager.[17] The variation was finally established to be of the β Lyrae type with somewhat variable period.

The Washburn Observatory observations go back to 1939. At that time a quartz-potassium cell of the Kunz type was in use. This cell, through the objective of the 15-inch refractor, had an effective wave length of 4500 A.[5] Later measures were made with 1P21 multiplier, which, after allowance for the objective, has an effective wave length of 4600 A.[18] The amplitudes of the eclipses being the same with the two installations, the curves were made to fit at maximum by applying the corrections given in the accompanying tabulation to equalize (approximately) the variable and comparison star at

Year	Correction (Mag.)	Cell
1939–1941	+0.440	Kunz
1947–1948	+0.458	1P21

maximum. The difference of 0.018 mag. between the two corrections can be interpreted as a seasonal variation, probably due to the color difference between the two types of cells used. The light-curve (Fig. 4) shows the individual observations with all adjustments included.

The phases were computed from

$$t_0 = \text{JD } 2429479.6164 + 1^d.6773522E\,.$$

TV CASSIOPEIAE

Prager[9] says: "The star has been observed many times" and lists eleven observers. He also calls attention to reported variations of the period. The heliocentric times of minima observed photoelectrically at the Washburn Observatory shown in Table 4 are satisfactorily represented by the period 1.81260983 days. The light-curve, with individual observations, is shown in Figure 5.

The details of the treatment of the original data to form normal magnitudes and the subsequent rectification of the light-curves are given in Section V at the end of the paper.

IV. DETERMINATION OF THE ELEMENTS

The elements of the photometric orbits of the five stars were derived at the Computation Laboratory of the Massachusetts Institute of Technology in February and March, 1950. The methods used are those described in chapters iii–iv of the *Manual of Computation of the Elements of Eclipsing Binary Systems*[19] by one of us, and the notations are consistent with the *Manual*. For each of the five stars under discussion, the secondary minima are found to be located exactly halfway between the primary minima, and no significant difference in durations of the alternate minima has been detected. In the obvious absence of any photometric or spectroscopic evidence of orbital eccentricity, circular orbits have been adopted for all five stars. In what follows, the particular properties and features presented by each system are briefly commented upon.

[16] *Geschichte und Literatur des Lichtwechsels*, 2, 86 (Leipzig, 1920).

[17] *Geschichte und Literatur des Lichtwechsels der veränderlichen Sterne*, Vol. 2, *Veröff. U.-Sternw. Berlin-Babelsberg*, p. 283, 1936.

[18] Stebbins and Whitford, *Ap. J.*, 108, 419, 1948.

[19] Cambridge, Mass.: Harvard College Observatory, 1950.

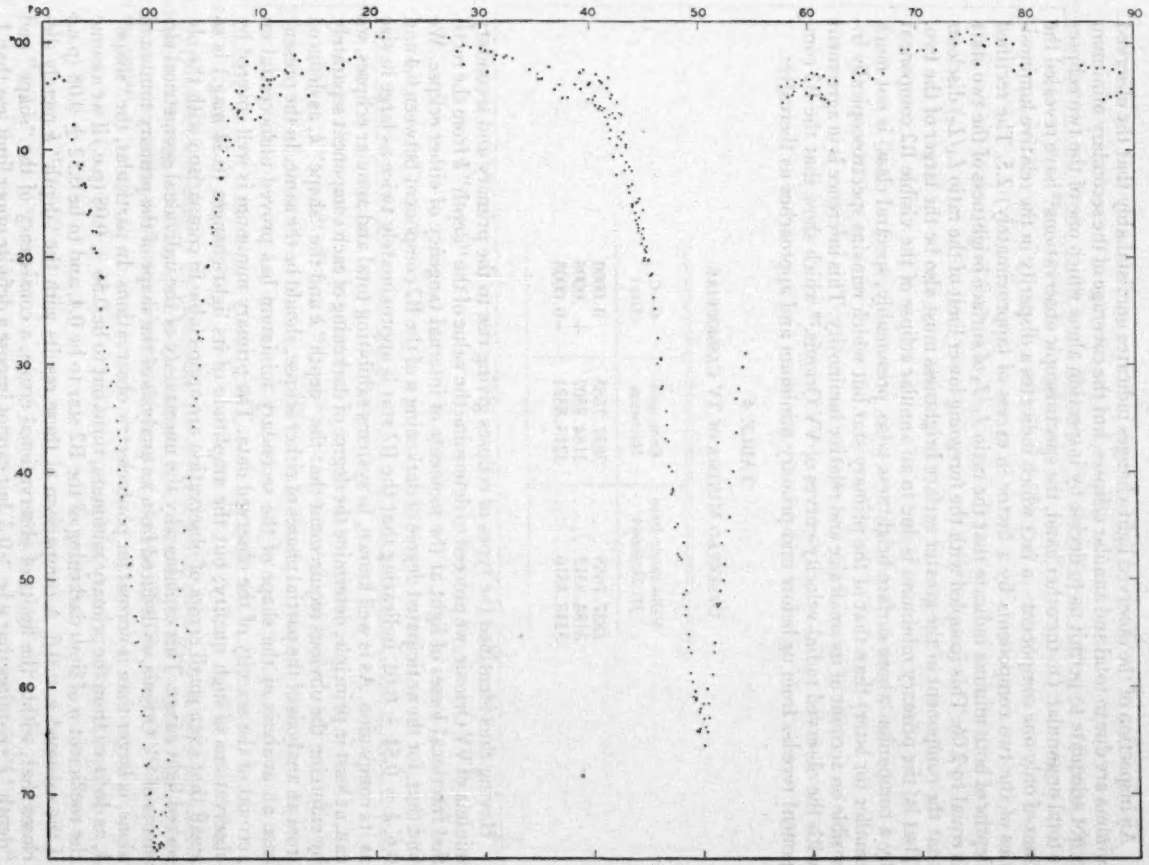

FIG. 4.—Photoelectric measures of U Ophiuchi made at the Washburn Observatory. The horizontal scale is given in decimals of the period.

VV ORIONIS

An inspection of the observed light-changes indicates unmistakably that the observed minima are due to total and annular eclipses, but the coverage of the secondary minimum is not adequate to permit us to decide by inspection alone which one of the two eclipses is total or annular. On the other hand, the spectroscopic observations[20] have revealed the lines of only one component—a fact which indicates a disparity in the relative luminosities of the two components by a factor in excess of (approximately) 2.5. The rectified depths of both minima indicate that the ratio J_1/J_2 of surface brightness of the two stars is equal to 2.06. This (coupled with the foregoing lower limit of the ratio L_1/L_2) discloses that the component of the greater surface brightness must also be the larger of the two. That is, the primary minimum is due to an annular eclipse of the visible B2 component by a companion whose surface brightness (also, presumably, spectral class) is not much smaller (or later) than that of the primary star but which remains spectroscopically invisible on account of its small size and relative luminosity. This inference is in agreement with the observed radial-velocity-curves of VV Orionis,[20] which show that the B2 component recedes from us before mid-primary minimum and approaches us thereafter.

TABLE 4

OBSERVED MINIMA OF TV CASSIOPEIAE

Heliocentric Date JD 2430000+	Computed Minimum	O−C (Day)
2827.7665.....	2827.7665	0.0000
3184.8515.....	3184.8507	+ .0008
3213.8516.....	3213.8524	−0.0008

Having thus identified the types of eclipses giving rise to the primary and secondary minima of VV Orionis, we proceed to determine the value of the "depth" k from the rectified fractional losses of light at the moments of internal tangency of either eclipse. We find that, for the anticipated degree of darkening u of the B2 component between 0.4 and 0.6, $k = 0.51 \pm 0.01$, indicating that the B2 star is approximately twice as large in size as its companion. As is well known, in systems exhibiting total and annular eclipses, we can, at least in principle, determine the degree of darkening of each component separately by enforcing the obvious requirement that the "depth" k and the "shape" k, as deduced from an analysis of the partial phases of either eclipse, should be the same. In the present case an analysis of the shape of the secondary minimum has proved unsuccessful on account of the scarcity of the observed data. The primary minimum is well covered by observations of high quality; but the amplitude of its light-changes (0.34 mag.) is so small that even small errors of observation are appreciable in comparison with the observed light-range. This explains why the uncertainty of the individual geometrical elements of VV Orionis, as deduced from an analysis of the shape of the primary minimum alone, is larger than is normal for photoelectric observations. In particular, the "shape" k, as deduced from the primary minimum, turns out to be 0.56 ± 0.08 (p.e.) if we assume the coefficient u of limb darkening of the B2 star to be 0.4, and to be 0.52 ± 0.08 (p.e.) if the assumed $u = 0.6$. A comparison of these results with the "depth" k merely discloses that, within the limits of observational errors, a consistency of the "shape" and "depth" k's requires that u be >0.3, but cannot impose a definite upper limit less than 1. In what follows, we assume for the B2 component that $u = 0.6$, mainly on the strength of the theoretical evidence tending to show that the opacity in the atmospheres of early-

[20] Daniel, *Pub. Allegheny Obs.*, **3**, 179, 1915; Struve and Luyten, *Ap. J.*, **110**, 160, 1949.

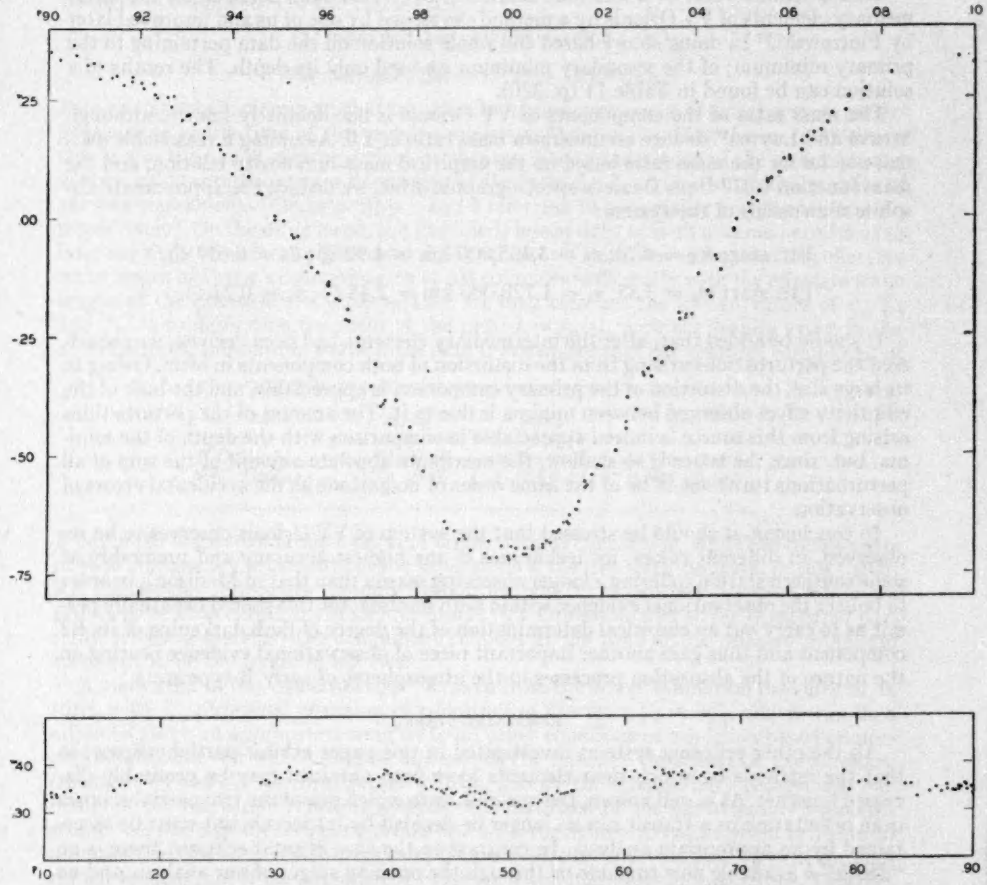

FIG. 5.—Photoelectric measures of TV Cassiopeiae. The vertical scales are the same in the upper and lower drawings. The horizontal scale in the upper drawing of the primary eclipse is four times that of the lower drawing (remainder of light-curve). The secondary eclipse can be seen approximately centered at phase $0^{P}.50$. The horizontal scale is expressed in decimals of the period.

type stars is due predominantly to electron scattering, as well as on the face of the observational evidence available[21] for other early-type stars, which lends an empirical support to this conclusion.

Once a definite value of u was thus assumed, we carried out a solution for the intermediary elements of VV Orionis by a method developed by one of us and improved later by Piotrowski.[22] In doing so, we based the whole solution on the data pertaining to the primary minimum; of the secondary minimum we used only its depth. The results of a solution can be found in Table 11 (p. 320).

The mass ratio of the components of VV Orionis is not definitely known, although Struve and Luyten[20] deduce an uncertain mass ratio of 1.0. Assuming a reasonable estimate of 2.0 for the mass ratio based on the empirical mass-luminosity relation, and the mass function 0.372 from Daniel's spectrographic orbit, we deduce the approximate absolute dimensions of the system:

$$\text{Btr. star: } m_b = 6.70;\ r_b = 3{,}405{,}000 \text{ km} = 4.90\ \odot;\ d_b = 0.057\ \odot.$$

$$\text{Ftr. star: } m_a = 3.35;\ r_a = 1{,}720{,}000 \text{ km} = 2.48\ \odot;\ d_a = 0.22\ \odot.$$

It should be added that, after the intermediary elements had been derived, we considered the perturbations arising from the distortion of both components in form. Owing to its large size, the distortion of the primary component is appreciable, and the bulk of the ellipticity effect observed between minima is due to it. The amount of the perturbations arising from this source is indeed appreciable in comparison with the depth of the minima, but, since the latter is so shallow, the maximum absolute amount of the sum of all perturbations turns out to be of the same order of magnitude as the accidental errors of observation.

In conclusion, it should be stressed that the system of VV Orionis deserves to be reobserved, in different colors, by techniques of the highest accuracy and preferably at some southern station (offering a longer observing season than that in Madison), in order to bolster the observational evidence within both minima; for this should eventually permit us to carry out an empirical determination of the degree of limb darkening of its B2 component and thus gain another important piece of observational evidence bearing on the nature of the absorption processes in the atmospheres of early B-type stars.

REMAINING STARS

All the other eclipsing systems investigated in this paper exhibit partial eclipses; so that the methods by which their elements have been obtained may be profitably discussed together. As is well known, the question as to which one of the two partial eclipses is an occultation or a transit can no longer be decided by inspection but must be ascertained by an appropriate analysis. In contrast to the case of total eclipses, there is no "depth" k available now to guide us through the opening stages of our analysis and no possibility of verifying a posteriori the adopted degrees of darkening of the components undergoing eclipse. In such cases we have to start by assuming a certain value of k, as well as a definite type of the eclipse for the primary minima, and to find subsequently whether or not our original assumptions are borne out by the iterative solution.

For RZ Cassiopeiae, the primary minimum is deep and the secondary shallow. In this case an identification of the primary minimum as an occultation offers but little difficulty, as can be seen immediately from the fundamental equations. For TV Cassiopeiae the same is true to a smaller extent (owing to the fact that the disparity in depths of both minima is smaller than for RZ Cas), except that the iterative solution converges (more slowly than in the preceding case) to the values indicating the primary eclipse to be a transit.

[21] Kopal, *op. cit.*, p. 84.

[22] *Ap. J.*, **108**, 36, 1948.

The remaining systems of U Ophiuchi and WW Aurigae prove to be two-spectrum binaries; and the relative intensities of the spectral lines of both stars have been measured with great care by R. M. Petrie,[23] who deduced from his measurements the following differences in magnitudes of the two stars:

$$\text{U Ophiuchi: } \Delta m = 0^{m}35 \pm 0^{m}03 \text{ (p.e.)};$$

$$\text{WW Aurigae: } \Delta m = 0^{m}25 \pm 0^{m}03 \text{ (p.e.)}.$$

Petrie established, moreover, that the more luminous component of either system undergoes eclipse at the time of the primary minimum,[24] indicating that the more luminous star is also the one of greater surface brightness. Now a knowledge of the difference Δm is obviously tantamount to a knowledge of the ratio L_a/L_b of fractional luminosities of the two components (the subscripts a and b referring to the smaller and the larger star, respectively). On the other hand, the (rectified) loss of light at both minima permits us to infer the ratio of surface brightnesses J_a/J_b of the two stars. Assuming that the effective wave length of Petrie's determination of Δm coincides sufficiently with the effective wave length of the photoelectric observations, we may combine the known values of L_a/L_b and J_a/J_b to determine the ratio of the radii $k = r_a/r_b$, with the results given in the accompanying tabulation. From these data it transpires that the brighter component of

Star	L_a/L_b	J_b/J_a	r_a/r_b
U Ophiuchi.....	0.72±0.02	1.15±0.02	0.926±0.015
WW Aurigae...	0.79±0.02	1.19±0.02	0.994±0.010

U Ophiuchi is approximately 8 per cent larger than its companion, while the components of WW Aurigae are practically of the same size. Of the five stars discussed in this paper, RZ Cassiopeiae represents the only system for which the primary (deeper) minimum proves to be an occultation; in all four others (VV Orionis as well as the three other partially eclipsing systems) the component eclipsed at the time of the primary minimum turns out to be the larger of the two.

A knowledge of the "spectroscopic" k taken from the above tabulation provides us, in turn, with an additional equation of condition of the form $C_1 = kC_2$, which was then adjoined (with an appropriate weight) to all other equations of condition based on normal points observed within minima and solved (by repeated iteration) for the auxiliary constants C_1 and C_2, which, together with p_0, specify the intermediary geometrical elements of the respective eclipsing system. A comparison of the initial purely "spectroscopic" k's listed in the foregoing tabulation with the definitive values given in Table 10 discloses that, for both WW Aurigae and U Ophiuchi, the "spectroscopic" k went through the subsequent mill of the photometric evidence without any significant change. This fact demonstrates forcefully the inability of even very precise photometric observations of partially eclipsing systems, which exhibit minima of nearly equal depths, to contribute much toward the determination of the ratio of the radii of such systems. In our present case their contribution toward fixing the value of k turned out to be almost insignificant in comparison with the weight with which k could have been deduced from Petrie's Δm's; but a combination of the photometric and spectroscopic observations was found to lead to a relatively precise determination of the elements of these systems, which would otherwise have remained largely indeterminate.

With respect to an application of the perturbations (arising from the unequal distortion in form of both components of an eclipsing system), the following comments should

[23] *Pub. Dom. Ap. Obs., Victoria*, 7, 205, 1939.

[24] Private communication.

be added. The components of WW Aurigae are much too far separated, and their distortion is consequently much too small, to make the perturbations of any consequence. The relative dimensions of the components of RZ and TV Cassiopeiae are large enough to give rise to significant perturbations, but their application is hampered by the fact that both these stars are single-spectrum systems and the ratio of masses of the components consequently remains unknown. The fact that there is so little evidence of the ellipticity effect between minima of both systems indicates that, in spite of their large relative sizes, their primary components must be very nearly spherical—i.e., that the masses of their companions may be relatively small. In the case of an apparently large disparity in mass, the ratio of the relative luminosities and the empirical mass-luminosity law are known to offer but a poor guide to the actual value of the mass ratio; and, as long as this holds true, the amplitude of the perturbations remains largely hypothetical. Therefore, the perturbations were not applied, and the elements given in the summarizing Table 11 are the intermediary ones. A derivation of the final elements of RZ and TV Cassiopeiae (taking account of the perturbations) must be postponed until more is known of the mass ratios of these two systems independently of the light-curve. The last system—U Ophiuchi—is a well-known two-spectrum binary, whose components are nearly equal in mass. The photometric perturbations of this eclipsing system are significant and have been duly applied by the "method of false position," so that the elements given in Table 10 can be regarded as the definitive ones.

In the case of RZ Cassiopeiae, the solution gives a difference of magnitude between the components of 2.74 mag. Since the loss of light of the brighter body at primary minimum is more than 80 per cent, it seemed from a preliminary solution that the spectrum of the fainter star should be visible at that phase. Accordingly, Dr. Otto Struve was consulted and agreed to examine the spectrum near primary eclipse in order to attempt to classify the fainter spectrum. No trace of the secondary spectrum was found.[25] A paper entitled "A Spectrographic Study of RZ Cassiopeiae," by Henry Horak,[26] is based on the series of spectrograms made by Struve in December, 1949, and January, 1950. The assumption of a circular orbit used in the computation of the photometric data in this paper is justified, since Horak's results give $e = 0.01 \pm 0.03$.

Horak further assumes a mass ratio of approximately 4, which, he concludes, "shows that this binary is a rather normal type of eclipsing variable. The fainter component does not obey the mass-luminosity relation." Using his data, which include $a_1 = 944{,}000$ km, we derive the following approximate data for the absolute dimensions of the system:

$$\text{Btr. star: } m_a = 2.0;\ r_a = 1{,}090{,}000 \text{ km} = 1.57\odot;\ d_a = 0.52\odot.$$

$$\text{Ftr. star: } m_b = 0.53;\ r_b = 1{,}290{,}000 \text{ km} = 1.85\odot;\ d_b = 0.08\odot.$$

In calculating the absolute dimensions of the two-spectrum binaries, Miss Lois Slocum's spectroscopic results have been used for WW Aurigae,[27] and J. S. Plaskett's for U Ophiuchi[28] and TV Cassiopeiae,[29] though the latter has a secondary spectrum so difficult to measure that the velocities are somewhat uncertain. The results are:

WW Aurigae:

$$\text{Btr. star: } m_b = 1.81\ \odot;\ r_b = 1{,}337{,}000 \text{ km} = 1.92\ \odot;\ d_b = 0.256\ \odot.$$

$$\text{Ftr. star: } m_a = 1.75\ \odot;\ r_a = 1{,}331{,}000 \text{ km} = 1.911\ \odot;\ d_a = 0.251\ \odot.$$

[25] Private communication.

[26] Prepublication communication.

[27] *Lick Obs. Bull.*, 19, 147, 1942.

[28] *Pub. Dom. Ap. Obs., Victoria*, 1, 138, 1919.

[29] *Ibid.*, 2, 141, 1922

U Ophiuchi:

Btr. star: $m_b = 5.30\ \odot$; $r_b = 2{,}336{,}000$ km $= 3.354\ \odot$; $d_b = 0.149\ \odot$.

Ftr. Star: $m_a = 4.65\ \odot$; $r_a = 2{,}194{,}000$ km $= 3.151\ \odot$; $d_a = 0.149\ \odot$.

TV Cassiopeiae:

Btr. star: $m_b = 1.66\ \odot$; $r_b = 1{,}844{,}000$ km $= 2.648\ \odot$; $d_b = 0.089\ \odot$.

Ftr. star: $m_a = 0.98\ \odot$; $r_a = 1{,}700{,}000$ km $= 2.441\ \odot$; $d_a = 0.067\ \odot$.

V. THE TABLES

Table 1 (p. 299) lists the catalogue data for the five variables and their comparison stars.

Tables 2, 3, and 4 give the times of minima of three of the five stars as determined from the present photoelectric measures.

In Tables 5–9 the normal magnitudes of the five variables are listed according to phase. The normals were formed in the usual manner by arranging the measures in order of phase and averaging all measures inside certain phase limits. The phase limits depended on the number of observations and were smallest during the eclipses, where the observations were most numerous. After the light-curves were examined and found to show no asymmetry, the measures were reflected about the middle of the eclipse and the normals formed. The tables therefore show the reflected normals at primary minima and at secondary minima where the eclipse is comparable in depth with the primary. All other normals are listed in order of phase. The first and second columns of Tables 5–9 give normal phases and the corresponding differences of magnitude. The magnitudes are referred to a convenient scale suitable for rectifying; that is, the magnitude differences are adjusted to approximately zero at the maximum between minima.

The rectification was performed by the process described recently by one of us.[30] The results, based on magnitudes between eclipses, are given in Table 10. The third columns in Tables 5–9 list the rectified light-values at the normal phases, and the fourth columns give the proportion of light lost, based on the rectified light-curve. The square roots of the weights ($\sqrt{w_0}$, $\sqrt{w_i}$) are given in the fifth and sixth columns. The first weight ($\sqrt{w_0}$) was assigned arbitrarily on the basis of the number of observations included in each normal and is equal to the number of observations divided by 10 in order to make the value near unity. The second weights ($\sqrt{w_i}$) are the intrinsic weights inside eclipse and depend on the position on the curve. Methods of computing these weights are discussed in the literature.[30] The final columns give the residuals obtained from the solution expressed in decimals of a magnitude.

The final summary of results is given in Table 11. This table is self-explanatory, with notations as given in Kopal's 1950 edition of *The Computation of Elements of Eclipsing Binary Systems.*

An inspection of the data presented in the foregoing table permits us also to draw certain conclusions regarding the general precision with which the individual elements of eclipsing binary systems can be determined from contemporary photometric data. The photoelectric light-curves analyzed in the present paper are based on observations which are so numerous and accurate that certainly a considerable effort would be required to improve upon them in the near future. Our analysis has then disclosed that such data permit us to determine the fractional radii of components of the respective systems within an uncertainty of the order of 1 per cent, and to establish the values of the orbital inclination within errors of the order of 0°.1. These conclusions are in agreement with recent experiences of other investigators dealing with other eclipsing systems observed with

[30] Kopal, *op. cit.*, Sec. 6.2.

TABLE 5

VV ORIONIS—NORMALS

PHASE	Δm	l_{res}	a	$\sqrt{w_0}$	$\sqrt{w_i}$	O−C
	Primary Minimum ($1-\lambda_0=0.245$; $a_0''=1$) (Reflected)					
0^{P}0024....	0^{m}367	0.754	1.000	3.0	.....	−0^{m}001
.0074....	.366	0.755	1.000	2.9	.....	.000
.0122....	.367	0.754	1.000	3.1	.....	− .001
.0170....	.363	0.756	1.000	2.5	.....	+ .001
.0227....	.360	0.758	0.980	2.0	2.31	− .001
.0278....	.339	0.773	0.929	2.0	2.30	+ .002
.0327....	.319	0.786	0.873	1.1	2.29	− .002
.0375....	.294	0.804	0.801	0.9	2.24	− .003
.0422....	.267	0.823	0.722	0.7	2.11	− .001
.0478....	.233	0.848	0.620	0.8	1.94	+ .001
.0529....	.202	0.872	0.524	1.3	1.74	+ .006
.0582....	.178	0.890	0.449	1.3	1.58	+ .001
.0627....	.160	0.896	0.424	1.0	1.53	− .014
.0682....	.130	0.928	0.294	0.7	1.24	+ .002
.0724....	.107	0.947	0.217	0.7	1.05	+ .006
.0775....	.079	0.970	0.122	0.8	0.81	+ .014
.0832....	.056	0.989	0.044	0.9	0.51	+ .018
.0880....	.055	0.989	0.044	1.0	0.51	− .003
.0922....	.049	0.994	0.026	0.9	0.40	+ .005
.0974....	.053	0.989	0.045	1.0	0.52	− .011
.1021....	.045	0.995	0.020	1.0	0.33	− .008
.1073....	.042	0.996	0.015	1.1	0.33	− .015
.1152....	.041	0.995	0.019	0.9	0.33	− .024
.1285....	.041	0.992	.....	1.5	.....	− .008
.1503....	.033	0.994	.....	0.8	.....	− .006
.1697....	.032	0.990	.....	1.5	.....	− .010
.1883....	.015	1.001	.....	1.4	.....	+ .001
.2274....	.010	1.000	.....	0.9	.....	.000
.2944....	.008	1.000	.....	0.6	.....	.000
0.3835....	0.027	0.996	.....	0.2	.....	−0.004
	Secondary Minimum ($1-\lambda_0=0.110$, $a_0=1$)					
0.4109....	0.042	0.987	0.083	1.4	.....	−0.004
.4301....	.063	0.971	0.286	1.6	.....	+ .002
.4513....	.117	0.927	0.614	2.0	.....	− .006
.4715....	.157	0.895	0.920	0.7	.....	− .004
.4902....	.159	0.894	1.000	0.7	.....	+ .004
.5098....	.166	0.888	1.000	1.0	.....	− .002
.5293....	.167	0.886	0.911	1.1	.....	− .014
.5482....	.125	0.920	0.622	1.1	.....	− .012
.5716....	.071	0.964	0.264	1.3	.....	− .007
.6004....	.025	1.002	0.022	1.1	.....	+ .004
.6838....	.017	0.994	.....	2.0	.....	− .006
.7117....	.014	0.994	.....	1.3	.....	− .006
.7319....	.003	1.004	.....	1.3	.....	+ .004
.7743....	.012	0.998	.....	1.0	.....	− .002
.7896....	.002	1.009	.....	1.4	.....	+ .009
0.8835....	0.046	0.991	.....	1.9	.....	−0.009

TABLE 6

RZ CASSIOPEIAE—NORMALS

PHASE	Δm	l_{res}	a	$\sqrt{w_0}$	$\sqrt{w_i}$	O−C
	Primary Minimum ($1-\lambda_0=0.755$; $a_0'=0.826$) (Reflected)					
0P0015	+1m661	0.244	0.823	0.5	1.23	−0m002
.0046	+1.635	0.250	.817	0.4	1.22	− .005
.0074	+1.581	0.267	.799	0.4	1.18	+ .012
.0104	+1.511	0.282	.781	0.3	1.14	+ .008
.0134	+1.402	0.302	.759	0.3	1.11	+ .004
.0166	+1.311	0.326	.734	0.3	1.07	− .008
.0194	+1.208	0.356	.702	0.3	1.01	− .002
.0225	+1.104	0.388	.666	0.2	0.95	− .004
.0255	+0.996	0.426	.625	0.4	0.90	+ .001
.0286	+0.901	0.462	.586	0.3	0.85	− .004
.0317	+0.808	0.501	.544	0.4	0.79	− .007
.0349	+0.717	0.542	.499	0.3	0.74	− .004
.0374	+0.649	0.575	.463	0.4	0.69	− .007
.0406	+0.577	0.612	.423	0.5	0.65	− .026
.0435	+0.493	0.659	.372	0.5	0.59	+ .009
.0464	+0.438	0.691	.336	0.5	0.53	+ .003
.0495	+0.374	0.731	.293	0.5	0.50	+ .003
.0525	+0.328	0.762	.260	0.7	0.47	− .008
.0556	+0.274	0.799	.219	0.5	0.42	− .009
.0583	+0.228	0.832	.183	0.6	0.38	+ .014
.0615	+0.189	0.861	.152	0.6	0.34	− .007
.0647	+0.148	0.893	.117	0.8	0.30	+ .013
.0677	+0.116	0.918	.089	0.6	0.25	+ .010
.0705	+0.094	0.936	.070	1.0	0.22	− .014
.0738	+0.064	0.961	.042	0.8	0.15	+ .018
.0764	+0.047	0.976	.027	1.3	0.11	+ .022
.0794	+0.036	0.985	.016	0.9	0.09	− .003
.0822	+0.038	0.983	.019	0.8	0.09	− .008
.0851	+0.018	1.000	0.000	1.6	0.00	+ .002
.0933	+0.014	1.003	.....	2.1	.....	+ .003
.1094	+0.017	0.998	.....	2.2	.....	− .002
.1325	+0.012	0.999	.....	2.7	.....	− .001
.1522	+0.003	1.004	.....	1.3	.....	+ .004
.1711	−0.002	1.005	.....	1.5	.....	+ .005
.1925	+0.003	0.997	.....	1.3	.....	− .003
.2453	−0.003	0.996	.....	2.1	.....	− .004
.2889	−0.008	0.997	.....	1.1	.....	− .003
.3122	+0.005	0.985	.....	0.9	.....	− .015
.3339	+0.009	0.981	.....	1.7	.....	− .019
.3886	−0.019	1.007	.....	1.5	.....	+ .008
0.4103	+0.003	0.988	.....	1.7	.....	−0.012

TABLE 6—*Continued*

PHASE	Δm	l_{rec}	a	$\sqrt{w_0}$	$\sqrt{w_i}$	O−C
	Secondary Minimum ($1-\lambda_b=0.046$)					
0P4269	+0m008	0.984	.....	2.1	.....	−0m004
.4509	+0.024	0.971	.....	1.9	.....	− .006
.4688	+0.032	0.964	.....	1.6	.....	+ .001
.4901	+0.045	0.953	.....	2.6	.....	+ .004
.5132	+0.041	0.956	.....	2.6	.....	+ .005
.5292	+0.035	0.961	.....	1.8	.....	− .002
.5494	+0.018	0.976	.....	1.4	.....	− .001
.5714	+0.005	0.987	.....	1.2	.....	− .001
.5928	−0.004	0.995	.....	0.9	.....	− .005
.6103	−0.018	1.007	.....	1.7	.....	+ .007
.6306	−0.018	1.006	.....	1.4	.....	+ .006
.6503	−0.020	1.007	.....	2.5	.....	+ .007
.6689	−0.018	1.005	.....	1.4	.....	+ .005
.6831	−0.012	1.000	.....	0.8	.....	.000
.7186	−0.009	0.998	.....	0.6	.....	− .002
.7397	−0.002	0.994	.....	0.8	.....	− .006
.7606	−0.010	1.003	.....	1.2	.....	+ .003
.7822	−0.011	1.006	.....	1.2	.....	+ .006
.8100	−0.004	1.004	.....	1.8	.....	+ .004
.8347	+0.002	0.998	.....	1.3	.....	− .002
.8886	−0.001	1.001	.....	2.7	.....	+ .001
0.9072	+0.004	0.997	.....	2.0	.....	−0.003

TABLE 7

U OPHIUCHI—NORMALS

PHASE	Δm	l_{res}	α	$\sqrt{w_0}$	$\sqrt{w_i}$	O−C
	Primary Minimum ($1-\lambda_0=0.464$; $a_0=0.938$) (Reflected)					
0P0019	+0m738	0.538	0.933	1.2	6.40	−0m002
.0045	+ .730	0.542	.925	1.2	6.18	− .004
.0082	+ .688	0.564	.882	1.2	5.11	− .001
.0136	+ .615	0.603	.803	1.2	3.88	+ .003
.0181	+ .548	0.641	.726	1.1	3.15	+ .008
.0229	+ .492	0.674	.658	1.1	2.67	+ .004
.0264	+ .449	0.701	.603	0.6	2.36	+ .005
.0307	+ .405	0.730	.546	0.8	2.11	− .001
.0341	+ .360	0.761	.484	1.0	1.84	+ .002
.0381	+ .324	0.786	.433	1.0	1.65	− .001
.0417	+ .286	0.813	.378	1.2	1.48	.000
.0453	+ .256	0.836	.332	0.8	1.33	− .002
.0499	+ .212	0.869	.265	1.2	1.12	+ .001
.0541	+ .179	0.895	.212	1.0	0.97	+ .001
.0583	+ .154	0.915	.172	1.2	0.85	− .003
.0622	+ .127	0.937	.127	1.0	0.70	.000
.0658	+ .114	0.948	.113	1.1	0.64	− .006
.0701	+ .096	0.962	.076	0.8	0.53	− .008
.0732	+ .077	0.979	.043	1.0	0.41	− .002
.0792	+ .056	0.996	0.008	1.2	0.13	+ .001
.0922	+ .050	0.997	.....	2.8	.....	− .003
.1103	+ .036	1.004	.....	3.3	.....	+ .004
.1364	+ .027	1.003	.....	2.0	.....	+ .003
.1753	+ .019	0.997	.....	2.0	.....	− .003
.2089	− .005	1.011	.....	1.4	.....	+ .011
.2825	+ .007	0.998	.....	2.2	.....	− .002
.3142	+ .014	0.998	.....	3.0	.....	− .002
.3603	+ .034	0.995	.....	2.4	.....	− .005
.3900	+ .042	0.998	.....	2.8	.....	− .002
.4061	+ .047	1.000	.....	3.0	.....	.000
0.4158	+0.060	0.991	.....	3.2	.....	−0.009

TABLE 7—*Continued*

PHASE	Δm	l_{res}	a	$\sqrt{w_0}$	$\sqrt{w_i}$	O−C
	Secondary Minimum ($1-\lambda_0=0.405$; $e_0=0.957$) (Reflected)					
0P4214	+0m060	0.992	0.019	1.1	0.22	−0m002
.4254	+ .066	0.988	.029	1.3	0.28	+ .002
.4299	+ .094	0.964	.088	1.0	0.50	− .009
.4344	+ .116	0.946	.133	1.0	0.62	− .010
.4372	+ .134	0.931	.170	1.0	0.73	− .011
.4427	+ .163	0.908	.218	1.4	0.85	− .012
.4467	+ .170	0.903	.230	1.4	0.89	+ .005
.4497	+ .197	0.881	.280	1.0	1.02	+ .001
.4542	+ .210	0.871	.304	0.8	1.07	+ .017
.4586	+ .270	0.825	.412	0.8	1.34	.000
.4623	+ .299	0.804	.463	1.0	1.48	− .003
.4670	+ .343	0.773	.537	1.0	1.71	+ .004
.4699	+ .374	0.751	.588	1.1	1.88	+ .003
.4739	+ .420	0.720	.660	1.2	2.16	− .001
.4774	+ .458	0.696	.719	1.0	2.43	.000
.4818	+ .490	0.676	.766	1.4	2.68	+ .009
.4857	+ .532	0.651	.826	1.6	3.11	+ .010
.4900	+ .585	0.621	.896	1.4	3.78	+ .005
.4943	+ .619	0.601	0.944	1.5	4.44	+ .005
.5897	+ .043	1.005	.....	2.8	.....	+ .005
.6111	+ .042	0.998	.....	3.5	.....	− .002
.6139	+ .032	0.997	.....	1.7	.....	− .003
.6605	+ .030	0.991	.....	1.7	.....	− .009
.7017	+ .007	1.004	.....	2.2	.....	+ .004
.7408	− .005	1.007	.....	2.2	.....	+ .007
.7622	+ .001	1.002	.....	2.6	.....	+ .002
.7931	+ .015	0.993	.....	2.2	.....	− .007
.8644	+ .029	1.001	.....	2.2	.....	+ .001
0.8861	+0.040	0.999	.....	2.4	.....	−0.001

TABLE 8

WW AURIGAE—NORMALS

PHASE	Δm	l_{rec}	e	$\sqrt{w_0}$	$\sqrt{w_i}$	O−C
	Primary Minimum ($1-\lambda_1=0.475$) (Reflected)					
0P0019...	0m723	0.528	0.867	0.91	2.24	−0m003
.0059...	.670	0.554	.818	0.50	1.80	− .002
.0105...	.580	0.602	.731	0.46	1.33	− .002
.0143...	.491	0.654	.636	0.44	1.04	+ .005
.0181...	.410	0.704	.543	0.46	0.84	+ .007
.0219...	.338	0.753	.455	0.53	0.70	+ .005
.0259...	.259	0.809	.350	0.59	0.56	+ .012
.0301...	.183	0.868	.243	0.63	0.42	− .021
.0343...	.141	0.902	.180	0.77	0.35	+ .009
.0378...	.094	0.942	.107	0.71	0.25	+ .015
.0416...	.067	0.965	.064	0.68	0.20	+ .009
.0461...	.045	0.985	0.028	0.91	0.12	+ .001
.0550...	.038	0.991	.....	2.1	.....	− .009
.0644...	.036	0.992	.....	3.6	.....	− .008
.0744...	.033	0.994	.....	2.8	.....	− .006
.0842...	.031	0.995	.....	1.9	.....	− .005
.0997...	.026	0.999	.....	1.5	.....	− .001
.1378...	.022	0.999	.....	2.2	.....	− .001
.2278...	.002	1.011	.....	1.4	.....	+ .011
.3147...	.004	1.011	.....	2.7	.....	+ .011
.4039...	.008	1.016	.....	1.3	.....	+ .016
.4244...	.018	1.008	.....	2.5	.....	+ .008
0.4403...	0.025	1.003	.....	1.5	.....	+0.003
	Secondary Minimum ($1-\lambda_2=0.398$) (Reflected)					
0.4532...	0.049	0.981	0.042	1.43	0.16	+0.009
.4581...	.068	0.964	.079	1.25	0.21	− .001
.4621...	.102	0.935	.144	1.00	0.30	− .003
.4662...	.141	0.902	.216	0.91	0.39	− .003
.4702...	.187	0.865	.297	0.56	0.46	+ .004
.4741...	.237	0.826	.382	0.59	0.60	− .003
.4780...	.294	0.784	.475	0.44	0.73	− .003
.4818...	.357	0.740	.572	0.50	0.90	+ .008
.4857...	.417	0.700	.659	0.56	1.10	− .003
.4899...	.485	0.657	.752	0.53	1.42	− .002
.4940...	.543	0.623	.827	0.63	1.85	+ .003
.4979...	.574	0.606	0.866	0.71	2.22	+ .004
.5631...	.031	0.997	.....	2.4	.....	− .003
.5747...	.032	0.995	.....	1.7	.....	− .005
.5853...	.030	0.996	.....	2.6	.....	− .004
.5944...	.036	0.990	.....	1.8	.....	− .010
.6053...	.038	0.987	.....	1.2	.....	− .013
.6836...	.027	0.990	.....	0.8	.....	− .010
.7283...	.036	0.979	.....	1.5	.....	− .021
.7822...	.017	0.997	.....	2.7	.....	− .003
.9175...	.022	1.004	.....	1.8	.....	+ .004
0.9408...	0.005	1.021	.....	2.7	.....	+0.021

TABLE 9

TV CASSIOPEIAE—NORMALS

PHASE	Δm	l_{res}	α	$\sqrt{w_0}$	$\sqrt{w_i}$	O−C
	Primary Minimum ($1-\lambda_0=0.593$; $\alpha_0''=0.718$) (Reflected)					
0P0026	+1m084	0.409	0.717	1.00	1.16	0m000
.0082	+1.062	0.416	.708	0.77	1.13	− .006
.0127	+1.022	0.430	.691	0.67	1.09	− .012
.0175	+0.916	0.471	.642	0.42	0.98	.000
.0235	+0.818	0.512	.592	0.36	0.88	− .003
.0278	+0.740	0.547	.549	0.33	0.81	− .003
.0330	+0.644	0.594	.492	0.48	0.72	− .001
.0374	+0.558	0.607	.437	0.40	0.64	+ .005
.0431	+0.481	0.684	.383	0.67	0.57	− .001
.0474	+0.412	0.726	.332	0.71	0.51	+ .003
.0525	+0.349	0.767	.283	0.53	0.45	− .001
.0574	+0.283	0.812	.228	0.56	0.39	+ .004
.0623	+0.239	0.844	.190	0.59	0.35	− .002
.0676	+0.182	0.887	.138	0.71	0.29	+ .004
.0727	+0.140	0.919	.098	0.59	0.24	+ .005
.0774	+0.110	0.944	.069	0.91	0.20	+ .003
.0840	+0.085	0.967	.040	1.25	0.15	− .002
.0938	+0.076	0.997	0.004	0.77	0.05	+ .002
.1011	+0.047	0.993	.....	1.4	.....	− .007
.1125	+0.042	0.996	.....	0.9	.....	− .004
.1267	+0.038	0.997	.....	0.7	.....	− .003
.1654	+0.025	1.000	.....	0.8	.....	.000
.1803	−0.012	1.011	.....	1.0	.....	+ .012
.2944	+0.013	0.992	.....	1.5	.....	− .008
.3181	−0.002	1.006	.....	2.1	.....	+ .006
0.3886	+0.007	1.000	.....	2.1	.....	0.000
	Secondary Minimum ($1-\lambda_0=0.050$; $\alpha_0'=0.76$)					
0.4137	+0.012	0.997	.....	2.8	.....	0.000
.4393	+0.036	0.977	.....	2.0	.....	− .008
.4617	+0.048	0.967	.....	2.8	.....	− .002
.4853	+0.063	0.954	.....	3.1	.....	.000
.5126	+0.066	0.952	.....	1.6	.....	− .001
.5371	+0.047	0.968	.....	1.6	.....	.000
.5527	+0.039	0.974	.....	0.7	.....	− .006
.6153	+0.007	1.000	.....	1.7	.....	.000
.6392	+0.008	0.998	.....	2.1	.....	− .002
.6625	+0.007	0.998	.....	1.8	.....	− .002
.6808	−0.004	1.004	.....	1.3	.....	+ .004
.7147	0.000	1.000	.....	1.5	.....	.000
.7322	+0.005	1.001	.....	0.9	.....	+ .001
.7942	+0.021	0.995	.....	0.9	.....	− .005
.8172	−0.002	1.001	.....	1.0	.....	− .001
.8567	+0.007	0.994	.....	1.8	.....	− .006
.8836	−0.001	1.000	.....	2.1	.....	.000
.8947	−0.007	1.006	.....	1.2	.....	+ .006
0.9028	−0.008	1.007	.....	1.3	.....	+0.007

TABLE 10

RESULTS OF RECTIFICATIONS

1. *VV Orionis:*

$$l_{obs} = 0.993 - 0.008 \cos\theta - 0.036 \cos^2\theta - \ldots$$
$$\pm 0.003 \pm 0.005 \qquad \pm 0.009 \text{ (p.e.)}$$
$$l_{rec} = \frac{l_{obs}(1 + 0.036 \cos^2\theta) + 0.008 (1 + \cos\theta)}{0.993 + 0.008}$$

2. *RZ Cassiopeiae:*

$$l_{obs} = 1.0072 - 0.0150 \cos\theta - 0.0150 \cos^2\theta + \ldots$$
$$\pm 0.0018 \pm 0.0015 \qquad \pm 0.0039 \text{ (p.e.)}$$
$$l_{rec} = \frac{l_{obs}(1 + 0.0150 \cos^2\theta) + 0.0150 (1 + \cos\theta)}{1.0072 + 0.0150}$$

3. *WW Aurigae:*

$$l_{obs} = 0.988 - 0.001 \cos\theta - 0.016 \cos^2\theta + \ldots$$
$$\pm 0.003 \pm 0.002 \qquad \pm 0.005 \text{ (p.e.)}$$
$$l_{rec} = \frac{l_{obs}(1 + 0.016 \cos^2\theta)}{0.988}$$

4. *U Ophiuchi:*

$$l_{obs} = 0.9980 + 0.0019 \cos\theta - 0.0602 \cos^2\theta - \ldots$$
$$\pm 0.0012 \pm 0.0010 \qquad \pm 0.0024 \text{ (p.e.)}$$
$$l_{rec} = \frac{l_{obs}(1 + 0.0602 \cos^2\theta)}{0.9980}$$

5. *TV Cassiopeiae:*

$$l_{obs} = 0.9924 - 0.0182 \cos\theta - 0.0221 \cos^2\theta - \ldots$$
$$\pm 0.0010 \pm 0.0009 \qquad \pm 0.0026 \text{ (p.e.)}$$
$$l_{rec} = \frac{l_{obs}(1 + 0.0221 \cos^2\theta) + 0.0182 (1 + \cos\theta)}{0.9924 + 0.0182}$$

Table 11

Summary of Results

	VV Ori	*RZ Cas*	*WW Aur*	*U Oph*	*TV Cas*
Pri. Min.	Transit	Occultation	Ambiguous	Transit	Transit
Period	$1^d.4853799$	$1^d.1952519$(var.)	$2^d.52501906$	$1^d.6773522$	$1^d.8126098$
$1-\lambda_a$(rect.)	0.110 ± 0.003	0.755 ± 0.002	0.398 ± 0.003	0.405 ± 0.006	0.050 ± 0.006
$1-\lambda_b$(rect.)	0.245 ± 0.004	0.046 ± 0.002	0.475 ± 0.003	0.464 ± 0.005	0.593 ± 0.007
u_a } adopted	0.6	0.6	0.6	0.6	0.6
u_b }	0.6	0.8	0.6	0.6	0.6
$Y(k,P_0)$	-	1.044	1.000	1.025	0.988
$Y(k,-1)$	1.081	1.107	1.000	1.039	1.048
α_0'	1	0.816 ± 0.004	0.873 ± 0.006	0.92 ± 0.01	0.76 ± 0.05
α_0''	1	0.769 ± 0.004	0.873 ± 0.006	0.91 ± 0.01	0.72 ± 0.05
P_0	-1	-0.612 ± 0.006	-0.749 ± 0.009	-0.82 ± 0.02	-0.52 ± 0.07
C_1	0.0450 ± 0.0013	0.0591 ± 0.0014	0.02579 ± 0.00037	0.0611 ± 0.0013	0.082 ± 0.004
C_2	0.0891 ± 0.0021	0.0697 ± 0.0002	0.02586 ± 0.00023	0.0651 ± 0.0008	0.0891 ± 0.0012
C_3	0.0169 ± 0.0019	-	-	-	-
r_a	0.2094 ± 0.0019	0.241 ± 0.002	0.1605 ± 0.0011	0.247 ± 0.002	0.283 ± 0.014
r_b	0.4145 ± 0.0036	0.284 ± 0.002	0.1612 ± 0.0011	0.263 ± 0.002	0.307 ± 0.015
k	0.505 ± 0.008	0.848 ± 0.018	0.997 ± 0.009	0.939 ± 0.013	0.92 ± 0.04
i	$80^\circ.9 \pm 0^\circ.2$	$82^\circ.14 \pm 0^\circ.06$	$87^\circ.65$	$86^\circ.57 \pm 0^\circ.07$	$80^\circ.8 \pm 0^\circ.3$
θ'	$37^\circ.6 \pm 0^\circ.5$	$30^\circ.8 \pm 0^\circ.3$	$18^\circ.64 \pm 0^\circ.08$	$30^\circ.5 \pm 0^\circ.2$	$35^\circ.1 \pm 0^\circ.8$
θ''	$7^\circ.6 \pm 0^\circ.4$	-	-	-	-
D	$0^d.209 \pm 0^d.003$	$0^d.171 \pm 0^d.002$	$0^d.1036 \pm 0^d.0004$	$0^d.169 \pm 0^d.001$	$0^d.195 \pm 0^d.004$
d	$0^d.042 \pm 0^d.003$	-	-	-	-
J_b/J_a	2.06 ± 0.06	0.0578 ± 0.0023	1.193 ± 0.012	1.118 ± 0.018	11.1 ± 1.3
L_a	0.110 ± 0.003	0.926 ± 0.004	0.456 ± 0.008	0.444 ± 0.009	0.071 ± 0.006
L_b	0.890 ± 0.003	0.074 ± 0.003	0.544 ± 0.008	0.556 ± 0.010	0.929 ± 0.007
L_a+L_b	1.000 ± 0.004	1.0000 ± 0.0004	1.000 ± 0.003	1.000 ± 0.002	1.000 ± 0.004

Table 12

Photoelectric Measures

Photoelectric Observations of RZ Cassiopeiae

J.D.	Phase	Δ Mag.	Note
2,429000+			
867.6832	0.9341	0.185	1
.6965	0.9394	0.189	1
.6987	0.9419	0.241	1
.6970	0.9455	0.299	1
.7016	0.9494	0.361	1
.7065	0.9535	0.439	1
.7106	0.9569	0.502	1
.7144	0.9601	0.565	1
873.6659	0.9042	-0.013	3
874.6626	0.1875	0.018	3
.7000	0.1720	0.005	3
.7146	0.1842	-0.007	3
875.7359	0.0306	0.583	1
.7410	0.0429	0.453	1
.7452	0.0454	0.418	1
.7495	0.0500	0.344	1
.7538	0.0536	0.301	1
.7581	0.0572	0.254	1
892.6256	0.8033	-0.006	3
.6406	0.8159	-0.012	3
.6540	0.8287	-0.012	3
895.6301	0.3171	0.004	3
.6447	0.3298	0.003	3
.6590	0.3379	0.005	3
.7276	0.3987	0.002	3
.7417	0.4105	0.000	3
.7569	0.4231	0.001	3
896.5635	0.1147	0.051	3
.5976	0.1297	0.033	3
.6118	0.1394	0.012	3
930.5874	0.9273	0.056	1
.5938	0.9301	0.049	1
.5984	0.9348	0.160	1
.6712	0.9388	0.208	1
.6787	0.9434	0.239	1
.5880	0.9479	0.324	1
.5878	0.9527	0.398	1
950.6917	0.7539	-0.088	3
.7049	0.7640	-0.086	3
.7215	0.7779	-0.084	3
.7340	0.7883	-0.082	3
954.6186	0.1275	0.012	3
.6514	0.1620	-0.013	3
.6672	0.1782	-0.009	3
957.6197	0.0146	1.350	1
.6236	0.0180	1.200	1
.6276	0.0213	1.080	1
.6313	0.0243	0.982	1
.6362	0.0284	0.852	1
.6403	0.0319	0.782	1
.6480	0.0386	0.635	1
.6498	0.0396	0.598	1
.6533	0.0425	0.448	1
.6599	0.0482	0.362	1
.6646	0.0521	0.322	1
.6682	0.0552	0.282	1
.6774	0.0636	0.224	1
.6908	0.0740	0.046	2
.6967	0.0807	0.027	2
.7079	0.0883	0.005	2
2,430000+			
000.5780	0.8418	-0.016	3
.5904	0.8535	-0.021	3
.6276	0.2830	-0.014	3
.6408	0.2938	-0.011	3
003.5776	0.9141	0.086	1
.5925	0.9182	0.083	1
.5972	0.9221	0.089	1
.6062	0.9280	0.176	1
.6131	0.9438	0.286	1
.6171	0.9471	0.338	1
.6227	0.9518	0.416	1
.6271	0.9555	0.496	1
.6317	0.9593	0.576	1
.6362	0.9631	0.680	1
.6406	0.9668	0.757	1
.6452	0.9721	0.930	1
.6518	0.9762	1.092	1
.6550	0.9872	1.404	1
.6588	0.9904	1.482	1
.6728	0.9955	1.567	1
.6763	0.9983	1.576	1
.6820	0.0014	1.572	1
.6868	0.0052	1.554	1
.6909	0.0089	1.538	1
.6951	0.0124	1.416	1
.7012	0.0176	1.282	1
.7184	0.0319	0.764	1
.7228	0.0356	0.666	1
.7269	0.0415	0.547	1
.7344	0.0453	0.458	1
.7365	0.0487	0.377	1
.7427	0.0542	0.323	1

J.D.	Phase	Δ Mag.	Note
2,430000+			
028.7486	0.0598	0.288	1
.7529	0.0631	0.215	1,
054.5983	0.9839	-0.002	1,
.6075	0.9906	-0.008	1,
229.7729	0.2451	-0.009	3
.7817	0.2579	-0.008	3
260.7132	0.1298	-0.001	2
.7202	0.1374	0.008	2
265.7153	0.8417	-0.035	3
.7328	0.8537	-0.031	3
276.6626	0.1647	0.006	3
.6958	0.1788	0.008	3
283.7611	0.4138	0.009	2
.7691	0.4197	0.010	2
.7972	0.4440	0.022	2
.8076	0.4527	0.025	2
.8451	0.4841	0.041	2
.8618	0.4981	0.049	2
314.5697	0.1880	0.001	3
.5812	0.2001	-0.008	3
322.5776	0.8905	-0.001	2
.5982	0.8992	0.005	2
.6033	0.9065	0.009	1
.6066	0.9146	0.011	1
.6139	0.9196	0.026	1
.6205	0.9252	0.051	1
.6274	0.9320	0.104	1
.6343	0.9378	0.168	1
.6396	0.9421	0.224	1
.6451	0.9468	0.301	1
.6509	0.9516	0.371	1
.6575	0.9572	0.476	1
.6639	0.9628	1.177	1
.6697	0.9641	1.339	1
.6967	0.9900	1.517	1
.7074	0.9989	1.541	1
.7145	0.0047	1.514	1
.7202	0.0096	1.527	1
.7255	0.0143	1.354	1
.7337	0.0209	1.152	1
.7392	0.0255	0.987	1
.7443	0.0298	0.859	1
.7524	0.0449	0.454	1
.7701	0.0514	0.326	1
.7763	0.0566	0.254	1
.7846	0.0635	0.186	1
.7915	0.0694	0.134	1
.7971	0.0740	0.099	1
.8040	0.0797	0.057	1
.8153	0.0892	0.059	2
.8250	0.0981	0.012	2
324.6908	0.9550	-0.001	3
.7056	0.9707	-0.008	3
.7194	0.9823	-0.004	2
325.6776	0.4254	0.008	2
.6801	0.4358	0.010	2
.6906	0.4446	0.016	2
.6931	0.4551	0.023	2
.6956	0.4656	0.033	2
.6979	0.4755	0.037	1,
.6990	0.4851	0.054	2
.7976	0.5090	0.047	2
.7189	0.5184	0.041	2
345.5679	0.1918	0.019	2
.5840	0.2010	0.016	2
374.7189	0.5101	0.051	3
.7319	0.5240	0.042	3
.7588	0.5415	0.028	3
.7739	0.5589	0.019	3
.7958	0.5775	0.006	3
.8160	0.5944	0.005	3
385.6601	0.9849	1.393	1
.6681	0.9916	1.582	1
.6838	0.9964	1.559	1
.6892	0.0009	1.541	1
.6944	0.0053	1.406	1,
410.5828	0.8170	0.040	3
.5983	0.8304	0.022	3
440.5697	0.8011	-0.038	3
.5847	0.8162	-0.030	3
2,430000+			
084.5692	0.0657	0.330	1
.5775	0.0707	0.218	1
.5819	0.0743	0.164	1
.5871	0.0787	0.104	1
.5935	0.0839	0.088	1
.5985	0.0782	0.076	1
.6038	0.0817	0.068	1
.6081	0.0853	0.068	1
.6144	0.0918	0.042	1
.6186	0.0950	0.026	1
.6228	0.0988	0.027	1
085.6454	0.9650	0.497	1
.6506	0.9684	0.563	1

J.D.	Phase	Δ Mag.	Note
2,430000+			
085.6540	0.9813	0.654	1
.6576	0.9844	0.719	1
.6618	0.9877	0.844	1
.6651	0.9908	0.931	1
.6689	0.9938	1.009	1
.6730	0.9764	1.077	1
.6754	0.9791	1.178	1
.6851	0.9867	1.402	1
.6976	0.9968	1.540	1
.7025	0.0019	1.670	1*
.7087	0.0071	1.638	1*
.7148	0.0120	1.585	1*
085.6146	0.8219	-0.016	3
.6318	0.8384	-0.019	3
.6451	0.8474	-0.020	3
086.6535	0.3276	0.007	3
.6648	0.3371	0.000	2
.6745	0.3462	0.009	3
.6921	0.4621	0.033	3
.8160	0.4839	0.030	3
096.7347	0.2535	0.014	3
.7472	0.2632	0.004	3
104.5745	0.1395	0.035	3*
.5864	0.1478	0.024	3*
112.5722	0.4835	0.028	2
.5782	0.4894	0.037	2
115.5342	0.9617	0.627	1
.5371	0.9641	0.696	1
.5429	0.9690	0.810	1
.5440	0.9698	0.840	1
.5467	0.9721	0.911	1
.5498	0.9749	0.946	1
.5519	0.9765	1.004	1
.5531	0.9775	1.101	1
.5564	0.9803	1.212	1
.5576	0.9813	1.252	1
.5589	0.9827	1.273	1
.5645	0.9870	1.369	1
.5661	0.9900	1.424	1
.5894	0.9911	1.527	1
.5758	0.9965	1.604	1
.5778	0.9982	1.677	1
.5819	0.0016	1.680	1
.5838	0.0035	1.644	1
.5862	0.0059	1.632	1
.5899	0.0093	1.634	1
.5931	0.0120	1.480	1
.5946	0.0128	1.412	1
.5986	0.0156	1.310	1
.5999	0.0168	1.287	1
.6047	0.0207	1.178	1
.6066	0.0213	1.105	1
.6091	0.0243	1.030	1
.6107	0.0257	0.976	1
.6152	0.0294	0.880	1
.6165	0.0306	0.845	1
.6194	0.0330	0.780	1
.6216	0.0340	0.750	1
147.6194	0.8084	-0.007	3
.6592	0.8146	-0.006	3
152.6904	0.9908	1.668	1
.6215	0.9914	1.676	1
.6249	0.9942	1.648	1
.6261	0.9952	1.670	1
.6284	0.9972	1.706	1
.6294	0.9980	1.706	1
.6335	0.0012	1.702	1
.6348	0.0020	1.680	1
.6374	0.0047	1.660	1
.6388	0.0054	1.645	1
.6427	0.0091	1.594	1
.6438	0.0098	1.577	1
.6470	0.0127	1.484	1
.6484	0.0139	1.440	1
.6515	0.0165	1.362	1
.6538	0.0174	1.305	1
.6562	0.0196	1.221	1
.6582	0.0204	1.200	1
405.6875	0.0407	0.567	1
.6910	0.0437	0.510	1
.6948	0.0465	0.457	1
.6976	0.0494	0.410	1
.7014	0.0526	0.362	1
.7049	0.0553	0.319	1
.7063	0.0581	0.276	1
.7118	0.0611	0.223	1
.7158	0.0640	0.196	1
.7189	0.0669	0.156	1
.7222	0.0692	0.121	1
.7257	0.0727	0.089	1
.7292	0.0758	0.064	1
.7330	0.0785	0.039	1
.7361	0.0814	0.019	1
.7394	0.0845	0.007	1
.7451	0.0878	0.002	1

Table 12 (cont'd)

Photoelectric Observations of RZ Cassiopeiae

J.D.	Phase	Δ Mag.	Sets
2,432000+			
405.7486	0.0932	-0.009	1
.7500	0.0960	-0.016	1
.7505			
.7670	0.0989	-0.020	3
.7674			
.7679			
.7874	0.1078	-0.014	3
.7708			
.7743			
.7778	0.1163	-0.013	3
.7812			
.7847			
.7882	0.1250	-0.014	3
.7917			
.7951			
.7998	0.1337	-0.010	3
.8021			
.8056			
.8091	0.1425	-0.009	3
.8125			
.8160			
.8195	0.1512	-0.006	3
.8229			
.8264			
.8299	0.1599	-0.002	3
.8333			
440.6507	0.2414	0.011	3
.7097	0.2552	-0.002	2
.7239	0.2942	-0.002	3
.7384	0.3082	0.015	2
.7527	0.3176	0.013	2
.7625	0.3274	0.005	3
.8444	0.3959	-0.007	3
.8678	0.4038	-0.019	2
.8960	0.4140	-0.016	2
.8743	0.4209	-0.011	2
.8954	0.4302	-0.007	3
452.5595	0.9236	0.063	1
.5660	0.9286	0.076	1
.5685	0.9314	0.094	1
.5660	0.9343	0.128	1
.5694	0.9372	0.155	1
.5729	0.9401	0.207	1
.5764	0.9430	0.280	1
.5799	0.9460	0.309	1
.5835	0.9488	0.384	1
.5868	0.9517	0.422	1
.5903	0.9547	0.476	1
.5938	0.9576	0.537	1
.5972	0.9604	0.600	1
.6007	0.9634	0.694	1
.6042	0.9663	0.766	1
.6076	0.9691	0.861	1
.6111	0.9721	0.960	1
.6181	0.9779	1.139	1
.6215	0.9808	1.227	1
.6250	0.9837	1.328	1
.6285	0.9866	1.418	1
.6319	0.9895	1.506	1
.6354	0.9924	1.580	1
.6389	0.9953	1.654	1
.6424	0.9982	1.676	1
.6458	0.0011	1.674	1
.6493	0.0040	1.694	1
.6528	0.0069	1.615	1
.6562	0.0098	1.565	1
.6597	0.0127	1.466	1
.6632	0.0156	1.349	1
.6667	0.0186	1.242	1
.6701	0.0214	1.145	1
.6736	0.0243	1.050	1
.6771	0.0273	0.938	1
.6806	0.0302	0.840	1
.6840	0.0330	0.760	1
.6875	0.0360	0.693	1
.6910	0.0389	0.616	1
.6944	0.0417	0.548	1
.6979	0.0447	0.490	1
.7014	0.0476	0.426	1
.7049	0.0505	0.372	1
.7083	0.0534	0.318	1
.7118	0.0563	0.268	1
.7153	0.0592	0.224	1
.7188	0.0622	0.186	1
.7222	0.0650	0.156	1
.7257	0.0679	0.124	1
.7292	0.0709	0.096	1
.7326	0.0737	0.072	1
.7361	0.0766	0.049	1
.7396	0.0796	0.029	1
.7430	0.0824	0.017	1
.7465	0.0853	0.017	1
.7500	0.0882	0.032	1
.7535	0.0912	0.022	1

J.D.	Phase	Δ Mag.	Sets
2,432000+			
452.7569	0.0940	0.022	1
.7604	0.0970	0.025	1
.7639	0.0999	0.027	1
454.8750	0.6152	-0.020	4#
.8889	0.6196	-0.018	4#
.8958	0.6218	-0.013	4#
.9028	0.6239	-0.008	4#
.9167	0.6283	0.008	4#
.9236	0.6304	0.012	4#
.9306	0.6326	-0.010	4#
472.6153	0.7184	-0.014	2
.6229	0.7197	-0.010	2
.6299	0.7246	-0.008	2
.6375	0.7260	-0.008	2
.6444	0.7297	-0.009	2
.6514	0.7298	0.002	2
.6583	0.7465	0.006	2
.6667	0.7554	0.026	2
.6736	0.7595	0.006	2
.6833	0.7598	-0.014	2
.6944	0.7745	0.001	2
.6979	0.7815	0.005	2
.7084	0.7979	0.011	2
.7229	0.8034	0.011	2
.7312	0.8082	0.001	2
.7424	0.8187	0.001	2
.7493	0.8245	0.019	2
.7569	0.8308	0.019	2
.7639	0.8397	0.013	2
.7708	0.8425	0.008	2
.7778	0.8483	0.007	2
.8125	0.8707	0.013	1
.8222	0.8855	0.052	2
.8306	0.8925	0.027	2
.8382	0.8988	0.041	2
.8473	0.9046	0.031	2
.8542	0.9122	0.030	2
.8618	0.9186	0.047	2
.8694	0.9241	0.055	1
.8721	0.9272	0.067	1
.8765	0.9307	0.087	1
.8800	0.9328	0.100	1
.8826	0.9358	0.126	1
.8868	0.9398	0.173	1
.8903	0.9424	0.207	1
.8941	0.9458	0.250	1
.8979	0.9488	0.297	1
473.5417	0.4874	0.039	2
.5614	0.4966	0.037	2
.5708	0.5118	0.052	2
.5792	0.5188	0.043	2
.5889	0.5259	0.037	2
.5979	0.5344	0.046	2
.6125	0.5457	0.018	2
.6284	0.5585	-0.025	24
.6354	0.5668	-0.020	24
.6437	0.5728	-0.020	24
.6521	0.5798	-0.046	24
.6597	0.5892	-0.061	24
.6722	0.5966	-0.038	24
.6854	0.6077	-0.041	24
.6944	0.6152	-0.038	24
.7014	0.6210	-0.044	24
479.5451	0.5104	0.084	3
.5568	0.5191	0.081	3
.5660	0.5278	0.088	3
.5764	0.5365	0.015	3
.5868	0.5452	0.012	3
.5972	0.5539	0.012	3
.6076	0.5626	0.010	3
.6163	0.5699	0.008	3
.6233	0.5758	-0.005	3
.6286	0.5807	-0.006	3
.6449	0.5955	-0.012	3
.6549	0.6022	-0.014	3
.6639	0.6097	-0.022	3
.6725	0.6169	-0.022	3
.6843	0.6266	-0.015	3
.6979	0.6382	-0.020	3
.7061	0.6448	-0.027	3
.7126	0.6501	-0.005	3
.7234	0.6597	-0.020	3
.7290	0.6648	-0.027	3
.7368	0.6699	-0.025	3
.7424	0.6754	-0.021	3
.7494	0.6813	-0.025	3
765.7870	0.9650	0.789	1
.7708	0.9718	0.871	1
.7743	0.9741	1.013	1
.7799	0.9789	1.197	1
.7847	0.9828	1.321	1
.7888	0.9865	1.377	1
.7918	0.9888	1.443	11
.7955	0.9919	1.526	11
801.7191	0.0489	0.317	18
.7256	0.0544	0.280	18

J.D.	Phase	Δ Mag.	Sets
2,432000+			
801.7301	0.0681	0.220	18
.7328	0.0611	0.188	18
.7371	0.0640	0.152	18
.7410	0.0673	0.120	18
.7449	0.0705	0.082	18
.7535	0.0777	0.004	28
.7804	0.1002	0.020	2
.7865	0.1058	0.054	2
.7965	0.1152	0.034	3
817.6811	0.4043	0.025	3
.6925	0.4138	0.022	3
.7054	0.4246	0.023	3
.7189	0.4359	0.023	3
.7298	0.4450	0.027	3
.7411	0.4546	0.034	3
.7524	0.4639	0.039	3
.7650	0.4745	0.049	3
.7737	0.4817	0.053	3
.7919	0.4970	0.071	3
.8098	0.5119	0.045	3
.8240	0.5238	0.056	2
7167	0.1074	0.061	3
.7365	0.1252	0.080	3
.7614	0.1265	0.021	2
820.6881	0.9035	0.021	2
.6923	0.9162	0.087	2
.6984	0.9239	0.056	1
.6979	0.9334	0.098	1
.7044	0.9389	0.138	1
.7097	0.9395	0.188	1
.7151	0.9428	0.226	1
.7205	0.9471	0.263	1
.7274	0.9531	0.459	1
.7308	0.9609	0.656	1
.7468	0.9685	0.831	1
.7530	0.9735	1.040	1
.7583	0.9799	1.219	1
.7640	0.9837	1.388	1
.7715	0.9900	1.594	1
.7777	0.9951	1.809	1
.7828	0.0005	1.977	1
.7915	0.0067	1.611	1
.7974	0.0116	1.507	1
.8039	0.0169	1.349	1
.8087	0.0211	1.181	1
.8160	0.0272	0.977	1
.8215	0.0318	0.814	1
.8272	0.0369	0.694	1
.8328	0.0412	0.611	1
.8700	0.0724	0.076	1
.8852	0.0851	0.034	3
.9047	0.1014	0.056	3
562.5476	0.9431	0.247	1
.5528	0.9458	0.297	1
.5597	0.9482	0.347	1
.5667	0.9507	0.384	1
.5698	0.9531	0.432	1
.5628	0.9557	0.490	1
.5559	0.9582	0.547	1
.5684	0.9605	0.610	1
.5712	0.9629	0.642	1
.5797	0.9700	0.808	1
.5859	0.9736	1.014	1
.5871	0.9762	1.109	1
.5899	0.9785	1.174	1
.5942	0.9821	1.317	1
.5970	0.9844	1.352	1
.6008	0.9868	1.447	1
.6038	0.9891	1.548	1
.6062	0.9913	1.597	1
.6080	0.9926	1.664	1
.6108	0.9950	1.681	1
.6140	0.9967	1.693	1
.6174	0.0015	1.694	1
.6201	0.0028	1.689	1
.6229	0.0061	1.643	1
.6271	0.0098	1.559	1
.6299	0.0120	1.493	1
.6330	0.0146	1.409	1
.6358	0.0169	1.328	1
.6392	0.0197	1.241	1
.6419	0.0220	1.166	1
.6447	0.0243	1.075	1
2,432000+			
827.7010	0.8776	0.005	2
.7069	0.8817	0.007	2
.7106	0.8858	0.005	2
.7155	0.8897	0.005	2
.7203	0.8937	0.015	2
.7252	0.8976	0.019	2
.7309	0.9025	0.015	2
.7356	0.9065	0.015	2
.7404	0.9106	0.014	2

Table 12 (cont'd)

Photoelectric Observations of RZ Cassiopeiae

J.D.	Phase	Δ Mag.	Sets
2,428000+			
157.7463	0.9147	0.011	2
.7525	0.9206	0.027	2
.7585	0.9267	0.074	1
.7599	0.9279	0.090	1
.7634	0.9308	0.115	1
.7648	0.9310	0.128	1
.7690	0.9345	0.135	1
.7704	0.9357	0.146	1
.7745	0.9391	0.195	1
.7759	0.9403	0.202	1
.7807	0.9443	0.290	1
.7821	0.9455	0.302	1
.7859	0.9487	0.348	1
.7873	0.9499	0.363	1
.7918	0.9538	0.456	1
.7932	0.9549	0.476	1
.7972	0.9581	0.520	1
.7986	0.9593	0.530	1
.8038	0.9638	0.651	1
.8042	0.9640	0.668	1
.8076	0.9668	0.768	1
.8090	0.9680	0.811	1
.8155	0.9732	0.961	1
.8167	0.9744	1.006	1
.8201	0.9772	1.085	1
.8215	0.9784	1.121	1
.8251	0.9814	1.241	1
.8265	0.9826	1.291	1
.8313	0.9865	1.411	1
.8327	0.9876	1.449	1
.8362	0.9907	1.525	1
.8376	0.9919	1.546	1
.8445	0.9977	1.651	1
.8459	0.9989	1.646	1
.8500	0.0023	1.642	1
.8514	0.0035	1.618	1
.8549	0.0064	1.601	1
.8563	0.0076	1.571	1
.8597	0.0104	1.479	1
.8611	0.0116	1.451	1
.8646	0.0145	1.379	1
.8660	0.0157	1.355	1
.8694	0.0186	1.246	1
.8708	0.0197	1.191	1
.8739	0.0223	1.091	1
.8753	0.0235	1.051	1
.8815	0.0278	0.908	1
.8829	0.0290	0.902	1
.8854	0.0319	0.804	1
.8868	0.0331	0.774	1
.8903	0.0360	0.694	1
.8917	0.0372	0.679	1
.8956	0.0404	0.672	1
.8970	0.0416	0.642	1
159.8921	0.9109	0.048	2
.8976	0.9155	0.082	2

J.D.	Phase	Δ Mag.	Sets
2,428000+			
159.7028	0.9207	0.045	2
.7090	0.9250	0.056	2
.7139	0.9291	0.080	2
.7206	0.9346	0.146	2
.7290	0.9415	0.225	2
.7368	0.9481	0.282	2
.7382	0.9492	0.298	2
.7421	0.9526	0.425	2
.7444	0.9547	0.446	2
.7489	0.9587	0.494	2
.7495	0.9579	0.528	2
.7522	0.9612	0.605	2
.7535	0.9623	0.654	2
.7549	0.9634	0.665	2
.7565	0.9648	0.702	2
.7577	0.9658	0.728	2
.7591	0.9670	0.776	2
.7606	0.9683	0.808	2
.7619	0.9728	0.923	2
.7672	0.9737	0.940	2
.7685	0.9749	0.976	2
.7699	0.9760	1.014	2
.7710	0.9769	1.041	1
.7755	0.9807	1.186	2
.7769	0.9818	1.241	2
.7810	0.9853	1.348	2
.7824	0.9864	1.376	2
.7838	0.9874	1.398	1
.7864	0.9895	1.451	2
.7908	0.9935	1.555	2
.7922	0.9946	1.608	2
.7936	0.9957	1.615	2
.7966	0.9975	1.646	2
.7970	0.9987	1.641	2
.7988	0.0002	1.649	2
.8005	0.0016	1.641	2
.8046	0.0050	1.599	2
.8060	0.0062	1.581	2
.8074	0.0074	1.568	2
.8089	0.0086	1.545	2
.8103	0.0102	1.478	2
.8122	0.0114	1.442	2
.8136	0.0125	1.395	2
.8176	0.0161	1.295	2
.8192	0.0172	1.297	2
.8206	0.0181	1.259	1
.8222	0.0201	1.089	2
.8276	0.0248	1.025	2
.8290	0.0264	0.966	2
.8305	0.0285	0.879	2
.8339	0.0295	0.851	2
.8355	0.0307	0.845	2
.8369	0.0315	0.816	1
.8403	0.0354	0.699	2
.8419	0.0368	0.692	1
179.6102	0.9788	-0.027	3

J.D.	Phase	Δ Mag.	Sets
2,428000+			
179.6185	0.9849	-0.028	3
.6230	0.9884	-0.040	2
242.5898	0.8765	0.004	2
.5928	0.8818	0.009	2
.5980	0.9018	0.014	2
.6024	0.9130	0.014	2
.6119	0.9209	0.027	1
.6182	0.9262	0.027	1
.6210	0.9286	0.080	1
.6278	0.9341	0.134	1
.6304	0.9364	0.152	1
.6366	0.9416	0.202	1
.6381	0.9429	0.222	1
.6431	0.9470	0.334	1
.6466	0.9498	0.355	1
.6480	0.9510	0.390	1
.6531	0.9554	0.460	1
.6561	0.9579	0.555	1
.6615	0.9623	0.645	1
.6641	0.9646	0.692	1
.6693	0.9691	0.770	1
.6708	0.9703	0.842	1
.6749	0.9738	0.972	1
.6773	0.9757	1.040	1
.6825	0.9804	1.196	1
.6861	0.9830	1.263	1
.6895	0.9858	1.543	1
.6921	0.9879	1.596	1
.7045	0.9982	1.643	1
.7072	0.0008	1.609	1
.7112	0.0040	1.630	1
.7140	0.0064	1.605	1
.7184	0.0100	1.478	1
.7212	0.0124	1.428	1
.7258	0.0167	1.230	1
.7312	0.0207	1.146	1
.7410	0.0289	0.960	1
.7444	0.0318	0.776	1
.7515	0.0377	0.695	1
.7535	0.0394	0.602	1
.7585	0.0440	0.482	1
.7649	0.0489	0.378	1
.7700	0.0532	0.309	1
.7739	0.0564	0.288	1
.7788	0.0618	0.192	1
.7804	0.0638	0.152	1
.7885	0.0670	0.110	1
.7894	0.0694	0.084	1
.7951	0.0742	0.052	1
.7976	0.0765	0.052	1
288.8795	0.4589	-0.012	2
.8851	0.4636	0.008	2
.8921	0.4695	0.018	2
.7052	0.4838	0.052	2
.7134	0.4899	0.046	2
.7205	0.4955	0.059	2
.7297	0.5044	0.088	2
.7362	0.5124	0.089	1

Photoelectric Observations of TV Cassiopeiae

J.D.	Phase	Δ Mag.	Sets
2,428000+			
480.8419	0.4974	0.298	2
.8512	0.5065	0.316	2
.8589	0.5068	0.318	2
.8626	0.5104	0.312	1
.8985	0.5255	0.315	2
.7014	0.5302	0.334	2
.7066	0.5350	0.335	2
.7156	0.5331	0.332	2
.7235	0.5419	0.341	2
.7305	0.5482	0.335	2
.7369	0.5508	0.338	2
.7467	0.5552	0.342	2
792.6498	0.8270	0.389	3
.6528	0.8288	0.383	3
.6738	0.8400	0.378	3
.6835	0.8459	0.359	3
.6949	0.8522	0.372	3
.7056	0.8583	0.386	3
.7254	0.8690	0.377	2
.7379	0.8759	0.390	2
.7451	0.8798	0.378	2
810.7786	0.9468	0.356	2
.7870	0.9519	0.385	2
.7946	0.9565	0.370	2
.8031	0.9592	0.382	2
.8108	0.9638	0.373	2
.8183	0.9681	0.386	2
.8267	0.9722	0.385	2

J.D.	Phase	Δ Mag.	Sets
2,428000+			
819.8347	0.6266	0.348	2
.8459	0.6311	0.354	2
.8492	0.6346	0.376	2
.8550	0.6393	0.376	2
.8635	0.6435	0.378	2
.8705	0.6464	0.374	2
.8774	0.6502	0.382	2
826.6553	0.8048	0.354	3
.6638	0.8096	0.366	3
.6725	0.8146	0.374	3
.6820	0.8199	0.370	3
.6904	0.8252	0.385	3
.7054	0.8172	0.389	2
.7131	0.8214	0.382	2
.7430	0.8378	0.388	1
.7565	0.8453	0.389	2
.7653	0.8502	0.316	2
.7722	0.8540	0.316	2
.7818	0.8594	0.327	3
.7953	0.8668	0.365	3
.8027	0.8742	0.307	3
.8206	0.8808	0.313	3
.8335	0.8878	0.316	3
.8452	0.8944	0.313	3
.8599	0.9006	0.316	3
.8705	0.9064	0.309	3
.8828	0.9132	0.310	3
.8948	0.9217	0.317	3

J.D.	Phase	Δ Mag.	Sets
2,428000+			
826.8060	0.8878	0.338	3
827.5416	0.8766	0.343	3
.5538	0.8848	0.339	3
.5624	0.8901	0.343	3
.5763	0.8990	0.348	3
.5839	0.9014	0.338	3
.5920	0.9064	0.332	2
.6000	0.9103	0.328	2
.6078	0.9148	0.296	2
.6149	0.9191	0.300	2
.6238	0.9257	0.298	2
.6303	0.9278	0.293	2
.6398	0.9311	0.217	2
.6438	0.9347	0.172	2
.6506	0.9389	0.132	2
.7561	0.9429	0.105	2
.7646	0.9464	0.095	2
.7710	0.9500	0.092	2
.7779	0.9535	-0.054	2
.7865	0.9580	-0.080	2
.7932	0.9617	-0.158	2
.8029	0.9654	-0.215	2
.7098	0.9709	-0.338	1
.7128	0.9728	-0.321	2
.7459	0.9913	-0.677	2
.7550	0.9964	-0.719	2
.7585	0.0004	-0.716	2
.7700	0.0068	-0.710	2

Table 12 (cont'd)

Photoelectric Observations of TV Cassiopeiae

J.D.	Phase	Δ Mag.	Sets
2,433000+			
827.7781	0.0091	−0.667	2
.7851	0.0135	−0.646	2
.7926	0.0171	−0.570	2
.7996	0.0205	−0.525	1
.8063	0.0265	−0.380	2
.8157	0.0296	−0.354	2
.8292	0.0374	−0.202	2
.8368	0.0415	−0.120	2
.8438	0.0452	−0.064	2
.8506	0.0491	−0.029	2
.8569	0.0528	0.012	1
.8724	0.0611	0.122	2
.8792	0.0649	0.168	2
.8871	0.0692	0.196	2
.8942	0.0732	0.234	2
.9020	0.0775	0.269	2
.9122	0.0831	0.318	3
834.8292	0.7869	0.310	3
.8368	0.7942	0.341	3
.8427	0.8421	0.354	3
.7349	0.8472	0.354	3
.7456	0.8531	0.338	3
.7540	0.8632	0.328	3
.7737	0.8683	0.348	3
.7826	0.8735	0.336	3
.7906	0.8780	0.351	3
.8003	0.8835	0.341	3
.8069	0.8886	0.342	3
.8208	0.8946	0.352	3
.8313	0.9004	0.336	2
849.5984	0.0309	−0.319	2
.6765	0.0353	−0.276	2
.6861	0.0401	−0.168	2
.6924	0.0441	−0.139	2
.6038	0.0498	−0.005	2
.6092	0.0535	0.040	2
.6148	0.0564	0.074	2
.6213	0.0600	0.125	2
.6288	0.0651	0.142	2
.6326	0.0663	0.176	2
.6329	0.0703	0.217	2
.6464	0.0739	0.254	2
.6532	0.0771	0.254	2
.6690	0.0974	0.326	3
.6978	0.1081	0.326	3
.7063	0.1089	0.325	3
.7135	0.1109	0.339	2
869.5730	0.1008	0.324	2
.5825	0.1088	0.342	3
.5982	0.1112	0.355	3
.6041	0.1177	0.343	3
.6138	0.1231	0.346	3
.6264	0.1300	0.332	3
.6326	0.1335	0.366	1
.6818	0.1606	0.347	2
.6908	0.1666	0.367	3
.7001	0.1707	0.358	3
.7089	0.1765	0.374	3
.7172	0.1801	0.376	3
.7251	0.1845	0.368	2
.7309	0.1877	0.362	2
2,433000+			
155.6967	0.9173	0.282	2
.7038	0.9211	0.286	2
.7081	0.9241	0.262	2
.7130	0.9268	0.268	2
.7185	0.9296	0.277	2
.7234	0.9325	0.300	2
.7290	0.9357	0.301	2
.7338	0.9383	0.148	2
.7385	0.9408	0.094	2
.7435	0.9437	0.069	2
.7469	0.9472	0.052	2
.7550	0.9500	−0.001	2
.7625	0.9542	−0.041	2
175.5808	0.8863	0.348	3
.5906	0.8937	0.323	3
.5998	0.8998	0.346	3
.6065	0.9035	0.326	3
.6147	0.9070	0.348	2
.6198	0.9096	0.325	2
.6239	0.9121	0.326	2

J.D.	Phase	Δ Mag.	Sets
2,433000+			
182.6751	0.8028	0.356	3
.6799	0.8066	0.361	3
.7010	0.8166	0.362	3
.7136	0.8226	0.366	2
.7221	0.8263	0.356	2
184.6876	0.9138	0.321	2
.6933	0.9158	0.302	2
.6998	0.9190	0.289	2
.7040	0.9217	0.276	2
.7096	0.9247	0.256	2
.7156	0.9282	0.220	2
.7217	0.9314	0.218	2
.7276	0.9347	0.185	2
.7331	0.9377	0.156	2
.7394	0.9412	0.134	2
.7565	0.9519	−0.005	1
.7642	0.9549	−0.039	2
.7690	0.9580	−0.103	2
.7762	0.9615	−0.140	2
.7798	0.9635	−0.170	2
.7836	0.9656	−0.192	2
.7883	0.9682	−0.252	2
.7949	0.9718	−0.328	2
.7990	0.9741	−0.384	2
.8032	0.9764	−0.384	2
.8088	0.9795	−0.440	2
.8128	0.9817	−0.470	2
.8168	0.9839	−0.501	2
.8231	0.9874	−0.654	2
.8279	0.9900	−0.677	2
.8327	0.9927	−0.700	2
.8379	0.9955	−0.708	2
.8425	0.9981	−0.716	2
.8471	0.0006	−0.732	2
.8518	0.0032	−0.696	2
.8565	0.0058	−0.700	2
.8611	0.0083	−0.696	2
.8657	0.0114	−0.660	2
.8707	0.0135	−0.628	2
.8747	0.0158	−0.600	2
.8797	0.0185	−0.548	2
.8839	0.0206	−0.451	2
.8898	0.0237	−0.320	2
.9042	0.0321	−0.301	2
.9087	0.0346	−0.278	2
.9142	0.0376	−0.216	2
.9163	0.0388	−0.212	1
.9284	0.0455	−0.080	2
185.5870	0.4533	0.337	3
.6831	0.4618	0.331	3
.7012	0.4718	0.328	3
.7136	0.4786	0.316	3
.7225	0.4836	0.326	2
.7308	0.4882	0.295	2
.8299	0.5483	0.338	3
.8513	0.5595	0.342	3
189.6723	0.6627	0.367	3
.6794	0.6666	0.371	3
.6902	0.6726	0.365	3
.7022	0.6795	0.376	3
.7094	0.6838	0.377	3
.7186	0.6882	0.383	3
.7522	0.7068	0.381	3
.7690	0.7165	0.377	3
.7885	0.7158	0.372	3
.7765	0.7202	0.373	3
.7949	0.7248	0.381	3
.7923	0.7289	0.386	3
.8003	0.7332	0.377	3
.8079	0.7376	0.383	3
212.7231	0.3799	0.369	3
.7314	0.3845	0.368	3
.7396	0.3890	0.371	3
.7471	0.3931	0.378	3
.7538	0.3968	0.385	3
.7590	0.3997	0.378	3
.7694	0.4049	0.374	3
.7768	0.4094	0.376	3
.7837	0.4133	0.369	3
.7914	0.4176	0.368	3
.7988	0.4217	0.366	3
.8060	0.4256	0.361	3
.8128	0.4297	0.347	3

J.D.	Phase	Δ Mag.	Sets
2,433000+			
218.6214	0.4341	0.351	3
.6299	0.4388	0.346	3
.6372	0.4428	0.342	3
.6449	0.4471	0.346	3
.6531	0.4516	0.329	3
.6606	0.4558	0.340	3
.6676	0.4594	0.329	3
.6744	0.4634	0.331	3
.6817	0.4674	0.329	3
.6898	0.4719	0.341	3
.6974	0.4761	0.327	3
.7047	0.4801	0.339	3
.9106	0.4833	0.328	2
.9147	0.4856	0.305	2
219.7688	0.9568	−0.080	2
.7732	0.9593	−0.118	2
.7775	0.9618	−0.134	2
.7816	0.9639	−0.178	2
.7859	0.9662	−0.216	2
.7897	0.9683	−0.270	2
.7963	0.9731	−0.396	2
.8017	0.9760	−0.434	2
.8051	0.9788	−0.461	2
.8107	0.9799	−0.510	2
.8149	0.9822	−0.535	2
.8190	0.9845	−0.560	2
.8231	0.9868	−0.640	2
.8289	0.9899	−0.660	2
.8308	0.9910	−0.670	2
.8356	0.9937	−0.685	2
.8404	0.9963	−0.682	2
.8453	0.9990	−0.693	2
.8501	0.0017	−0.715	2
.8540	0.0038	−0.710	2
.8578	0.0059	−0.693	2
.8630	0.0088	−0.682	2
.8680	0.0109	−0.664	2
.8710	0.0128	−0.646	2
.8779	0.0170	−0.556	3
.8863	0.0227	−0.434	2
.8902	0.0249	−0.382	2
.8962	0.0271	−0.344	2
221.5886	0.2874	0.362	3
.5954	0.2918	0.367	3
.6417	0.3247	0.361	3
.5514	0.3001	0.375	3
.5576	0.3036	0.372	3
.5653	0.3077	0.383	3
.5719	0.3114	0.364	3
.5792	0.3154	0.376	3
.5854	0.3188	0.386	3
.5917	0.32023	0.374	3
.5979	0.3257	0.376	3
.6042	0.3293	0.382	3
224.6035	0.0011	−0.694	2
.6097	0.0041	−0.689	2
.6156	0.0079	−0.689	2
.6198	0.0102	−0.662	2
.6240	0.0125	−0.645	2
.6288	0.0152	−0.617	2
.6330	0.0175	−0.565	2
.6372	0.0198	−0.523	2
.6442	0.0237	−0.481	2
.6483	0.0259	−0.445	2
.6525	0.0282	−0.407	2
.6581	0.0313	−0.326	2
.6622	0.0338	−0.307	2
.6664	0.0356	−0.279	2
.6716	0.0388	−0.206	2
.6803	0.0436	−0.157	2
.6853	0.0463	−0.118	2
.6904	0.0492	−0.085	2
.6963	0.0524	−0.028	2
.6804	0.0541	0.003	1
.7005	0.0547	0.062	2
.7035	0.0564	0.077	2
.7061	0.0575	0.080	2
.7083	0.0590	0.092	2
.7122	0.0612	0.125	2
.7170	0.0638	0.159	2
.7208	0.0659	0.182	2
.7247	0.0681	0.194	2

Table 12 (cont'd)

Photoelectric Observations of VV Orionis

J.D.	Phase	Δ Mag	Sets
2,432000+			
129.7150	0.9725	-0.174	1
.7276	0.9762	-0.180	1
.7329	0.9844	-0.183	1
.7416	0.9904	-0.190	1
.7502	0.9952	-0.192	1
.7583	0.0027	-0.178	1
.7707	0.0100	-0.178	1
.7823	0.0176	-0.185	1
.8100	0.0394	-0.157	1
.8160	0.0418	-0.134	1
.8245	0.0462	-0.094	1
.8300	0.0500	-0.060	1
.8408	0.0572	-0.062	1
.8496	0.0632	-0.008	1
.8578	0.0687	0.036	1
.8682	0.0745	0.057	1
129.7768	0.0784	0.040	1
.7842	0.0788	0.068	1
.7926	0.0841	0.065	1
.8008	0.0898	0.078	1
.8094	0.0965	0.087	1
.8190	0.1019	0.104	1
193.5396	0.0090	-0.181	2
202.5128	0.9822	-0.178	1
.5195	0.9870	-0.190	1
.5262	0.9913	-0.197	1
.5320	0.9960	-0.198	1
.5384	0.0004	-0.190	1
.5401	0.0048	-0.198	1
.5546	0.0105	-0.189	1
.5654	0.0177	-0.180	1
.5729	0.0228	-0.170	1
.5812	0.0283	-0.163	1
.5872	0.0324	-0.132	1
.5940	0.0370	-0.116	1
.6004	0.0418	-0.104	1
.6068	0.0456	-0.074	1
.6348	0.0644	0.028	1
.6414	0.0689	0.044	1
.6480	0.0733	0.081	1
.6541	0.0774	0.100	1
.6598	0.0813	0.116	1
.6732	0.0856	0.128	1
.6985	0.0959	0.116	1
.6981	0.1082	0.106	2
210.5708	0.4070	0.128	1
.5858	0.4169	0.128	1
.6010	0.4272	0.094	1
.6206	0.4472	0.058	1
239.5107	0.0818	0.054	1
.5282	0.9408	0.002	1
.6014	0.9496	-0.060	1
.6128	0.9594	-0.112	1
.6256	0.9696	-0.150	1
.6352	0.9784	-0.178	1
.6390	0.9774	-0.184	1
.6510	0.9830	-0.180	1
.6580	0.9878	-0.170	1
.6652	0.9928	-0.177	1
.6907	0.0030	-0.184	1
245.7283	0.0632	-0.082	1
.7417	0.0645	-0.084	1
.7468	0.0648	-0.012	1
.7480	0.0667	-0.007	1
.7508	0.0690	0.000	1
.7525	0.0694	0.012	1
.7542	0.0642	0.022	1
.7597	0.0668	0.020	1
.7651	0.0699	0.040	1
.7684	0.0711	0.040	1
.7699	0.0735	0.078	1
.7727	0.0767	0.088	1
.7774	0.0786	0.102	1
.7808	0.0807	0.122	1
.7828	0.0828	0.121	1
.7868	0.0848	0.128	1
.7894	0.0866	0.128	1
.7927	0.0888	0.124	1
.7958	0.0909	0.112	1
.7995	0.0934	0.104	1
.8035	0.0961	0.106	1
.8065	0.0981	0.108	1
.8092	0.0999	0.111	1
.8119	0.1017	0.116	1
259.6100	0.4853	0.018	1
.6228	0.4940	-0.004	1
.7008	0.5455	0.044	2
.7129	0.5548	0.056	2
.7271	0.5642	0.078	2
.7476	0.5779	0.095	2
264.6078	0.6499	0.150	1
.6265	0.6626	0.116	2
.6484	0.6772	0.120	2
.6579	0.6836	0.115	2
.6738	0.6943	0.120	2

J.D.	Phase	Δ Mag.	Sets
2,432000+			
924.6838	0.9010	0.128	2
.6961	0.9088	0.122	2
.7068	0.9161	0.132	2
925.5427	0.5028	0.004	2
.5589	0.5197	-0.005	2
.5865	0.5167	0.007	2
.5760	0.5228	-0.009	2
.5885	0.5296	0.000	2
.6003	0.5376	0.018	2
.6094	0.5437	0.028	2
.6184	0.5484	0.044	1
.6415	0.5663	0.094	2
.6519	0.5722	0.114	2
.6622	0.5785	0.128	2
.6742	0.5878	0.142	2
.6856	0.5960	0.150	2
.6962	0.6018	0.132	2
.7049	0.6080	0.152	2
.7165	0.6170	0.135	2
946.5427	0.8942	0.110	2
.5544	0.8992	0.122	2
.5667	0.9034	0.122	2
.5778	0.9079	0.105	2
.5898	0.9153	0.122	2
.5948	0.9223	0.120	2
.6097	0.9294	0.044	2
.6167	0.9341	0.042	1
.6307	0.9435	-0.004	2
.6432	0.9519	-0.044	2
.6541	0.9595	-0.135	2
.6634	0.9649	-0.130	1
948.5201	0.6897	0.141	1
.5274	0.6936	0.134	1
.5339	0.6979	0.124	1
.5387	0.9012	0.118	1
.5440	0.9047	0.108	1
.5594	0.9104	0.088	1
.5708	0.9228	0.074	1
.5758	0.9262	0.080	1
.5808	0.9296	0.060	1
.5861	0.9331	0.044	1
.5988	0.9378	0.012	1
.5997	0.9422	-0.002	1
.6115	0.9508	-0.052	1
.6229	0.9579	-0.082	1
.6282	0.9614	-0.104	1
.6356	0.9651	-0.127	1
.6401	0.9694	-0.156	1
.6468	0.9740	-0.186	1
.6522	0.9778	-0.183	1
.6576	0.9812	-0.172	1
.6638	0.9853	-0.186	1
.6701	0.9898	-0.200	1
.6779	0.9948	-0.192	1
.6844	0.9992	-0.184	1
.6904	0.0032	-0.192	1
.6948	0.0065	-0.184	1
.6996	0.0094	-0.176	1
.7048	0.0139	-0.198	1
976.5482	0.0819	0.094	2
.5489	0.0837	0.100	2
.5531	0.0865	0.110	2
.5556	0.0883	0.106	2
.5579	0.0897	0.116	2
.5621	0.0922	0.119	2
.5669	0.0957	0.124	2
.5694	0.0974	0.122	2
.5750	0.1015	0.130	2
.5795	0.1045	0.130	2
.5831	0.1067	0.136	2
980.5490	0.7745	0.148	3
.5522	0.7767	0.154	3
.5589	0.7822	0.158	3
.5625	0.7853	0.168	3
.5722	0.7921	0.178	3
.5853	0.7996	0.182	3
982.5497	0.1213	0.122	2
.5568	0.1279	0.122	2
.5654	0.1338	0.118	2
.5727	0.1388	0.125	2
.5794	0.1435	0.132	2
.5871	0.1485	0.144	2
.5930	0.1526	0.130	2
.6000	0.1571	0.141	2
.6078	0.1624	0.134	3
988.5545	0.1658	0.142	3
.5606	0.1698	0.138	3
.5666	0.1737	0.142	3
.5716	0.1771	0.148	3
.5784	0.1816	0.158	3
.5840	0.1854	0.163	3
.5924	0.1910	0.162	3
.5944	0.1924	0.160	3
.5989	0.1954	0.167	3
994.5872	0.2125	0.160	3

J.D.	Phase	Δ Mag.	Sets
2,432000+			
994.5776	0.8256	0.148	3
2,433000+			
179.6535	0.9887	-0.078	2
.6598	0.9898	-0.095	2
.6642	0.9929	-0.113	2
.6682	0.9965	-0.138	2
.6744	0.9701	-0.186	2
.6787	0.9738	-0.170	2
.6847	0.9787	-0.178	2
.6910	0.9809	-0.178	2
.6964	0.9848	-0.171	2
.7014	0.9879	-0.173	2
.7065	0.9914	-0.178	2
.7129	0.9957	-0.167	2
.7192	0.9999	-0.182	2
.7235	0.0027	-0.176	2
.7286	0.0062	-0.176	2
.7359	0.0112	-0.180	3
182.6132	0.9482	-0.097	2
.6180	0.9520	-0.080	2
.6230	0.9558	-0.095	2
.6318	0.9607	-0.113	2
.6374	0.9648	-0.121	2
.6428	0.9690	-0.157	2
.6482	0.9718	-0.166	2
.6535	0.9764	-0.170	2
.6583	0.9788	-0.168	2
.6638	0.9825	-0.184	2
.6699	0.9861	-0.180	2
.6761	0.9896	-0.190	2
.6811	0.9938	-0.182	2
.6886	0.9989	-0.174	3
.6965	0.0039	-0.178	2
.6993	0.0064	-0.186	2
.7049	0.0100	-0.181	2
.7108	0.0136	-0.170	2
.7167	0.0172	-0.180	2
.7218	0.0211	-0.188	2
.7282	0.0256	-0.177	2
188.6253	0.9946	-0.174	2
.6316	0.9987	-0.184	2
.6354	0.0018	-0.184	2
.6427	0.0061	-0.178	2
.6476	0.0094	-0.171	2
.6538	0.0138	-0.178	2
.6588	0.0170	-0.179	2
.6628	0.0197	-0.188	2
.6681	0.0232	-0.182	2
.6728	0.0262	-0.174	2
.6794	0.0308	-0.180	2
.6856	0.0350	-0.148	2
.6914	0.0389	-0.158	2
.6972	0.0428	-0.089	2
.9017	0.0469	-0.075	2
.9068	0.0498	-0.046	2
.9108	0.0518	-0.051	2
.9150	0.0548	-0.014	2
.9219	0.0595	-0.018	2
.9287	0.0650	-0.008	2
.9338	0.0648	0.000	2
.9376	0.0700	0.009	2
189.5269	0.6697	0.126	3
.6351	0.6742	0.151	3
.6459	0.6808	0.148	3
.6514	0.6856	0.158	3
.6608	0.4915	0.152	3
.6661	0.6955	0.154	3
.6787	0.7038	0.154	3
.6861	0.7086	0.167	3
.6941	0.7140	0.166	3
.9012	0.7187	0.162	3
.9156	0.7217	0.172	3
.9276	0.7298	0.176	3
.9340	0.7341	0.182	2
.9397	0.7375	0.186	2
200.7655	0.0456	-0.094	2
.7692	0.0496	-0.048	2
.7751	0.0535	-0.028	2
.8006	0.0672	-0.008	2
.8049	0.0701	-0.004	2
.8082	0.0730	0.003	2
.8109	0.0676	0.016	2
.8139	0.0702	0.051	2
.8240	0.0750	0.062	2
.8295	0.0797	0.082	2
.8340	0.0797	0.105	2
.8396	0.0827	0.124	2
.8440	0.0864	0.134	2
.8482	0.0895	0.134	2
.8524	0.0921	0.132	2
.8595	0.0962	0.139	2
.8628	0.0990	0.137	2
.8668	0.1018	0.143	2
.8725	0.1066	0.142	2

Table 12 (cont'd)

Photoelectric Observations of VV Orionis

J.D.	Phase	Δ Mag.	Sets
2,428000+			
200.9784	0.1063	0.148	2
.9808	0.1111	0.150	2
.9865	0.1151	0.153	2
.9910	0.1181	0.150	2
.9966	0.1232	0.142	2
.0049	0.1274	0.139	2
.0089	0.1301	0.136	2
202.9038	0.4060	0.159	2
.9060	0.4089	0.122	2
.9122	0.4116	0.132	2
.9189	0.4161	0.115	2
.9252	0.4190	0.119	2
.9278	0.4230	0.124	2
.9336	0.4260	0.108	2
.9426	0.4321	0.085	2
.9467	0.4348	0.091	2
.9507	0.4376	0.092	2
.9579	0.4424	0.079	2
.9690	0.4489	0.057	2
.9751	0.4540	0.042	2
.9818	0.4581	0.031	2
212.9128	0.8860	0.134	2
.9215	0.8912	0.128	2
.9330	0.8984	0.119	2

J.D.	Phase	Δ Mag.	Sets
2,428000+			
213.9390	0.9088	0.119	2
.9464	0.9080	0.126	2
.9519	0.9117	0.120	2
.9585	0.9161	-0.116	2
220.6343	0.9735	-0.165	2
.6415	0.9783	-0.144	2
.6472	0.9822	-0.150	2
.6528	0.9859	-0.159	2
.6606	0.9912	-0.168	2
.6663	0.9970	-0.175	2
.6754	0.0012	-0.191	2
.6821	0.0043	-0.201	2
.6860	0.0076	-0.194	2
.6890	0.0103	-0.192	2
.6930	0.0130	-0.205	2
.6996	0.0174	-0.179	2
.7039	0.0205	-0.179	2
.7063	0.0223	-0.177	2
.7139	0.0271	-0.169	2
.7181	0.0299	-0.169	2
.7222	0.0327	-0.153	2
.7278	0.0364	-0.129	2
.7317	0.0391	-0.116	2

J.D.	Phase	Δ Mag.	Sets
2,428000+			
255.7355	0.0416	-0.107	2
.7403	0.0449	-0.078	2
.7446	0.0479	-0.057	2
.7494	0.0510	-0.042	2
.7551	0.0548	-0.022	2
.7589	0.0574	-0.012	2
.7627	0.0599	0.000	2
.7678	0.0632	0.017	2
.7697	0.0646	0.022	1
.7811	0.0723	0.063	1
.7832	0.0737	0.074	2
.7881	0.0770	0.088	2
.7951	0.0817	0.101	2
.7996	0.0848	0.111	2
.8052	0.0886	0.111	2
.8119	0.0930	0.109	2
.8162	0.0959	0.106	2
.8203	0.0990	0.106	2
.8251	0.1019	0.110	2
.8307	0.1057	0.125	2
.8347	0.1084	0.130	2
.8414	0.1129	0.131	2
.8461	0.1174	0.121	2

Photoelectric Observations of VV Aurigae

J.D.	Phase	Δ Mag.	Sets
2,428000+			
478.8231	0.5605	0.002	2
.8315	0.5638	0.005	2
.8382	0.5669	0.018	2
.8458	0.5695	0.016	2
.8546	0.5769	0.006	2
.8729	0.5802	0.018	2
480.7040	0.9232	0.020	2
.7126	0.9298	0.018	2
.7805	0.9397	0.016	2
.7998	0.9430	0.011	2
.8071	0.9453	0.008	2
.8255	0.9488	0.008	1
.8311	0.9558	0.032	1
.8358	0.9578	0.045	1
.8335	0.9595	0.052	1
.8341	0.9610	0.062	1
.8376	0.9634	0.072	1
.8414	0.9659	0.085	1
.8451	0.9683	0.105	1
.8490	0.9699	0.120	1
.8538	0.9684	0.146	1
.8570	0.9701	0.170	1
.8611	0.9717	0.185	1
.8648	0.9731	0.215	1
.8681	0.9745	0.238	1
.8713	0.9757	0.262	1
.8767	0.9776	0.286	1
.8810	0.9798	0.328	1
.8847	0.9810	0.358	1
.8881	0.9824	0.405	1
.8923	0.9840	0.432	1
.8958	0.9854	0.462	1
.9004	0.9868	0.539	1
.9048	0.9910	0.598	1
.9128	0.9928	0.642	1
.9187	0.9945	0.662	1
.9231	0.9958	0.702	1
.9289	0.9977	0.727	1
528.8957	0.9824	0.827	1
.8992	0.9842	0.885	1
.9040	0.9857	0.707	1
.9072	0.9870	0.709	1
.9010	0.9865	0.709	1
.9041	0.9887	0.712	1
535.8801	0.7005	0.004	3
.9010	0.7708	-0.005	3
.9211	0.7788	-0.006	3
.9316	0.7839	-0.008	3
.9405	0.7894	0.001	2
.9486	0.7896	0.000	2
567.8722	0.3980	0.007	3
.8819	0.3998	0.017	3
.9005	0.4002	-0.004	2
619.8389	0.9318	-0.007	2
.8448	0.9348	-0.005	2
.8516	0.9372	0.006	2
.8569	0.9397	0.002	2
.8637	0.9424	0.002	2
.8708	0.9450	-0.002	2
.8765	0.9474	0.002	2
.8810	0.9492	-0.014	2

J.D.	Phase	Δ Mag.	Sets
2,428000+			
619.8899	0.9626	0.018	1
.8934	0.9641	0.030	1
.8972	0.9656	0.035	1
.9006	0.9670	0.042	1
.9038	0.9683	0.060	1
.9080	0.9699	0.070	1
.9118	0.9714	0.080	1
.9151	0.9727	0.090	1
622.8481	0.1242	0.028	3
.8582	0.1284	0.020	3
.8662	0.1328	0.021	3
.8805	0.1389	0.019	3
.8924	0.1417	0.016	3
.9127	0.1462	0.025	3
.9192	0.1486	0.029	2
.9196	0.1526	0.015	2
640.5674	0.8802	-0.009	3
.5776	0.8845	-0.002	3
.5884	0.2886	0.015	3
.5960	0.2927	-0.006	3
.6078	0.2981	-0.001	2
666.6815	0.4787	0.255	1
.6931	0.4832	0.300	1
.6969	0.4903	0.317	1
.7005	0.4928	0.495	1
.7034	0.4955	0.515	1
.7080	0.4951	0.527	1
.7110	0.4963	0.547	1
.7147	0.4978	0.570	1
.7177	0.4990	0.590	1
.7206	0.5001	0.627	1
.7235	0.5038	0.615	1
.7265	0.5048	0.580	1
.7256	0.5061	0.517	1
.7286	0.5074	0.513	1
.7293	0.5100	0.380	1
.7309	0.5161	0.355	1
.7340	0.5173	0.328	1
.7363	0.5190	0.348	1
.7710	0.5201	0.340	1
.7737	0.5211	0.322	1
.7765	0.5223	0.310	1
.7792	0.5233	0.308	1
.7820	0.5244	0.290	1
.7848	0.5255	0.270	1
.7888	0.5271	0.216	1
.7920	0.5284	0.175	1
.7951	0.5296	0.186	1
.7979	0.5307	0.165	1
.8006	0.5318	0.150	1
.8048	0.5335	0.120	1
.8076	0.5345	0.125	1
.8117	0.5362	0.112	1
.8144	0.5373	0.106,	1
.8180	0.5387	0.098	1
.8286	0.5430	0.072	1
.8316	0.5441	0.060	1
.8365	0.5459	0.041	2
.8444	0.5491	0.048	2
.8520	0.5522	0.020	2
.8579	0.5545	0.046	2

J.D.	Phase	Δ Mag.	Sets
2,428000+			
669.7519	0.9086	0.025	3
.7609	0.9181	0.027	3
.7699	0.9157	0.021	3
.7795	0.9194	0.022	3
.7880	0.9238	0.015	3
.7969	0.9284	0.020	2
692.7052	0.0782	0.044	3
.7146	0.0819	0.032	3
.7276	0.0910	0.027	3
.7475	0.0960	0.035	3
.7605	0.1000	0.027	3
.7727	0.1049	0.021	3
.7812	0.1083	0.018	3
907.7401	0.0327	0.147	2
.7480	0.0350	0.155	2
.7522	0.0376	0.140	2
.7596	0.0404	0.100	3
.7705	0.0471	0.068	3
.7849	0.0604	0.032	3
.7944	0.0548	0.026	3
.8033	0.0577	0.042	3
.8119	0.0611	0.054	3
.8211	0.0648	0.053	3
.8293	0.0680	0.062	3
.8385	0.0717	0.042	3
.8464	0.0740	0.057	2
.8517	0.0759	0.052	2
938.6788	0.4823	0.532	1
.6821	0.4846	0.555	2
.6869	0.4868	0.602	2
.6903	0.4888	0.587	2
.6993	0.5015	0.558	3
.7028	0.5052	0.564	3
.7072	0.5048	0.574	3
.7117	0.5094	0.548	3
.7159	0.5094	0.602	2
.7206	0.5100	0.480	3
.7243	0.5114	0.475	3
.7285	0.5130	0.449	3
.7328	0.5150	0.427	2
.7374	0.5168	0.401	3
.7427	0.5186	0.363	3
.7462	0.5200	0.363	3
.7504	0.5217	0.351	3
.7544	0.5233	0.350	3
.7590	0.5251	0.322	3
.7633	0.5268	0.353	3
939.7527	0.3147	0.000	3
.7610	0.3179	-0.007	3
.7698	0.3212	-0.014	3
.7774	0.3244	-0.017	3
.7841	0.3271	-0.018	2
945.5455	0.0047	0.567	1
.5512	0.0070	0.559	1
.5572	0.0093	0.552	1
.5634	0.0118	0.567	1
.5695	0.0139	0.522	1
.5752	0.0157	0.497	1
.5787	0.0179	0.451	1
.5854	0.0205	0.359	1
.5904	0.0225	0.332	1

Table 12 (cont'd)

Photoelectric Observations of BW Aurigae

J.D.	Phase	Δ Mag.	Sets
2,433000+			
945.5961	0.0249	0.295	1
.6020	0.0271	0.240	1
.6079	0.0291	0.192	1
.6119	0.0310	0.172	1
.6174	0.0332	0.155	1
.6198	0.0341	0.140	1
.6243	0.0359	0.102	1
.6284	0.0391	0.075	1
.6331	0.0475	0.042	1
.6374	0.0490	0.018	1
946.7079	0.4651	0.167	1
.7107	0.4682	0.167	1
.7247	0.4717	0.190	1
.7311	0.4743	0.215	1
.7393	0.4775	0.255	1
.7462	0.4802	0.347	1
956.7756	0.4124	-0.008	1
.7809	0.4157	0.010	2
.7918	0.4187	0.015	2
.7953	0.4202	0.012	2
.8040	0.4217	0.026	3
.7028	0.4232	0.022	2
.7059	0.4248	0.012	2
.7103	0.4261	-0.014	2
.7148	0.4277	0.005	2
.7180	0.4296	0.026	2
.7215	0.4308	0.026	2
.7253	0.4321	0.008	2
.7294	0.4337	0.020	2
.7328	0.4350	0.020	2
.7352	0.4364	0.024	2
.7415	0.4386	0.026	2
.7455	0.4401	0.025	2
.7490	0.4418	0.022	2
.7538	0.4439	0.022	2
.7556	0.4441	0.018	2
.7599	0.4454	0.029	1
964.6521	0.5727	0.022	3
.6625	0.5764	0.022	3
.6707	0.5810	0.011	3
.6794	0.5856	0.028	3
.6921	0.5897	0.027	3
970.6028	0.3036	0.009	3
.6097	0.3060	0.023	3
.6145	0.3083	0.016	3
.6199	0.3104	0.018	3
988.6087	0.0260	0.023	3
.6141	0.0601	0.028	3
.6197	0.0622	0.029	3
.6247	0.0643	0.025	3
.6314	0.0670	0.031	3
.6360	0.0690	0.032	3
.6418	0.0711	0.021	3
.6465	0.0732	0.019	3
.6570	0.0771	0.016	3
.6647	0.0802	0.027	3
.6694	0.0820	0.020	3
.6758	0.0844	0.019	3
.6801	0.0865	0.017	3
.6944	0.0920	0.046	2
.6978	0.0938	0.041	2
994.6044	0.4585	0.035	2
.6099	0.4606	0.060	2
.6156	0.4626	0.049	2
.6219	0.4650	0.082	2
.6269	0.4669	0.086	2
2,433000+			
215.7361	0.0098	0.611	2
.7425	0.0118	0.549	2
.7494	0.0145	0.480	2
.7563	0.0169	0.449	2
.7597	0.0183	0.408	2
.7639	0.0202	0.377	2
.7687	0.0222	0.355	2
.7732	0.0240	0.320	2
.7777	0.0257	0.298	2
.7835	0.0280	0.250	2
.7897	0.0305	0.199	2
.7945	0.0325	0.162	2
.8010	0.0350	0.142	2
.8041	0.0368	0.120	2
.8090	0.0381	0.102	2
.8131	0.0398	0.089	2
.8175	0.0414	0.082	2
.8239	0.0438	0.056	2
.8280	0.0451	0.054	3
.8297	0.0461	0.041	3
.8438	0.0518	0.044	3
.8490	0.0545	0.056	3
.8560	0.0579	0.035	3
.8668	0.0606	0.035	3
.8722	0.0628	0.042	3
.8785	0.0657	0.036	3

J.D.	Phase	Δ Mag.	Sets
2,433000+			
215.8851	0.0683	0.054	3
.8925	0.0712	0.055	3
.9001	0.0742	0.053	3
.9065	0.0764	0.059	2
225.6965	0.9642	0.052	3
.7042	0.9673	0.068	3
.7104	0.9697	0.077	3
.7181	0.9838	0.114	2
.7221	0.9844	0.145	2
.7261	0.9859	0.159	2
.7317	0.9881	0.162	2
.7380	0.9899	0.178	2
.7424	0.9718	0.204	2
.7489	0.9739	0.249	2
.7540	0.9746	0.288	1
.7547	0.9773	0.295	2
.7587	0.9789	0.330	2
.7638	0.9804	0.355	2
.7676	0.9824	0.414	2
.7714	0.9839	0.448	2
.7759	0.9854	0.472	2
.7804	0.9874	0.539	2
.7842	0.9890	0.569	2
.7881	0.9905	0.586	2
.7933	0.9926	0.650	2
.7976	0.9943	0.662	2
.8017	0.9959	0.704	2
.8078	0.9981	0.787	2
.8110	0.9996	0.745	2
.8149	0.0011	0.748	2
.8232	0.0040	0.706	2
.8282	0.0056	0.701	2
.8308	0.0078	0.678	2
.8358	0.0094	0.605	2
.8410	0.0114	0.602	2
.8468	0.0135	0.582	2
.8501	0.0150	0.479	2
.8539	0.0166	0.447	2
.8577	0.0181	0.451	2
.8622	0.0198	0.392	2
.8664	0.0215	0.344	2
.8708	0.0232	0.311	2
.8765	0.0254	0.273	2
.8795	0.0265	0.242	1
249.8799	0.4598	0.065	2
.8860	0.4626	0.088	2
.8898	0.4645	0.071	2
.8963	0.4674	0.085	2
.7021	0.4719	0.096	2
.7071	0.4738	0.110	2
.7140	0.4768	0.139	2
.7197	0.4789	0.175	2
.7261	0.4710	0.199	2
.7296	0.4728	0.219	2
.7342	0.4748	0.249	2
.7397	0.4769	0.276	2
.7450	0.4794	0.317	2
.7510	0.4818	0.348	2
.7557	0.4832	0.376	2
.7618	0.4865	0.427	2
.7662	0.4870	0.451	2
.7695	0.4895	0.486	2
.7739	0.4912	0.494	2
.7821	0.4933	0.517	2
.7848	0.4945	0.533	2
.7891	0.4964	0.558	2
.7929	0.4975	0.571	2
.7967	0.4994	0.570	2
.8016	0.5013	0.581	2
.8058	0.5029	0.582	2
.8098	0.5045	0.598	2
.8138	0.5065	0.549	2
.8166	0.5078	0.528	3
.8207	0.5115	0.445	3
.8255	0.5139	0.416	3
.8314	0.5157	0.420	3
.8424	0.5197	0.366	2
.8502	0.5207	0.323	2
.8564	0.5230	0.277	2
.8607	0.5247	0.252	2
.8651	0.5265	0.231	2
.8706	0.5287	0.211	2
.8750	0.5304	0.198	2
.8793	0.5321	0.185	2
.8838	0.5347	0.139	2
.8903	0.5368	0.128	2
.8963	0.5386	0.105	2
.9008	0.5406	0.078	2
.9065	0.5424	0.065	2
.9098	0.5446	0.057	2
.9124	0.5454	0.048	2
.9165	0.5480	0.043	2
.9201	0.5496	0.037	2
265.8068	0.8896	0.201	2

J. D.	Phase	Δ Mag.	Sets
2,433000+			
265.6158	0.9728	0.241	2
.6220	0.9763	0.252	2
.6280	0.9777	0.330	2
.6339	0.9795	0.307	2
.6377	0.9811	0.398	2
.6706	0.9948	0.659	2
.6744	0.9957	0.655	2
.6782	0.9972	0.719	2
.6881	0.0001	0.728	2
.6876	0.0008	0.729	2
.6918	0.0025	0.718	2
.6964	0.0044	0.692	2
.7008	0.0061	0.688	2
.7048	0.0077	0.645	2
.7110	0.0102	0.582	2
.7158	0.0118	0.548	2
.7198	0.0135	0.496	2
.7230	0.0141	0.507	2
.7289	0.0163	0.460	2
.7329	0.0180	0.468	2
.7365	0.0192	0.389	2
.7354	0.0196	0.384	2
.7421	0.0235	0.316	2
.7462	0.0241	0.288	2
.7504	0.0259	0.259	2
152.6555	0.4614	0.089	2
.6607	0.4634	0.109	2
.6648	0.4658	0.125	2
.6684	0.4678	0.157	2
.6445	0.4698	0.152	2
.6801	0.4711	0.167	2
.6840	0.4727	0.195	2
.6880	0.4745	0.219	2
.6923	0.4771	0.261	2
.6701	0.4780	0.317	2
.6742	0.4807	0.358	2
.6781	0.4828	0.360	2
.6823	0.4845	0.388	2
.6880	0.4861	0.416	2
.6925	0.4880	0.442	2
.6978	0.4900	0.462	2
.7020	0.4917	0.507	2
.7078	0.4939	0.527	2
.7449	0.5087	0.528	2
.7490	0.5108	0.492	2
.7538	0.5120	0.452	2
.7590	0.5148	0.418	2
.7630	0.5159	0.397	2
.7670	0.5174	0.387	2
.7719	0.5194	0.353	2
.7760	0.5210	0.313	2
.7801	0.5228	0.279	2
.7850	0.5248	0.228	2
.7894	0.5265	0.206	2
.7940	0.5281	0.217	2
.8000	0.5305	0.183	2
.8037	0.5320	0.165	2
.8111	0.5349	0.146	2
.8194	0.5382	0.111	2
267.7488	0.4835	0.494	2
.7531	0.4860	0.504	2
.7575	0.4888	0.560	2
.7619	0.4905	0.572	2
.7681	0.4972	0.582	2
.7703	0.4986	0.582	2
.7751	0.5007	0.586	2
.7795	0.5021	0.576	2
.7819	0.5034	0.573	2
.7861	0.5051	0.554	2
.7899	0.5068	0.541	2
.7930	0.5081	0.517	2
.7981	0.5099	0.482	2
.8018	0.5115	0.468	2
.8060	0.5128	0.438	2
.8104	0.5147	0.405	2
.8138	0.5159	0.388	2
.8181	0.5178	0.366	2
.8219	0.5195	0.342	2
.8257	0.5208	0.314	2
.8290	0.5225	0.301	2
.8344	0.5242	0.289	2
.8381	0.5257	0.280	2
.8418	0.5276	0.259	2
.8465	0.5290	0.218	2
.8505	0.5305	0.209	2
200.8009	0.8908	0.038	3
.8066	0.8918	0.029	3
.8347	0.9028	0.044	3
.8409	0.8921	0.038	3
.8478	0.8944	0.033	3
.8547	0.8015	0.039	3
.8610	0.8040	0.029	3
.8678	0.8067	0.028	3
.8736	0.8091	0.044	3

Table 12 (cont'd)

Photoelectric Observations of WW Aurigae

J.D.	Phase	Δ Mag.	Sets
2,433000+			
300.7568	0.8811	0.083	3
.7833	0.8842	0.086	3
.7992	0.8865	0.083	2
306.6028	0.7677	0.085	3
.6178	0.7906	0.046	3
.6149	0.7935	0.047	3
.6323	0.7964	0.058	3
315.6003	0.8609	0.055	3
315.6095	0.8634	0.045	3
.6157	0.8659	0.040	3
.6239	0.8687	0.047	3
.6294	0.8712	0.045	3
.6356	0.8737	0.054	3
.6440	0.8771	0.054	3
.6548	0.8814	0.050	3
.6614	0.8840	0.048	3
315.6976	0.5865	0.036	3
.7142	0.5890	0.025	3
.7811	0.5918	0.033	3
.7893	0.5950	0.028	3
323.5994	0.7233	0.034	3
.6054	0.7251	0.028	3
.6081	0.7299	0.029	3
.6094	0.7314	0.043	3
.6156	0.7329	0.037	3

Photoelectric Observations of U Ophiuchi

J.D.	Phase	Δ Mag.	Sets
2,429000+			
378.770	0.0965	0.051	4
.788	0.1006	0.046	4
.798	0.1078	0.039	4
.815	0.1180	0.054	4
382.805	0.2865	0.005	4
.815	0.2915	0.005	4
.830	0.3004	0.006	4
.837	0.3046	0.009	4
.846	0.3100	0.009	4
.856	0.3159	0.012	4
.870	0.3243	0.013	4
.880	0.3302	0.015	4
428.664	0.6265	0.035	4
.680	0.6330	0.032	4
.699	0.6478	0.028	4
.707	0.6521	0.026	4
431.6852	0.4278	0.026	2
.6904	0.4307	0.054	2
.6947	0.4335	0.098	2
.6998	0.4365	0.118	2
.7095	0.4420	0.120	2
.7137	0.4448	0.164	2
.7176	0.4471	0.179	2
.7224	0.4498	0.194	2
434.668	0.2059	-0.005	4
.678	0.2119	-0.005	4
437.7371	0.0356	0.358	2
.7419	0.0385	0.332	2
.7472	0.0418	0.301	2
.7517	0.0445	0.276	2
.7604	0.0495	0.209	2
.7648	0.0520	0.198	2
.7694	0.0545	0.170	2
.7739	0.0569	0.159	2
.7774	0.0598	0.143	2
.7822	0.0625	0.127	2
.7864	0.0650	0.112	2
.7920	0.0689	0.108	2
.7966	0.0719	0.096	2
.8044	0.0767	0.081	2
.8090	0.0798	0.069	2
.8135	0.0811	0.071	2
439.6430	0.8727	0.041	4
.6528	0.8816	0.034	4
.6657	0.8966	0.057	4
.6727	0.9058	0.035	4
454.721	0.1807	0.024	4
.744	0.1744	0.021	4
.755	0.1810	0.016	4
.762	0.1852	0.014	4
456.722	0.7576	0.027	4
.730	0.7622	0.032	4
458.6308	0.4915	0.438	2
.6347	0.4939	0.434	2
.6392	0.4965	0.432	2
.6427	0.4987	0.406	2
.6492	0.5026	0.428	2
.6541	0.5055	0.407	2
.6578	0.5078	0.395	2
.6633	0.5110	0.361	2
.6745	0.5185	0.305	2
.6814	0.5218	0.249	2
.6851	0.5240	0.227	2
.6901	0.5270	0.202	2
.6949	0.5299	0.185	2
.6998	0.5327	0.134	2
.7035	0.5350	0.108	2
.7081	0.5377	0.090	2
.7174	0.5432	0.065	2
.7221	0.5460	0.011	2
.7255	0.5481	0.015	2
.7298	0.5508	-0.015	2
.7337	0.5541	-0.018	2
.7418	0.5574	-0.057	2
.7450	0.5597	-0.077	2
.7505	0.5629	-0.076	2
460.628	0.6870	0.007	4
460.647	0.6938	0.006	4
.660	0.7013	0.007	4
.670	0.7073	0.007	4
.680	0.7192	0.007	4
468.6429	0.4803	0.300	2
.6473	0.4838	0.323	2
.6543	0.4871	0.370	2
.6598	0.4898	0.396	2
.6632	0.4724	0.421	2
.6681	0.4763	0.452	2
.6719	0.4776	0.477	1
.6796	0.4822	0.515	2
.6879	0.4871	0.564	2
.6911	0.4890	0.588	2
.6951	0.4914	0.610	2
.6998	0.4942	0.642	2
.7042	0.4969	0.674	2
.7093	0.4999	0.716	2
.7158	0.5038	0.802	2
.7226	0.5084	0.869	2
.7281	0.5111	0.869	2
.7320	0.5134	0.865	2
.7363	0.5160	0.811	2
.7418	0.5193	0.801	2
.7504	0.5244	0.410	2
479.6040	0.8946	0.850	2
.6087	0.8974	0.716	2
.6154	0.9014	0.747	2
.6201	0.9042	0.728	2
.6244	0.9068	0.710	2
.6291	0.9096	0.698	2
.6324	0.0140	0.608	2
.6369	0.0166	0.572	2
.6449	0.0190	0.542	2
.6496	0.0218	0.510	2
.6531	0.0239	0.484	2
.6573	0.0264	0.454	2
.6642	0.0305	0.406	2
.6732	0.0359	0.339	2
.6769	0.0381	0.313	2
.6825	0.0413	0.275	2
480.6266	0.8043	0.022	4
.6348	0.8092	0.039	4
.6444	0.8149	0.051	4
.6548	0.8207	0.035	4
485.6216	0.5819	0.051	4
.6318	0.5880	0.048	4
.6413	0.5966	0.047	4
.6496	0.6046	0.050	4
.6736	0.6129	0.052	4
.6795	0.6159	0.053	2
.6849	0.6197	0.056	4
499.4328	0.9260	0.114	2
.4382	0.9277	0.132	2
.4452	0.9318	0.158	2
.4501	0.9347	0.176	2
.4555	0.9380	0.196	2
.4609	0.9418	0.218	2
.4672	0.9549	0.286	2
.4724	0.9580	0.308	2
.4768	0.9601	0.320	2
.4817	0.9638	0.339	2
.4854	0.9658	0.353	2
.4908	0.9686	0.371	2
500.4241	0.8314	0.303	2
.4294	0.8339	0.323	2
.4457	0.8383	0.305	2
.4602	0.8410	0.291	2
511.655	0.7892	0.045	4
.844	0.8046	0.072	4
515.5706	0.4264	0.135	2
.5763	0.4283	0.151	2
.5794	0.4477	0.109	2
.5846	0.4439	0.173	2
.5913	0.4478	0.188	2
.5954	0.4501	0.195	2
.6010	0.4531	0.203	2
515.6044	0.4556	0.216	2
520.5762	0.4194	0.053	2
.5797	0.4214	0.055	2
.5825	0.4231	0.071	2
.5877	0.4262	0.088	2
.5908	0.4282	0.106	2
.5972	0.4319	0.120	2
.6041	0.4360	0.140	2
.6087	0.4387	0.158	2
.6135	0.4416	0.168	2
.6176	0.4440	0.176	2
.6212	0.4462	0.188	2
.6261	0.4491	0.204	2
796.3374	0.0040	0.546	2
.6468	0.0080	0.502	2
.6527	0.0149	0.436	2
.6598	0.0215	0.376	2
.6781	0.0383	0.298	2
.6880	0.0546	0.234	2
.6901	0.0608	0.180	2
.7084	0.0859	0.128	2
.7479	0.0589	-0.003	3
.7674	0.0815	-0.022	2
.7780	0.0862	-0.030	2
797.656	0.6115	0.048	2
807.6839	0.8776	0.056	2
.6765	0.8863	0.049	2
.6824	0.8948	0.040	3
.7042	0.9017	0.034	5
812.7405	0.6040	0.052	2
.7599	0.6139	0.048	2
815.6813	0.3873	0.054	2
.6948	0.3984	0.044	3
.7123	0.3768	0.052	3
816.6598	0.9288	0.091	2
.6803	0.9350	0.133	2
.6992	0.9405	0.161	2
.6994	0.9457	0.193	2
.6782	0.9516	0.249	2
.6873	0.9571	0.300	2
.7086	0.9685	0.410	2
.7196	0.9765	0.486	2
.7292	0.9814	0.534	2
.7394	0.9875	0.627	2
.7472	0.9867	0.706	2
.7557	0.9978	0.759	2
.7639	0.0028	0.745	2
.7723	0.0077	0.761	2
.7842	0.0148	0.614	2
819.5972	0.3462	0.028	2
.6125	0.3543	0.034	2
822.5910	0.3221	0.014	2
875.5896	0.0710	0.091	2
.6026	0.0798	0.044	3
876.5775	0.0801	0.034	2
.5838	0.0957	0.029	2
2,430000+			
122.7708	0.3991	0.040	2
.7882	0.4096	0.056	2
.8021	0.4197	0.083	2
125.8901	0.6888	0.112	2
.7067	0.9281	0.135	2
.7142	0.9425	0.157	2
.7223	0.9474	0.177	2
.7277	0.9584	0.219	2
.7393	0.9675	0.296	2
.7478	0.9824	0.316	2
.7564	0.9877	0.394	2
.7646	0.9725	0.416	2
.7728	0.9775	0.479	2
.7814	0.9828	0.539	2
.7893	0.9878	0.604	2
.7973	0.9921	0.672	2
.8083	0.9969	0.730	2
164.6722	0.4132	0.068	2
.6892	0.4283	0.090	2

Table 12 (cont'd)

Photoelectric Observations of U Ophiuchi

J.D.	Phase	Δ Mag.	Sets
2,430000+			
184.6979	0.4256	0.112	2
.7080	0.4303	0.132	2
.7147	0.4435	0.170	2
.7229	0.4484	0.201	2
.7372	0.4569	0.258	2
.7477	0.4632	0.295	2
.7563	0.4683	0.367	2
.7651	0.4736	0.419	2
.7748	0.4792	0.480	2
.7928	0.4944	0.534	2
.7951	0.4902	0.596	2
.8027	0.4930	0.606	2
.8106	0.5007	0.630	2
222.6418	0.9787	0.496	2
.6488	0.9807	0.559	1
.6674	0.9860	0.625	2
.6779	0.9922	0.702	2
.6747	0.9953	0.745	2
.6849	0.0024	0.719	2
223.5047	0.5121	0.523	2
.6132	0.5172	0.466	2
.6235	0.5225	0.455	3
228.6044	0.4824	0.606	2
.6138	0.4978	0.621	2
.6232	0.5026	0.643	2
229.5940	0.0823	0.048	3
.6096	0.0918	0.068	3
.6218	0.0969	0.070	2
2,430000+			
342.6376	0.8725	0.053	3
.6478	0.8796	0.051	3
.6568	0.8839	0.049	3
.6644	0.8885	0.048	2
.6799	0.8978	0.045	3
.6912	0.9045	0.038	3
.7017	0.9108	0.034	3
.7100	0.9157	0.032	2
.7197	0.9197	0.036	2
.7304	0.9279	0.077	2
.7392	0.9351	0.119	3
384.6519	0.9820	0.471	2
.6665	0.9876	0.536	2
.6410	0.9904	0.609	2
.6489	0.9953	0.606	2
.6611	0.9994	0.606	2
.6656	0.9989	0.643	2
.6697	0.0016	0.626	2
.6839	0.0041	0.631	2
.6881	0.0068	0.596	2
.6724	0.0091	0.588	2
.6769	0.0118	0.536	2
.6803	0.0140	0.506	2
.6858	0.0171	0.468	2
.6892	0.0191	0.443	2
.6927	0.0212	0.419	2
.6968	0.0231	0.396	2
.7073	0.0299	0.323	2
.7125	0.0320	0.289	2
.7185	0.0354	0.276	2
.7205	0.0376	0.256	2
.7243	0.0401	0.236	2
.7286	0.0427	0.221	2
.7340	0.0459	0.199	2
.7371	0.0477	0.179	2
.7412	0.0501	0.155	2
.7456	0.0528	0.120	2
.7631	0.0672	0.066	2

J.D.	Phase	Δ Mag.	Sets
2,430000+			
384.7549	0.0895	0.075	2
386.6847	0.2827	0.023	3
.7019	0.3780	0.040	3
.7139	0.3801	0.051	3
.7248	0.3846	0.039	3
.7342	0.3922	0.044	3
.7451	0.3987	0.063	3
.7526	0.4031	0.054	1
.7670	0.4088	0.089	1
.7816	0.4085	0.082	1
.7884	0.4114	0.084	1
.7706	0.4139	0.082	1
.7748	0.4154	0.077	1
.7796	0.4197	0.090	1
.7834	0.4216	0.107	1
.7876	0.4242	0.122	1
415.6998	0.9660	0.378	1
.8023	0.9689	0.398	1
.8067	0.9695	0.423	1
.8102	0.9718	0.446	1
.8157	0.9738	0.468	1
.8171	0.9767	0.486	1
.8206	0.9778	0.504	1
.8250	0.9804	0.534	1
.8295	0.9851	0.558	1
.8330	0.9862	0.581	1
.8372	0.9877	0.654	1
.8406	0.9897	0.674	1
.8455	0.9928	0.698	1
.8490	0.9947	0.734	1
.8528	0.9970	0.749	1
.8566	0.9982	0.752	1
.8608	0.0017	0.760	1
.8649	0.0042	0.747	1
.8688	0.0065	0.717	1
424.6045	0.7373	0.000	3
.6181	0.7464	-0.001	3
.6320	0.7527	-0.003	3
.6481	0.7633	0.005	3
662.7764	0.7328	-0.006	3
.7825	0.7406	-0.008	3
.8044	0.7477	-0.010	3
.8217	0.7580	-0.008	3
.8360	0.7666	-0.004	3
.8500	0.7749	-0.000	3
.8641	0.7835	-0.005	3
.8747	0.7896	0.001	2
665.7132	0.4062	0.080	2
.7218	0.4114	0.038	2
.7300	0.4163	0.043	2
.7372	0.4205	0.049	2
.7444	0.4248	0.056	2
.7518	0.4292	0.068	2
.7593	0.4337	0.096	2
.7671	0.4384	0.120	2
.7752	0.4432	0.149	2
.7832	0.4480	0.176	2
.7941	0.4546	0.218	2
.8044	0.4608	0.270	2
.8118	0.4660	0.321	2
.8195	0.4696	0.372	2
.8264	0.4737	0.418	2
.8376	0.4805	0.482	2
.8451	0.4849	0.528	2
.8524	0.4892	0.569	2
.8596	0.4935	0.611	2
.8657	0.4977	0.640	2
.8740	0.5021	0.638	2
.8796	0.5048	0.630	1

J.D.	Phase	Δ Mag.	Sets
2,430000+			
699.7117	0.7902	0.088	3
.7535	0.7972	0.081	3
.7569	0.8052	0.089	3
720.6190	0.1015	0.040	3
.6312	0.1087	0.055	3
.6427	0.1156	0.051	3
.6531	0.1218	0.028	3
.6752	0.1350	0.017	4
727.6143	0.2717	-0.004	3
.6256	0.2791	0.009	3
.6368	0.2845	0.021	2
.6722	0.3048	0.029	3
.6844	0.3135	0.018	3
729.6482	0.4949	0.511	2
.6765	0.5010	0.555	2
.6840	0.5056	0.516	2
.6915	0.5100	0.568	2
.7008	0.5155	0.523	2
.7080	0.5198	0.486	2
.7151	0.5240	0.442	2
.7223	0.5283	0.400	2
.7272	0.5313	0.384	1
730.6172	0.0618	0.127	2
.6251	0.0666	0.098	2
.6348	0.0722	0.058	2
.6439	0.0777	0.048	3
.6591	0.0868	0.018	3
.6732	0.0946	0.024	3
.6880	0.1005	0.030	2
.6908	0.1056	0.026	2
733.6192	0.8514	0.021	2
.6315	0.8588	0.023	2
.6436	0.8659	0.024	2
.6560	0.8734	0.023	2
.6674	0.8802	0.025	2
.6786	0.8868	0.026	2
734.6156	0.4434	0.148	2
.6250	0.4511	0.191	2
735.6132	0.0401	0.270	2
.6202	0.0443	0.241	2
.6276	0.0497	0.210	2
.6361	0.0558	0.173	2
.6435	0.0601	0.147	2
.6507	0.0635	0.115	2
.6618	0.0697	0.078	3
779.6239	0.7918	0.089	2
.6276	0.7946	0.086	2
.6371	0.8005	0.088	2
.6458	0.8051	0.061	2
.6532	0.8099	0.060	2
.6605	0.8142	0.070	2
.6686	0.8191	0.062	2
.6794	0.8255	0.086	2
782.5814	0.1187	0.049	3
.5928	0.1238	0.039	3
.6046	0.1306	0.018	3
.6156	0.1372	0.029	3
.6247	0.1426	0.060	2
800.5569	0.4480	0.187	2
.5658	0.4530	0.204	2
.5743	0.4583	0.249	2
.5826	0.4633	0.296	2
.5911	0.4684	0.344	2
.5995	0.4732	0.400	2
.6079	0.4776	0.449	2
.6146	0.4824	0.496	2
.6228	0.4873	0.558	2
.6321	0.4928	0.612	2

comparable precision, and they set the limit of accuracy with which we can at present hope to learn the principal characteristics of eclipsing binary systems and which we can hope to exceed only under exceptionally favorable circumstances.

Table 12 is the table of photoelectric measures of all five variables. The first column gives the phase expressed in decimals of the period and the second column the difference of magnitude referred to one or to the mean of two comparison stars. This difference of magnitude (Δ mag.) is the final photoelectric magnitude used after all corrections have been made for extinction and with reductions applied for changes of shade glasses or attenuator steps. The third column gives the number of "sets" averaged for a single magnitude. This is in accordance with the standard practice at the Washburn Observatory since the beginning of the photoelectric observations. One set means a single reading on the Esterline-Angus chart or a comparable series of deflections of the galvanometer. During an eclipse, when the magnitude of the star was changing rapidly, a single set was used. Outside eclipse, several sets were averaged into one Δ mag. to improve the measure, since the time co-ordinate is not important. Other small figures in Table 12 refer to footnotes at the end of the section where they occur.

We are indebted to the American Academy of Arts and Sciences for a grant from the Rumford fund, a portion of which was used for the computations and preparation of this paper. The photometer was built under the supervision of Dr. A. E. Whitford. Observations were shared with Mr. Burt Nelson, graduate assistant at the University of Wisconsin. Computations were performed at the Massachusetts Institute of Technology by Mr. F. Gilbert Davoren, who also assisted in the preparation of the tables.

COUDÉ RADIAL VELOCITIES OF TU CASSIOPEIAE, DT CYGNI, AND U VULPECULAE

ROSCOE F. SANFORD
MOUNT WILSON AND PALOMAR OBSERVATORIES
CARNEGIE INSTITUTION OF WASHINGTON
CALIFORNIA INSTITUTE OF TECHNOLOGY
Received March 9, 1951

ABSTRACT

In each of these cepheid stars, various classes of absorption lines give the same velocity displacements, and hence no selection was needed in deriving velocities.

A plot of the coudé velocities of TU Cas indicates a variation of the systemic velocity and perhaps of the velocity amplitude, which probably accounts for the large scatter of the one-prism velocities about their mean curve. Plots of the coudé velocities of DT Cyg show a smooth variation, and those of U Vul consistently indicate a pause in the rising branch, but with an otherwise smoothly progressing variation.

Light-maxima and velocity minima seem to be coincident for TU Cas and for U Vul, but the relation is not clear for DT Cyg.

Coudé spectrograms (10 A/mm) of TU Cassiopeiae, DT Cygni, and U Vulpeculae were obtained because their velocity-curves determined earlier from one-prism spectrograms seemed poorly defined. All classes of absorption lines of these three cepheids give essentially the same velocity displacements, and therefore no selection of lines was made except on the basis of quality. The coudé spectrograms are listed in Table 1, with phases, in the third column, reckoned from the epochs and periods given in Table 2. A plot of the velocities in Table 1 and of light-curves for each of the variables is in Figure 1.

TU Cassiopeiae.—The minimum velocity of this cepheid seems to agree with maximum light as obtained (at about the same time) by Gordon and Kron. But the coudé velocities in different cycles do not agree. It is therefore concluded that the large scatter found in the one-prism velocities[1] is, for the most part, caused by variable systemic velocity, by a variable velocity amplitude, or by a combination of the two. Gordon and Kron found that the light-variation did not repeat itself with faithful regularity (see Fig. 1). Earlier photometric observers[2] had also noted irregularities in their observations.

DT Cygni.—The coudé velocities define a very satisfactory curve, although these velocities belong to widely different cycles. The amplitude of velocity variation is small, which probably accounts for the apparent scattering of the one-prism velocities[3] about their mean curve. Minimum velocity lags behind maximum light by $0.06P$, and maximum velocity behind minimum light by $0.10P$ in Figure 1. This assumes that the period is constant. Since this period does not serve to superpose the phase of maximum and minimum velocity of the one-prism velocities upon these phases for the coudé velocities, the constancy of the period may be doubted. Therefore, the relations of the phases of light and velocity shown by Figure 1 are open to question. They need to be established by simultaneous observations of light and velocity.

U Vulpeculae.—The coudé velocities define a new curve without scatter. But there is a definite pause on the increasing-velocity branch from phase 0.3 to $0.5P$ after maximum light. No such pause at the corresponding phase interval has as yet been found in any of its light-curves, although there may be a slight pause at a somewhat earlier phase in one

[1] R. F. Sanford, *Mt. W. Contr.*, No. 367; *Ap. J.*, 68, 169, 1928.

[2] See, e.g., L. V. Robinson, *Harvard Bull.*, No. 866, 1929.

[3] R. F. Sanford, *Mt. W. Contr.*, No. 404; *Ap. J.*, 72, 46, 1930.

TABLE 1

COUDÉ RADIAL VELOCITIES OF TU CAS, DT CYG, AND U VUL

PLATE NO. CE	JD	PHASE	VEL. (KM/SEC)
	TU Cas		
3866	2431655.963	0.740P	+ 1.9
3872	1656.960	.206	−30.3
3879	1657.905	.649	− 1.8
3972	1716.951	.248	−26.8
3985	1718.880	.150	−42.0
4286	1983.969	.064	−25.8
4356	2043.919	.087	−40.9
4360	2044.874	.535	− 4.5
4389	2070.793	.650	− 0.2
4395	2071.894	.164	−24.4
4467	2108.769	.402	−17.2
4483	2159.752	.233	−25.1
4503	2168.774	.450	−15.0
4505	2169.745	.905	−31.9
4532	2194.670	.555	− 7.8
4536	2195.639	.008	−45.2
4542	2196.683	0.497	− 8.3
	DT Cyg		
3902	1687.797	0.910	− 3.0
3909	1688.771	.300	− 1.3
3968	1716.709	.479	+ 3.5
3988	1719.614	.641	+ 7.9
4352	2042.949	.022	− 7.3
4361	2044.951	.823	+ 3.2
4862	2435.625	0.148	− 7.0
	U Vul		
3860	1654.969	0.503	−12.8
3864	1655.838	.611	− 3.3
3870	1656.836	.735	+ 5.6
3877	1657.799	.857	− 4.4
3976	1717.765	.362	−15.0
4355	2043.853	.170	−19.9
4359	2044.772	.287	−15.8
4853	2433.725	.962	−22.1
4858	2434.792	.096	−21.7
4864	2435.793	.221	−16.7
4868	2455.647	.705	+ 6.5
4873	2456.638	.830	+ 2.9
4880	2457.701	.960	−21.8
5281	2781.807	0.524	−12.7

TABLE 2

EPOCHS AND PERIODS

Star	Epoch of Light-Max. (JD)	Period (Days)	Reference
TU Cas.....	2425041.820	2.139295	Gordon and Kron, *Ap. J.*, **106**, 322, 1947
DT Cyg.....	2424305.651	2.49911	*Kat. u. Eph. Ver. Sterne*, No. 21, 1940
U Vul.....	2420400.228	7.990571	L. V. Robinson, *Harvard Ann.*, **90**, 49, 1940

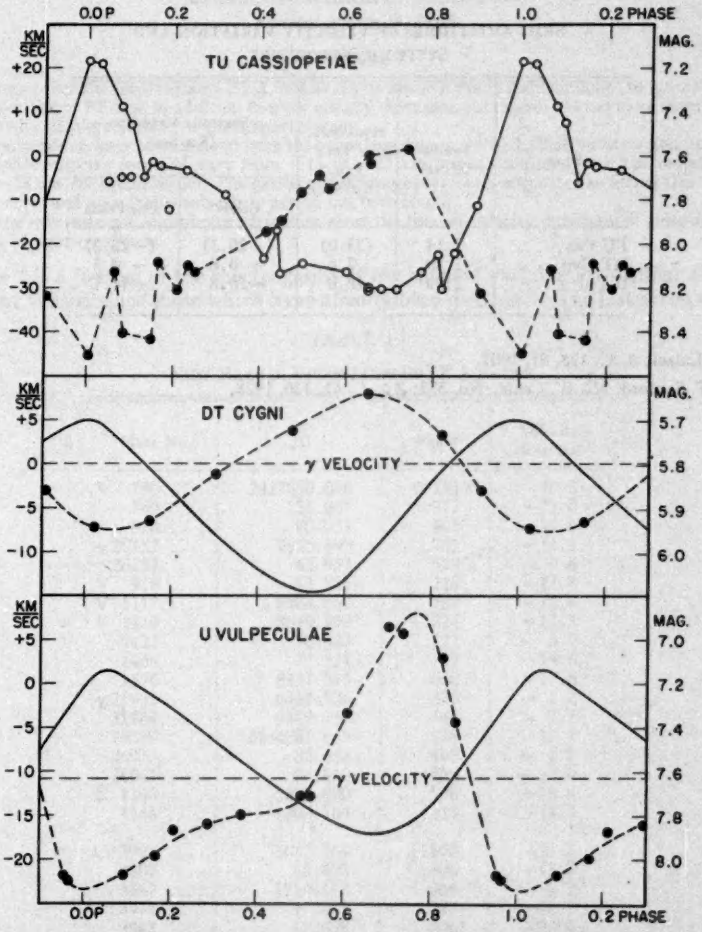

FIG. 1.—Light- and velocity-curves of TU Cassiopeiae, DT Cygni, and U Vulpeculae. Abscissae are phases in decimals of the periods. The velocities (left-hand ordinates) are connected by broken lines. The light-curves (right-hand ordinates) are given by solid lines. The sources of the light-curves are: TU Cas, Gordon and Kron, *Ap. J.*, **106**, 318, 1947; DT Cyg, C. M. Huffer, *Pub. Wash. Obs.*, **15**, 132, 1928; and U Vul, L. V. Robinson, *Harvard Ann.*, **90**, 49, 1940. The maximum for DT Cyg was arbitrarily assumed to be 5.7 mag.

of them.[4] The scatter of the earlier observations[5] about the mean velocity is probably largely the effect of errors of measurement of the one-prism spectrograms. Robinson's formula for light-maximum represents the velocity minimum derived from the earlier one-prism plates as well as the minimum given by the coudé spectrograms, and hence velocity minimum and light-maximum seem to be closely coincident.

The new values of the semi-amplitude of velocity variation read from curves of Figure 1 and of the systemic velocities determined by planimeter are compared with the old values in Table 3.

TABLE 3

SEMI-AMPLITUDES OF VELOCITY VARIATION AND SYSTEMIC VELOCITIES

Star	Period (Days)	Semi-ampl. of Vel. Var. (Km/Sec)	Systemic Velocity (Km/Sec)	
			Coudé	One-Prism
TU Cas.....	2.14	(23.0)	(−20.3)	(−22.2)
DT Cyg.....	2.50	7.6	− 0.6	− 0.5
U Vul.....	7.99	16.0	−10.8	−11.7

[4] M. Luizet, *A.N.*, 175, 81, 1907.

[5] R. F. Sanford, *Mt. W. Contr.*, No. 352; *Ap. J.*, 67, 326, 1928.

RADIAL VELOCITIES OF FF AQUILAE

ROSCOE F. SANFORD
MOUNT WILSON AND PALOMAR OBSERVATORIES
CARNEGIE INSTITUTION OF WASHINGTON
CALIFORNIA INSTITUTE OF TECHNOLOGY
Received March 19, 1951

ABSTRACT

Eighteen prismatic spectrograms (35 A/mm at $H\gamma$) and seven coudé spectrograms (10 A/mm) provide radial velocities of FF Aql, in addition to sixty already discussed. All classes of lines have essentially the same velocity displacement for a given spectrogram.

Annual residuals have been derived from the curve based upon the Lick Observatory velocities of 1933. The systemic velocity seems to vary from −13 to −25 km/sec as compared with the variation from −14 to −28 km/sec found earlier. The period of 4109 days previously suggested as fitting this variation will not serve, and no suitable substitute period has been found.

Existing spectroscopic and photometric data show the time of velocity minimum in close agreement with that of light-maximum.

Table 1 is a journal of the spectrograms of the cepheid variable FF Aquilae obtained at Mount Wilson since those which have already been discussed.[1] The last seven spectro-

TABLE 1

NEW RADIAL VELOCITIES OF FF AQUILAE

Plate No.	JD	Phase	Velocity (Km/Sec)
V 780	2427850.076	0.755 P	−18.5
789	51.067	.977	−21.0
828	80.057	.461	−13.6
γ 20752	7916.899	.701	−11.2
20757	42.953	.529	− 9.6
V 918	72.935	.235	−23.8
V 1117	8064.669	.752	−12.8
V 1419	8349.796	.524	−12.3
1422	50.633	.722	− 6.9
1466	79.721	.217	−14.6
1596	8441.611	.060	−27.6
γ 21961	9449.724	.536	− 7.2
21962	9449.765	.546	− 9.7
26030	2431281.685	.278	−13.2
26033	82.658	.495	− 4.9
26041	83.840	.758	−13.0
E 1140	1302.890	.996	−19.4
1146	1303.764	.214	−12.4
Ce 3901	1687.764	.100	−21.7
3907	88.682	.306	−15.3
3967	1716.672	.566	− 8.2
3974	17.617	.777	−18.7
3982	18.638	.006	−23.9
4214	1926.002	.385	−13.7
4726	2365.865	0.766	−15.6

[1] R. F. Sanford, *Mt. W. Contr.*, No. 508; *Ap. J.*, **81**, 132, 1935.

grams have a dispersion of 10 A/mm; the remaining spectrograms are prismatic, with a dispersion of approximately 35 A/mm at $H\gamma$, like those previously obtained at Mount Wilson.

With the coudé dispersion the absorption lines of FF Aql are still very sharp and well suited to accurate measurement. Furthermore, all classes of lines on a given plate have similar velocity displacements; hence only the quality of the lines influenced their choice for use in the mean plate velocities (Table 1).

The phases in the third column are in decimals of the period and are derived from

$$\text{Velocity minimum} = \text{JD } 2431718.612 + 4^{d}471033E \text{ (G.M.T.)}. \quad (1)$$

The epoch is from the minimum for the Mount Wilson velocities of 1945–1946, and the period is derived from the interval separating the velocity minimum of the Lick observations of 1933 from that of the Mount Wilson velocities of 1945–1946.

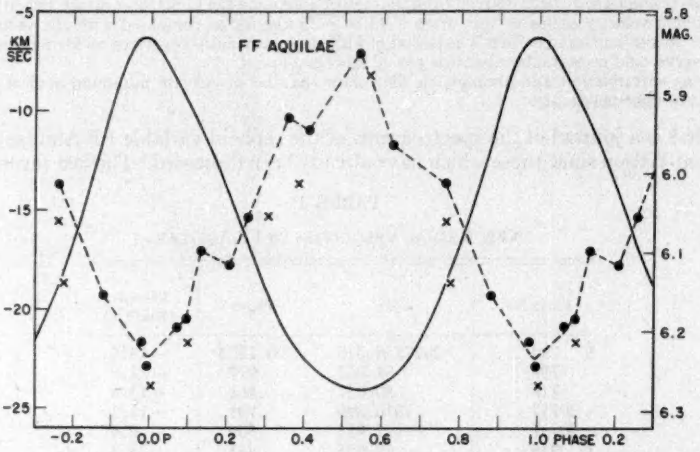

FIG. 1.—Velocity-curve of FF Aquilae (*dashed line*), Lick 1933 (*dots*), and Mount Wilson coudé (*crosses*). Abscissae are decimals of the period and ordinates are (*left*) velocities, (*right*) magnitudes. The light-curve (*solid line*) is that by Huffer.

The last seven velocities of Table 1 are plotted in Figure 1, together with the Lick observations of 1933. The two sets have a similar variation but show some systematic difference. In the previous study of the velocities of FF Aql[1] its systemic velocity, γ, was found to be variable, and it was suggested that the variation fitted a period of 4109 days. It now seems best to redetermine the residuals for the published velocities on account of changes here introduced in epoch and period and to refer all velocities to the Lick observations of 1933. Residuals on the same basis were also derived for the velocities given in Table 1. Annual means were then found to be as in Table 2.

The extreme values in Table 2 indicate that γ varies from -12.8 to -25.4 km/sec; in the previous paper the range was quite similar, from -13.9 to -28.4 km/sec. But the period of 4109 days previously suggested for the γ variation does not fit the new data; more observations will be needed to give a reliable determination of the period.

The photoelectrically determined time of maximum light is JD 2425065.32 (G.M.T.). The nearest velocity minimum according to equation (1) is JD 2425065.71 (G.M.T.).

The difference of 0.39 day is not conclusive evidence of a difference in time of light-maximum and velocity minimum, for the velocity and light-observations were made at very different times.[2]

TABLE 2

MEAN ANNUAL VELOCITY RESIDUALS OF FF AQUILAE

Year	JD	v (Km/Sec)	No. of Plates
1914	2420302	−10.4	5
1918	1891	− 5.3	1
1919	2121	−10.4	1
1922	3250	− 3.0	5
1930	6281	− 1.7	3
1931	6603	− 5.0	5
1932	6945	+ 0.2	14
1933	7266	− 4.1	9
1934	7580	− 8.6	5
1935	7920	− 2.9	7
1936	8254	− 0.9	4
1939	9450	− 0.5	2
1944	2431291	+ 2.2	5
1945	1706	− 2.0	5
1946	1926	− 3.1	1
1947	2366	− 0.9	1

[2] C. M. Huffer, *Pub. Washburn Obs. U. Wisconsin*, 15, 205, 1931.

DISPLACED HELIUM LINES IN THE SPECTRUM OF BD+11°4673

PAUL W. MERRILL
MOUNT WILSON AND PALOMAR OBSERVATORIES
CARNEGIE INSTITUTION OF WASHINGTON
CALIFORNIA INSTITUTE OF TECHNOLOGY
Received May 29, 1951

ABSTRACT

The *He* I line λ 3888 in the spectrum of the peculiar Be star BD+11°4673 exhibits from two to eight narrow absorption components having displacements of from −56 to −428 km/sec. The components vary rapidly and apparently irregularly in position and intensity; their behavior does not seem to be related to the 800-day cycle in the velocities and intensities of numerous bright lines. Individual components, illustrated by tracings in Figures 1 and 2, are listed in Table 1. The lines probably arise in a layer far above the photosphere. The discrete outward motions, possibly related to the rapid motions of eruptive prominences, offer a promising subject for theoretical discussion.

In certain stellar spectra with hydrogen emission lines, the dark helium line λ 3888 exhibits the characteristics of a shell line, being sharper and stronger than other lines of helium. Because this line arises from a strongly metastable energy state, 2^3S, in the helium atom, its enhancement indicates that it is produced at an unusually low density, and hence in an unusually high level, in the star's atmosphere.

One of the stars in whose spectrum λ 3888 is of special interest is BD+11°4673.[1] The spectrum of this star has been extensively investigated. It exhibits many remarkable changes, some of which recur in a cycle of 800 days, while others appear to be progressive. A general description of the changes observed during the interval 1943–1950 on numerous spectrograms with dispersion 10 A/mm was recently published.[2]

The present article describes the extraordinary behavior of the absorption components of the *He* I line λ 3888, $2^3S - 3^3P$, in the spectrum of BD+11°4673. From two to eight narrow absorption components having large shortward displacements exhibit rapid and apparently irregular variations in position and intensity. The only progressive change appears to be the occasional addition, as time goes on, of components having greater and greater displacement. This is in line with the general increase of negative displacements of absorption lines indicated in Figure 11 of the previous paper.[2]

The tracings in Figure 1 exhibit the wide range of variation which individual components undergo. For examples of quick changes compare plates Ce 6337, 6350, and 6355. For comparison with λ 3965 and λ 4471 see Figure 2.

Because of their great diversity, the displacements of individual components are not easy to tabulate. Some degree of continuity is evidenced, however, by the recurrence of certain preferred displacements. To exhibit this partial continuity, Table 1 has been drawn up in columnar form. This table gives results for most of the plates on which well-defined components have been measured.

Component I, with a mean displacement of −72 km/sec, is very persistent. It is well marked on a few plates, but on most of them it is represented by a weak shoulder on the shortward side of the *He*, *Hε* emission. This component is seldom recognizable in other helium lines. On Ce 3989, however, a corresponding displacement was measured in the following lines of *He* I: λλ 3447, 3613, 3819, 3888, 3965, 4026, 44[illegible] on Ce 4932 in λ 3888 and λ 3965. The displacement is nearly constant, but on a few plates—for example, Ce 4932—the measured velocity differs appreciably from the mean velocity.

[1] AG Pegasi, HD 207757; 1900 R.A., 21^h46^m2; Decl., +12°9′; mag. 7.6; spec. Bep.

[2] P. W. Merrill, *Mt. W. and P. Reprint* No. 36; *Ap. J.*, 113, 605, 1951.

TABLE 1

VELOCITIES OF PRINCIPAL DARK COMPONENTS OF HELIUM LINES*
(Km/Sec)

Plate Ce	Date	Lines (A)	I	II	III	IV	V	VI
3082	1943 June 23	3888	69	151	.....	227	.....	.....
		4471	.....	156	.....	214	.....	.....
3531	1944 Aug. 3	3888	tr†	.....	184	221	.....	.....
		3965	tr	.....	183	.....	.....	.....
		4026	tr	(116)‡	181	.....	.....	.....
		4471	tr	(146)	197	.....	.....	.....
3989	1945 Sept. 25	3888	72	(145)	.....	(232)	.....	.....
		3965	68	.....	.....	.....	.....	.....
		4026	66	.....	162	.....	.....	.....
		4471	65	.....	(173)	.....	.....	.....
4459	1946 Oct. 12	3888	tr	.....	179	223	.....	.....
		3965	.....	.....	(170), (200)	.....	.....	.....
		4026	.....	123	161, 200	.....	.....	.....
		4471	.....	(136)	198	.....	.....	.....
4807	1947 Aug. 25	3888	75	122	187	.....	.....	.....
		3965	.....	117	.....	.....	.....	.....
		4026	.....	119	.....	.....	.....	.....
		4471	.....	(138)	.....	.....	.....	.....
4810	Aug. 26	3888	75	125	185	.....	.....	.....
		3965	.....	116	.....	.....	.....	.....
		4026	.....	115	.....	.....	.....	.....
		4471	.....	(128)	.....	.....	.....	.....
4932	Oct. 25	3888	56	131	197	.....	.....	.....
		3965	53	121	195	.....	.....	.....
		4026	.....	.....	(179)	.....	.....	.....
		4471	.....	.....	(175)	.....	.....	.....
5208	1948 June 17	3888	tr	.....	170	234	.....	.....
		4026	.....	.....	.....	217	.....	.....
		4471	.....	.....	.....	222	.....	.....
5312	Sept. 11	3888	tr	.....	175	231	.....	.....
		4026	.....	.....	169	.....	.....	.....
		4471	.....	(145)	(194)	.....	.....	.....
5808	1949 Aug. 3	3888	.....	.....	183	243	.....	.....
		4026	.....	.....	.....	(214)	.....	.....
		4471	.....	.....	.....	235	.....	.....
6245	1950 May 25	3888	(91)	135	.....	230	318	394
		4026	.....	.....	.....	228	310	.....
		4471	.....	.....	(208)	(224)	315	.....
6337	June 29	3888	tr	103, 154	(189)	230	292, 315	378§
		4026	.....	.....	.....	.....	319	381
		4471	.....	.....	.....	.....	313	380
6350	July 1	3888	66	106, 152	tr	233	286, 340	.....
		4026	.....	.....	.....	.....	330	.....
		4471	.....	.....	.....	.....	329	.....
6355	July 2	3888	70	105, 151	(186)	236	279, 340	404
		4026	.....	.....	.....	(233)	.....	.....
		4471	.....	.....	.....	(244)	.....	.....
6369	July 25	3888	78	143	.....	246	317	(373)
		4026	.....	.....	.....	.....	(320)	.....
		4471	.....	.....	.....	.....	320	.....
6377	July 27	3888	(82)	155	.....	247	299, 332	.....
		4026	.....	.....	.....	.....	302	.....
		4471	.....	.....	.....	.....	304	.....
6429	Aug. 4	3888	72	127, 158	187	226	294, 343	.....
6435	Aug. 5	3888	73	(122)	.....	227	294, 333	.....
6444	Aug. 7	3888	71	132	.....	230	303	.....
6483	Aug. 29	3888	73	143	.....	223	275, 323	.....
6540	Sept. 24	3888	74	.....	170	230	288, 336	.....
6619	Oct. 20	3888	72	.....	.....	216	324	362
6696	Nov. 28	3888	(60)	(154)	(185)	215	292, 322	.....

* All values are negative.

† tr = trace.

‡ Values in parentheses refer to poor or blended components.

§ There is an additional component at −428 km/sec and possibly one at −452.

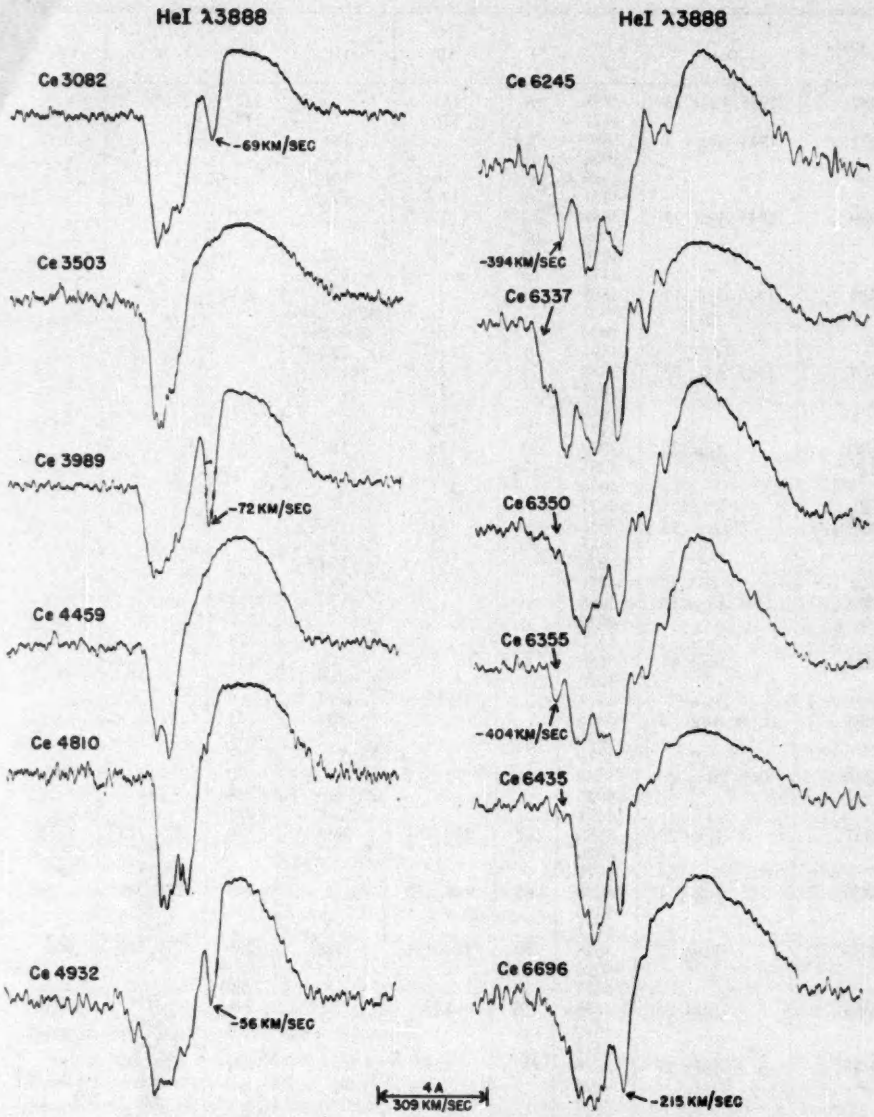

FIG. 1.—Tracings of *He* I λ 3888 in the spectrum of BD+11°4673

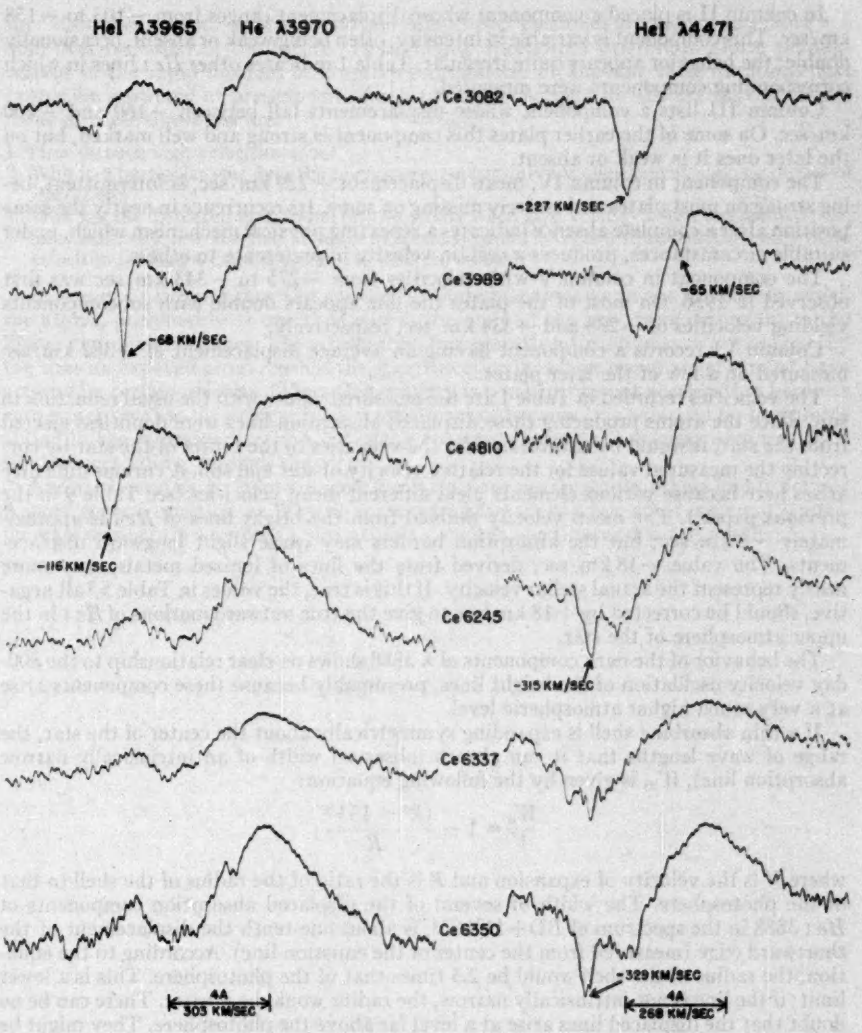

FIG. 2.—Tracings of two *He* I lines in the spectrum of BD+11°4673

In column II is placed a component whose displacement ranges from −103 to −158 km/sec. This component is variable in intensity, often being weak or absent, occasionally double; the behavior appears quite irregular. Table 1 indicates other *He* I lines in which corresponding components were measured.

Column III lists a component whose displacements fall between −160 and −200 km/sec. On some of the earlier plates this component is strong and well marked, but on the later ones it is weak or absent.

The component in column IV, mean displacement −229 km/sec, is intermittent, being strong on most plates and entirely missing on some. Its recurrence in nearly the same position after a complete absence indicates a repeating physical mechanism which, under suitable circumstances, produces a certain velocity in preference to others.

The component in column V with velocities from −275 to −343 km/sec was first observed in 1950. On most of the plates the line appears double with subcomponents yielding velocities of −288 and −334 km/sec, respectively.

Column VI records a component having an average displacement of −382 km/sec measured on a few of the later plates.

The velocities recorded in Table 1 are the measured values with the usual reduction to sun. Since the atoms producing these displaced absorption lines were doubtless ejected from the star, it would be natural to refer the velocities to the center of the star by correcting the measured values for the relative velocity of star and sun. A curious difficulty arises here because various elements yield different mean velocities (see Table 9 in the previous paper[2]). The mean velocity derived from the bright lines of *He* I is approximately −8 km/sec; but the absorption borders may cause slight longward displacements. The value −18 km/sec, derived from the lines of ionized metals, may more nearly represent the actual stellar velocity. If this is true, the values in Table 5,[2] all negative, should be corrected by +18 km/sec to give the true outward motions of *He* I in the upper atmosphere of the star.

The behavior of the dark components of λ 3888 shows no clear relationship to the 800-day velocity oscillation of the bright lines, presumably because these components arise at a very much higher atmospheric level.

If a thin absorbing shell is expanding symmetrically about the center of the star, the range of wave lengths that it can absorb (observed width of an intrinsically narrow absorption line), W_a, is given by the following equation:

$$\frac{W_a}{V} = 1 - \frac{(R^2 - 1)^{1/2}}{R},$$

where V is the velocity of expansion and R is the ratio of the radius of the shell to that of the photosphere. The width of several of the displaced absorption components of *He* I 3888 in the spectrum of BD+11°4673, is about one-tenth the displacement of the shortward edge (measured from the center of the emission line). According to the equation, the radius of the shell would be 2.3 times that of the photosphere. This is a lower limit; if the line is not intrinsically narrow, the radius would be greater. There can be no doubt that the displaced lines arise at a level far above the photosphere. They might be called "circumstellar" to distinguish them from lines arising in the normal reversing layer just above the photosphere.

The cause of these multiple displaced lines is evidently quite selective; in BD+11°4673 it appears to operate only on neutral helium atoms and to become especially important in those upper strata where the atoms are mostly in stable or metastable states. Comparable phenomena are shown by the H and K lines of *Ca* II in HD 190073[3] and XX Ophiuchi[4] and possibly by the displaced hydrogen lines in *v* Sagittarii[5] and by lines of

[3] P. W. Merrill, *Mt. W. and P. Reprint* No. 30; *Ap. J.*, **113**, 55, 1951.

[4] P. W. Merrill, *Mt. W. and P. Reprint* No. 44; *Ap. J.*, **114**, 37, 1951.

[5] W. P. Bidelman, *Ap. J.*, **109**, 544, 1949.

the "diffuse enhanced" spectra of novae. A few other examples are known and more will doubtless be found in the future. These highly specialized discrete motions, perhaps related to the rapid motions of eruptive prominences on the sun, raise questions that cannot be answered at present but offer a promising subject for theoretical discussion. Some of these questions are:

1. How do such high velocities arise?
2. Why in a particular star does the phenomenon occur only for one element and one degree of ionization?
3. Why are the displaced lines frequently so strong when zero velocity is not represented? Or, more generally, how is it that atoms of a certain type and in certain strata can have only those velocities forming a definite pattern of discrete values?

It is easy to surmise that the answers to these questions lie in the manner in which the atoms, presumably at one time within the body of the star, were driven up to the higher circumstellar zones. The accelerating forces apparently act in such a way that, by the time an expelled atom reaches the spectroscopically active upper zone, it must have acquired a certain velocity. When this velocity is reached, the net acceleration becomes zero either because the driving force ceases to act or because it is balanced by some force acting in the opposite direction (as in the constant "terminal" velocity acquired by a small object falling through the air).

A related question is: Why are some shells stable or nearly stable, others highly active? A more general question is: Why do some stars have shells while other apparently similar stars do not? Or why does a star exhibit a shell at one time and not at another?

AN EMISSION BAND SYSTEM ATTRIBUTED TO THE MOLECULE NH^+*

M. W. FEAST†
Division of Physics, National Research Council, Ottawa, Canada
Received March 30, 1951

ABSTRACT

Two red degraded bands at 2725 and 2885 A have been excited in a hollow-cathode discharge tube in flowing ammonia. Their rotational structures have been analyzed, and they are shown to be the (1, 0) and (0, 0) bands, respectively, of the $^2\Sigma^+ - {}^2\Pi_r$ transition of NH^+. Large perturbations in the $^2\Pi_r$ state are caused by a $^4\Sigma^-$ state. Wave numbers of the band lines and molecular constants for the three states are listed. Weaker bands at 2614 and 2825 A probably belong to the same system.

I. INTRODUCTION

Recent astrophysical work, especially on the spectroscopic study of comets and of interstellar matter, has led to an increased interest in the study of the spectra of ionized diatomic molecules. For example, CH and CH^+ have both been identified in emission from comets and in absorption from interstellar matter, and NH is found in emission from comets, though there seems to be no evidence at present for its identification in interstellar space. Consideration of these facts suggests that NH^+ may be an astrophysically important molecule. Furthermore, a study of NH^+ is of interest to the spectroscopist, since this molecule is isoelectronic with CH and the two molecules would be expected to bear considerable resemblance to each other. For these reasons it was decided to investigate the possibility of obtaining emission bands due to NH^+ in the laboratory.

Apparently the only previous observation regarding an NH^+ spectrum that has been published is a brief note by Lunt, Pearse, and Smith.[1] In giving a preliminary account of their work on the spectrum of NH obtained in a hollow-cathode discharge in flowing ammonia, they state: "In addition we have obtained four weaker bands at λλ 2730, 2835, 2885 and 2980 which appear to be due to the ion NH^+." These authors did not, however, proceed any further with an investigation of these bands.[2] In the present work, bands, apparently identical to those obtained by Lunt, Pearse, and Smith, have been secured, and their analysis and assignment to NH^+ forms the basis of this paper. No other bands attributable to NH^+ have yet been observed. Since the bands to be described all lie in the region of atmospheric ozone absorption, their astrophysical investigation will probably have to await the wider application of V2 rocket techniques. However, there remains the possibility of finding other band systems of NH^+ in more accessible regions of the spectrum, as is discussed at the end of Section IV.

II. EXPERIMENTAL

The spectrum was excited by means of a hollow-cathode discharge in flowing ammonia. The hollow cathode was in the form of an aluminum cylinder 18 cm long, 5 cm in external diameter, and 1.5 cm in internal diameter. A short, hollow cylinder, also of aluminum, placed concentric with the cathode and 3.5 cm from the nearer face of it served as the anode. The discharge was viewed through the hole in the anode. Ammonia

* *Contributions from the National Research Council*, No. 2494.

† National Research Laboratories Postdoctorate Fellow.

[1] *Nature*, 136, 32, 1935.

[2] I am indebted to Dr. R. W. B. Pearse for this information.

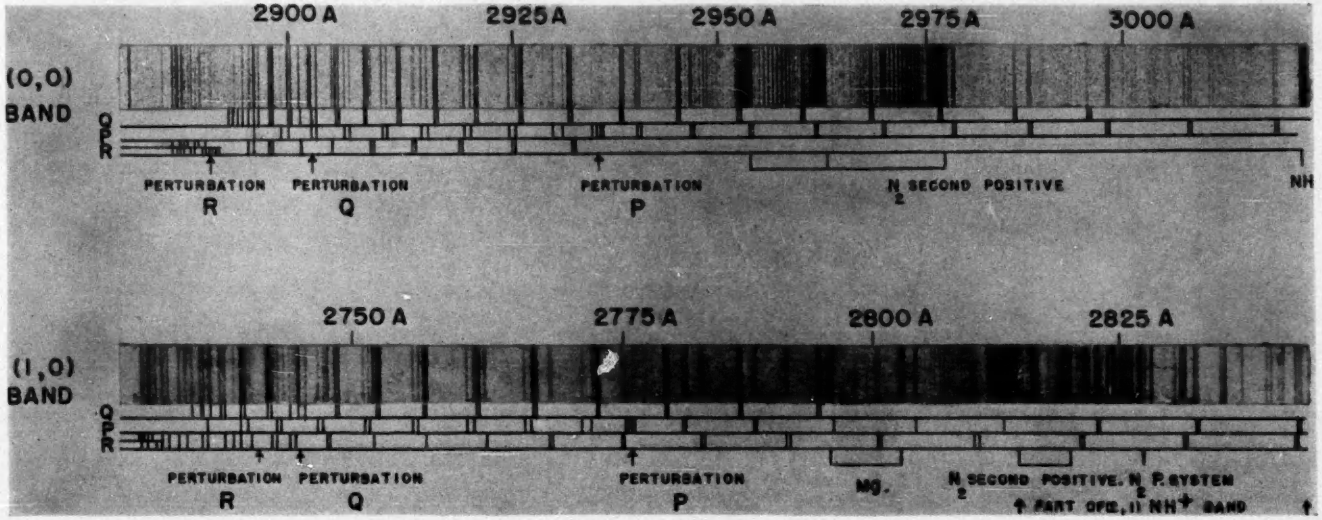

FIG. 1.—The 2725 and 2885 A bands of NH^+, showing the perturbations

obtained from a cylinder of compressed gas was streamed into the discharge tube through the hollow cathode and was condensed out of the system by a liquid nitrogen trap attached to the discharge tube by a ground-glass joint near the anode. In this manner a very rapid flow of gas could be maintained. The nitrogen and hydrogen formed in the discharge tube were pumped off by an oil-diffusion pump backed by a rotary pump. The discharge tube was cooled by immersing it in a water bath. Power was supplied by a transformer–mercury-rectifier circuit, which gave 1500 volts. Preliminary experiments showed that, in order to obtain the bands reported by Lunt, Pearse, and Smith with sufficient intensity, it was necessary to stream the gas very rapidly through the tube at a relatively high pressure and to use quite low currents (~0.1 amp.). Unless this was done, the bands either could not be found at all or were badly confused with N_2 second positive bands and the H_2 continuum. Using this method of excitation, spectrograms were obtained with a Hilger Quartz Littrow spectrograph (E. 478). Good spectrograms of the strongest band at 2885 A were obtained with exposures of about 12 hours, whereas the next strongest band at 2725 A required 30 hours' exposure in order to secure a spectrogram of high density.

The visible region of the spectrum so obtained consisted partly of the many-line spectrum of H_2 and partly of the α band of ammonia (NH_2?). The H_2 continuum, N_2 second positive, and N_2^+ first negative bands were present, though relatively weak. All four known NH systems appeared with considerable intensity. Apart from the red degraded bands at 2725 and 2885 A (the 2730 and 2885 A bands of Lunt, Pearse, and Smith), weaker red degraded bands of similar structure and probably belonging to the same system were found near 2614 and 2825 A. The 2614 A band is overlapped by another weak band at 2684 A, degraded to shorter wave lengths. This is probably the (0, 1) band of the NH $d^1\Sigma - c^1\Pi$ system. The 2825 A band (the 2835 A band of Lunt, Pearse, and Smith) is overlapped by the high K lines of the 2725 A band. No separate band has been found near 2980 A, but the high K lines of the 2885 A band lie in this region and may give the appearance of another band, since they are separated from the low K lines by the (2, 0) N_2 second positive sequence at 2977 A. A weak red degraded band found near 4120 A may be the (1, 0) band of the NH $c^1\Pi - b^1\Sigma$ system. The only other band structure found was a violet degraded band near 2827 A. This is the (0, 0) band of one of the N_2 singlet systems (Gaydon's P system; Herman's ζ system).

III. ANALYSIS OF THE BANDS ATTRIBUTED TO NH^+

The 2725 and 2885 A bands are shown in the plate (Fig. 1). They are of similar structure, consisting of a strong doublet Q branch and weaker doublet P and R branches. Perturbations are seen to occur in one component of the Q branch and in both components of the P and R branches in each band. Table 1 lists the wave numbers of the band lines (probable error ± 0.2 cm^{-1}). The structure of the bands immediately suggests a $^2\Sigma - {}^2\Pi$ transition with the $^2\Pi$ state near case b. This is shown to be correct by the detailed analysis. Transitions of this type have been adequately described in the literature[3] and will not be described in detail here. The perturbations occur at the same places in both bands, showing that the bands have a state in common. That this is the lower state is shown by the fact that the perturbations occur at the same value of K in the P and R branches. The fine structure of this lower state due to Λ and spin doubling, as well as the fact that the perturbations in the Q branch are at a K value different from the common K value for the P and R branch perturbations, shows that this state is the $^2\Pi$ state. It is safest to rely on these facts rather than on the missing lines at the origin, since lines of low K usually tend to be weak and overlapped and, in the case of $^2\Sigma - {}^2\Pi$ transitions, lines of satellite branches are sometimes found near the origin in the position of expected

[3] See, e.g., G. Herzberg, *Molecular Spectra and Molecular Structure*, Vol. 1: *Spectra of Diatomic Molecules* (New York: Van Nostrand Co., 1950).

TABLE 1

WAVE NUMBERS OF THE $^2\Sigma^+ - {}^2\Pi$ SYSTEM OF NH^+

K	R_1	Q_1	P_1	R_2	Q_2	P_2
	2885 A Band (0, 0)					
1	34604.9	34553.5	34527.3	34598.7	34542.3	.....
2	619.8	542.3	491.6	611.0	533.2	34482.3
3	629.0	527.3	450.9	623.6	520.8	443.4
4	636.1	507.2	405.6	629.0	502.2	398.5
5	636.1	482.3	356.2	629.0	478.3	349.0
6	632.4	452.7	302.1	623.6	466.9	294.7
	.....	.....	.....	.....	443.4	.....
7	623.6	418.4	244.0	614.6	414.2	235.5
8	611.0	378.7	183.1	600.4	375.1	173.0
9	533.2	334.2	056.1	542.3	330.5	065.1
	598.7	.....	123.0	584.6	.....	109.4
10	584.6	284.3	060.1	592.8	280.7	070.6
	533.2	.....	011.1	527.3	.....	005.5
11	507.2	229.0	33936.9	502.2	225.5	33934.9
12	466.9	168.4	854.3	466.9	165.0	854.3
13	422.3	102.6	765.2	422.3	099.0	766.5
14	369.9	031.0	670.7	372.0	027.8	673.1
15	311.4	33954.0	571.0	314.3	33950.7	573.5
16	246.0	871.2	465.8	248.9	867.7	468.8
17	173.0	783.0	355.0	177.2	779.7	358.5
18	094.2	689.2	238.6	099.0	686.0	242.7
19	.....	N_2	117.0	.....	N_2	121.2
20	.....	488.2	.....	.....	485.5	.....
21	.....	386.9	.....	.....	384.4	.....
	2725 A Band (1, 0)					
1	36608.7	36556.5	36536.0	36593.5	36546.6	.....
2	616.4	542.4	496.1	605.9	532.8	36485.4
3	618.9	522.4	450.8	610.9	515.9	443.1
4	616.4	496.1	400.7	608.7	491.2	393.8
5	608.7	463.8	345.0	601.4	459.6	338.0
6	593.5	424.8	283.0	586.0	436.1	275.9
	.....	.....	.....	.....	416.0	.....
7	572.3	379.4	215.8	563.9	375.2	207.5
8	546.6	327.7	144.3	536.0	323.8	134.0
9	450.8	269.0	005.3	459.6	265.8	613.5
	518.7	.....	072.3	505.0	.....	058.4
10	481.5	203.8	35991.8	502.0	200.6	608.6
	436.1	.....	945.7	431.2	.....	35940.8
11	390.0	132.2	856.8	388.0	128.8	854.7
12	332.6	053.5	757.6	332.6	050.1	757.6
13	269.0	35968.2	651.0	269.0	35964.8	651.0
14	192.0	875.8	536.8	192.0	872.5	536.8
15	109.7	776.2	415.8	112.3	773.0	417.9
16	019.4	669.4	288.2	022.5	666.2	290.9
17	35920.6	555.8	153.8	35924.2	552.6	157.0
18	813.6	435.9	012.4	815.5	432.4	016.4
19	697.9	309.4	34864.3	701.9	306.8	34868.4
20	574.5	176.4	709.4	578.0	.....	713.6

main-branch lines. However, the present assignments of lines near the origin agree with $^2\Pi$'s being the lower state.

The 2885 A band, being the strongest band observed, is taken as the (0, 0) band of the system. The 2725 A band is then obviously the (1, 0) band. The *NH* bands unfortunately overlap the region where one would expect to find the (0, 1) band. If, however, the common lower level had $v'' = 1$ instead of $v'' = 0$, one would expect a (0, 0) band on the short-wave-length side of the 2725 A band [which would then be the (1, 1) band]. No such band is observed. On the other hand, if the upper-state quantum number were increased by one unit, the two observed bands would become the (1, 0) and (2, 0) bands, respectively. The (0, 0) band would be overlapped by *NH* bands, but the (0, 1) and (0, 2) bands should be observed in the near ultraviolet. These bands are not found, however. Thus the vibrational assignments of the bands appear established. The weak 2614 A band is probably the (2, 0) band, and the 2835 A band the (2, 1) band. Neither of these two bands was strong enough for a complete rotational analysis to be made, but some weak branches could be picked out, and rough values for band origins are 38,255 and 35,500 cm^{-1}. The determination of the origins of the 2725 A and 2885 A bands is discussed below. Using the average of the origins of the two subbands in each case [since the values for the (2, 0) and (2, 1) bands are rough average values], we obtain the very approximate vibrational scheme given in Table 2. The various vibrational constants are listed in Table 3. The ω_0'' value was obtained from Kratzer's relation $\omega = \sqrt{4B^3/D}$. It must, of course, be borne in mind that this relation is only approximately true.

a) UPPER STATE $^2\Sigma$

The upper-state differences $\Delta_2F_i'(K) = R_i(K) - P_i(K)$ were determined for the two components ($i = 1, 2$) of each band. It was found that in both bands $\Delta_2F_1'(K) = \Delta_2F_2'(K)$ within the limits of experimental error. Thus the spin doubling in the $^2\Sigma$ state is too small to be observed with the dispersion used in the present experiment. Assuming for the moment that the bands are due to NH^+, the spin doubling should be comparable with that in the $^2\Sigma$ states of the isoelectronic molecule *CH*. The splitting in the case of the two $^2\Sigma$ states of *CH* is shown graphically as a function of K by Gerö,[4] and a similar splitting in the present bands would be within the experimental error. In all calculations the average values $\Delta_2F'(K) = \frac{1}{2}[\Delta_2F_1'(K) + \Delta_2F_2'(K)]$ were therefore used. Proceeding in the usual manner,[3] $[\Delta_2F(K)]/(4K + 2)$ $[= B_v - 2D_v(K + \frac{1}{2})^2]$ was plotted against $(K + \frac{1}{2})^2$, and from the straight line so obtained the constants B_v and D_v for the two levels $v' = 0$ and $v' = 1$ were determined. By means of the formulae $B_v = B_e - \alpha(v + \frac{1}{2})$ and $D_v = D_e + \beta(v + \frac{1}{2})$, values for B_e, α, D_e, and β were then calculated. The quantity r_e was calculated from the formula $r_e = \sqrt{h/8\pi^2 c\mu B_e}$ by means of the atomic constants of DuMond and Cohen[5] and with the assumption that the emitter is NH^+. The constants for the $^2\Sigma$ are listed in Table 3. In a later section it is shown that this state is $^2\Sigma^+$.

b) THE LOWER STATE $^2\Pi$ AND THE STATE PERTURBING IT

Owing to the considerable perturbations occurring in the lower state $^2\Pi$, the normal molecular constants for this state (B, D, etc.) have a rather restricted meaning, as have the band origins, and it is convenient to discuss their determination and the perturbations simultaneously. This discussion will be facilitated by frequent reference to Figure 2, which shows the finally accepted scheme for the two mutually perturbing states, as well as certain other cases which will be eliminated by the arguments given below.

Considering, first, the P and R branches, we can determine combination differences $\Delta_2F_{1e}''(K)$ and $\Delta_2F_{2e}''(K)$ in the normal way. Proceeding as if there were no perturbations and plotting $[\Delta_2F_e''(K)]/4K + 2$—where $\Delta_2F_e''(K) = \frac{1}{2}[\Delta_2F_{1e}''(K) + \Delta_2F_{2e}''(K)]$, using averaged values of the differences from both bands—against $(K + \frac{1}{2})^2$, we find that, apart

[4] *Zs. f. Phys.*, **118**, 27, 1941. [5] *Rev. Mod. Phys.*, **20**, 82, 1948.

from the region of great perturbation, the points fall accurately on a straight line and yield $B_0'' = 15.252\ \text{cm}^{-1}$ and $D_0'' = 14.3 \times 10^{-4}\ \text{cm}^{-1}$. However, this does not mean that the formula $F(K) = BK(K+1) - DK^2(K+1)^2$ applies outside the region of great perturbation; for, actually, all the levels above this region are displaced upward (i.e., are perturbed) by a constant amount (about $17.7\ \text{cm}^{-1}$) relative to the levels calculated from the above formula. This is clearly seen when an attempt is made to determine the band origins for each of the subbands. The most accurate method is to make use of the formula

$$R_i(K-1) + P_i(K) - 2(B_v' - B_v'')K^2 + 2(D_v' - D_v'')K^2(K^2+1) = 2\nu_0$$

and plot the left-hand side of this equation against K^2. The quantity ν_0 is determined as the intercept at $K = 0$, while any deviation of the curve from the horizontal indicates the need for a small correction to the difference $(B_v - B_v'')$. Furthermore, deviations

TABLE 2

DESLANDRES TABLE FOR NH^+

	v''		
v'	0		1
0	34553.0 2004.0		
1	36557.0 1698		
2	38255	2755	35500

TABLE 3

MOLECULAR CONSTANTS FOR NH^+

Constants for the $^2\Sigma^+$ State

$$\left.\begin{aligned} B_0' &= 12.848\ \text{cm}^{-1} \\ B_1' &= 12.082\ \text{cm}^{-1} \\ B_e' &= 13.231\ \text{cm}^{-1} \end{aligned}\right\} \pm 0.005\ \text{cm}^{-1} \qquad \left.\begin{aligned} D_0' &= 18.9 \times 10^{-4}\ \text{cm}^{-1} \\ D_1' &= 18.3 \times 10^{-4}\ \text{cm}^{-1} \\ D_e' &= 19.2 \times 10^{-4}\ \text{cm}^{-1} \end{aligned}\right\} \pm 0.1 \times 10^{-4}\ \text{cm}^{-1}$$

$$\alpha' = 0.766\ \text{cm}^{-1} \qquad \beta' = -0.6 \times 10^{-4}\ \text{cm}^{-1}$$

$$r_e' = 1.164 \times 10^{-8}\ \text{cm}$$

$$\Delta G_{1/2}' = 2004.0\ \text{cm}^{-1} \qquad \omega_e' \sim 2310\ \text{cm}^{-1} \qquad x_e'\omega_e' \sim 153\ \text{cm}^{-1}$$

Constants for the $^2\Pi$ State

$$B_0'' = 15.252 \pm 0.005\ \text{cm}^{-1} \qquad D_0'' = 14.3\ (\pm 0.1) \times 10^{-4}\ \text{cm}^{-1}$$

$$r_0'' = 1.084 \times 10^{-8}\ \text{cm}$$

$$\Delta G_{1/2}'' \sim 2755\ \text{cm}^{-1} \qquad \omega_0''\ \text{(Kratzer's relation)} \sim 3150\ \text{cm}^{-1}$$

Constants for the $^4\Sigma^-$ State

$$B_v = 14.94\ \text{cm}^{-1} \qquad D_v = 15 \times 10^{-4}\ \text{cm}^{-1}\ \text{(assumed)}$$

$$r_v = 1.095 \times 10^{-8}\ \text{cm}$$

from linearity would indicate a slight error in $(D'_v - D''_v)$. Using this method and ignoring points in the greatly perturbed region, we obtain, for each subband, two parallel straight lines displaced relative to each other by a constant amount. Such behavior was predicted by Dieke[6] for perturbations in which the quantum number Λ differs by unity in the perturbing and perturbed states ($\Delta\Lambda = \pm 1$). This type of perturbation is variously described as "heterogeneous," "rotational," and "Class A" and differs from the type with $\Delta\Lambda = 0$ (homogeneous, vibrational, Class B) for which theory predicts a return

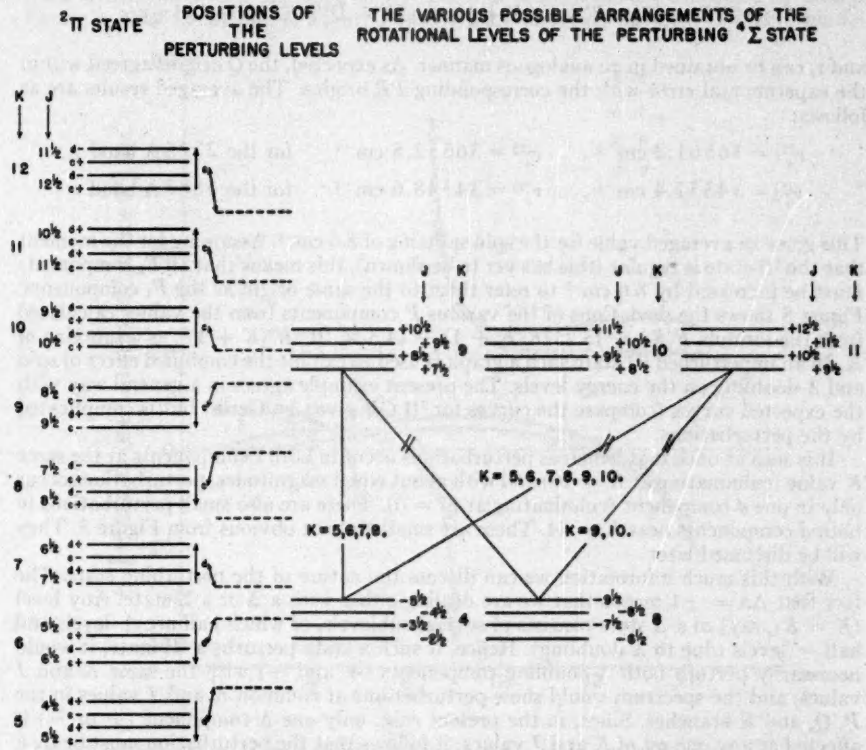

FIG. 2.—Schematic representation of the energy levels of the $^2\Pi$ and $^4\Sigma^-$ states to illustrate the explanation of the perturbations.

to the theoretically unperturbed levels above the region of perturbation. Very often several perturbations occur in the same set of energy levels, making it difficult to test Dieke's theory; and the present example appears to be one of the few cases in which such a test is possible.

To examine the perturbations in the Q branches, the differences $\Delta_2 F''_{1d}(K)$ and $\Delta_2 F''_{2d}(K)$ were determined by the following relation:

$$\Delta_2 F''_{id}(K) = Q_i(K-1) - Q_i(K+1) + \Delta_2 F'(K).$$

From these differences and the ones previously obtained for the c-components (using, in

[6] *Phys. Rev.*, **47**, 870, 1935.

each case, the averages of the values from the two bands) the term values $F''_{1d}(K)$, $F''_{2d}(K)$, $F''_{1c}(K)$, and $F''_{2c}(K)$ were determined. In doing this, it was necessary to use calculated values for $F''_{ic}(1)$, $F''_{id}(1)$, $F''_{ic}(2)$, and $F''_{id}(2)$. The origins (for the K values near the origin) were calculated for the eight sets of branches, viz.: $(P_1R_1)_{2885}$, $(P_1R_1)_{2725}$, $(P_2R_2)_{2885}$, $(P_2R_2)_{2725}$, $(Q_1)_{2885}$, $(Q_2)_{2725}$, $(Q_2)_{2885}$, and $(Q_2)_{2725}$. The formula for this calculation in the case of the P and R branches has been given above. For the Q branches the formula is

$$Q(K) - (B'_v - B''_v)K(K+1) + (D'_v - D''_v)K^2(K+1)^2 = \nu_o ,$$

and ν_o can be obtained in an analogous manner. As expected, the Q origins agreed within the experimental error with the corresponding PR origins. The averaged results are as follows:

$\nu_o^{(1)} = 36561.2$ cm^{-1}, $\nu_o^{(2)} = 36552.8$ cm^{-1} for the 2725 A band;

$\nu_o^{(1)} = 34557.4$ cm^{-1}, $\nu_o^{(2)} = 34548.6$ cm^{-1} for the 2885 A band.

This gives an averaged value for the spin splitting of 8.6 cm^{-1}. Assuming for the moment that the $^2\Pi$ state is regular (this has yet to be shown), this means that all F_2 components must be increased by 8.6 cm^{-1} to refer them to the same origin as the F_1 components. Figure 3 shows the deviations of the various F components from the values calculated from the formula $F(K) = 15.252K(K+1) - 14.3 \times 10^{-4}K^2(K+1)^2$, as a function of K. In an unperturbed $^2\Pi$ state such a graph is used to exhibit the combined effect of spin and Λ doubling on the energy levels. The present example agrees in a general way with the expected curves (compare the curves for $^2\Pi$ CH given by Gerö[4]) but is complicated by the perturbations.

It is seen at once that, whereas perturbations occur in both c components at the same K value (culminating at $K = 10$) and with about equal magnitudes, perturbations occur only in one d component (culminating at $K = 6$). There are also small perturbations in both d components near $K = 14$. These are small and not obvious from Figure 3. They will be discussed later.

With this much information we can discuss the nature of the perturbing state. The fact that $\Delta\Lambda = \pm 1$ means that we are dealing either with a Δ or a Σ state. Any level ($K = K_1$, say) of a Δ state consists of several sublevels, of which half are $+$ levels and half $-$ levels (due to Λ doubling). Hence, if such a state perturbs a $^2\Pi$ state, it would necessarily perturb both Λ-doubling components ($+$ and $-$) with the same K and J values, and the spectrum would show perturbations at common K and J values in the P, Q, and R branches. Since, in the present case, only one Λ component ($+$ or $-$) is affected at any one set of K and J values, it follows that the perturbation must be by a Σ state, where the sublevels of any one K value are either all $+$ or all $-$.

Since the observed transition involves doublet states, it follows that the perturbing Σ state must have even multiplicity. It will be found easiest to discuss the interpretation of the results on the assumption that the perturbing state is a $^4\Sigma$ state. Then $^2\Sigma$ states etc., will be considered. In the case of intercombinations ($\Delta S \neq 0$), the selection rules $\Delta J = 0$, $+ \rightarrow +$, $- \rightarrow -$, apply, but the further restriction $\Delta K = 0$ does not hold.

If we consider the case of the c levels of the $^2\Pi$ state at $K = 10$ (see Fig. 2), then, since both c components are affected, the perturbing level must contain the sublevels $J = 9\frac{1}{2}$ and $J = 10\frac{1}{2}$. The only three numberings that satisfy this condition are shown in Figure 2. (The $+$ and $-$ signs in the $^2\Pi$ and $^4\Sigma$ levels are as yet only relative.) At $K = 6$, only one component of the d levels is affected. This could either be the d level with $J = 5\frac{1}{2}$ or that with $J = 6\frac{1}{2}$, since we have not yet determined which of these levels lies lowest (i.e., whether the $^2\Pi$ state is normal or inverted). If we take the first alternative, the $^4\Sigma$ perturbing level must contain a sublevel $J = 5\frac{1}{2}$ but not $J = 6\frac{1}{2}$, since the $K = 6$,

$J = 6\frac{1}{2}$ level of the $^2\Pi$ state is unperturbed. Similarly, if we take the second alternative, the $^4\Sigma$ perturbing level must contain $J = 6\frac{1}{2}$ but not $J = 5\frac{1}{2}$. The only level satisfying the first condition is $K = 4$, while $K = 8$ is the only level satisfying the second condition. These numberings are indicated in Figure 2. But the numberings of the level causing the perturbation at $K = 10$ and the one causing the perturbation at $K = 6$ cannot be chosen independently, since the two levels must have opposite parity. Thus, for instance, we cannot choose $K = 10$ and $K = 8$ of the $^4\Sigma$ state as the perturbing levels, since these levels always have the same parity. The four possibilities are connected by lines in Figure 2. Now the arrows in Figure 2 indicate the direction in which the $^2\Pi$ levels are

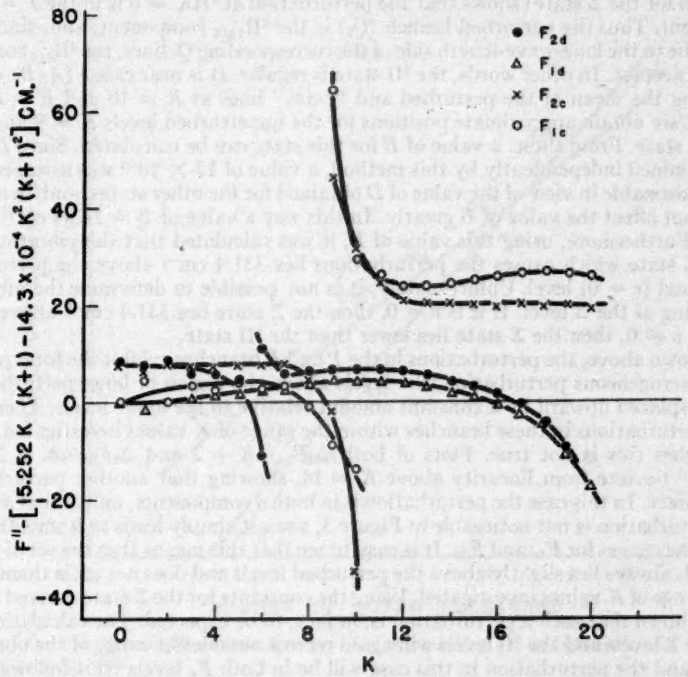

FIG. 3.—The deviations of the sublevels of the $^2\Pi$ state from the formula $15.252K(K+1) - 14.3 \times 10^{-4}K^2(K+1)^2$ due to the combined effects of Λ doubling, spin doubling, and the perturbations.

shifted by the perturbation. Since perturbations are always in the sense of repulsions, it at once follows that the perturbing levels must lie roughly as indicated by the dotted lines, and the number of perturbing levels between $K = 10$ and $K = 6$ of the perturbed state is uniquely defined (as four). Only the combination of $K = 9$ and $K = 4$ of the perturbing levels satisfies this condition, and hence this must be the correct arrangement of levels in the $^4\Sigma$ state.

If we assume the perturbing state to be $^2\Sigma$, the $\Delta K = 0$ rule holds, since the perturbation is then permitted ($\Delta S = 0$). Hence the only level that can perturb $^2\Pi K = 6$ would be $^2\Sigma K = 6$; but such an interaction would cause perturbations in both Q branches in the two bands, whereas only one of the branches is found to be affected. Thus $^2\Sigma$ states can be eliminated. However, similar arguments to those given above for $^4\Sigma$ states may

be given in the case of Σ states of higher multiplicity, and it is not possible to eliminate them from the discussion by direct application of the observational data. On the other hand, low-lying states of these high multiplicities are not possessed by possible emitters of the spectrum, and the large change of spin involved in such an interaction as $^2\Pi - {}^6\Sigma$ makes it unlikely that perturbations of the magnitude observed would occur. Though it is not possible to determine whether the state is Σ^- or Σ^+, application of the parity selection rules for radiative transitions and perturbations shows that, if it is Σ^-, then the upper state $^2\Sigma$ is Σ^+ and vice versa.

The analysis of the perturbations (on the assumption of any even multiplicity greater than two for the Σ state) shows that the perturbation at $^2\Pi K = 6$ is in the $J = 5\frac{1}{2}$ spin component. Thus the perturbed branch (Q_2) is the $^2\Pi_{1\,1/2}$ component, and, since the Q_2 lines all lie to the long-wave-length side of the corresponding Q_1 lines, the $^2\Pi_{1/2}$ component must lie deepest. In other words, the $^2\Pi$ state is regular. It is near case b ($A/B_v = 0.56$).

Taking the mean of the perturbed and "extra" lines at $K = 10$ and $K = 6$ of the $^2\Pi$ state, we obtain approximate positions for the unperturbed levels $K = 9$ and $K = 4$ of the Σ state. From these, a value of B for this state can be calculated. Since D cannot be determined independently by this method, a value of 15×10^{-4} was assumed, which seems reasonable in view of the value of D obtained for the other states, and, in any case, it does not affect the value of B greatly. In this way a value of $B = 14.94$ cm^{-1} was obtained. Furthermore, using this value of B, it was calculated that the vibrational level of the Σ state which causes the perturbations lies 331.4 cm^{-1} above the perturbed $^2\Pi$ vibrational ($v = 0$) level. Unfortunately, it is not possible to determine the vibrational numbering of the Σ level. If it is $v = 0$, then the Σ state lies 331.4 cm^{-1} above the $^2\Pi$ state; if $v \neq 0$, then the Σ state lies lower than the $^2\Pi$ state.

As shown above, the perturbations in the P and R branches exhibit the form predicted for a heterogeneous perturbation, the levels above the region of large perturbation all being displaced upward by a constant amount relative to the lower levels. There are no other perturbations in these branches within the range of K values investigated. For the Q branches this is not true. Plots of both $\Delta_2 F_{1d}/4K + 2$ and $\Delta_2 F_{2d}/4K + 2$ against $(K + \frac{1}{2})^2$ deviate from linearity above $K = 14$, showing that another perturbation is taking place. In this case the perturbation is in both d components, unlike that at $K = 6$. The perturbation is not noticeable in Figure 3, since it simply leads to a smooth depression of the curves for F_{1d} and F_{2d}. It is easy to see that this means that the set of perturbing levels always lies slightly above the perturbed levels and does not cross them, at least in the range of K values investigated. Using the constants for the Σ state derived above, it can be shown that such a perturbation is, in fact, to be expected. The calculations show that the Σ levels and the $^2\Pi$ levels will again recross outside the range of the observed K values, and the perturbation in this case will be in both F_d levels (this follows from an inspection of the selection rules). The Q-branch lines of high K value are just beginning to be affected by this perturbation. Because of this second perturbation, it is difficult to estimate B_0'' for the F_d components, and the more reliable value for the F_e components, as calculated above, has been used wherever necessary in this paper.

IV. THE NATURE OF THE EMITTER

The B values derived above for the various states of the band system show that the emitter must be a diatomic hydride of an element in the first row of the periodic table. All the experimental evidence indicates a compound of nitrogen and hydrogen, since the only other bands observed were due to N_2, H_2, NH, and NH_2. Under conditions in which OH bands occurred, the new bands were absent. No trace of bands due to carbon compounds was found. Furthermore, the B values do not agree with any known B values. Moreover, NH is eliminated, since it gives rise to odd multiplicity states, and we are left with NH^+ and NH^- as alternatives (omitting NH^{+++} and NH^{---}, which both seem extremely unlikely). The molecule NH^+ is isoelectronic with CH, and NH^- with OH;

both these molecules have $^2\Pi$ ground states and no other stable low-lying $^2\Pi$ states; hence we may reasonably assume that the observed $^2\Pi$ state is the corresponding state of the molecule. Theory predicts a regular $^2\Pi$ ground state (or very low-lying $^2\Pi$ state—see later) for *CH* and NH^+, but an inverted $^2\Pi$ state for *OH* and NH^-. The observed state is regular, and hence the emitter cannot be NH^-, and we are left with NH^+ as the only alternative. Furthermore, a very low-lying $^4\Sigma^-$ state is predicted for NH^+, which could be used to explain the perturbations observed. None of the other possible molecules (apart from *CH*, which can be eliminated, since its $^2\Pi$ state is well known) has a very low-lying Σ state.

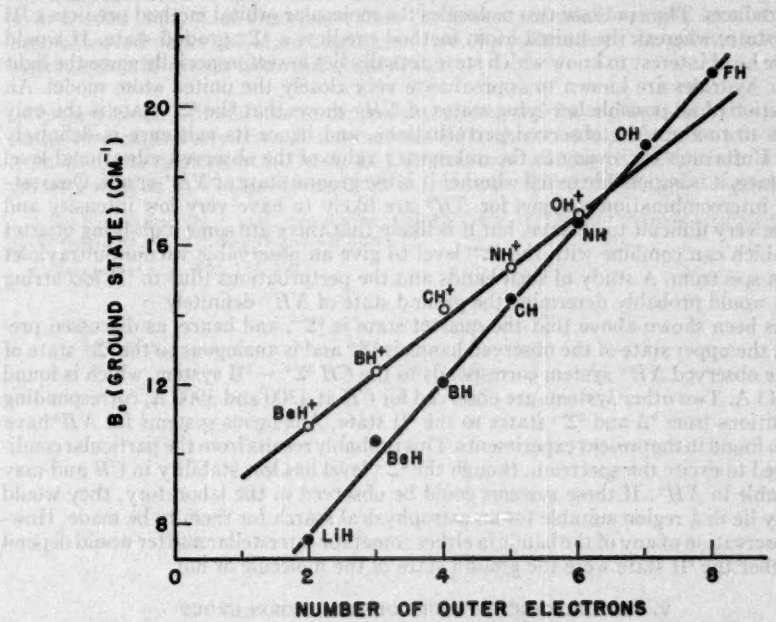

FIG. 4.—Ground state B_e values for the neutral and ionized diatomic hydride molecules of the first row of the periodic table.

As has been shown by Douglas and Herzberg,[7] the ionized and neutral diatomic hydrides of the first row of the periodic table show a smooth, almost linear, variation of B_e (ground state) with the number of outer electrons in the molecule. Such a plot is shown in Figure 4. Plotting the observed B value for the $^2\Pi$ state (B_0'', not B_e'', which cannot be determined), it is seen that the value fits well with the expected value for NH^+. The molecules NH^{+++}, NH^{----}, and NH^- would be expected to fall on different curves, and hence the observed B value is not consistent with any of them being the emitter of the spectrum.

We may thus conclude with a considerable degree of certainty that the emitter is NH^+ and that the observed $^2\Pi$ state corresponds to the known $^2\Pi$ state of *CH*. All the low-lying states of *CH* have been predicted by Mulliken,[8] and an analogous scheme applies for NH^+, except that the dissociation products may differ in this case, since we have to

[7] *Canadian J. Res.*, A, 20, 71, 1942. [8] *Rev. Mod. Phys.*, 4, 5, Fig. 36, 1932.

consider dissociation into both $N^+ + H$ and $N + H^+$. Since the ionization potential of hydrogen is less than that of nitrogen, the lowest pair of dissociation products is $N(^4S_u) + H^+(^1S_g)$, and the first excited pair $N^+(^3P_u) + H(^2S_g)$. The lowest pair of dissociation products can give rise only to a $^4\Sigma^-$ state, as also can the lowest level of the united atom $O^+(^4S_u)$. Thus it would seem very likely that this state is the ground state of the molecule, though its electron configuration, $K(2s\sigma)^2 2p\sigma(2p\pi)^2$, is an excited configuration. The lowest electron configuration is $K(2s\sigma)^2(2p\sigma)^2 2p\pi$, and this gives rise to the $^2\Pi$ state. This state correlates with the first excited state of the united atom $O^+(^2D_u)$ and the first excited state of the dissociation products. This is the same scheme as for CH, except that in the latter the $^2\Pi$ and $^4\Sigma^-$ states both dissociate into the same (ground-state) products. Thus in these two molecules the molecular orbital method predicts a $^2\Pi$ ground state, whereas the united atom method predicts a $^4\Sigma^-$ ground state. It would therefore be of interest to know which state actually lies lowest, especially since the light diatomic hydrides are known to approximate very closely the united atom model. An examination of all possible low-lying states of NH^+ shows that the $^4\Sigma^-$ state is the only one able to produce the observed perturbations, and hence its existence is definitely proved. Unfortunately, owing to the unknown v value of the observed vibrational level of this state, it is impossible to tell whether it is the ground state of NH^+ or not. Quartet-doublet intercombination systems for NH^+ are likely to have very low intensity and would be very difficult to observe, but it is likely that there are some high-lying quartet levels which can combine with the $^4\Sigma^-$ level to give an observable vacuum-ultraviolet emission spectrum. A study of such bands and the perturbations (due to $^2\Pi$)occurring in them would probably determine the ground state of NH^+ definitely.

It has been shown above that the quartet state is $^4\Sigma^-$, and hence, as discussed previously, the upper state of the observed bands is $^2\Sigma^+$ and is analogous to the $^2\Sigma^+$ state of CH. The observed NH^+ system corresponds to the $CH\ ^2\Sigma^+ - {}^2\Pi$ system, which is found near 3143 A. Two other systems are observed for CH at 4300 and 3900 A, corresponding to transitions from $^2\Delta$ and $^2\Sigma^-$ states to the $^2\Pi$ state. Analogous systems for NH^+have not been found in the present experiments. This probably results from the particular conditions used to excite the spectrum, though the $^2\Sigma^-$ level has low stability in CH and may be unstable in NH^+. If these systems could be observed in the laboratory, they would probably lie in a region suitable for an astrophysical search for them to be made. However, observation of any of the bands in either comets or interstellar matter would depend on whether the $^2\Pi$ state were the ground state of the molecule or not.

V. THE DIATOMIC HYDRIDES OF THE CARBON GROUP

Diatomic hydride spectra have been analyzed for CH, SiH, SnH, and PbH. For all these molecules there should be a low-lying (as yet unobserved) $^4\Sigma^-$ state. No perturbations have been observed in the $^2\Pi$ states of any of these molecules, though PbH has not yet been thoroughly investigated.[9] Since quartet-doublet transitions in these molecules would have a very low probability, one of the few ways of determining the positions of the $^4\Sigma^-$ states would be to investigate quantitatively the Λ doublings in the $^2\Pi$ states. It is well known that the Λ doublings in a Π state are due to an interaction (perturbation) of this state and the various Σ states in the term manifold. The theory of this effect has been worked out, with certain simplifying assumptions, by Van Vleck[10] and by Mulliken and Christy,[11] and the theoretically computed Λ doublings are found to agree well with those determined experimentally for most molecules. For SiH, SnH, and PbH no such calculations are possible, since the positions of the low-lying $^2\Sigma^-$ states are not known. However, for CH, Mulliken and Christy have carried out the calculations, taking into account the fact that the $^2\Pi$ state interacts with both the $^2\Sigma^-$ and $^2\Sigma^+$ states. The cal-

[9] See Howell, *Proc. Phys. Soc.*, **57**, 37, 1945.

[10] *Phys. Rev.*, **33**, 467, 1929.

[11] *Phys. Rev.*, **38**, 87, 1931.

culated Λ doublings do not agree with those experimentally observed.[12] This is no doubt partly due (as stated by Mulliken and Christy) to the inadequacy of the formulae used in the case of a molecule with three outer p electrons, but it would seem that a low-lying $^4\Sigma^-$ state would also affect the Λ doublings considerably. Although the interaction constant will be small, the separation of the two states will also be small, and the effect may therefore not be negligible. A more detailed theoretical study might allow the position of the $^4\Sigma^-$ level in *CH* to be predicted. It may be mentioned that if the discrepancy of theory and experiment was all to be ascribed to the effect of the $^4\Sigma^-$ state, it would lie above the $^2\Pi$ state. Indeed, it seems certain that the $^2\Pi$ state is the ground state, since molecules in this state are found to exist in interstellar space. Bands of *SiH* are found in absorption in solar spectra, but, since absorption from the lowest metastable singlet level of *NH* has been observed under the same conditions,[13] no conclusion as to the ground state of the molecule can be drawn from this observation.

In conclusion I should like to express my sincere thanks to Dr. G. Herzberg, F.R.S., for his interest and advice on all matters related to this research. I have benefited greatly from many discussions with Dr. A. E. Douglas, to whom my thanks are also due. I am grateful to Miss R. Craig, who assisted in the measurement of the spectrograms.

[12] See Fagerholm, *Ark. f. mat., astr. och fys.*, Vol. 27 *A*, No. 19, 1940, for the most accurate evaluation of the constants of the Λ doubling in *CH* and *CD*.

[13] Babcock, *Ap. J.*, **102**, 154, 1945.

CHARACTERISTICS OF SOLAR FLARES

ROBERT S. RICHARDSON
MOUNT WILSON AND PALOMAR OBSERVATORIES
CARNEGIE INSTITUTION OF WASHINGTON
CALIFORNIA INSTITUTE OF TECHNOLOGY
Received May 17, 1951

ABSTRACT

Attention is called to certain characteristics of the changes in area of solar flares which, on a much reduced time scale, are suggestive of the light-curves of novae. Different types of flares are discussed on the basis of these characteristics.

A flare has been called "fast" if it attains maximum area within less than 0.4 of its lifetime. A flare is "slow" if it attains maximum after 0.4 of its lifetime. About 75 per cent of all flares are fast. But very slow flares of low intensity do occur.

A region has been called "recurrent" if 5 or more distinct flares are observed there at one station in one transit of the disk or if 10 or more have been reported by all co-operating observatories. Recurrent regions are most often in or near spot groups of complex magnetic polarity (γ and $\beta\gamma$ groups). Although flares are least likely to occur over stable unipolar groups, there are recurrent regions in the *Quarterly Bulletins* that were associated with groups predominantly unipolar.

In the *Quarterly Bulletins* the active regions are given a new number at each rotation, regardless of whether a region appeared at preceding rotations. When the results are reduced to *individual active regions*, it was found that 159 such regions over which recurrent flares appeared produced 4187 of the 8056 flares recorded from October, 1935, to December, 1949. That is, 159 individual active regions, which constituted 12 per cent of the whole number of 1371, produced 52 per cent of the flares.

Occasionally a flare appears abnormally bright for several hours or even days with only minor changes in form and intensity. Such flares have been called "persistent." An interesting example is described which was apparently the cause of exceptionally intense reception on the 80 Mc/sec band.

The name of "flash" has been given to weak flares with a duration of 5 minutes or less. Some flash flares may possibly be prominence "surges" seen on the disk. Owing to difficulties of observation, the flash flares may be more numerous than we suppose and may possibly make a considerable contribution to the solar ultraviolet radiation.

Flares of intensity 3+ have been called "superflares." About 70 per cent are associated with spot groups of complex magnetic polarity. A comparison of complex groups and simple bipolar groups of the same area shows that the number of flares over the complex groups is always greater.

The question has been investigated of whether two or more flares occur nearly simultaneously over widely separated spot groups more often than would be expected by chance. The number of multiple flares observed was found to be higher than the number calculated, if they occurred at random, from Poisson's law. It is felt, however, that a definite conclusion cannot be drawn until data are available for another cycle.

The total emission from the flare of February 21, 1950, at maximum intensity in the K line was found by photographic photometry to be 3.2×10^{26} erg/sec. The radiation from the hemisphere of the sun at 6000° K in the same width of neighboring spectrum is 1395×10^{26} erg/sec.

I. INTRODUCTION

Despite the fact that solar flares have been widely discussed since their ionospheric effects were first clearly recognized about 1936, no general method of describing them exists beyond the eye estimates of intensity in the *Quarterly Bulletins on Solar Activity*. There are times, however, when a ready method of describing a flare would seem desirable, rather than launching into a detailed account of its rise and fall. We usually distinguish between objects by their appearance, but flares occur in such a variety of forms that it is doubtful whether this method could be applied to them. In our work we have found that changes in the area of flares have certain characteristics which remind us of the changes in brightness displayed by novae and which would seem to form a handy means of describing some of their most outstanding features. In borrowing from the terminology used in referring to novae, however, it should be emphasized that there is no intention of implying that any real similarity exists between the two phenomena.

Table 1 contains the classes into which flares have been divided. Owing to the variety of instruments used by different solar observers and the lack of exact quantitative measurements, it was decided, except where otherwise stated, to restrict the discussion to flares recorded at Mount Wilson from October 1, 1935, to June 30, 1950. This material should be on a fairly uniform scale, since the observing program during this interval has remained essentially unchanged and all the estimates of intensity are my own.

Although definite limits have been set in Table 1, they are strictly applicable only to our own observations. It is doubtful whether a hard-and-fast set of rules applicable to all observers is possible or even desirable. No special significance, therefore, should be attached to these definitions. It is hoped only that they may be found useful as general reference terms in describing flares in somewhat the same way that we speak of a star as being of "early" or "late" type.

TABLE 1

A TERMINOLOGY FOR SOLAR FLARES

Name	Description
Fast	A flare that reaches maximum area at or before 0.4 of its lifetime.
Slow	A flare that reaches maximum area after 0.4 of its lifetime.
Flash	A flare of intensity 1 or 1− with a life of 5 minutes or less.
Persistent	A flare that is abnormally bright for 2 hours or more.
Recurrent	A region in which 5 or more flares have been recorded at one station in a single transit across the disk, or for which 10 or more flares are given in the *Bulletins* in a single transit.
Superflare	A flare of intensity 3+.

II. FAST AND SLOW FLARES

Figure 1 shows the changes in area of a flare of maximum intensity 3, which began at 23^h40^m on February 21, 1950. At 23^h45^m the flare had an area of 2200,[1] had dropped to 750 by 23^h53^m, after which it declined more slowly, so that at 24^h40^m it was about intensity 1, with an area of 400. The relative speed with which the flare rose to maximum area reminds one of the light-curve of a fast nova.

Figure 2 shows the changes in area of a flare which began at 15^h09^m on July 3, 1941. At 15^h26^m it was of intensity 2 with an area of 750. The bright material began to decline as if fading away, but at 15^h59^m it began to brighten again, so that by 16^h21^m it was of intensity 3, with an area of 1000. It then declined, with small fluctuations in intensity, but was still brighter than the normal quiescent calcium flocculi when observations ended about 18^h. In this flare the relative changes in the area-curve remind us of a slow nova, such as Nova Pictoris or Nova Herculis.

Whereas the light-curves of novae are so distinctive that there is seldom any doubt as to whether it is fast or slow, no correspondingly sharp division was found for flares. Figure 3 shows the times required to reach maximum area for 490 flares for which we have complete life-histories. The time interval to maximum is seen to vary smoothly from 5 to 60 minutes and probably longer in rare cases.

If we plot the time interval required to reach maximum—not in minutes but as a fraction of the total lifetime of the flare—we obtain quite a different distribution, as shown in Figure 4. Instead of a smooth curve, there is a fairly sharp break at 0.4, such that about 75 per cent of the flares reach maximum within 0.4 of their lifetime. We have called a flare "fast" or "slow," depending upon whether it reaches maximum area before or after 0.4 of its lifetime has elapsed, respectively.

This division was found to hold fairly well for both weak and strong flares. Of 408 flares

[1] Areas on the solar disk are customarily expressed in millionths of the sun's visible hemisphere. Thus a spot group with an area of 1000 covers a thousand millionths, or 0.1 per cent, of the visible hemisphere.

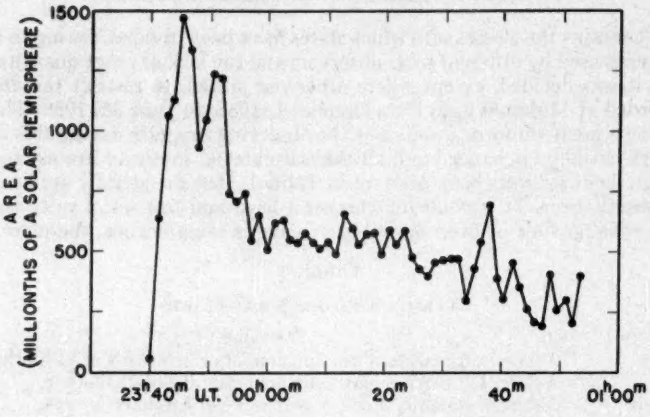

FIG. 1.—The "fast" flare which began at 23^h40^m on Feb. 21, 1950

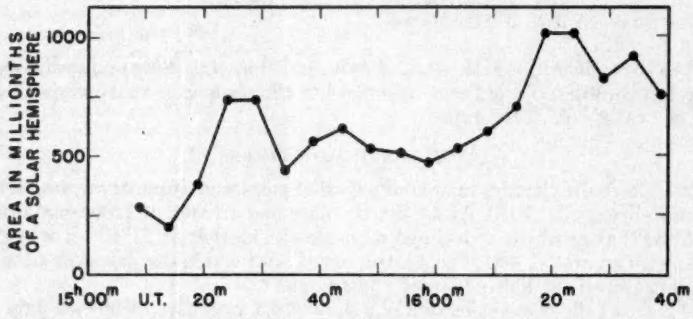

FIG. 2.—The "slow" flare which began at 15^h09^m on July 3, 1941

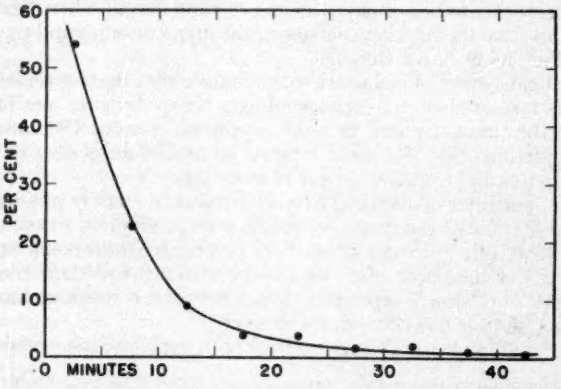

FIG. 3.—Frequency of flares according to actual time required to reach maximum intensity

of intensity 1 and 1−, there were 74.3 per cent that attained maximum within 0.4 of their lifetime. Of the remaining 82 flares of intensity 2 and 3, there were 79.3 that reached maximum within 0.4 of their lifetime. But the time in minutes required to reach maximum for weak and strong flares is quite different. Thus, among flares of intensity 2 and 3, there were 80 per cent that reached maximum within 20 minutes or less, while, for flares of intensity 1 and 1−, the same proportion reached maximum within less than 10 minutes.

It is interesting to note, however, that well-observed weak flares have sometimes required more than an hour to reach maximum, with a correspondingly slow decline. The "lightning-like" speed with which flares often increase in brightness has perhaps been overemphasized.

III. RECURRENT FLARES

From October 1, 1935, to June 30, 1950, 1118 flares were recorded at Mount Wilson over 577 regions. From October 1, 1935, to December 31, 1949, there are 8056 flares given in the *Bulletins* which occurred over 1867 active regions. Table 2 shows the frequency with which flares occurred over the active regions as recorded at Mount Wilson

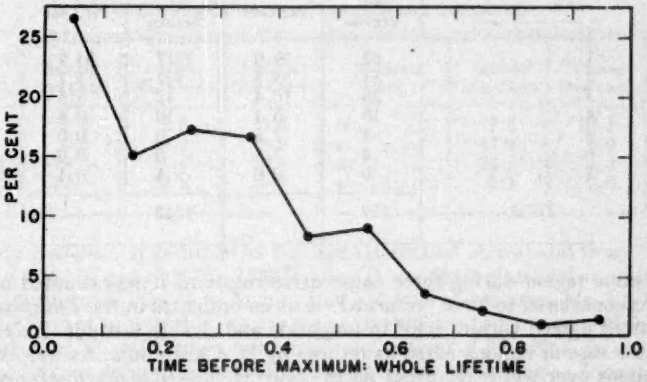

FIG. 4.—Frequency of flares according to fraction of lifetime required to reach maximum intensity

TABLE 2

DISTRIBUTION OF FLARES OVER ACTIVE REGIONS

No. of Flares	Mount Wilson (Per Cent of Regions)	All Observatories (Per Cent of Regions)	No. of Flares	Mount Wilson (Per Cent of Regions)	All Observatories (Per Cent of Regions)
1.....	62.9	34.6	9.....	0.0	1.5
2.....	17.0	20.2	10.....	0.5	1.6
3.....	8.1	11.4	11.....	0.5	1.0
4.....	4.9	7.0	12.....	0.0	1.0
5.....	0.9	5.0	13.....	0.2	1.0
6.....	1.9	3.5	14.....	0.0	0.8
7.....	2.4	3.2	⩾15.....	0.2	5.5
8.....	0.5	2.7			

and by all co-operating observatories during these intervals. From inspection of Table 2 a region has been (rather arbitrarily) considered to be exceptionally active or "recurrent" if 5 or more flares were recorded over it in one rotation at Mount Wilson or 10 or more by all co-operating observatories.

In the *Quarterly Bulletins* the "régions actives" are numbered in the order of their central meridian passage during the months included in that bulletin, although some of the regions may have appeared at previous rotations. For example, an active region that survived two rotations and returned a third time would be recorded under three different numbers.

In Table 3 the figures refer to *individual active regions*. That is, if flares were observed

TABLE 3

COMPARATIVE DURATION OF RECURRENT AND NONRECURRENT ACTIVE REGIONS

No. Rotations Observed	Recurrent		Nonrecurrent	
	No. Regions	Per Cent	No. Regions	Per Cent
1	62	39.0	1017	83.9
2	53	33.3	142	11.7
3	26	16.4	42	3.5
4	10	6.3	10	0.8
5	4	2.5	0	0.0
6	4	2.5	0	0.0
7	0	0.0	1	0.1
Total	159	.....	1212	.....

over the same region during three consecutive rotations it was counted only *once*. A region was considered to have "returned" if its co-ordinates in the *Bulletins* for successive rotations agreed within $\pm 10°$ in longitude and $\pm 5°$ in latitude. Exceptions were made in the case of regions noted as returns by L. d'Azambuja. As was expected, the active regions over which recurrent flares occurred showed a much stronger tendency to return than did the active regions over which nonrecurrent flares occurred. The 159 individual active regions over which the recurrent flares occurred produced 4187 of the 8056 flares recorded from October, 1935, to December, 1949. That is, 12 per cent of the active regions produced 52 per cent of the flares.

The spot groups over which the flares recurred were examined for special features that might account for their exceptional activity. The only feature that seemed significant was the magnetic classification of the group on the day the flare occurred, a large percentage being complex groups of the γ and $\beta\gamma$ class.[2]

A sample distribution of the daily magnetic classification of all spot groups was obtained from our records for the years of maximum activity of 1937 and 1947, as shown in the second column of Table 4. The third column gives the distribution in the magnetic classification of spot groups over which flares were observed. The increase in the percentage of spot groups classified as γ and $\beta\gamma$ is noteworthy. If, however, we restrict the count to groups over which 5 or more flares were observed, the increase in the percentage of complex groups, as shown in the fourth column, becomes very impressive indeed. It is seen that, although, on the average, complex groups constitute only 6 per cent of the total number, yet they constitute 56 per cent of the recurrent flares. This

[2] Hale and Nicholson, *Mt. W. Contr.*, No. 300; *Ap. J.*, **62**, 270, 1925.

subject has been discussed from a somewhat different point of view by R. G. Giovanelli,[3] who arrived at essentially the same results.

Although flares seldom occur in or near stable unipolar spot groups, yet there are 11 groups of this type in the *Quarterly Bulletins* with which 10 or more flares were associated. Our records show, however, that 10 of these active unipolar groups were very close either to groups of opposite polarity or to groups undergoing rapid changes in form and area, or to both.

The lone exception is Mount Wilson No. 5914 (Greenwich No. 12844), a stable, isolated spot in latitude 6° S., longitude 192°, first seen on the east limb on May 31, 1938. This group displayed none of the characteristics commonly supposed to be associated with flares; yet a dozen flares were observed over it, one of which was of intensity 2+. While the spot group was of the stable type, still the region itself was active over an unusually long interval. The first group to appear in this region was No. 5877 (Greenwich No. 12808) from May 4 to May 16, a bipolar group in which the penumbra of the following and preceding portions merged on May 8 and over which 8 flares are recorded in

TABLE 4

MAGNETIC CLASSIFICATION OF ALL SPOT GROUPS COMPARED WITH GROUPS OVER WHICH FLARES WERE OBSERVED

Magnetic Class.	Sample (Per Cent)	1 Flare (Per Cent)	5 Flares (Per Cent)	Magnetic Class.	Sample (Per Cent)	1 Flare (Per Cent)	5 Flares (Per Cent)
γ	1.4	7.8	20.4	βf	7.2	10.5	5.7
βγ	4.6	20.2	35.5	α	13.3	6.9	0.0
β	19.8	16.6	7.4	αp	24.1	6.3	4.1
βp	27.6	30.9	26.9	αf	2.1	0.8	0.0

the *Quarterly Bulletins*. It returned as No. 5914 described above; and from June 27 to July 8 as No. 5962 (Greenwich No. 12887), when it was again classified as unipolar. But, at its next return from July 24 to August 5 as No. 6017 (Greenwich No. 12934), it appeared in the form of an unstable bipolar group, over which 15 flares were observed. It is uncertain whether No. 6017 was a new group or a revival of No. 5962. In any case, the region around a spot group of the stable type was active for as long as 3 months.

H. W. Newton[4] has called attention to the fact that intense flares and great magnetic storms frequently occur in pairs or even in groups of three, the members of each pair being separated by 3 or 4 days, on the average. An example of this effect seems to have occurred in February, 1950. According to Newton, the available evidence points to a flare over the big spot group of February 17 observed between 01^h50^m and 03^h05^m as the antecedent of a great magnetic storm which began February 20 at 15^h16^m, after an interval of 86 hours. Three days after the great storm the magnetometer at Mount Wilson showed an apparently new storm beginning February 23 at 10^h42^m, or 35 hours after the flare of February 21 previously described.

IV. PERSISTENT FLARES

Occasionally a flare, instead of fading away and leaving the region much as it was before, will remain abnormally bright for several hours or even days. In other cases a bright region appears which, at first glance, gives the impression that a flare is in progress, but continued observations fail to show any of the rapid changes in intensity characteristic of flares. Flares that remain abnormally bright for about 2 hours or more have been

[3] *Ap. J.*, **89**, 555, 1939.

[4] *Observatory*, **70**, 233, 1950.

called "persistent," by analogy with stars such as P Cygni which show permanent nova characteristics.

An interesting example of a persistent flare occurred over Mount Wilson No. 10373, a spot group in latitude 18° S. that crossed the central meridian June 15.0, 1950. A flare of intensity 1 was observed over the group when first seen on the east limb on June 8, and 4 more flares were seen on June 9, one of which was of intensity 2. No further activity was seen by us that seemed significant until observations were begun at 14^h51^m on June 11, when a small bright area that had not been there the previous day was noticed some 5° northwest of the tip of the leading member of the group. The area slowly increased in brightness until, on June 16 from about 15^h to 18^h, it would probably have been called a flare of intensity 1− if we had had only a single observation. The area then began to fade but was still abnormally bright when 71° W. on June 19.

According to A. Maxwell,[5] of Manchester University, England,

> from June 13 to June 15 we recorded very intense radio reception from the sun on the 80 Mc/s band. It would appear that the sunspot responsible for this was a very small one[6]; 600 millionths (June 8), 18°.5 S., C.M.P. June 14.5—the only active region on the visible hemisphere between the above dates. The radiation was some 1000 times above the normal "quiescent" level (corresponding to a half-degree source of temperature of 10^9 deg. K, compared with the quiescent 10^6 deg. K at 80 Mc/s). Intensities of this magnitude are usually only associated with major sunspot groups.

The observations indicate that important ionospheric effects may be produced by persistently active regions, even when of low intensity, as well as by those of the more spectacular type.

V. FLASH FLARES

The name of "flash" has been given to flares of intensity 1 and 1− with a life of 5 minutes or less. Although they seem trivial, yet it is possible that in the aggregate they may be of considerable importance. We know that there are more flares of intensity 2 than of intensity 3 and many more flares of intensity 1 than of intensity 2. The question is: How many flares are there much fainter than 1 which escape detection? I recall that, with the 43-cm solar image at the 150-foot tower, small flares could be seen practically any time over the great spot group of February, 1946. Multitudes of weak flares of short life might make a significant contribution to the radiation from the sun in the ultraviolet.

It is possible that some flash flares may be prominence "surges" seen on the disk.

VI. SPOTLESS FLARES

Of 1118 flares recorded at Mount Wilson from 1935 to 1950, 10, or 0.9 per cent, occurred where no spot group was observed. In almost every case, however, either a group could be found within less than 15° of the flare, or a group had been observed near the position a few days before. An exception is flare No. 4 in Table 5, which apparently was wholly independent of any spot group. The only possibility is a tiny spot of 1-day duration on October 9, 1936.

VII. SUPERFLARES

H. W. Newton[7] has used the term "superflares" in referring to flares of exceptional brightness designated 3+. He lists 37 such flares from 1859 to 1942, to which 4 more should probably be added to bring the list up to date. Superflares are distinguished by their great area, by possible peculiarities of spectrum, and by the fact that they are al-

[5] Personal letter.

[6] Solar observers would hardly call a spot group with an area of 600 a "very small one." Spots of that size have been seen without a telescope.

[7] *M.N.*, 103, 244, 1943.

most invariably followed by a great magnetic storm about 24 hours later. It is still uncertain, however, whether superflares are ordinary flares of great brightness or whether they differ in some special way from the others.

Newton found that 70 per cent of the superflares occured over spot groups classified as γ or $\beta\gamma$, but he remarked that this may merely reflect the tendency for great spot

TABLE 5

FLARES WHICH OCCURRED WHERE NO SPOT GROUP WAS OBSERVED

No.	Date	First Seen	Approx. Lat.	Approx. Long.	Max. Int.	Group Nearest Flare: Date	Class.	Lat.	Long.
1.....	1918 Sept. 15	18^h20^m	10° N.	267°	2	Sept. 14	βp	11° N.	266°
2.....	1926 Mar. 14	16 36	20 N.	37	1	Feb. 27	γ	22 N.	28
3.....	1936 Mar. 12	22 51	15 N.	226	1	Mar. 3	dxd	16 N.	222
4.....	Oct. 12	16 41	22 N.	197	2	Oct. 9	dxd	19 N.	210
5.....	1937 Jan. 4	21 25	16 N.	202	1	Jan. 4*	?	15 N.	211
6.....	July 16	22 45	18 S.	156	3	July 16	1βpd	15 S.	141
7.....	Oct. 20	15 51	21 S.	330	1	Oct. 19	dβpd	21 S.	332
8.....	1938 Nov. 24	16 14	17 N.	126	1	Nov. 20	1βd	16 N.	129
9.....	1942 Dec. 10	17 41	12 S.	88	1	Dec. 7	1βpd	12 S.	92
10.....	1949 June 23	14 33	14 N.	171	1	June 21	1ad	12 N.	177
11.....	Oct. 15	16 30	19 N.	188	1	Oct. 15	1β1	19 N.	173
12.....	Nov. 2	15 23	6 N.	261	1	Oct. 31	dxd	12 N.	258

* No. 12158 of the Greenwich series was observed at this position from December 28, 1936, to January 5, 1937. It was a group of maximum area 94, described as "a regular spot breaking up and disappearing rapidly after January 3" (*Grn. Phot. Results*, 1936, p. C139). No solar observations were made in the United States or Canada from December 29, 1936, to January 3, 1937, inclusive.

TABLE 6

MEAN AREAS OF SPOT GROUPS OF DIFFERENT MAGNETIC CLASS

Magnetic Classification	Per Cent	Mean Area	Standard Error	Magnetic Classification	Per Cent	Mean Area	Standard Error
α.....	13	125	± 4	βp.....	27	255	± 6
αp.....	28	145	± 3	βf.....	7	158	± 9
αf.....	3	70	± 8	$\beta\gamma$.....	4	416	±25
β.....	16	191	±10	γ.....	1	887	±80

groups to be of complex magnetic type. To investigate the size of complex groups relative to others, the areas of 6743 groups observed at Mount Wilson from 1917 to 1924, inclusive, were arranged according to their magnetic classification on each day. The magnetic classifications were taken from the *Magnetic Classifications of Sunspots 1917–1924*,[8] and the areas from the *Greenwich Photoheliographic Results*. The mean areas for the different magnetic classifications are given in Table 6.

The difference between the mean areas of the γ groups and the βp groups is 632, which is 8 times the standard error of the difference. The difference between the mean areas of the $\beta\gamma$ groups and the βp groups is 161, which is 6 times the standard error of the difference. It appears, therefore, that complex groups are actually larger than simple bipolar groups.

[8] Hale and Nicholson, *Carnegie Inst. Washington*, Pub. No. 498, Part I.

To determine whether complex groups are more effective in producing flares than simple bipolar groups of the same area, a list was made of the predominant magnetic classification of the groups associated with the active regions in the *Quarterly Bulletins* for 1936 and 1938. (The *Greenwich Photoheliographic Results* are not yet available for 1937, and the years before 1936 had to be omitted, since observations of flares were then too scarce to be of statistical significance.) The number of flares, N, was assumed to be related to the total area of the spot group, S, by the equation,

$$N = aS + bS^2 . \qquad (1)$$

The curve was forced through the origin, since, as we have already seen, flares practically never occur over spotless regions.[8]

Values of N obtained from least-square solutions for the complex and bipolar groups are given in Table 7. For both types of groups the number of flares increases almost

TABLE 7

FREQUENCY OF FLARES OVER COMPLEX AND SIMPLE BIPOLAR GROUPS

Area	Number of Flares		Area	Number of Flares	
	Complex Groups	Bipolar Groups		Complex Groups	Bipolar Groups
250	6	4	1000	22	16
500	12	8	2000	33	26
750	18	12			

linearly up to an area of 2000, but the number of flares is always larger for the complex groups.

VIII. MULTIPLE FLARES OVER WIDELY SEPARATED SPOT GROUPS

In 1936 attention was called to cases in which flares occurred nearly simultaneously over widely separated spot groups.[9] The question has been reinvestigated with the material that has accumulated since that time. Because different observers differ in their methods of recording and enumerating flares and because it is highly essential for this investigation that the data be on a uniform basis, the material has been restricted to our own.

The problem is an intricate one, and it is doubtful whether any two people would approach it by quite the same method. The one chosen here was to compare the observed frequency distribution with a theoretical distribution calculated from the laws of probability, such as Poisson's law. This law states that the probability $P_m(n)$ of n successes in m trials is given by

$$P_m(n) = \frac{e^{-\epsilon}\epsilon^n}{n!}, \qquad (2)$$

where $\epsilon = mp$, p being the probability of success in a single trial and e the natural base of logarithms.

It will be recalled that Poisson's law rests upon two basic assumptions; namely, that (*a*) the probability of one or more points lying within a definite interval is not influenced by any knowledge we may have concerning the states of the other intervals and that (*b*) each point in any such interval lies at random, independently of all the rest.

[9] *Ann. Rept. Director Mt. W. Obs.*, No. 35, p. 171, 1935–1936.

The procedure consisted in counting the number of flares 0, 1, 2, etc., recorded during a certain time interval and comparing the distribution obtained, calculated from equation (2).

Since flares almost always occur over spot groups, the probability of observing flares during a given time interval will obviously be greater, the more groups there are on the disk. But, for Poisson's law to apply, the probability of an event's occurring must be the same for all intervals. This difficulty was partially avoided by confining the observations to days when the number of groups upon the disk gave roughly the same number of flares per 100 hours of observation. Table 8 shows the number of flares per 100 hours

TABLE 8

FLARES PER 100 HOURS FOR DIFFERENT NUMBER OF SPOT GROUPS ON THE DISK OBSERVED AT MOUNT WILSON

No. Groups on Disk	Flares per 100 Hours	No. Groups on Disk	Flares per 100 Hours
0	0.0	10	6.5
1	0.2	11	5.4
2	0.8	12	4.7
3	1.2	13	5.0
4	0.9	14	6.2
5	1.9	15	7.4
6	4.0	16	7.3
7	3.7	17	4.6
8	4.7	18	6.3
9	5.1	19	14.0
		20–23	11.4

for days when there were 0, 1, 2, . . . , 23 groups upon the disk from 1937 to 1949, inclusive. It is seen that the number of flares per 100 hours is fairly constant when there were 6–14 groups, inclusive, upon the disk. The material was therefore confined to days when the number of groups fell within these limits.

The time intervals chosen were 0.5, 1.0, and 4.0 hours; that is, a flare was not counted unless it was first seen within, say, an interval of 1.0 hour. Furthermore, the interval was always counted from the *beginning* of a period of observation. For example, if we had observations from 19^h00^m to 20^h17^m, the interval was counted only from 19^h00^m to 20^h00^m. A flare first seen at 20^h03^m would not have been counted. Otherwise, by juggling the time intervals about, it would have been possible to alter the form of the distribution considerably.

Table 9 shows the distributions obtained compared with those calculated from Poisson's law. In no case does the number of multiple flares observed conform to the number calculated. Application of the χ^2 criterion for the goodness of fit gives a probability of less than 0.01 in each case.

Although the formal statistical results as well as the visual impression conveyed from inspection of the photographs suggests that some form of coupling may exist between widely separated spot groups, it is felt that the question must still be regarded as open. Probably another cycle must elapse before sufficient data will be available to provide a definite answer.

IX. RADIATION FROM THE K LINE DURING A FLARE

Photographs of the flare of February 21, 1950, were calibrated by means of diaphragms placed automatically over the grating at the beginning of each exposure. The intensity,

I, of the larger portion of this flare was measured with respect to the intensity, I_0, of the undisturbed disk as recorded on the spectroheliogram in the center of the K line. These ratios are given in Table 10. From calibrations on our film the intensity at the center of K in the undisturbed disk is about 0.11 of that of the neighboring continuous spectrum. From measures on the spectra of several flares photographed on previous occa-

TABLE 9

NUMBER OF FLARES OBSERVED COMPARED WITH NUMBER CALCULATED FROM POISSON'S LAW

No. of Flares	0b5		1b0		4b0	
	Obs.	Calc.	Obs.	Calc.	Obs.	Calc.
0	19,246	19,230	7908	7880	1576	1533
1	494	527	431	484	251	324
2	24	7	36	15	55	34
3			4	0	10	2
4					1	0
5					1	0

TABLE 10

RADIATION FROM THE K LINE IN THE FLARE OF FEBRUARY 21, 1950

Exposures (Minutes)	I/I_0	Area (Cm^2)	Radiation (Erg/Sec)
1.3	27.0	3.23×10^{19}	4.4×10^{28}
5.3	17.0	4.06×10^{19}	3.4×10^{28}
8.9	12.0	3.16×10^{19}	1.9×10^{28}

sions the width of emission in K was found to be about 0.5 A. The radiation from a black body at 6000° K at λ 3950 in 1 A is 9.16×10^6 erg/cm²/sec. The total radiation from the flare in the K line should therefore be given by

$$\frac{I}{I_0}(0.11)\ (0.5)\ (9.16\times10^6)\ (\text{area flare cm}^2)\ .$$

The results obtained from exposures made 1.3, 5.3, and 8.9 minutes, respectively, after the flare commenced are shown in Table 10. The radiation from one hemisphere of the sun in 0.5 A at λ 3950 at a temperature of 6000° K is 1395×10^{26} erg/sec.

I am indebted to R. P. Dilworth, of the mathematics department of the California Institute of Technology, for advice on the investigation of multiple flares, and to Miss Elizabeth Keely for help in reducing much of the material.

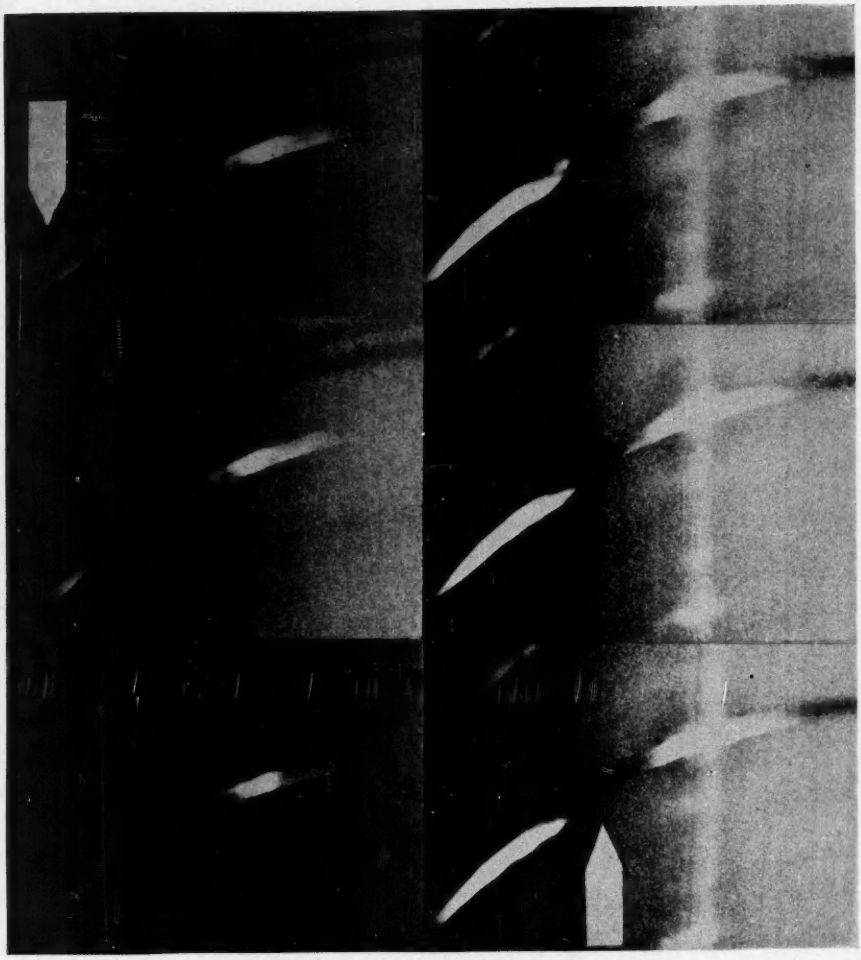

FIG. 1.—Three wide-slit exposures of the corona spectrum, showing a dark filament in the *Hα* line (*right*) and to some extent also in the helium D3 line (*left*). Climax, July 26, 1949.

SOME OBSERVATIONS OF DARK FILAMENTS IN PROMINENCES

YNGVE ÖHMAN
Stockholm Observatory, Saltsjöbaden, Sweden
Received January 25, 1951

ABSTRACT

During a year's stay at the High Altitude Observatory in Boulder, Colorado, the writer had the opportunity to study a number of spectrum plates of the corona obtained with a wide slit. A great number of photographs of prominences have also been examined. Indications have been found of the presence in many prominences of apparently dark filaments, when observations are made in the *Hα* line. Though it is generally difficult to distinguish between "dark" filaments and rifts, some rather convincing cases suggesting the presence of faintly luminous lanes of absorbing matter have been detected. The observations have been confirmed by spectroheliographic material kindly put at my disposal by the Mount Wilson and the McMath-Hulbert Observatories. Photographs of prominences selected in 1948 and 1949 at the Stockholm Observatory and examined after my return to Sweden have also given evidence in favor of the opinion that a "dark" structure is often associated with prominences.

I. EVIDENCE FROM WIDE-SLIT SPECTRA OF THE CORONA

In connection with a polarimetric study of the corona, using the deep Fraunhofer lines and analyzing the polarization by means of Savart interference fringes[1] the writer took a number of spectra of the corona with the Climax Observatory coronagraph. For this work it was found preferable to use a wide slit in the spectrograph. From a careful study of such plates the writer has sometimes found traces of dark lanes in the *Hα* line. Wide-slit spectra have also been taken, therefore, without the Savart plates. In some cases the dark lanes can be seen in front of bright prominences (and also in the helium D3 line); in other cases dark lanes have been detected in the *Hα* absorption line projected against the faint background formed by the corona or by extended and very faintly luminous prominences.

Figure 1 shows an example in which dark lanes extend partly in front of and partly between two prominences. The observations were made with the Climax spectrograph at the east limb on July 26, 1949. The images to the left give the helium D3 line,[2] the images to the right are the same exposures in the *Hα* line. Several similar cases have been observed with the Climax coronagraph.

In order to check the observations, similar plates were taken with the Sacramento Peak Station coronagraph. Figure 2 shows in the *Hα* line a narrow dark lane between two prominences at the east limb. The spectrograms were obtained on Sacramento Peak on November 6, 1949. On some occasions helix-shaped dark lanes have been observed in the *Hα* line. The dark filaments visible on these plates indicate the presence of absorbing matter of a very low brightness above the surface of the sun.

II. EVIDENCE FROM PHOTOGRAPHS OF PROMINENCES OUTSIDE THE LIMB

After the discovery of several examples of dark lanes on spectrum plates of the corona, the writer examined a great number of prominence photographs taken on Climax and at

[1] Cf. *Ark. f. Astr.*, Vol. 1, No. 1, 1949; and R. W. Wood's article in *Ap. J.*, 12, 281, 1900.

[2] Considering the fact that D3 filaments are seldom seen on the disk and that self-absorption is, as a rule, insignificant in the D3 line (cf. Unsöld, *Physik der Sternatmosphären* [Berlin: J. Springer, 1938], p. 411), the dark D3 filament in Fig. 1 is possibly not a real object but is due to a rift or a radial-velocity shift. On the other hand, even if a filament does not show up in D3 on the disk, it might appear dark in front of a hot prominence, though probably with lower contrast than in *Hα*. Another explanation would be that the filament is situated in the prominence itself and that this is a flat object. A low-excitation filament could in this case show up dark simply because of its low luminosity.

the McMath-Hulbert and Stockholm Observatories. Though apparent filaments can often be seen on the photographs, it is, in general, very difficult to prove that the dark objects are real ones and not caused by rifts in the bright prominences.

But in such cases, when a dark filament in front of a prominence extends as a faintly luminous object outside the prominence, it seems very likely that the filament in front of the prominence is a real object. Examples of this kind are presented in Figure 3. These prominences were photographed by L. Dahlmark at the Stockholm Observatory on February 7, August 31, and September 14, 1949, with a birefringent monochromator built by me in 1937. The dotted lines in the schematic drawings indicate the objects in question. It seems very probable that the "dark" filaments in Figure 3 are real ones. They have, of course, a much higher intrinsic brightness than the objects traced in Figures 1 and 2.

III. EVIDENCE FROM SPECTROHELIOGRAMS

All dark filaments which appear in $H\alpha$ outside the limb should be expected to appear as dark objects when projected against the solar disk and observed on $H\alpha$ spectroheliograms. As a matter of fact, it has been a puzzling problem to explain why very dark filaments on the disk sometimes appear as rather feeble prominences outside the limb. But, if these objects have a very low intrinsic brightness, it is quite natural that they should almost disappear when observed outside the limb.

In extended filaments on the disk it is often possible to see dark, narrow threads. The writer wants to draw special attention to the cases in which such a filament is visible partly on the disk and partly outside the limb. It sometimes happens that the dark, narrow threads also appear as dark objects in the prominence seen outside the limb, as indicated by the schematic Figure 4. Plate II, 3 on page 24 in the extensive paper of M. and Mme d'Azambuja[3]) seems to give an example of such an object. A rather clear case was found at the McMath-Hulbert Observatory on July 2, 1949, and was privately communicated to me by Dr. Helen Dodson. A similar object was recorded by me on January 13, 1950, with the Stockholm Observatory spectroheliograph.[4] The phenomenon strongly confirms the conclusion drawn above that objects of low intrinsic brightness sometimes appear in connection with prominences and may produce strong absorption effects not only when viewed against the disk but also when viewed against a prominence outside the limb.

It is a general opinion that flat prominences, seen edgewise, produce many of the very dark and narrow filaments on spectroheliograms. As the prominences in such a case are almost opaque in $H\alpha$, it is the intrinsic brightness of such an object which gives its residual intensity. Now many of these objects are really darker than many prominences seen outside the limb. Consequently, there must be a considerable variation in temperature (excitation) from one object to the other and not merely a question of different transparency.[5] It does not seem improbable that a network of low-excitation matter appearing in the flat prominences may contribute to the low residual intensity of these objects when seen edgewise as filaments.

IV. SOME SUGGESTIONS FOR FUTURE WORK

The best way to study the relatively dark filaments outside the limb would probably be to use a birefringent monochromator attached to a coronagraph and built in such a

[3] *Ann. Obs. Paris, Meudon*, Vol. 6, Fasc. VII, 1948.

[4] The writer is indebted to Mr. A. Dollfus, who has kindly communicated to me an interesting observation of such an object made by him at Meudon on June 14, 1950, with the birefringent monochromator. The observation was made after conference with the writer. Phenomena of a similar kind seem to have been observed before in Meudon by Deslandres and D'Azambuja, though not specifically reported in the literature.

[5] Internal variations of excitation within prominences have been found before by H. A. Brück and W. Moss from a study of the intensity ratio between $H\alpha$ and D3 (*M.N.*, 105, 282, 1945).

FIG. 2.—Two wide-slit exposures of the corona spectrum, showing a faint narrow dark filament between two prominences in the $H\alpha$ line. Sacramento Peak, November 6, 1949.

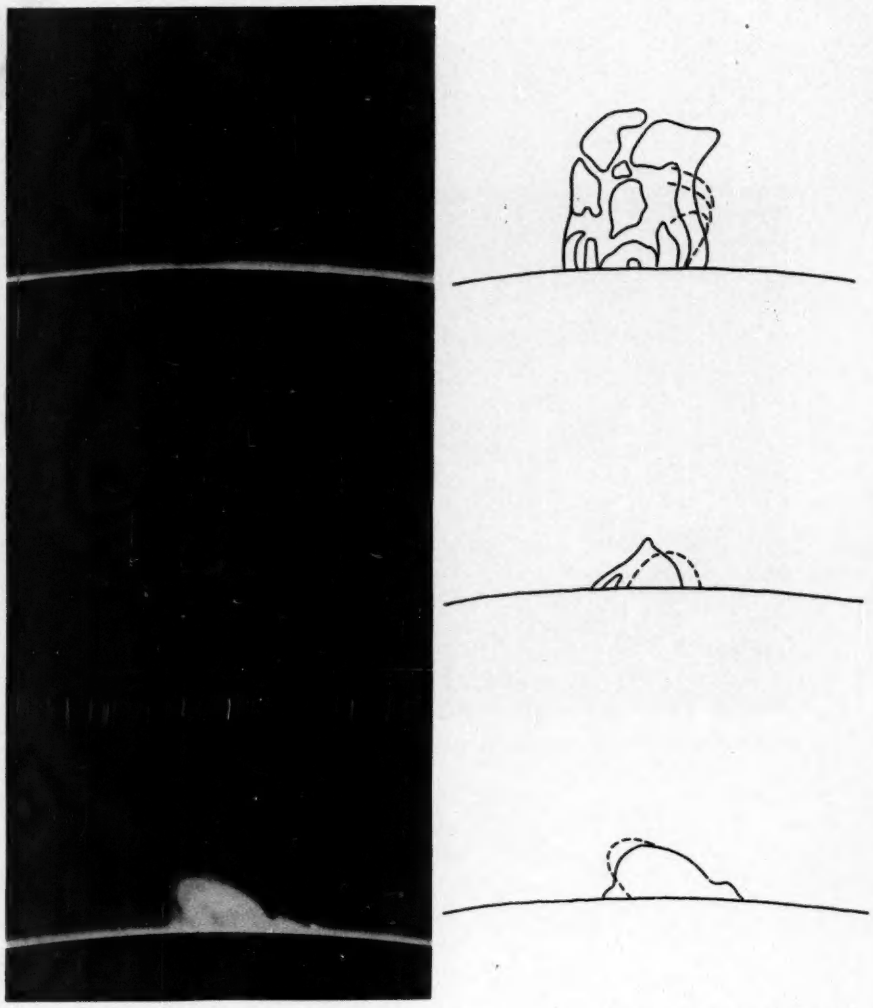

FIG. 3.—Prominences photographed on February 7, August 31, and September 14, 1949, at the Stockholm Observatory. Low-intensity filaments are indicated by the dotted lines in the schematic drawings.

way that only 1 angström or less is transmitted at $H\alpha$. The exposures should be long enough to show the corona as a uniform background. The same arrangement should, if possible, be used when observing eclipses.

More information might be gained from an extensive study of filaments inside and outside the limb of the sun. Special attention should also be paid to those extremely narrow filaments which sometimes appear on the disk and often connect ordinary filaments. (Such narrow objects can be seen on some large-scale spectroheliograms put at my disposal by the Mount Wilson Observatory.)

FIG. 4.—Schematic drawing, showing a dark narrow filament appearing in front of a prominence which is partly visible on the disk and partly outside the limb.

The observations presented here cannot be fully understood without an elaborate theory. The "dark" filaments are likely to be objects of relatively low excitation; but whether the temperature is low or the pressure high or both effects are present seems to be a point of great interest for a theoretical study.

The work presented here has been carried out partly with the support of Harvard University research contract W 19-122 ac-17 administered by the Air Force Cambridge Research Laboratories. It is a pleasant duty to express my deep appreciation for this support. I want to express my gratitude to Dr. Harlow Shapley, Dr. Donald H. Menzel, and Dr. Walter Orr Roberts for the kind interest they have taken in my work and for valuable help in various respects. My thanks are due also to other members of the staffs of the Harvard College Observatory and the High Altitude Observatory, and I want to mention particularly Mr. William Fleming at the Climax station, Mr. Rudolph Cook at the Sacramento Peak station, and the photographer, Mr. H. L. McLeland. I also want to express my deep gratitude for the material put at my disposal by the courtesy of the Mount Wilson and the McMath-Hulbert Observatories.

NOTES

THE SPECTROSCOPIC BINARY 47 ANDROMEDAE

At the suggestion of Dr. O. Struve, observations were made of the star 47 And (HD 8374) for the purpose of determining its spectroscopic orbit. From observations by R. K. Young,[1] plates taken by W. W. Morgan at Yerkes Observatory during the interval 1933–1935, and plates taken at the McDonald Observatory during the interval 1947–1949, three of the elements were found to be:

$$P = 39^{d}.393 \; ; \; e \cong 0.6 \; ; \; \omega \cong 0^{\circ} \, .$$

The values of e and ω were derived by using the best fit on the velocity-curves of E. S. King.[2] Double lines are observed for a duration of about 4 days during the period. There is no evidence of diffuse lines between the times of the measured separations.

The time of maximum velocity separation of the spectral lines is given by the relation

$$T = \text{JD } 2432896.10 + 39.393\, E \, .$$

P. D. Jose

McDonald Observatory
February 26, 1951

[1] *Pub. Dom. Ap. Obs. Victoria*, **1**, 166, 1920.

[2] *Harvard Ann.*, **81**, 231, 1920.

REVIEWS

Atlas der Restlinen, Vol. III: *Spektren seltener Metalle und einiger Metalloide*. By A. GATTERER and J. JUNKES. Vatican City: Specola Vaticana, 1949. Pp. 80+42 double-weight photographic charts, 30×40 cm. $25.00.

For many years the publication of wave-length tables, though extensive and with accurate measures, left much to be desired; the individual who has taken a set of tables and a new spectrum in hand and attempted to identify features on the latter has invariably felt himself baffled. The transformation necessary to change a table of wave lengths into what the physical appearance might be is difficult; and there are all too many cases in the history of spectroscopy in which an investigator has blithely taken a set of wave-length tables and some wave lengths measured on spectrograms and gone methodically down the list making "identifications." Although the tables can hardly be blamed for such a procedure, such tables do present the opportunity.

The preparation of this third and final volume of the *Atlas der Restlinen* shows that the authors were well aware of the problems involved in spectral analyses. Their tables for each element are concise, giving the important spectral features and the impurities present. In numerous applications the impurities are often as important as the substance; certainly, a table telling only what ought to be present is missing an important point—one of the most useful things is what also might be present.

The crowning beauty of this atlas is the inclusion of superb-quality photographic prints of the actual spectra. The amount of painstaking care that went into the preparation of the spectra and of the volume itself is reflected in the potential usefulness of the atlas. Reproductions are given of the arc and spark spectra for the metals and of electrodeless discharge spectra for the metalloids. The spectra are all obtained with sufficient dispersion to be useful for many purposes; the several prismatic spectrographs used to cover the range from 6340 to 2100 A gave mean dispersions of the order of 1.5 A/mm, with the exception of the red region, where the highest dispersion is 4 A/mm. For convenience the most notable impurities and unrelated band emissions, as well as the wave lengths of the principal lines, are marked upon the spectra.

While the primary concern of the authors was a study of the prominent atomic lines of the various elements, the spectra frequently show molecular bands of the oxides. A comparison with the complete table of molecular bands published by Herzberg[1] shows immediately a number of unstudied band systems. Some of the more prominent bands recorded are *CbO* (*Cb* = niobium), *TaO*, *TeO*, and *HfO*. The band analyses for these systems could actually be done directly from the excellent photographic reproductions, since the rotational structures are well resolved.

The publication of this third volume of the *Atlas der Restlinen* definitely marks a new high point in the publication of photographic atlases. It will make a most valuable addition to every astrophysical or physical laboratory; and it certainly should be welcomed by the metallurgical laboratories, in view of the prominent role that spectroscopy plays in these industries.

A. B. MEINEL

Yerkes Observatory

Ninth Astronomer Royal: The Life of Frank Watson Dyson. By MARGARET WILSON. Cambridge: W. Heffer & Sons, Ltd., 1951. Pp. 294+xiv. 25*s*. net.

"If I'm remembered in the future it will be because of my association with Eddington. People will say—'Dyson? Oh yes—he was Astronomer Royal, when Eddington was Chief Assistant.'" So Dyson told everyone: and that is a measure of his innate modesty. But Eddington has said: "To his contemporaries it is axiomatic that the name of Dyson must rank among the greatest of

[1] *Spectra of Diatomic Molecules* (New York: D. Van Nostrand Co., Inc., 1950).

the makers of modern astronomy; and if the reasons do not appear obvious on the surface, it is because they are deeper than the surface. His influence went far beyond the work which appears under his name—or more usually under his name joined with that of a collaborator. As for viewing his achievement impartially, no-one could judge Dyson impartially; the universal affection in which he was held was too strong for that. . . . The root of his great influence was his personal character. The qualities which endeared him to us, his complete unselfishness, his sincerity, his sociability, shone the more brightly because they were innate in his nature. . . . Time after time, in scientific progress as in human fellowship, his was the inconspicuous yet indispensable part." And the charming biography of one of the great astronomers of our times by his daughter reveals the lovable personality that was Dyson's.

In an age and a period different from ours, there should have been no need for the author's apologetic remark: "Such an unsettled and critical period in the world's history may seem a strange time to publish the life of a scientist of only secondary importance. Frank Dyson fought no wars, framed no policies, declaimed no speeches." Dyson was by no means a scientist of only "secondary importance." Together with Eddington, Schwarzschild, and Seeliger, Dyson was the founder of modern statistical astronomy. And Dyson's was an indispensable part in what Eddington has described as "the most exciting event I can recall in my own connection with astronomy, [namely,] the verification of Einstein's prediction of the deflection of light at the eclipse of 1919." And Jeans, paying tribute to Dyson, has written: "In 1918, in the darkest days of the war, two expeditions were planned, one by the Greenwich Observatory and one by Cambridge, to observe, if the state of civilization should permit when the time came, the eclipse of May, 1919, with a view to a crucial test of Einstein's generalized relativity. The Armistice was signed in November, 1918; the expeditions went and returned, bringing back news which changed, and that irrevocably, the astronomer's conception of the nature of gravitation and the ordinary man's conception of the nature of the universe in which he lives. If the credit of this achievement had to be divided between Sir Frank Dyson and Professor Eddington I frankly do not know in what proportion the division should be made. To my mind, however, it is not so much an occasion for sharing out credit as for attributing the whole credit to each, for if either had failed to play his part, either from want of vision, of enthusiasm, or of capacity for seizing the right moment, I doubt if the expeditions would have gone at all, and the great credit of first determining observationally what sort of things space and time really are would probably have gone elsewhere." And reading Dyson's biography, we can well envy the sense of absolute values which motivated the astronomers of an earlier epoch.

S. CHANDRASEKHAR

Yerkes Observatory

ASTROPHYSICAL

Contributions from the Princeton University

...LES OF STELLAR DYNA...

...ARCHAR

...CTRA OF LONG-PERIOD V...

...RUSSELL

...MASSES OF THE STARS ...
...CULE OF DYNA...

...RUSSELL and ...

...DISTRIBUTION OF TE...

...FOX

...UNIVERSITY OF C...